IAEA-BIOMASS-2

Testing of environmental transfer models using data from the atmospheric release of Iodine-131 from the Hanford site, USA, in 1963

Report of the Dose Reconstruction Working Group of the Biosphere Modelling and Assessment (BIOMASS) Programme, Theme 2

INTERNATIONAL ATOMIC ENERGY AGENCY

The originating Section of this publication in the IAEA was:

Waste Safety Section
International Atomic Energy Agency
Wagramer Strasse 5
P.O. Box 100
A-1400 Vienna, Austria

TESTING OF ENVIRONMENTAL TRANSFER MODELS USING DATA FROM
THE ATMOSPHERIC RELEASE OF IODINE-131 FROM THE HANFORD SITE, USA, IN 1963
IAEA, VIENNA, 2003
ISBN 92–0–102603–X

Printed by the IAEA in Austria
March 2003

FOREWORD

The IAEA Programme on *BIO*sphere *M*odelling and *ASS*essment (BIOMASS) was launched in Vienna in October 1996. The programme was concerned with developing and improving capabilities to predict the transfer of radionuclides in the environment. The programme had three themes:

Theme 1: Radioactive Waste Disposal. The objective was to develop the concept of a standard or reference biosphere for application to the assessment of the long term safety of repositories for radioactive waste. Under the general heading of "Reference Biospheres", six Task Groups were established:

Task Group 1: Principles for the Definition of Critical and Other Exposure Groups.

Task Group 2: Principles for the Application of Data to Assessment Models.

Task Group 3: Consideration of Alternative Assessment Contexts.

Task Group 4: Biosphere System Identification and Justification.

Task Group 5: Biosphere System Descriptions.

Task Group 6: Model Development.

Theme 2: Environmental Releases. BIOMASS provided an international forum for activities aimed at increasing the confidence in methods and models for the assessment of radiation exposure related to environmental releases. Two Working Groups addressed issues concerned with the reconstruction of radiation doses received by people from past releases of radionuclides to the environment and the evaluation of the efficacy of remedial measures.

Theme 3: Biosphere Processes. The aim of this Theme was to improve capabilities for modelling the transfer of radionuclides in particular parts of the biosphere identified as being of potential radiological significance and where there were gaps in modelling approaches. This topic was explored using a range of methods including reviews of the literature, model inter-comparison exercises and, where possible, model testing against independent sources of data. Three Working Groups were established to examine the modelling of: (1) long term tritium dispersion in the environment; (2) radionuclide uptake by fruits; and (3) radionuclide migration and accumulation in forest ecosystems.

This report describes results of the studies undertaken by the Dose Reconstruction Working Group under Theme 2. The IAEA Scientific Secretary for this publication was initially K.-L. Sjoeblom and subsequently C. Robinson both of the Division of Radiation and Waste Safety. The IAEA wishes to acknowledge the contribution of the Working Group Leader, K. Thiessen of the United States of America, for help with this report.

EDITORIAL NOTE

The use of particular designations of countries or territories does not imply any judgement by the publisher, the IAEA, as to the legal status of such countries or territories, of their authorities and institutions or of the delimitation of their boundaries.

The mention of names of specific companies or products (whether or not indicated as registered) does not imply any intention to infringe proprietary rights, nor should it be construed as an endorsement or recommendation on the part of the IAEA.

CONTENTS

SUMMARY

This BIOMASS Theme 2 Working Document has been produced by Working Group 1 which is concerned with the evaluation of the reliability of methods used for dose reconstruction for specific individuals and members of specific population subgroups.

This Working Group has developed and used model-testing scenarios to examine one or more aspects of the dose reconstruction assessment process. This process includes the following elements:

(1) Evaluation of the source term, or the nature, amount, and conditions of the release;

(2) Evaluation of the environmental transport of the contaminants, including dispersion, chemical transformation, persistence, and time-dependent concentrations of the contaminants in various environmental media;

(3) Description and evaluation of potential pathways for human exposure to the contaminants;

(4) Estimation of the internal and external doses to humans; and

(5) Estimation of the resulting health risks to exposed individuals and populations.

This exercise provides an opportunity for comparison of assessment methods and conceptual approaches, for testing models for the specified level of the assessment with actual measurements, and for identifying the most important sources of uncertainty with respect both to that part of the assessment and to the overall assessment.

The scenario discussed in this Report relates to an inadvertent release of ^{131}I to atmosphere from the Hanford Purex Chemical Separations Plant on 2–5 September 1963. The details of the scenario are discussed in the Report. Two groups of possible calculational endpoints were identified: quantities for which measurement data exist and quantities that can only be predicted (such as radiation dose).

1. INTRODUCTION

1.1. BACKGROUND AND OVERALL OBJECTIVES OF BIOMASS

BIOMASS (**Bio**sphere **M**odelling and **Ass**essment Methods) is the fourth in a series of international programmes aimed at the improvement of methods for assessing the impact of radionuclides in the environment; the first three were the VAMP programme, sponsored by the International Atomic Energy Agency (IAEA), and BIOMOVS (**Bio**spheric **Mo**del **V**alidation **S**tudy) Phases I and II, supported by organizations from Canada, Spain and Sweden. These programmes have served to provide forums to promote international collaboration, information exchange, and peer review in the area of modelling and assessment of the movement of radionuclides and other pollutants in the environment.

The scope of the BIOMASS programme is the scientific, experimental, and technical aspects related to the analysis and assessment of the behaviour of radionuclides in the environment and their associated impacts. Special emphasis is being placed on the improvement of the accuracy of model predictions, on the improvement of modelling techniques, and on the promotion of experimental activities and field data gathering to complement assessments.

The programme is designed to address important radiological issues associated with accidental and routine releases and with solid waste management. Three important areas involving environmental assessment modelling are being covered: Theme 1, Radioactive waste disposal (emphasis on reference biospheres); Theme 2, Environmental Releases (including remediation of areas contaminated as a result of nuclear accidents, unrestricted releases or poor management practices, and reconstruction of radiation doses received due to accidental or poorly controlled releases); and Theme 3, Biosphere Processes (current emphases on tritium, fruit trees, and forests).

The general goals of the BIOMASS programme can be summarized as follows:

(1) To provide an international focal point in the area of biospheric assessment modelling for the exchange of information and in order to respond to biospheric assessment needs expressed by other international groups (within and outside IAEA).

(2) To develop methods (including models, computer codes and measurement techniques) for the analysis of radionuclide transfer in the biosphere for use in radiological assessments.

(3) To improve models and modelling methods by model testing, comparison and other approaches.

(4) To develop international consensus, where appropriate, on biospheric modelling philosophies, approaches, and parameter values.

1.2. THEME 2: ENVIRONMENTAL RELEASES

Theme 2 of BIOMASS, Environmental Releases, focuses on issues of dose reconstruction and remediation assessment. Many national agencies and authorities have a growing interest in:

— addressing concerns about the effects of historic releases, both planned and accidental;

— gaining information to improve understanding of processes of migration, accumulation, exposure and exposure consequences;

— making better informed decisions about remediation requirements at contaminated sites, through the assessment of future impacts; and

— guiding decisions on alternative technologies and techniques available for remediation of contaminated sites.

Dose reconstruction and evaluation of remediation alternatives both involve assessment of radionuclide releases to the environment. Such assessments make use of a great variety of information gained from site characterization studies, source term evaluation, and so on. Ultimately, however, this information has to be combined in some sort of assessment model involving assumptions about how the system has behaved (or will behave). Mathematical modelling of this type is required because it is simply not possible today to measure directly what has happened in the past or what will happen in the future.

The overall objective of BIOMASS Theme 2 is to provide an international forum to increase the credibility of and confidence in methods and models for the assessment of radiation exposure in the context of dose reconstruction and remediation activities. Consideration is being given to assessment of concentrations of radionuclides in relevant environmental media and the associated radiation doses and risks to humans.

Secondary objectives of BIOMASS Theme 2 include the following:

(1) To provide a forum for review, independent scrutiny and intercomparison of methods and models used in dose reconstruction and remediation assessment.

(2) To provide a forum for model testing, and where possible, validation.

(3) To develop the consideration and presentation of conceptual and parameter uncertainties within dose reconstruction and remediation assessment.

(4) To test the transparency and adequacy of modelling assumptions in the context of specified assessment objectives.

(5) To identify assessment shortcomings in terms of model structure and data and hence identify critical research areas.

(6) To identify those components of assessment assumptions that are arbitrary, matters of policy, or simple value judgments, as opposed to those which are objectively verifiable.

Two Working Groups have been established within BIOMASS Theme 2:

(1) Working Group 1 is concerned with the evaluation of the reliability of methods used for dose reconstruction for specific individuals and members of specific population subgroups.

(2) Working Group 2 is concerned with the evaluation of the reliability of dose and risk assessment methodologies applied in support of decisions to determine the cost-effectiveness of risk-reduction measures within an environmental remediation programme.

1.3. BACKGROUND ON DOSE RECONSTRUCTION

The goal of a dose reconstruction is the estimation of human exposures, doses, and health risks due to an historical release (or set of releases) of one or more contaminants. Different

amounts and types of information may be available, depending on such things as the nature of the release and how long ago the release took place. The completeness and the site-specific relevance of the available data influence the degree of confidence or uncertainty that can be placed on the assessment results.
In general, the assessment process includes the following aspects:

(1) Evaluation of the source term, or the nature, amount, and conditions of the release;

(2) Evaluation of the environmental transport of the contaminants, including dispersion, chemical transformation, persistence, and time-dependent concentrations of the contaminants in various environmental media;

(3) Description and evaluation of potential pathways for human exposure to the contaminants;

(4) Estimation of the internal and external doses to humans; and

(5) Estimation of the resulting health risks to exposed individuals and populations.

Each of these aspects of the assessment process presents its own set of potential sources of uncertainty, all of which contribute to the uncertainty in the assessment endpoint.

The model-testing scenarios developed and used in this part of the BIOMASS project each examine one or more aspects of the dose reconstruction assessment process. For each aspect of an assessment question, the exercise provides an opportunity for comparison of assessment methods and conceptual approaches, for testing models for the specified level of the assessment with actual measurements, and for identifying the most important sources of uncertainty with respect both to that part of the assessment and to the overall assessment.

1.4. INITIAL CASE IN DOSE RECONSTRUCTION: HANFORD SCENARIO

1.4.1. Background

The Hanford test scenario is an inadvertent acute release of ^{131}I to the environment from the Hanford Purex Chemical Separations Plant stack that occurred on September 2–5, 1963 (Soldat, 1965) [1]. Monitoring data were collected in nine counties in the northwestern United States over the two-month period following the release. The pathways contributing to dose are primarily through the air and terrestrial environments (Farris et al., 1994) [2].

This initial dose reconstruction scenario could be used for a number of different purposes:

(1) To test a number of different types of environmental dosimetry models (atmospheric transport and deposition, food chain transport, intake by humans) by comparing model predictions with measurements;

(2) To compare assessment methods that can be used to arrive at a specific user-selected endpoint, e.g. process-level models vs. assessment models;

(3) To compare methods and approaches used for selecting parameter values, performing and interpreting sensitivity analyses, and performing, interpreting, and presenting uncertainty estimation; and

(4) To examine approaches to the management of accidental releases of radioactivity to the environment, including how the approach used depends on the data available to the manager.

This scenario was designed to be used by a variety of dose assessment professionals; each participant in this exercise could select the aspects of the scenario that best fit his or her needs.

The Hanford scenario involved an acute release of ^{131}I to the atmosphere. While the specific release occurred in the northwestern USA, the assessment methods addressed with this scenario have wide application. Many dose reconstructions either currently underway or being considered in many parts of the world involve the release of ^{131}I to the atmosphere. These include:

— Chernobyl Unit 4 accident, Ukraine;
— Mayak Nuclear Weapons Production Facility, Russian Federation;
— Semipalatinsk Test Site, Altai Region, Kazakhstan;
— Maralinga Test Site, Australia;
— Republic of the Marshall Islands;
— Oak Ridge Historic Fuel Reprocessing, Tennessee, United States of America;
— Nevada Test Site, United States of America;
— Windscale Accident, United Kingdom.

The insights gained from participation in this Hanford scenario are directly applicable to those dose reconstructions as well as to any other radiological assessments involving ^{131}I. In addition, some aspects of this scenario, e.g. atmospheric dispersion and deposition, will also be applicable to assessments that do not necessarily include ^{131}I.

1.4.2. Scenario description

An acute, inadvertent release of ^{131}I from the 60 m stack of a nuclear chemical separations plant (centrally located on the 1450 km^2 Hanford Site) occurred beginning 2 September 1963. This release resulted from the inadvertent charging of short-aged fuel elements into a dissolver of the Purex separation plant. Plant operations were shut down as soon as the abnormal release was detected. Steps were immediately taken to retain as much of the ^{131}I as possible within the plant. Laboratory analyses of stack effluent samples were made. These were provided as a possible starting point for calculations. The routine program of environmental surveillance was augmented with additional sampling. Measurements of wind velocity and temperature are made routinely at the site meteorology tower. Similar data from additional weather stations within a few hundred kilometres were also available for those who wished to use them in dispersion modelling.

No significant rainfall occurred in the test region during the test period. No protective measures were taken following the release. No atmospheric nuclear test explosions occurred in the several months prior to this event. Routine atmospheric releases of ^{131}I prior to and following this event were on the order of 0.1 Ci per month, or less.

The Hanford Site is located in a rural, semi-arid region of southeastern Washington State in the USA and occupies an area of about 1450 km^2. The Site lies about 320 km northeast of Portland, Oregon, 270 km southeast of Seattle, Washington, and 200 km southwest of Spokane, Washington. The semi-arid land on which the Hanford Site is located has a sparse covering of desert shrubs and drought-resistant grasses. The most broadly distributed type of vegetation on the Site is the sagebrush/cheatgrass/bluegrass community. Most abundant of the mammals is the Great Basin pocket mouse. Of the big-game animals, the mule deer is most widely found, while the cottontail rabbit is the most abundant small game animal. Coyotes are also plentiful. The bald eagle is a regular winter visitor to the area along the Columbia River.

The terrain of the central and eastern parts of the Hanford Site is relatively flat. The northern and western parts of the Site have moderate to steep topographic ridges composed of basalt and sediments. The elevations of the alluvial plain that covers much of the Site vary from 105 m (345 ft) above mean sea level in the southeast corner to 245 m (803 ft) in the northwest. The central plateau of the Site varies in elevation from 190 to 245 m (623 to 803 ft). The highest point is on Rattlesnake Mountain (1093 m or 3585 ft) at the southwestern border of the Site.

The Columbia River, which originates in the mountains of eastern British Columbia, Canada, flows through the northern edge of the Hanford Site and forms part of the northern edge of the Hanford Site and part of the Site's eastern boundary. Land surrounding the Hanford Site is used primarily for agriculture and livestock grazing. Agricultural lands are found north and east of the Columbia River and south of the Yakima River. These areas contain orchards, vineyards, and fields of alfalfa, wheat, and vegetables. The Hanford Site north of the Columbia River contains both a state wildlife management area and a federal wildlife refuge. The northeast slope of the Rattlesnake Hills along the southwestern boundary of the Site is designated as the Arid Lands Ecology Reserve and is used for ecological research.

The population in the area surrounding the Site is rural, with the exception of the area near the southeast boundary where the cities of Richland, Pasco, and Kennewick are located. Smaller communities in the vicinity are Benton City, West Richland, Mesa, and Othello. Altogether about 80 000 people lived in the vicinity of the Site at the time the event took place.

The prevailing regional winds are from the northwest, with occasional cold-air drainage into valleys and strong crosswinds. The region is a typical desert basin, where frequent strong temperature inversions occur at night and break during the day, resulting in unstable and turbulent wind conditions.

Increased vegetation sampling was begun on 2 September and continued for the next week. Leafy sagebrush (approximately 40% moisture) was collected whenever possible at on-site locations. A few samples consisted of leafy weeds, cheat grass, and in one case, bare sage stems (20% moisture) where a fire had previously destroyed the normal vegetation growth. Off-site vegetation samples consisted of pasture grass samples (approximately 80% moisture) from local dairy farms and native vegetation (leafy weeds, approximately 40% moisture) along highways and at the permanent atmospheric monitoring stations. Sampling of grass and milk was extended up to 100 km southeast of the release point. The maximum off-site vegetation contamination of 0.5 Bq/g was measured on a sample of green hay from a farm 32 km SSE of the release point where no cattle were being grazed. Maximum on-site vegetation contamination was found within 3 km of the stack.

Twenty-two permanent atmospheric monitoring stations were maintained in the environs of the Hanford site. Equipment installed in these stations included an HV-70 filter and a caustic scrubber in series. These permanent air sampling stations were supplemented by several temporary caustic scrubber and charcoal cartridge samples during September 1963. The concentrations provided in the scenario are daily values which were averaged (divided) evenly over the varying sampling periods.

Routine milk collection in 1963 included daily to weekly samples from seven local dairy farms, two milk-shed composites twice per month, and three commercial brands of milk twice per month. Spot sampling at several other dairy farms brought the total number of farms where milk and grass were sampled up to fifteen during the month of September 1963. The Twin City Dairy processed milk from both the east and the south of the test region, and Darigold creamery processed milk from the east of the region.

A complete description of the Hanford scenario and the input information is provided in Annex I.

1.4.3. Assessment tasks

The possible calculational endpoints for this scenario can be separated into two groups. The first group includes quantities for which measurements exist and against which model predictions can be tested. The second group includes quantities which can only be predicted but not tested (such as radiation dose). The latter were included because they are the most common and useful endpoints in radiological assessments. For all quantities, a 90% confidence level (5% and 95%, respectively, lower and upper bound estimates) was requested to quantify the expected uncertainty in the result. These values are 'subjective' confidence intervals, given the nature of the data provided for this scenario.

The following types of calculations for model testing could be performed:

— daily air concentrations of ^{131}I;

— average time-integrated air concentrations;

— average deposition;

— total inventory over the region;

— time-integrated concentrations in milk;

— average time-integrated concentrations in specified vegetation;

— thyroid burden of two specified children.

The following calculations could be performed for model comparison purposes only:

— mean external dose to specified individuals from the overhead cloud and contaminated ground;

— mean inhalation dose to the thyroid of specified individuals;

— mean ingestion dose to the thyroid of specified individuals;

— total dose;

— estimates of the risks that result from these doses.

Users were permitted to start at different points in the scenario and calculate different items from the list above. This decision depended on the needs and interests of the user and the capability of the models being examined.

1.5. STRUCTURE OF THE REPORT

Section 1 of this report contains an introduction to BIOMASS, the Theme 2-Dose Reconstruction Working Group, and the initial test exercise (the Hanford scenario). Section 2 summarizes the participation in the exercise and provides a description of the characteristics of the models used. A summary and discussion of the results of the test exercise are given in Section 3. Major factors affecting the model outcomes (e.g., reasons for good predictions or mispredictions) are discussed in Section 4. Section 5 contains a discussion of the uncertainty analyses carried out in the modelling exercise, and Section 6 provides concluding remarks.

Three annexes supplement the main text of this report. Annex I contains a detailed description of the Hanford Scenario, including both input and observed data. Annex II contains descriptions of the models and individual evaluations of model predictions by the participants in the exercise. A complete summary of the model predictions is given in Annex III.

2. PARTICIPANTS AND MODELS

Six individuals or groups participated in the test exercise, in addition to the scenario author, who contributed both observations when available and calculations performed as a part of the Hanford Environmental Dose Reconstruction (HEDR) programme. The participants, their nationalities, and the endpoints for which they made calculations are summarized in Table I. The modelling approaches used for different parts of the exercise are described briefly in Table II, and a comparison of values used for key model parameters is provided in Tables III and IV. Model documentation is provided in Annex II, together with each participant's evaluation of his model's performance.

TABLE I. SUMMARY OF PARTICIPANTS AND ENDPOINTS MODELLED

Participant	Napier	Filistovic	Homma	Krajewski	Kryshev	Kanyár/ Nényei	Tveten
Country	USA	Lithuania	Japan	Poland	Russia	Hungary	Norway
Deposition	x	x	x	x	x	x	x
Vegetation concentrations	x	x	x	x	x	x	x
Milk concentrations	x	x	x	x	x	x	
Daily averages at dairies					x	x	
Human intake			x	x	x	x	
Thyroid burdens			x	x	x	x	
Dose Estimates:							
External (cloud)	x	x	x	x	x	x	
External (ground)	x	x	x	x	x	x	
Inhalation	x	x	x	x	x	x	
Ingestion	x	x	x	x	x	x	
Total	x	x	x	x	x	x	
Dispersion contours	x	x	x			(x)[a]	

[a] Dispersion contours were developed, but not submitted.

TABLE II. SUMMARY OF MODELLING APPROACHES USED IN THE HANFORD TEST EXERCISE

Participant	Atmospheric Transport	Deposition	Terrestrial Foodchain	Uncertainty Estimation
Napier (HEDR)	$1/r^2$ wind field interpolation from observations, all 12 met stations, 10 km grid	dry and wet deposition	time-dependent compartmental	Monte Carlo
Filistovic	segmental diffusion-convection model, 1 km grid, Hanford Met Station data	dry deposition velocity	time-dependent compartmental	Monte Carlo
Homma	Lagrangian trajectory, Gaussian puff model (1) hourly met data at release height, meso scale wind and stability fields from 12 surface met stations, $1/r^2$ interpolation (2) hourly met data at release height, Hanford Met Station data	dry deposition velocity and washout rate	time-dependent, analytical	Monte Carlo
Krajewski	reconstructed from vegetation and air measurements	reconstructed from vegetation measurements	time-dependent compartmental	error propagation
Kryshev	Pasquill-Gifford straight-line Gaussian model, segmented, Hanford Met Station data	deposition velocity	transfer factors	judgment
Kanyár /Nényei	multi-puff Gaussian model, hourly met data at the release height, Hanford Met Station data, Smith-Hosker relationships and trajectories, 1-12 hourly releases, 2 km grid	effective dry deposition rate	time-dependent compartmental	Monte Carlo
Tveten	straight-line Gaussian model (MACCS), hourly met data at release height, Hanford Met Station data, day and night conditions separately	dry deposition velocity	not done	not done

TABLE III. SUMMARY OF VALUES USED FOR SELECTED MODEL PARAMETERS[a]

Parameter	Napier (HEDR)	Filistovic	Homma	Krajewski	Kryshev	Kanyár/Nényei	Tveten
iodine speciation (%)							–[c]
reactive gas (I_2)	40–60	40	40	40	45	40	
particulate	5–45	25	25	25	25	25	
organic	remainder[b]	35	35	35	35	35	
dry deposition velocity ($m \cdot s^{-1}$)							
all (weighted average)			0.0043		0.013	0.0083	0.006
reactive gas (I_2)	0.002–0.07	0.01	0.01	0.01	0.03	0.02	
particulate	0.0015–0.0095	0.001	0.001	0.0016	0.002	0.001	
organic		0.0005	0.0001	1×10^{-5}	0.0001	0.0005	
pasture yield ($kg\ m^{-2}$)	0.3 (dry)	0.519 (wet)	–[c]	0.7 (wet)	0.12 (wet)	0.5 (dry)	0.52 (dry)
biomass growth rate ($kg \cdot m^{-2} \cdot d^{-1}$)	by crop type	–[c]	–[c]	–[c]	6.4×10^{-4}	–[c]	–[c]
weathering rate constant (d^{-1})	0.0495	0.074	0.0495	0.046	0.05	0.07	–[c]
interception fraction (pasture)	function of biomass	–[c]	–[c]	0.3	–[c]	0.4	0.4
absorption coefficient or mass interception factor (pasture; $m^2\ kg^{-1}$)	1.0–4.0	1.0	2.0	2.8	2.8	–[c]	–[c]
milk transfer coefficient for ^{131}I ($d\ L^{-1}$)	0.0092	0.00117	0.01 (model equivalent)	0.00168	0.01 $d\ kg^{-1}$	0.008 (model equivalent)	–[c]
transfer in cow (d^{-1})	–[c]	–[c]	–[c]	–[c]	–[c]		–[c]
GI tract–to–blood						10	
blood–to–milk						0.5	
milk production ($L\ d^{-1}$)	–[c]	–[c]	–[c]	–[c]	–[c]	11	–[c]
fraction of daily intake of ^{131}I secreted per liter of milk (L^{-1})	–[c]	–[c]	$0.0091\ e^{(0.021t)} * [1\text{-}e^{(-0.292t)}]$	–[c]	–[c]	–[c]	–[c]

TABLE III (cont.)

Parameter	Napier (HEDR)	Filistovic	Homma	Krajewski	Kryshev	Kanyár/Nényei	Tveten
cattle feed intake (kg d^{-1})					–[c]		–[c]
fresh (grass)		60.0		45			
dry	9		9.0	9		9.5	
grain	1						
milk intake rates (L d^{-1})					–[c]		–[c]
adult (male)		0.377	0.377	0.4		0.38	
adult (female)			0.260	0.4		0.59	
child			0.497	1		0.72	
boy (Farm B)	4		4.0	4		4.0	
girl (Farm B)	1		1.0	1		1.0	
vegetable intake rate (kg d^{-1})	–[c]				–[c]		–[c]
adult (male)		0.047	0.047	lettuce 0.03,		0.049	
adult (female)			0.050	spinach 0.03		0.050	
child			0.0072	0		0.018	
inhalation rate (adult male) (m^3 d^{-1})	22	23	23 (2.66×10^{-4} m^3 s^{-1})	24	23.3 (2.7×10^{-4} m^3 s^{-1})	23	–[c]
external dose reduction factor		none	none		none		–[c]
time spent indoors	0.66			0.6		0.3	
shielding factor	0.5			0.1			
inhalation dose reduction factor		none	none		none		–[c]
time spent indoors	0.35–1.0			0.6		0.4	
filtration factor				0.6			

[a] In most cases, values represent either point estimates or the best estimate (e.g., midpoint or mean) of a probability distribution. Ranges are given in a few cases where no midpoint was specified. For more details, see the individual reports by the participants.

[b] The specified ranges were sampled for reactive gas and particulate iodine, with the total limited to 100%; if the total for these two fractions was less than 100%, the difference was assumed to be organic iodine.

[c] The parameter was not used by the participant, or the value was not given in the model description.

TABLE IV. SUMMARY OF VALUES USED FOR DOSE FACTORS

Participant	Dose Factor	Units	Source
External dose to thyroid (cloud)			
Filistovic	1.35×10^{-9}	Sv d^{-1} Bq^{-1} m^3	[4] Kocher, 1980
Homma	5.65×10^{-7}	Sv y^{-1} Bq^{-1} m^3	[4] Kocher, 1980
Kryshev	1.80×10^{-14}	Sv s^{-1} Bq^{-1} m^3	[5] Romanov, 1993
External dose-effective (cloud)			
Krajewski (adult)	1.44×10^{-6}	mSv d^{-1} Bq^{-1} m^3	[6] Jacob et al., 1990
External dose to body surface (cloud)			
Filistovic	3.72×10^{-9}	Sv d^{-1} Bq^{-1} m^3	[4] Kocher, 1980
External dose to thyroid (ground)			
Filistovic	2.87×10^{-11}	Sv d^{-1} Bq^{-1} m^2	[4] Kocher, 1980
Homma	1.32×10^{-8}	Sv y^{-1} Bq^{-1} m^2	[4] Kocher, 1980
Kryshev	3.10×10^{-11}	Sv d^{-1} Bq^{-1} m^2	[5] Romanov, 1993
External dose-effective (ground)			
Krajewski (adult)	2.14×10^{-8}	mSv d^{-1} Bq^{-1} m^2	[6] Jacob et al., 1990
External dose to body surface (ground)			
Filistovic	7.62×10^{-11}	Sv d^{-1} Bq^{-1} m^2	[4] Kocher, 1980
Inhalation dose to thyroid			
Filistovic	3.70×10^{-7}	Sv Bq^{-1}	[7] Johnson, 1981
Homma	2.67×10^{-7}	Sv Bq^{-1}	[8] ICRP, 1979
Kryshev	2.70×10^{-7}	Sv Bq^{-1}	[5] Romanov, 1993
Inhalation dose-effective			
Krajewski (child, 1 year)	7.20×10^{-5}	mSv Bq^{-1}	[9] IAEA, 1996
Ingestion dose to thyroid			
Filistovic	3.70×10^{-7}	Sv Bq^{-1}	[7] Johnson, 1981
Homma	4.35×10^{-7}	Sv Bq^{-1}	[8] ICRP, 1979
Krajewski (child, 1 year)	1.29×10^{-3}	mSv Bq^{-1}	[10] Snyder et al., 1974
Kryshev	4.40×10^{-7}	Sv Bq^{-1}	[5] Romanov, 1993
Ingestion dose-effective			
Krajewski (child, 1 year)	1.80×10^{-4}	mSv Bq^{-1}	[9] IAEA, 1996
External doses			
Kanyár/Nényei			[6] Jacob et al., 1990
Internal doses			
Kanyár/Nényei			[9] IAEA, 1996

3. SUMMARY AND DISCUSSION OF RESULTS

The Hanford scenario was designed to provide several optional starting points and endpoints. In the spirit of a true dose reconstruction, available measurements of ^{131}I concentrations in vegetation and milk were provided in the scenario description. Thus the Hanford scenario did not provide a blind test such as was carried out in the VAMP Multiple Pathways test exercises (Scenarios CB and S). Comparison of model predictions with observations was possible for only a few endpoints (^{131}I concentrations in vegetation and milk, thyroid burdens in two specified individuals). For all other endpoints, model predictions were compared with each other and with the HEDR calculations. The predictions described below were the participants' final predictions following an opportunity for intercomparison of predictions among the participants. All participants made predictions for five test locations (Farm A, Farm B, Mesa, Eltopia, and Pasco; Figure 1); two participants also made predictions for a sixth location (Ringold).

3.1. ATMOSPHERIC TRANSPORT

Several different approaches were used to calculate the atmospheric transport of ^{131}I from the release point (Table II). These varied in complexity from reconstruction of air concentrations from measurements of ^{131}I in air and vegetation made after the release, to simple straight-line models, to complex models using detailed meteorological data from as many as 12 stations. Homma performed two sets of calculations, the first (Approach 1) using data from all 12 meteorological stations and the second (Approach 2) using only the hourly meteorological data at the release site (results from both approaches are shown in the figures).

Napier, Filistovic, and Homma provided contour maps of the air concentrations over the first few days of the release (Figures 2–5). The dispersion patterns predicted by HEDR (Figure 2), Filistovic (Figure 3), and Homma's second approach (Figure 5) were very similar, with the highest air concentrations along a line approximately northwest to southeast with an important southerly component (including Farms A and B) and minimum concentrations at the test sites east of the release (Mesa and Eltopia; Homma had high concentrations for Ringold, also to the east, but his modelled plume did not extend as far as Mesa and Eltopia). Filistovic predicted higher concentrations toward the northwest than did HEDR or Homma; both HEDR and Homma (approach 2) predicted higher concentrations to the far southeast (Pasco). Homma's two approaches produced similar predictions for the test sites south-southeast of the release (Farms A and B), but his first approach (Figure 4) gave lower predictions for Pasco and predicted the highest concentrations for the test sites to the east (Ringold, Mesa, and Eltopia).

Air concentrations at the test locations were not requested as a scenario endpoint, although Filistovic and Homma compared their calculations (both time-dependent and time-integrated) with the observations provided in the scenario description (Annex II). However, modelled air concentrations were used to predict deposition at the specified test sites, so the effects of the atmospheric dispersion modelling are apparent in the predicted values for deposition at the various sites (next section).

3.2. DEPOSITION

Predicted deposition (Bq/m^2) at the specified test sites is shown by site and participant in Figures 6–7. Predictions by different participants vary by a factor of about 5–7 for Farms A and B, while for Mesa, predicted values of deposition vary by about two orders of magnitude (Tveten predicted that the plume never reached Mesa at all, giving zero deposition for that location). HEDR, Filistovic, Kryshev, Kanyár, and Krajewski all predicted the highest deposition for Farms A and B (also Pasco for HEDR) and the lowest for Mesa and Eltopia. Homma (Approach 1) predicted the highest deposition for Mesa, Eltopia, and Ringold (only Homma and Kanyár included predictions for Ringold). In his second set of calculations (Approach 2), Homma had predicted values for Mesa and Eltopia that were more similar to those of other participants and to the HEDR calculations; however, this time he obtained his highest values for Pasco and Ringold, rather than for Farms A and B. Tveten had his highest prediction for Eltopia and his lowest (zero) for Mesa.

Predicted values for deposition at the test sites were dependent on the treatment of atmospheric transport and iodine speciation, as well as deposition itself. Most participants calculated deposition from modelled air concentrations and a dry deposition velocity (Table II). Homma included a washout rate as well as dry deposition, and HEDR included both wet and dry deposition; however, since rainfall was essentially non-existent during the

time period in question, neglect of wet deposition or washout should not have been important. Krajewski reconstructed the deposition from measurements of ^{131}I in vegetation. In most cases, participants used the estimated proportions of reactive gas, particulates, and organic iodine that were given in the scenario description. Most participants used a dry deposition velocity of about 0.01 m/s for gaseous iodine (I_2) (Table III); weighted average deposition velocities ranged from 0.0043–0.013 m/s.

On the whole, however, the treatment of atmospheric transport was the most important factor determining the range of model results for deposition in this exercise. Thus, there seems to have been general agreement about the amount of contamination that reached Farms A and B, south-southeast of the release point. However, there is much less consensus about whether the plume went primarily east (Ringold) and turned south either before or after reaching Mesa and Eltopia, or whether it went more to the southeast (Pasco). Krajewski's calculations, which were based on measured concentrations in vegetation rather than on an atmospheric dispersion model, suggest that deposition in Mesa was higher than predicted by most modelers and that deposition in Eltopia and Pasco was midway between the extreme predictions. Some of Krajewski's estimates were based on very limited sample sizes, however. It should be pointed out that none of the modellers considered terrain effects. The presence of 'coulees' (dry or nearly dry river channels) and other terrain features could have caused some very specific local wind conditions, with a plume either missing an area entirely or being funnelled to a particular location. Thus it is not unreasonable that model predictions may vary an order of magnitude or more in either direction (as was the case for Mesa) from estimates based on measurements.

3.3. ^{131}I CONCENTRATIONS IN VEGETATION

Predictions and observations for time-integrated ^{131}I concentrations in vegetation are shown in Figures 8–10 (confidence intervals on the observations were not available). Predictions for pasture grass ranged from a factor of 15 below to 18 above the observations, depending on the participant and the site. Most participants used a mass interception factor or absorption coefficient to calculate the ^{131}I concentrations on vegetation (Table III); Kanyár and Tveten each used an interception fraction of 0.4. Root uptake was not considered. Values of the mass interception factor or absorption coefficient varied from 1.0–2.8 m^2/kg (dry weight), and the weathering rate constant from about 0.05–0.07 d^{-1}. Estimates of pasture yield varied from 0.3–0.52 kg/m^2 (dry) or 0.12–0.7 kg/m^2 (wet).

In general, the predicted concentrations in grass or hay were driven primarily by the predicted deposition; for each participant, the vegetation (fresh weight)-to-deposition ratio was the same (or nearly so) for all test sites (Figure 11). However, differences in the vegetation-to-deposition ratio among participants varied by a factor of about 14, probably due to different assumptions about the moisture content of the vegetation. Most participants had vegetation-to-deposition ratios of about 3–6, but Kryshev had ratios of about 15 and HEDR about 1.1 (essentially all of the vegetation concentrations by HEDR were underpredicted by about a factor of 3).

3.4. ^{131}I CONCENTRATIONS IN MILK

Predictions and observations for time-integrated ^{131}I concentrations in milk are shown in Figures 12–13 (confidence intervals on the observations were not available). Predictions for milk ranged from a factor of 14 below to 34 above the observations, depending on the

participant and the site. For Mesa, most participants underpredicted, while for Eltopia and Pasco, most overpredicted. The total range of predictions was about a factor of 4.5 for Farms A and B and almost 300 for Mesa. Two participants also predicted time-dependent concentrations of milk for selected dairies; although both sets of predictions were close (factor of 4 or better) to the measurements (Figure 14), too few data were available to permit evaluation of the predicted dynamic behaviour of ^{131}I in commercially produced milk.

Most participants used a milk transfer coefficient of about 0.01 d/L or the equivalent in terms of a more detailed model (Homma and Kanyár); Filistovic used a value of about 0.001 d/L based on site-specific information reported near the time of the release (Soldat, 1963) [3]. Observed milk-to-vegetation (fresh weight) ratios range from 0.04–0.12 (Figure 15); predicted milk-to-vegetation (fresh weight) ratios vary from about 0.05–0.3. For any single participant, the milk-to-vegetation ratios are nearly constant from site to site, thus reflecting differences among participants both in the modelling of milk transfer and in the choice of intake rate of vegetation by cows. Milk-to-deposition ratios varied from about 0.2–1.5 (Figure 16), reflecting the additional differences among modellers in the predicted interception and retention by vegetation.

3.5. INTAKE OF ^{131}I BY HUMANS

Four participants made calculations of the amount of human intake of ^{131}I for reference individuals, either by dairy or by test location (Figure 17). Predicted intakes vary by about a factor of 5 (Carnation) to 30 (Darigold), depending on the predicted sources of milk for each dairy, the predicted concentrations of ^{131}I in milk contributing to each dairy, and the estimated milk consumption rates for men, women, and children (Table III).

3.6. THYROID BURDENS

Thyroid burdens of ^{131}I for two specified individuals at Farm B were calculated by four participants (Figure 18). Comparison with measurements was possible for these two individuals, both of whom were children with higher-than-average milk consumption. Most of the predictions included the measured value within their confidence intervals. The major difficulty with this endpoint is that the measurements were made approximately six weeks after the release, when the thyroid burden was considerably lower than its peak level soon after the release (see figures in Krajewski's report in Annex II). Measurements were in the range of the detection limits, and uncertainties on the measurements were not available.

3.7. DOSE ESTIMATES

3.7.1. External doses (cloud and ground)

Predicted external doses from cloud exposure are shown in Figures 19–20. Predictions varied by a factor of about 20 (Farm B) to 500 (Mesa), depending on the site. The variation is due to differences in predicted air concentrations, adjustments for shielding or time spent indoors, and dose factors. The calculations by Napier (HEDR), Krajewski, and Kanyár included adjustments for shielding and for time spent indoors (Table III). Homma and Kryshev calculated doses to the thyroid (Table IV), Filistovic calculated doses both to the thyroid and to the body surface, and Krajewski and Kanyár calculated effective doses. The differences in

predicted air concentrations at each site are probably more important than differences in shielding factors or dose factors.

Predicted external doses from ground exposure from September 2 to October 1 are shown in Figures 21–22 (predictions for September 2–5 are included in Annex III but are not shown here). Predictions varied by a factor of about 10 (Farm B) to 300 (Mesa). The variation is due to differences in predicted deposition, adjustments for shielding or time spent indoors, and dose factors. The calculations by Napier (HEDR), Krajewski, and Kanyár included adjustments for shielding and for time spent indoors (Table III). As with the doses from cloud exposure, Homma and Kryshev calculated doses to the thyroid (Table IV), Filistovic calculated doses both to the thyroid and to the body surface, and Krajewski and Kanyár calculated effective doses. When the ground exposure doses are normalized for deposition (Figure 23), the dose-to-deposition ratios range from about 5×10^{-8} (HEDR, effective dose, shielding included) to 1×10^{-6} (Filistovic, dose to body surface, no shielding included).

3.7.2. Inhalation doses

Predicted doses to the thyroid of specified individuals from inhalation of ^{131}I are shown in Figures 24–25. Predictions varied by as much as a factor of 2000–3000 (Mesa and Pasco). These differences reflect the predicted air concentrations, reduction for filtering and time spent indoors, inhalation rates (primarily adults vs. children), and dose factors. The calculations by Napier (HEDR), Krajewski, and Kanyár included adjustments for filtering and for time spent indoors (Table III). Filistovic, Homma, and Kryshev calculated doses to the thyroid (Table IV), while Krajewski and Kanyár calculated effective doses. The lowest calculated doses represent effective doses to a reference child (1 year old), with adjustment for filtering and time spent indoors. The highest doses represent doses to the thyroid of an adult with no adjustment for filtering or time spent indoors. However, the differences in predicted air concentrations at each site are probably more important overall than differences in filtration factors, inhalation rates, or dose factors.

3.7.3. Ingestion doses

Predicted doses to the thyroid of reference individuals from ingestion of ^{131}I are shown in Figures 26–27, along with predictions for specified children at Farm B (Figure 28). Predictions for Farm B ranged from about 5×10^{-3} mSv for an adult to 0.26 mSv for a reference child (Figure 27). The predicted doses to the two specified children at Farm B were higher (up to 0.45 mSv), in accordance with the higher milk intakes of these children. The ingestion doses were based primarily on ingestion of milk, although some participants also included a contribution from leafy vegetables (Table III). The highest doses were obtained for the specified individuals (real children) at Farm B (Figure 28), due both to the high deposition at Farm B and the exceptionally high milk intake of these children. In most cases, predicted doses for the children at Farm B were in good agreement with the doses predicted for these children by HEDR.

As expected from the results obtained for the scenario midpoints (^{131}I concentrations in vegetation and milk), the ingestion dose-to-deposition ratio across sites is nearly constant for a given participant (Figure 29). However, the value of this ratio varies from about 10^{-4} to 10^{-3}, depending primarily on whether the participant calculated doses for a child or an adult, and whether a different (higher) dose factor was used for children (Table IV). The ingestion dose-

to-deposition ratio also reflects differences in calculated milk and vegetable concentrations and estimated ingestion rates.

3.7.4. Total dose

Predictions of total dose from all pathways are shown in Figures 30–31. Most participants submitted estimates of total doses for each test site. For the others, best estimates of total dose were calculated for this discussion by adding the best estimates of doses submitted for each exposure pathway. In all cases, the ingestion dose was the major contributor to the total dose. This is expected for ^{131}I, both because of the importance of the iodine-milk pathway and because the half-life of ^{131}I is too short for it to be a major concern with respect to external exposure.

4. MAJOR FACTORS AFFECTING MODEL PREDICTIONS

Measurements for use as test data were available for only a few endpoints, and these measurements were not ideally suited for model testing purposes (i.e., either they were not entirely representative of the test locations or the sample sets were incomplete). The available measurements also did not always include the time periods in which the peak concentrations probably occurred. In addition, participants had access to most of the available measurements from the beginning of the test exercise. For these reasons, this exercise did not include blind testing of model predictions. On the other hand, this exercise was representative of an actual dose reconstruction in that the existing data, whatever their limitations, were available for use in calculations or in calibration of models.

This test exercise did provide an opportunity to compare predictions made with the same information using several different approaches for atmospheric transport modelling as well as a range of approaches to various parts of the terrestrial transport modelling. It is encouraging that most dispersion models gave results similar to those obtained by Krajewski, who started with measurements of air and vegetation concentrations. It is also apparent that complex models do not necessarily perform better than simpler models. In general, atmospheric dispersion models based on a wide grid will not necessarily predict well for specific point locations, especially as the distance to a target site increases or in situations such as this with complex terrain effects.

Compensatory effects (a high prediction in one model compartment being offset by a low prediction in another compartment) were quite common in this test exercise. The participants with the highest predicted deposition for a site did not necessarily have the highest predictions for milk concentrations or doses, depending on the approach and parameter values used for other parts of the calculation. As is seen in the comparisons of normalized predictions (Figures 11, 15–16, 23, 29), the ratio of two endpoints may vary considerably among participants (e.g., a factor of 10 for ingestion dose-to-deposition). This situation reflects differences in the state of knowledge about the various processes or parameter values. In an actual dose reconstruction, the state of knowledge about various processes or parameter values should be reflected in terms of detailed rationales for the approach or for the selection of key parameter values, as well as in the estimates of uncertainty about the predictions.

5. UNCERTAINTY ESTIMATION

Several approaches were used by participants to estimate uncertainties in their model predictions (Table II). HEDR, Filistovic, Homma, and Kanyár used Monte Carlo approaches for estimation of uncertainties in their model predictions (Their parameter values in Table III represent the midpoints or means of their parameter distributions). Krajewski used error propagation based on uncertain parameter values. Kryshev used professional judgment to apply an uncertainty factor to his predictions. Major sources of uncertainty include atmospheric transport (which could contribute as much as a factor of 20–50), representativeness of available measurements, iodine speciation, treatment or neglect of terrain effects, actual consumption and metabolic rates, and dosimetry for actual individuals; these latter sources of uncertainty are minor in comparison to the uncertainty in the atmospheric transport calculations.

6. CONCLUDING REMARKS

The Hanford scenario described a short-term atmospheric release of ^{131}I and served as the basis for calculations of atmospheric transport, deposition, and doses to humans from external and internal exposure pathways. Radioiodine releases are important for most radiation accidents (large and small). Because data on the results of these releases are often incomplete, models for estimating ^{131}I transport and exposure are essential in dose reconstruction efforts. The Hanford scenario has therefore provided a valuable opportunity to intercompare model predictions among several assessors and to compare model predictions with data, albeit incomplete data.

Most of the attention by this group of participants was focused on the atmospheric transport part of the scenario, and several different approaches were used to estimate transport and deposition at several specified locations. The primary exposure pathway in terms of contribution to human doses was ingestion of contaminated milk and vegetables. Predicted mean doses to the thyroid of reference individuals from ingestion of ^{131}I ranged from 0.0003 mSv (lower bound for an adult at Pasco) to 0.8 mSv (upper bound for a child at Farm B). Predicted doses to actual children with high milk consumption at Farm B ranged from 0.006 to 2 mSv. The predicted doses varied with location (specifically the predicted deposition at each location) and the receptor (adult vs. child). The predicted deposition at any given site (central value or best estimate) varied among participants by a factor of 6–7 up to about 2 orders of magnitude, depending on the site. The predicted ingestion doses for children, normalized for predicted deposition, varied by about a factor of 10 among participants, reflecting differences in approaches or selection of parameter values for the deposition-to-dose calculations.

Overall, the Hanford scenario provided an excellent opportunity to compare a number of modelling approaches to a single assessment problem, in a dose reconstruction context. Several major points and recommendations can be made from the experience.

First, in many if not most dose reconstruction situations, the data available are incomplete or imperfect. Modelling must often be carried out to determine the quantities (e.g., contaminant concentrations) needed in the dose assessment. However, when data are available, they should be used, either as part of the calculational approach or as a check on the validity of the calculations. In addition, uncertainties about the model inputs or parameter values should be large enough to allow for inadequacies, incompleteness, or uncertainties in the data.

Secondly, when several assessors are given the same starting information, considerable variability in the predicted endpoints may be expected. This may occur due to different approaches (e.g., different model types or different interpretations of the scenario) to part or all of the assessment problem, different choices of parameter values, or different adjustments for site-specific conditions. In addition, misunderstanding of the scenario or errors in coding or units conversion can lead to different results obtained by different individuals (even when efforts are made to reduce mistakes). Comparison of results among several assessors provides an opportunity to explain discrepancies (e.g., the predicted values of deposition at Mesa) and correct problems. At the same time, the fact that similar, although not necessarily identical, results were obtained by several assessors using a variety of approaches permits a greater level of confidence in the overall results of this assessment. To the extent possible, an assessment should include adequate time for evaluation of model calculations, as well as opportunities for comparison of predictions with available data and with predictions made by independent assessors.

Finally, inclusion of uncertainty estimates for model predictions is essential for describing the level of confidence that should be placed in a prediction. In a dose reconstruction, the uncertainty estimates should reflect the amount and quality of data that were available to the assessment as well as the state of knowledge (or lack of knowledge) about various components of the assessment.

Text cont. on page 43.

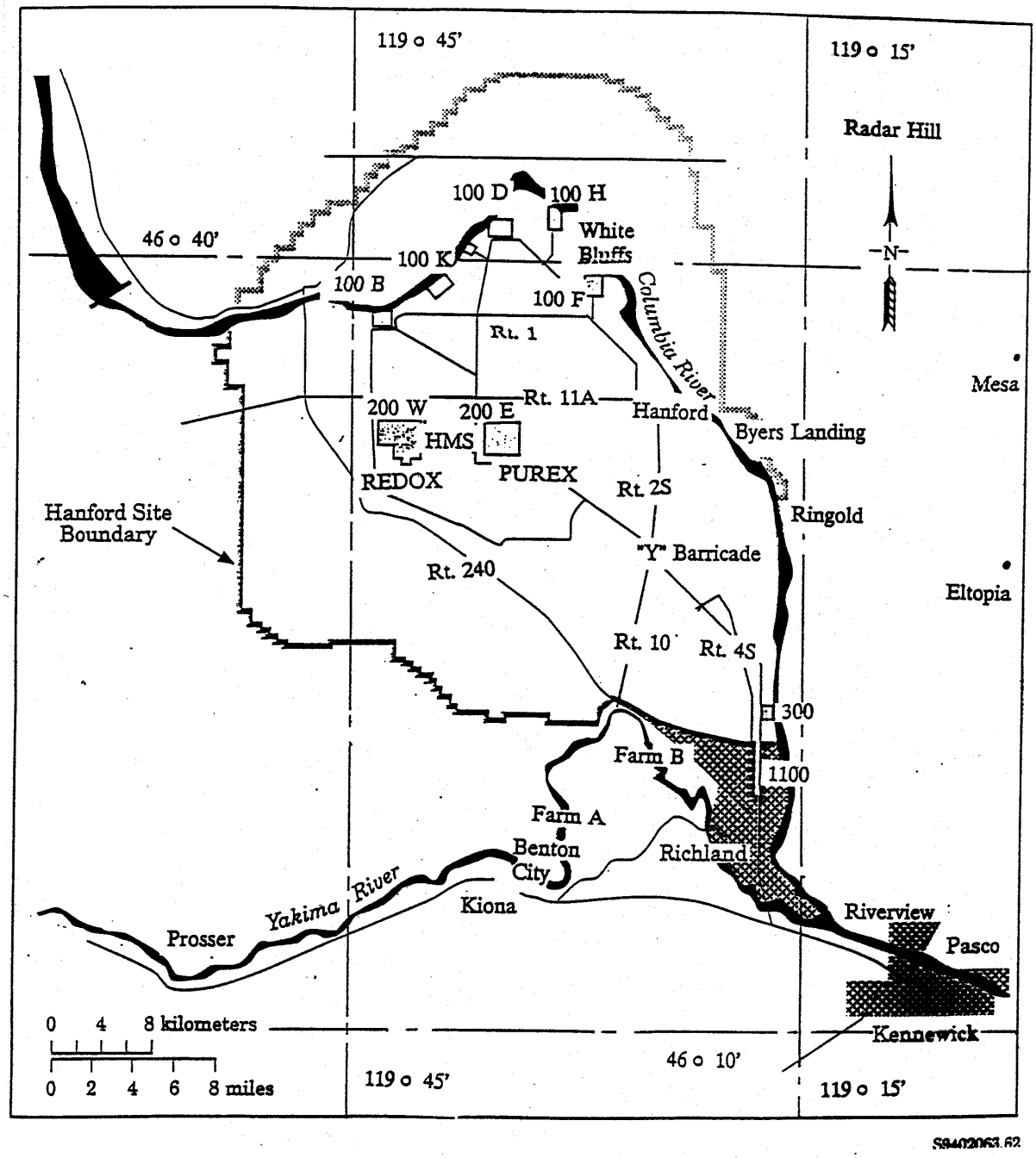

FIG. 1. Map of the Hanford site. The release originated at the Purex plant (PUREX). The Hanford Meteorological Station (HMS) is adjacent. Test locations included Farm A, Farm B, Mesa, Eltopia, Pasco and Ringold.

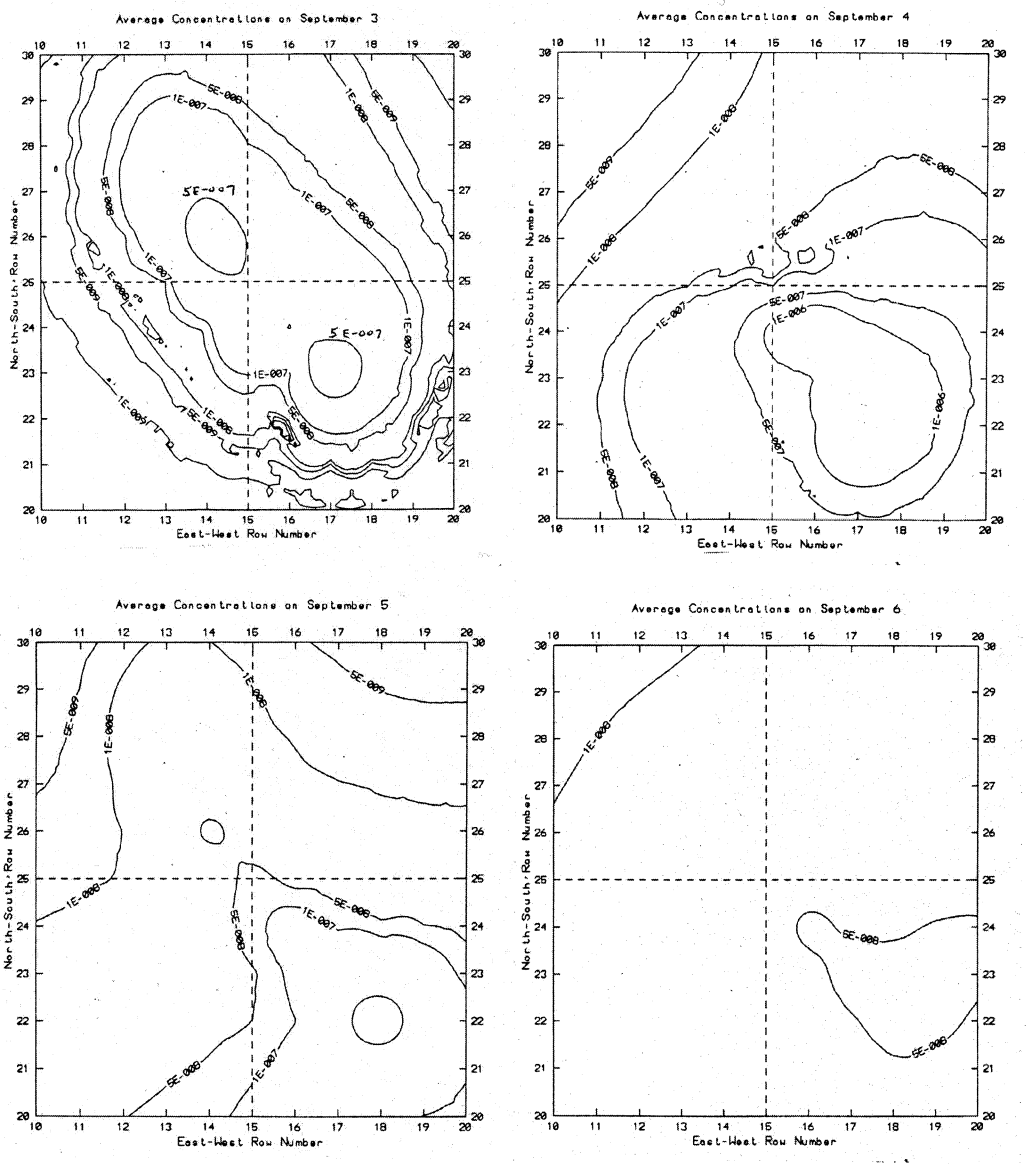

FIG. 2. Predicted time-integrated concentrations of ^{131}I in air (Ci s m^{-3}) from Napier (HEDR). Upper left, 3 September; upper right, 4 September; lower left, 5 September; lower right, 6 September.

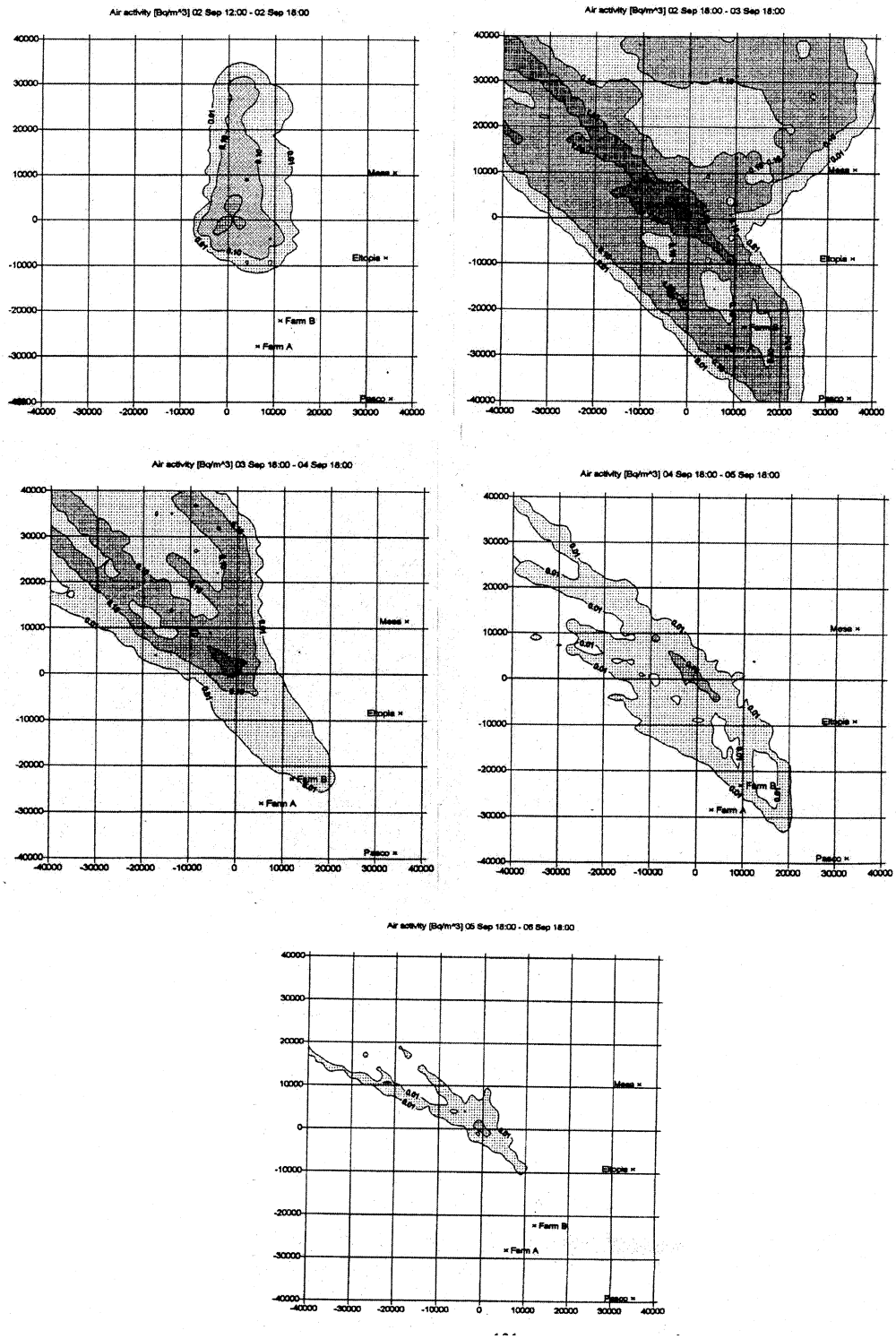

FIG. 3. Predicted average concentrations of ^{131}I in air (Bq m^{-3}) from Filistovic. Upper left, 2 September, 12:00–18:00; upper right, 2 September 18:00 to 3 September 18:00; centre left, 3 September 18:00 to 4 September 18:00; center right, 4 September 18:00 to 5 September 18:00; bottom, 5 September 18:00 to 6 September 18:00.

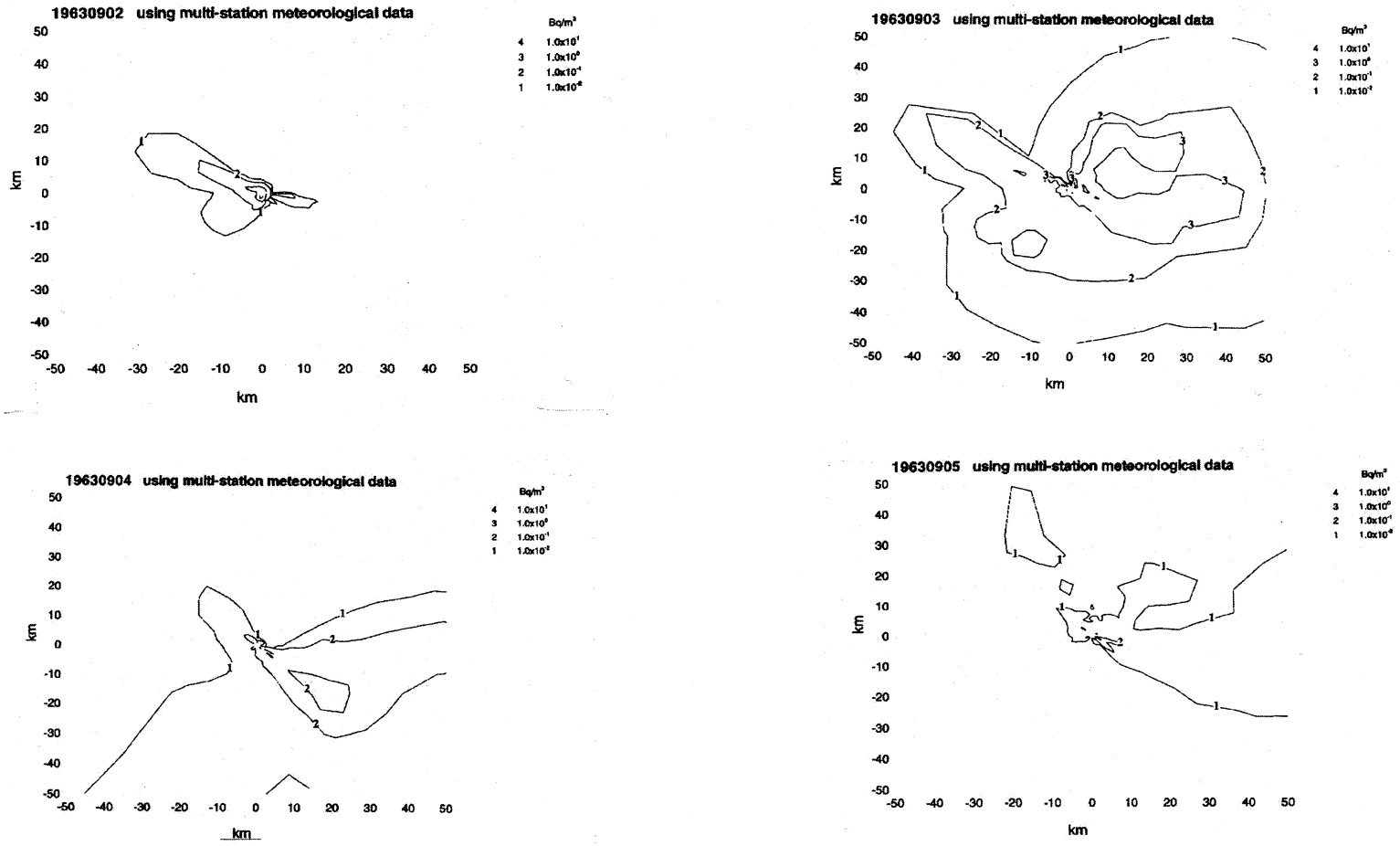

FIG. 4. Predicted average concentrations of ^{131}I in air (Bq m^{-3}) from Homma, Approach 1 (data from all 12 meteorological stations). Upper left, 2 September; upper right, 3 September; lower left, 4 September; lower right, 5 September.

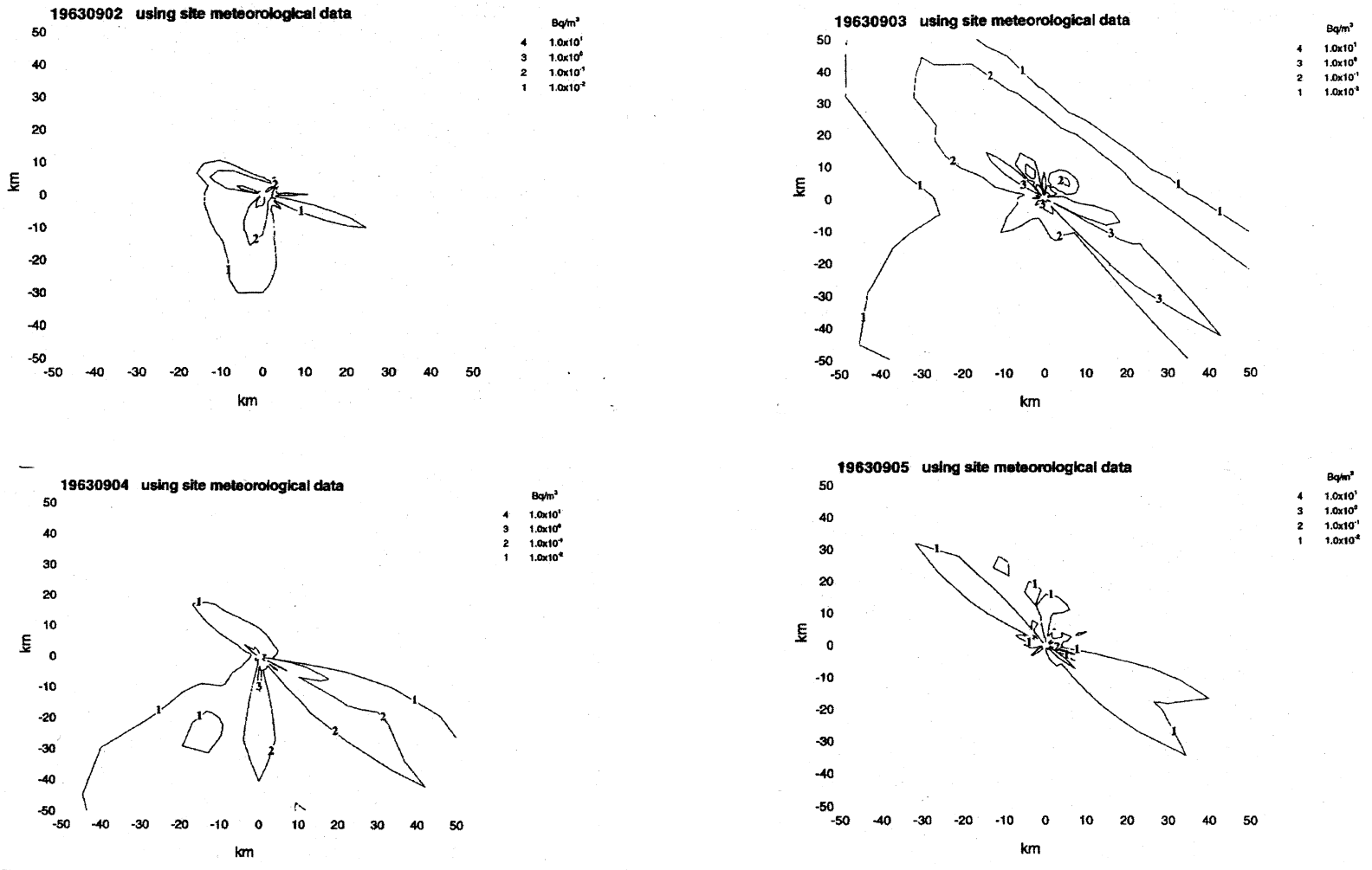

FIG. 5. Predicted average concentrations of ^{131}I in air (Bq m^{-3}) from Homma, Approach 2 (data from only one meteorological station). Upper left, 2 September; upper right, 3 September; lower left, 4 September; lower right, 5 September.

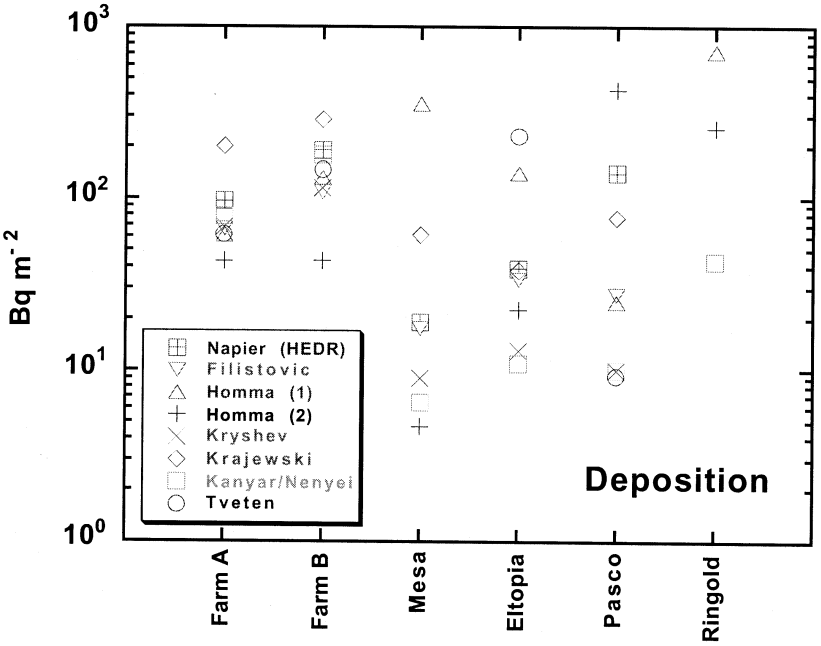

FIG. 6. Comparison of model predictions for the mean deposition of ^{131}I at six sites near Hanford. Uncertainties on the model predictions are not shown.

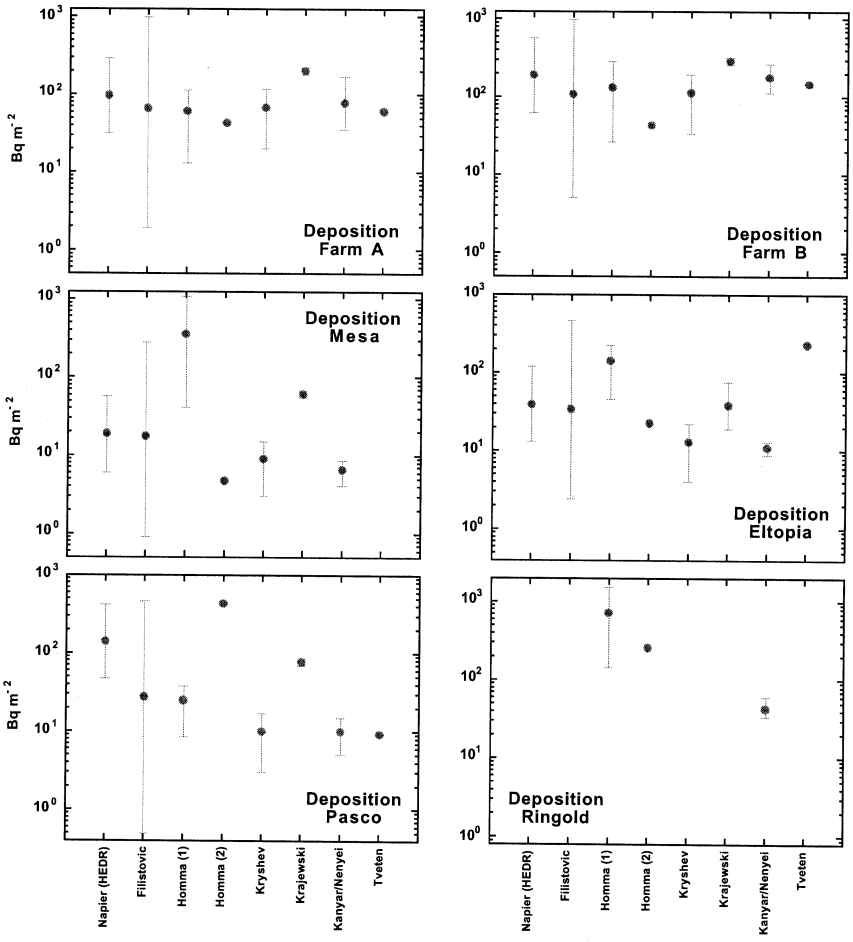

FIG. 7. Comparison of model predictions for the mean deposition of ^{131}I at six sites near Hanford. Vertical lines indicate the uncertainties on the model predictions.

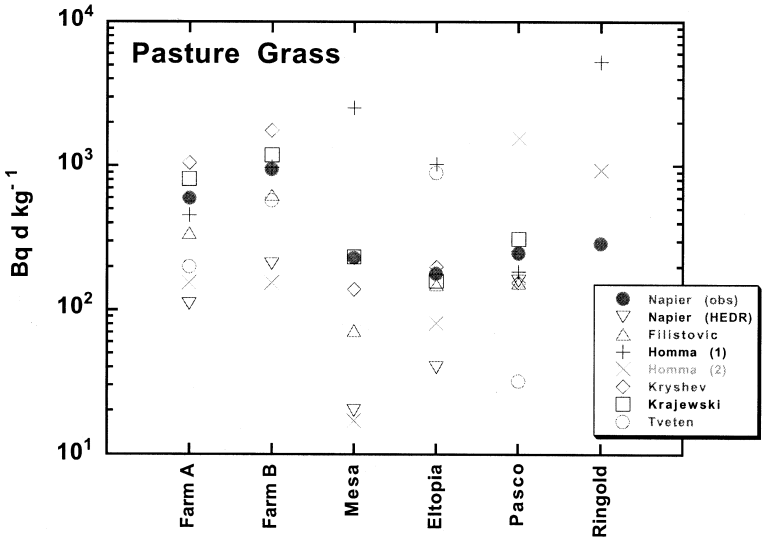

FIG. 8. Comparison of measured (dark circles) vs. predicted mean time-integrated concentrations of ^{131}I on pasture grass at six sites near Hanford. Uncertainties on the model predictions are not shown.

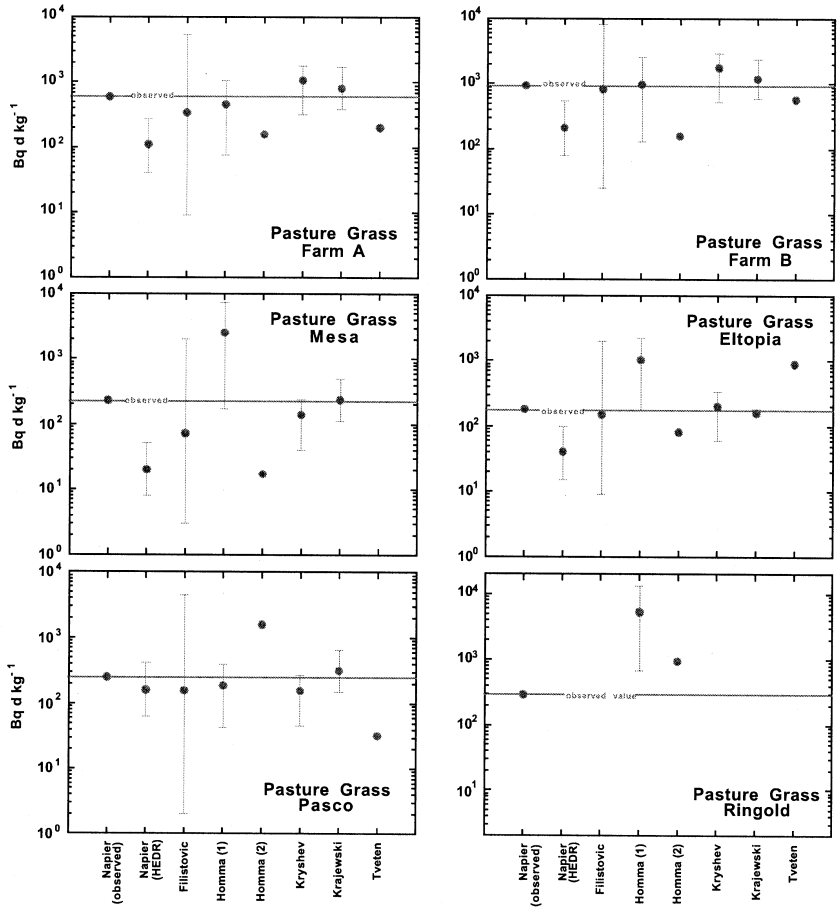

FIG. 9. Comparison of measurements (horizontal line) and model predictions for mean time-integrated concentrations of ^{131}I on pasture grass at six sites near Hanford. Vertical lines indicate the uncertainties on the model predictions. Uncertainties on the measurements are not available.

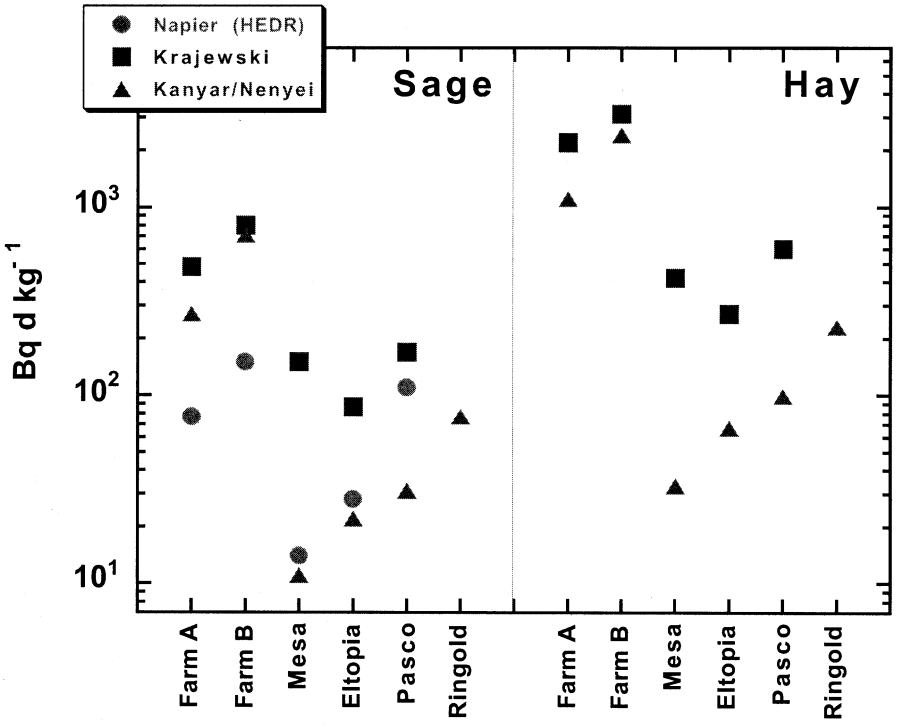

FIG. 10. Comparison of predicted mean time-integrated concentrations of ^{131}I on sage or hay at six sites near Hanford. Uncertainties on the model predictions are not shown.

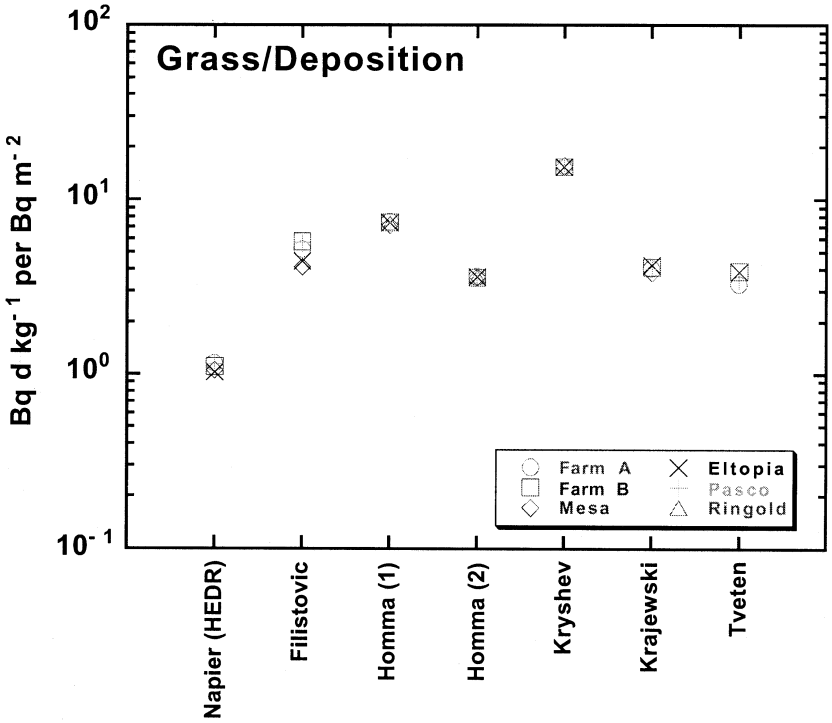

FIG. 11. Comparison of model predictions for mean time-integrated concentrations of ^{131}I on pasture grass at six sites near Hanford, normalized for predicted mean deposition at each site.

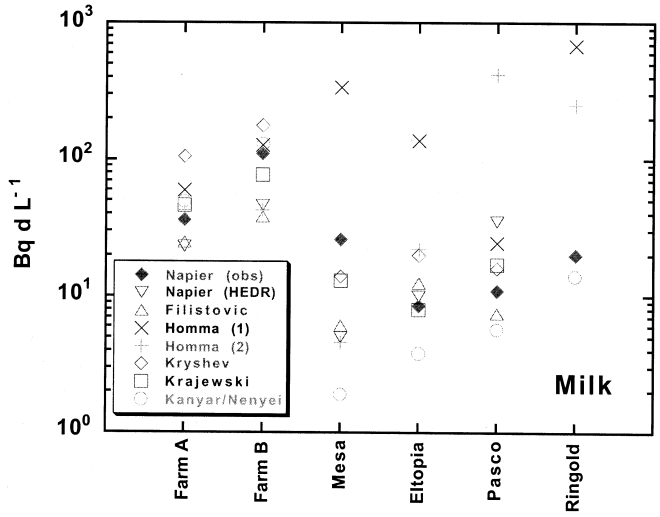

FIG. 12. Comparison of measured (dark diamonds) vs. predicted mean time-integrated concentrations of ^{131}I in milk at six sites near Hanford. Uncertainties on the model predictions are not shown.

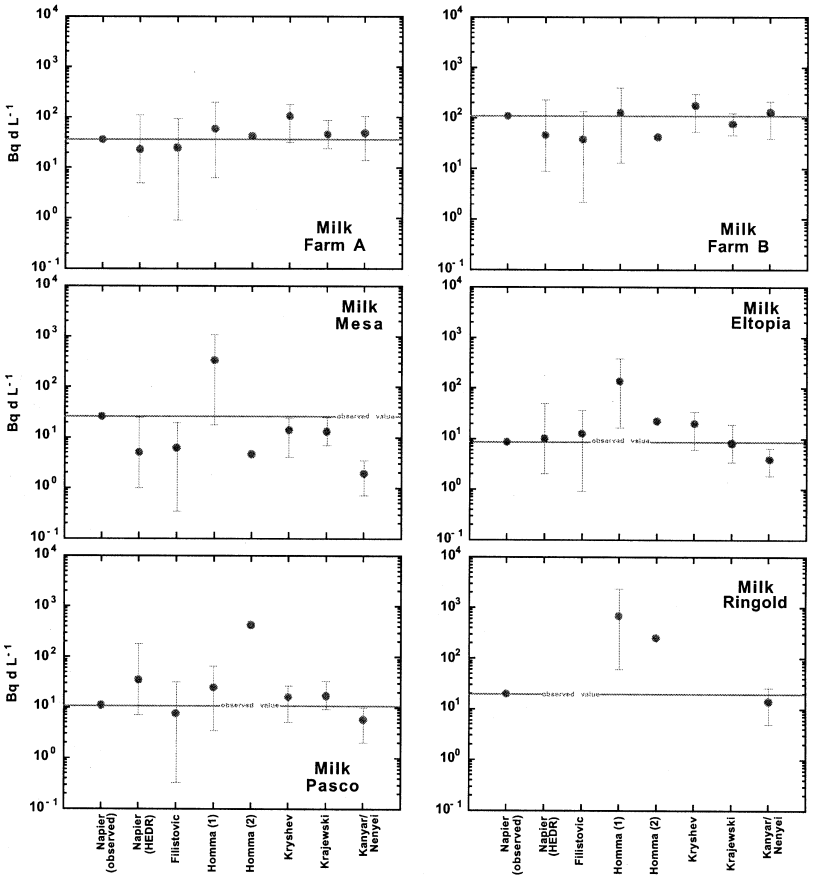

FIG. 13. Comparison of measurements (horizontal line) and model predictions for mean time-integrated concentrations of ^{131}I in milk at six sites near Hanford. Vertical lines indicate the uncertainties on the model predictions. Uncertainties on the measurements are not available.

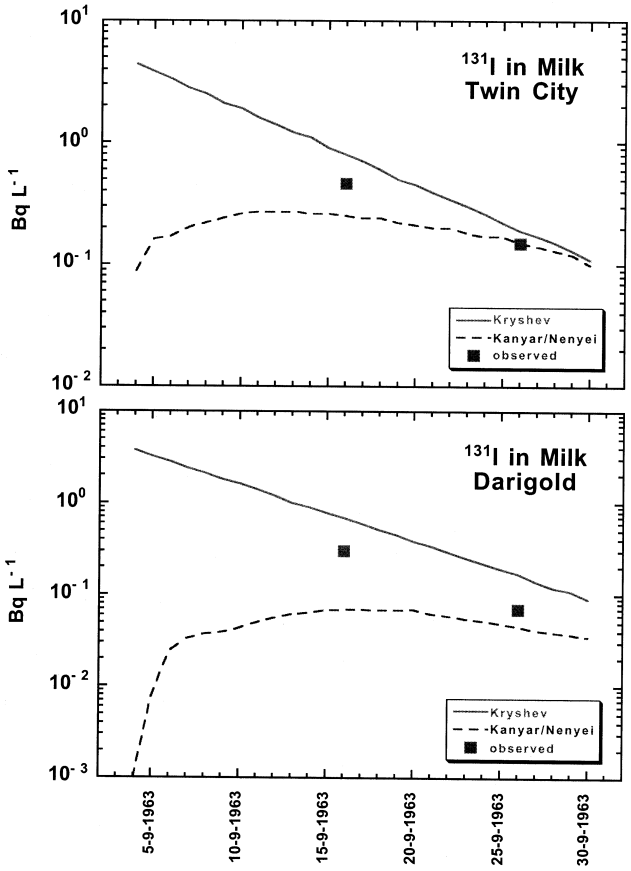

FIG. 14. Predicted concentrations of ^{131}I in milk at two dairies during the period 4–30 September 1963.

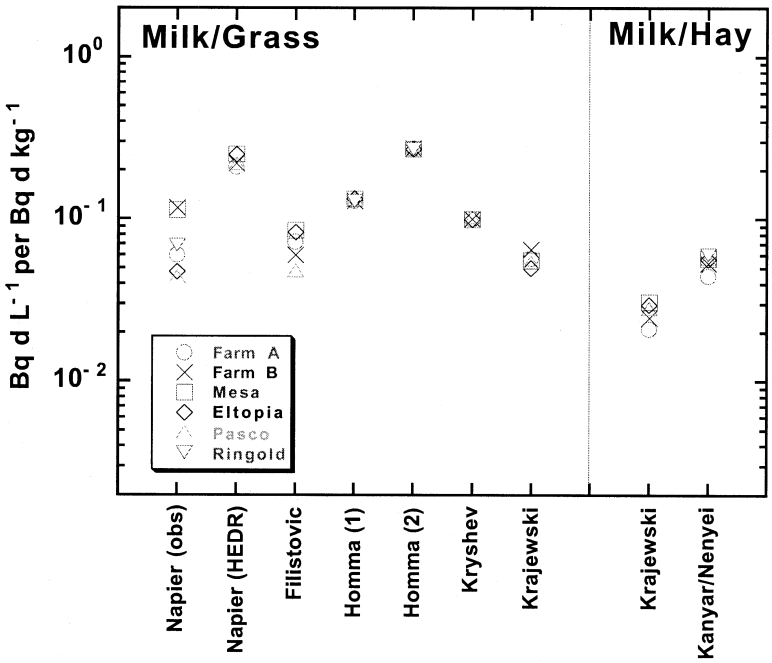

FIG. 15. Comparison of model predictions for mean time-integrated concentrations of ^{131}I in milk at six sites near Hanford, normalized for predicted mean time-integrated concentrations of ^{131}I in pasture grass or hay at each site.

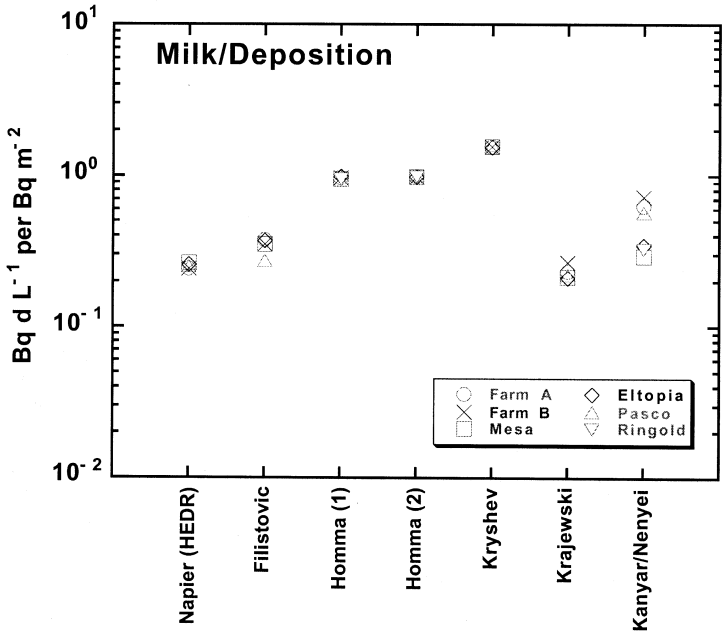

FIG. 16. Comparison of model predictions for mean time-integrated concentrations of ^{131}I in milk at six sites near Hanford, normalized for predicted mean deposition at each site.

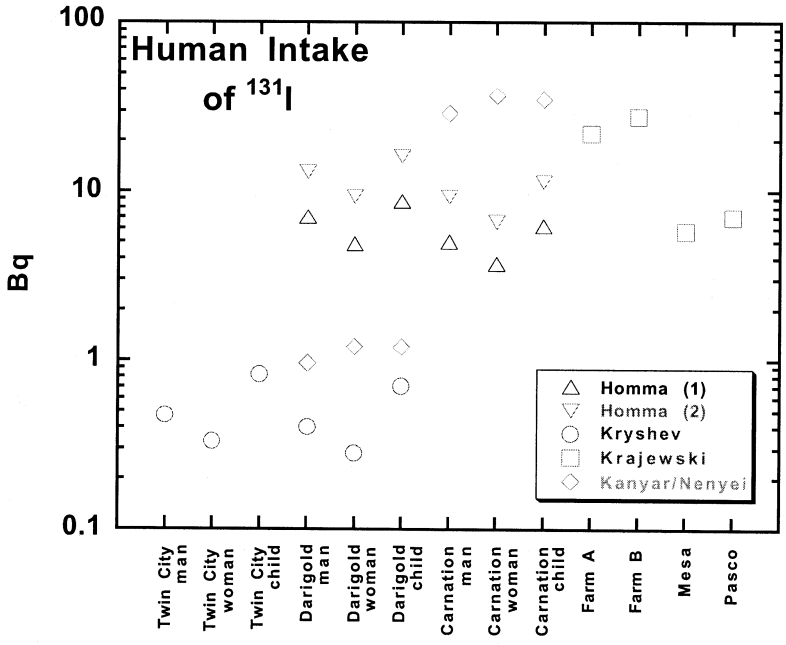

FIG. 17. Predicted total intake of ^{131}I by reference individuals, by either dairy or location. Uncertainties on the predictions are not shown.

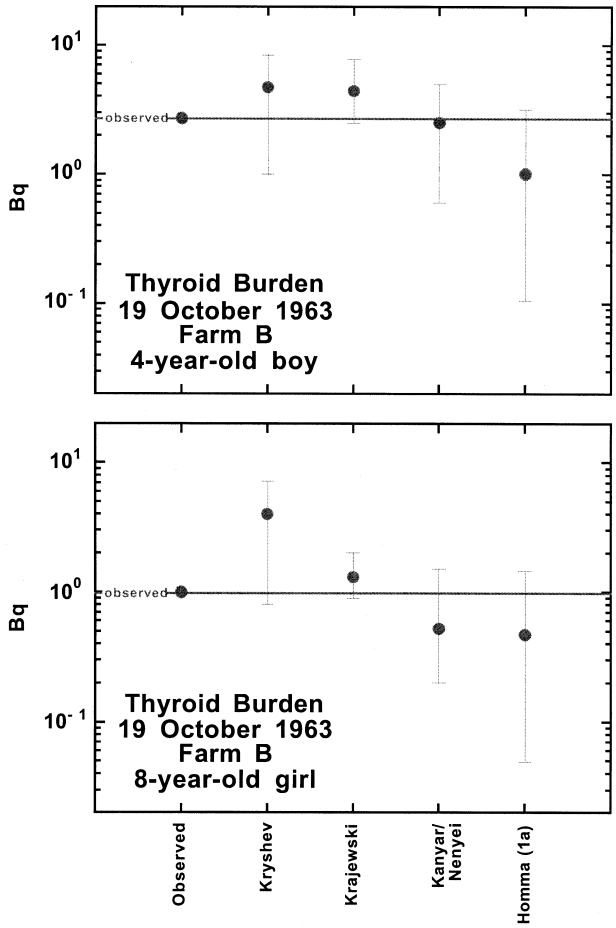

FIG. 18. Comparison of measured (horizontal lines) and predicted thyroid burdens of ^{131}I for two children at Farm B on 19 October 1963. Vertical lines indicate uncertainties on the model predictions. Uncertainties on the measurements are not shown.

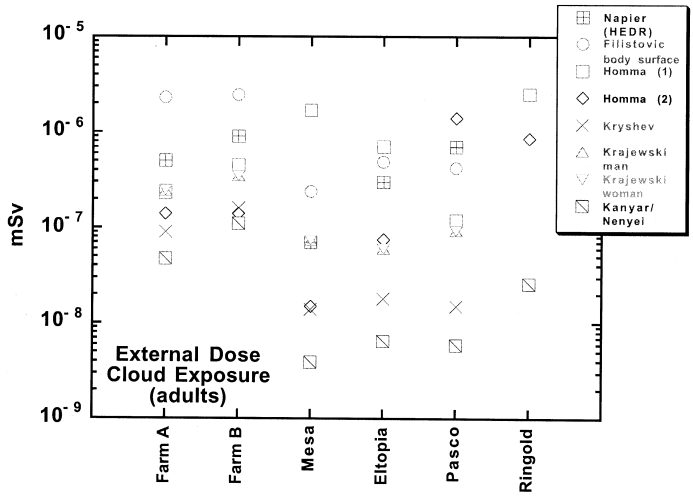

FIG. 19. Comparison of model predictions for mean external doses from cloud exposure to ^{131}I for reference adults at six sites near Hanford. Uncertainties on the model predictions are not shown.

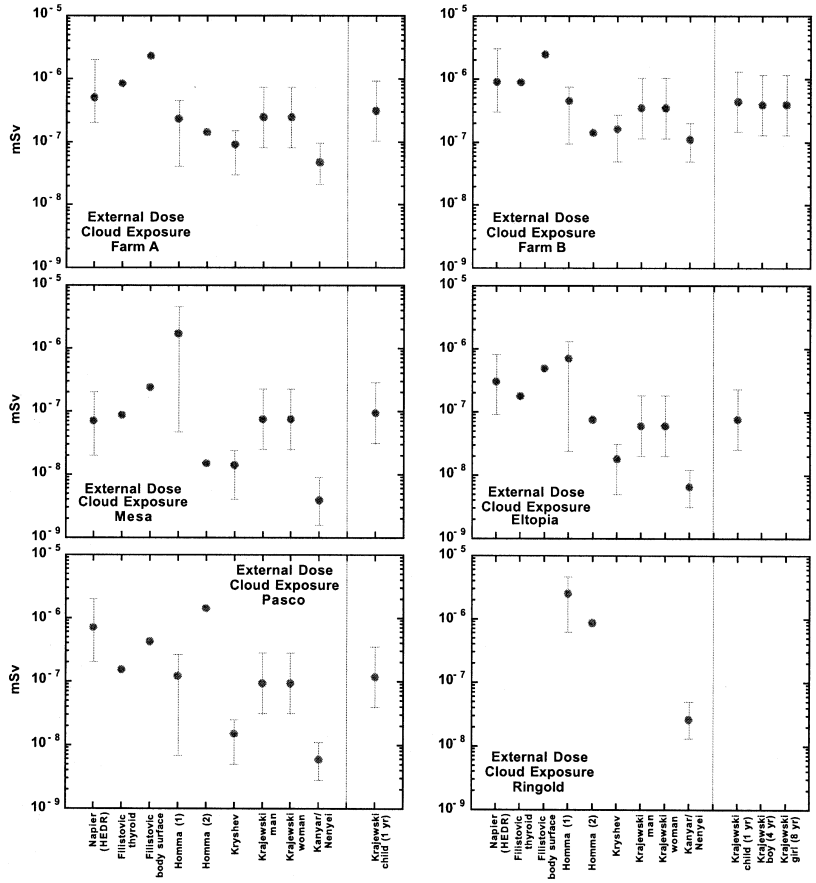

FIG. 20. Comparison of model predictions for mean external doses from cloud exposure to ^{131}I for specified individuals at six sites near Hanford. Vertical lines indicate the uncertainties on the model predictions.

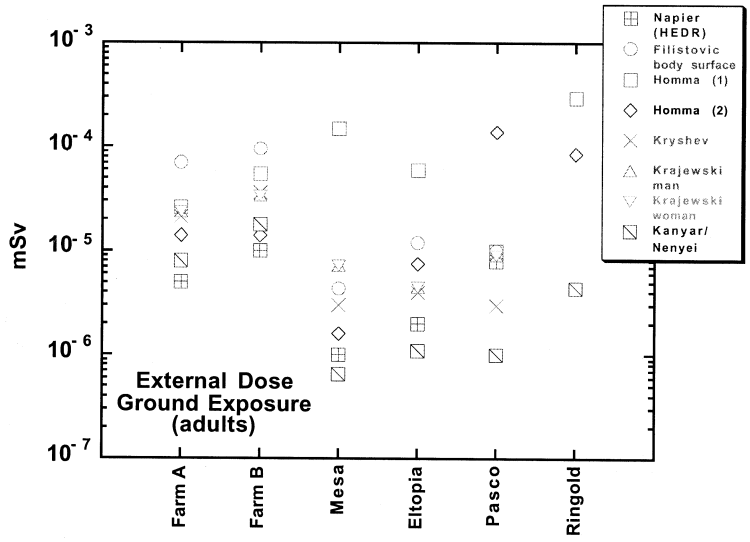

FIG. 21. Comparison of model predictions for mean external doses from ground exposure to ^{131}I for reference adults at six sites near Hanford (2 September to 1 October). Uncertainties on the model predictions are not shown.

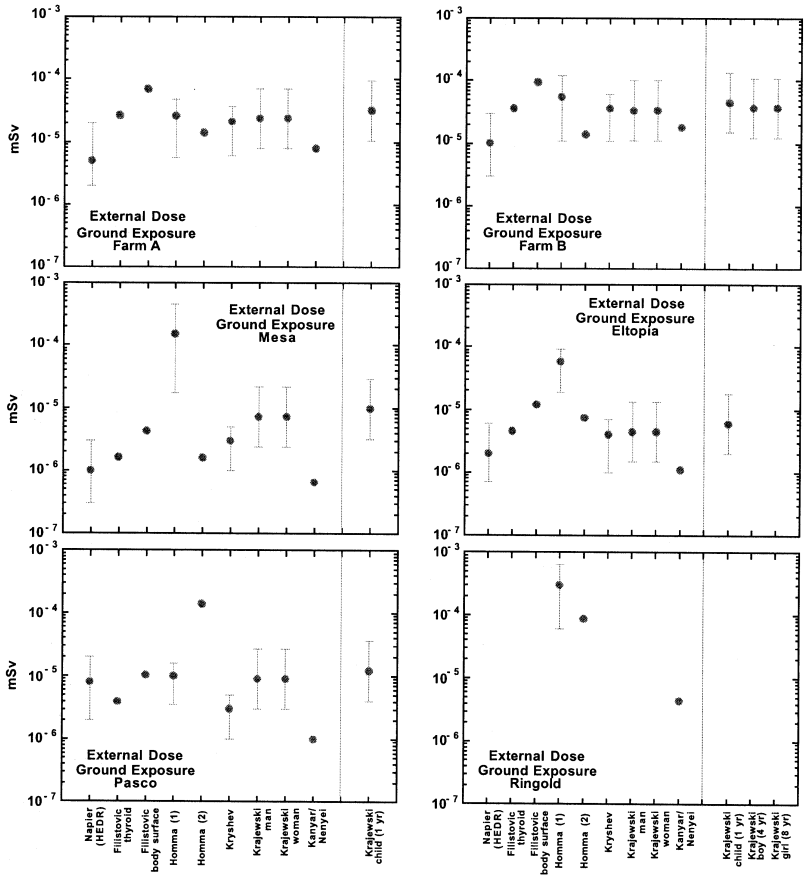

FIG. 22. Comparison of model predictions for mean external doses from ground exposure to ^{131}I for specified individuals at six sites near Hanford (2 September to 1 October). Vertical lines indicate the uncertainties on the model predictions.

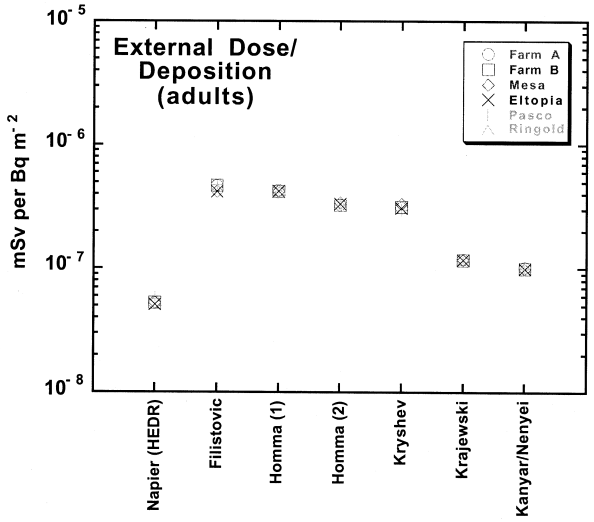

FIG. 23. Comparison of model predictions for mean external doses from ground exposure to ^{131}I for reference adults at six sites near Hanford, normalized for predicted mean deposition at each site.

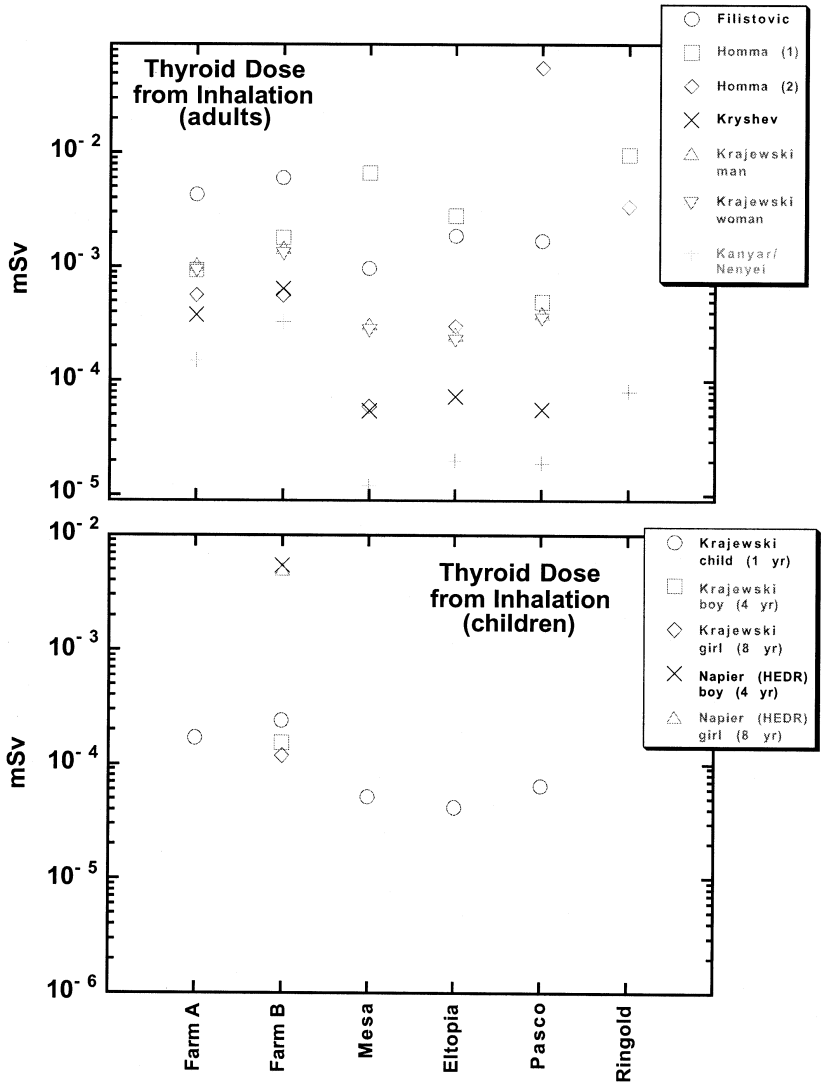

FIG. 24. Comparison of model predictions for mean doses to the thyroid from inhalation of ^{131}I for specified adults (top) and children (bottom) at six sites near Hanford. Uncertainties on the model predictions are not shown.

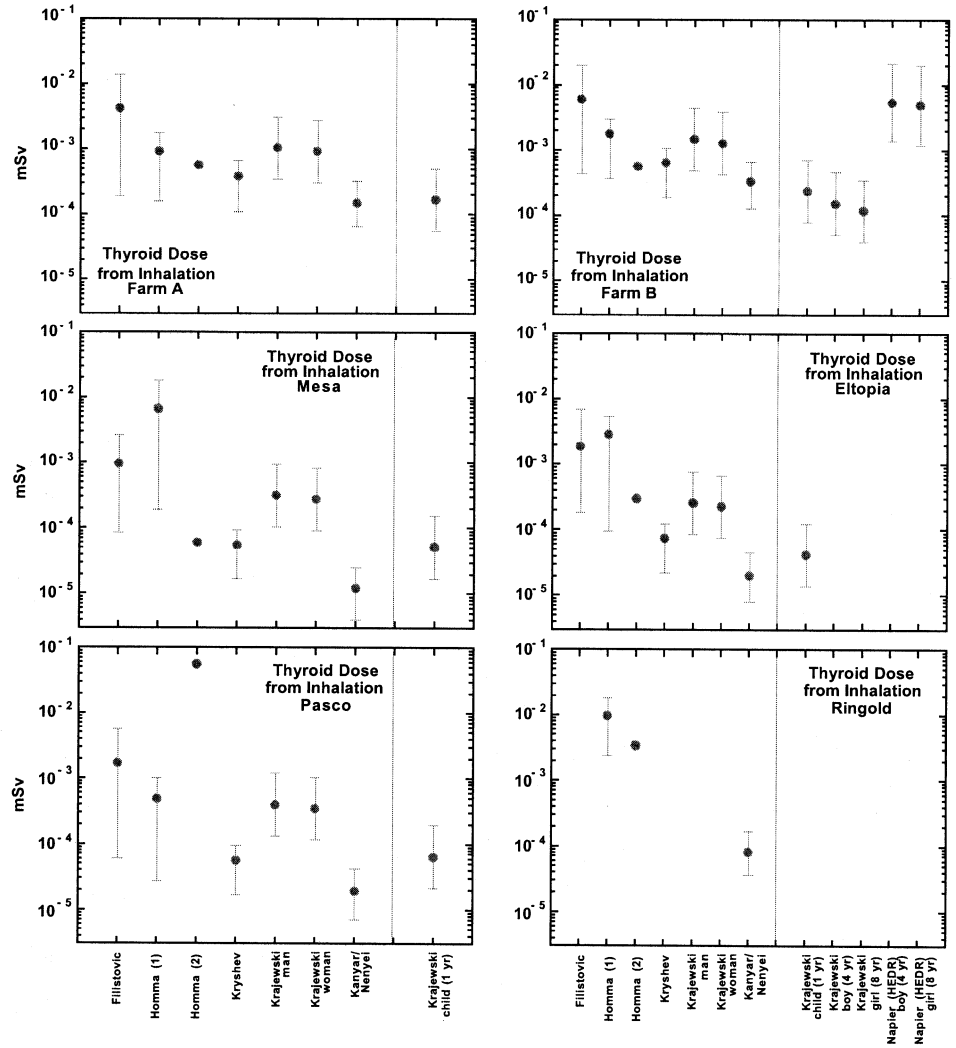

FIG. 25. Comparison of model predictions for mean doses to the thyroid from inhalation of ^{131}I for specified individuals at six sites near Hanford. Vertical lines indicate the uncertainties on the model predictions.

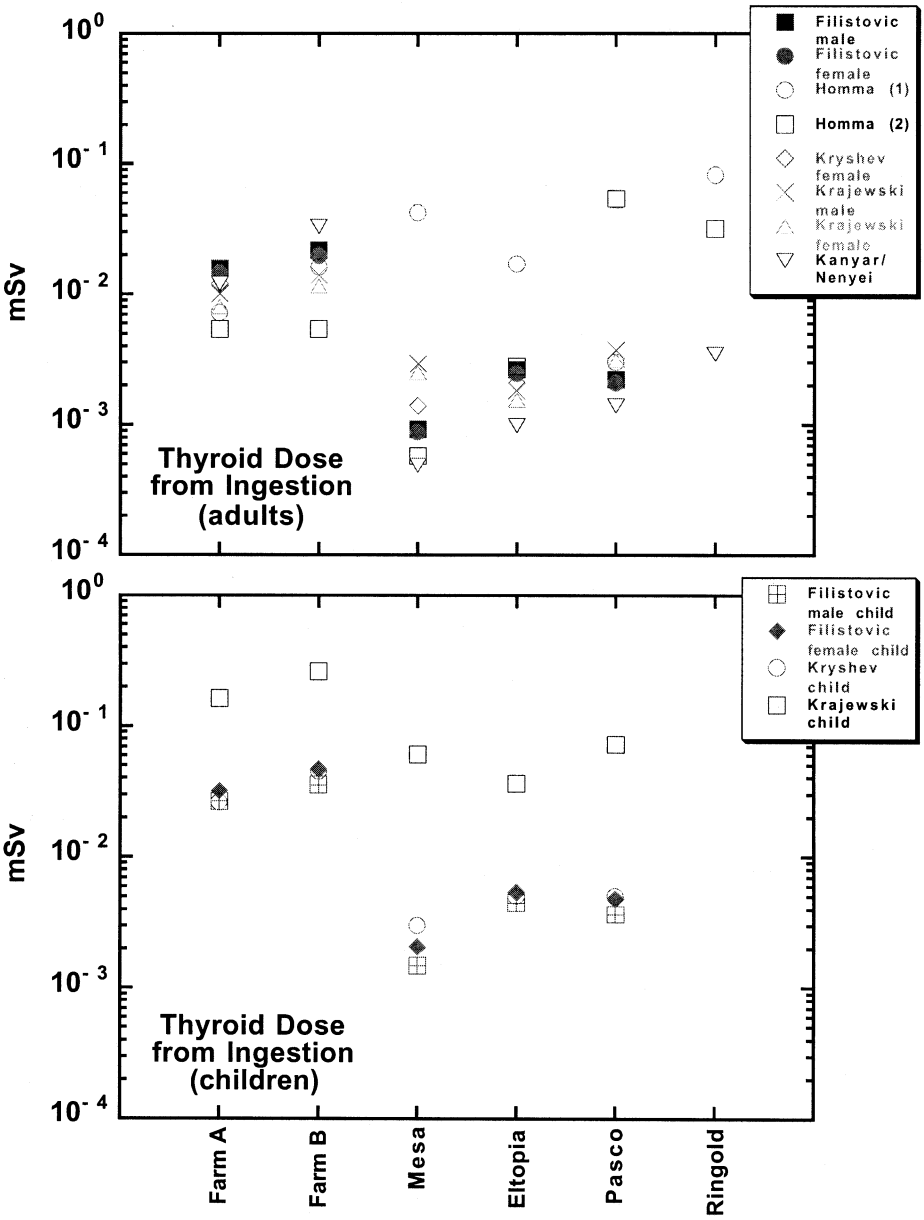

FIG. 26. Comparison of model predictions for mean doses to the thyroid from ingestion of ^{131}I for reference adults (top) and children (bottom) at six sites near Hanford. Uncertainties on the model predictions are not shown.

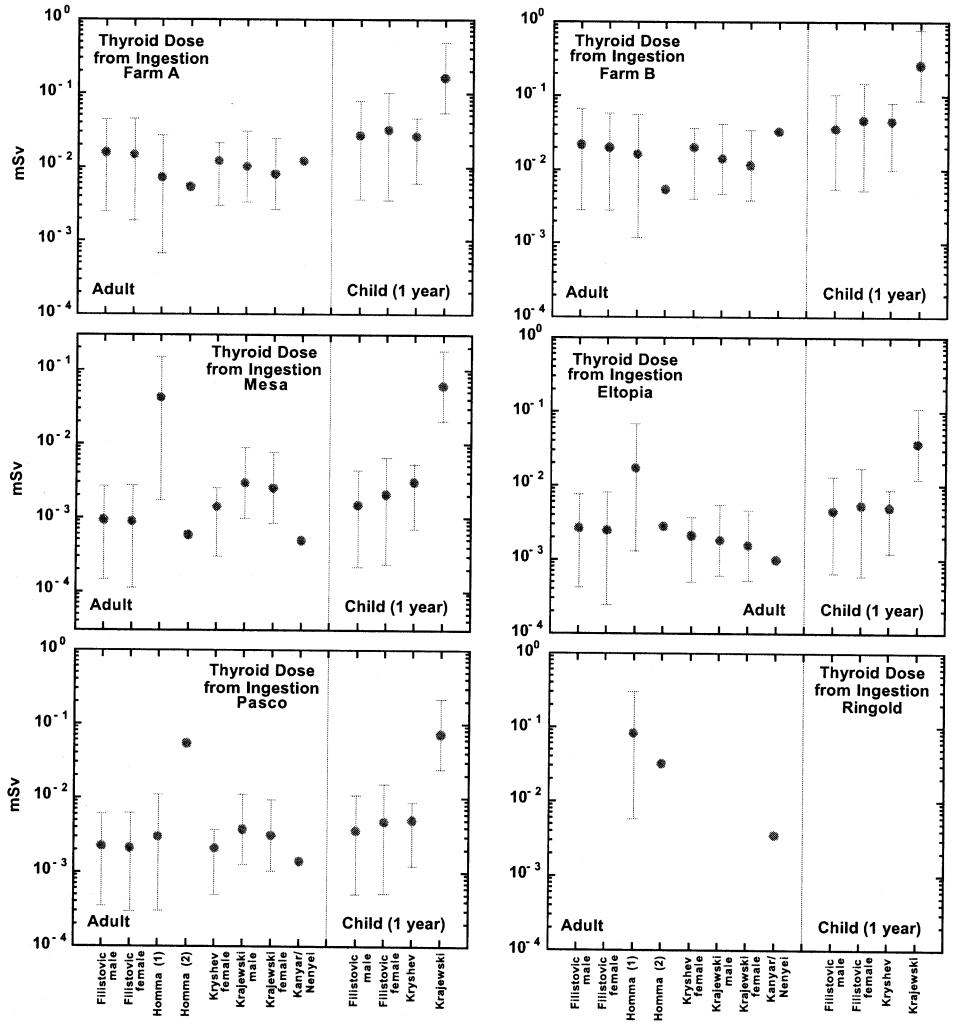

FIG. 27. Comparison of model predictions for mean doses to the thyroid from ingestion of ^{131}I for reference individuals at six sites near Hanford. Vertical lines indicate the uncertainties on the model predictions.

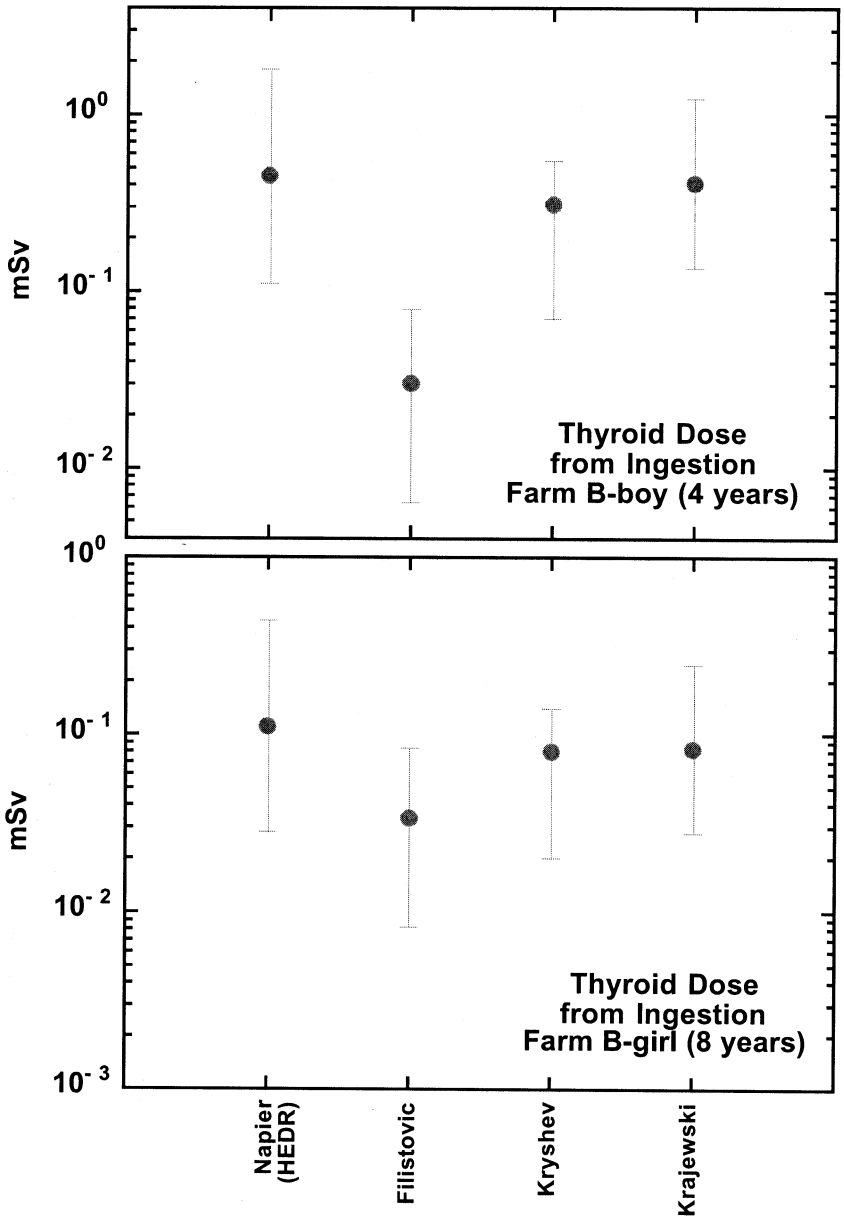

FIG. 28. Comparison of model predictions for mean doses to the thyroid from ingestion of ^{131}I for specified children at Farm B. Vertical lines indicate the uncertainties on the model predictions.

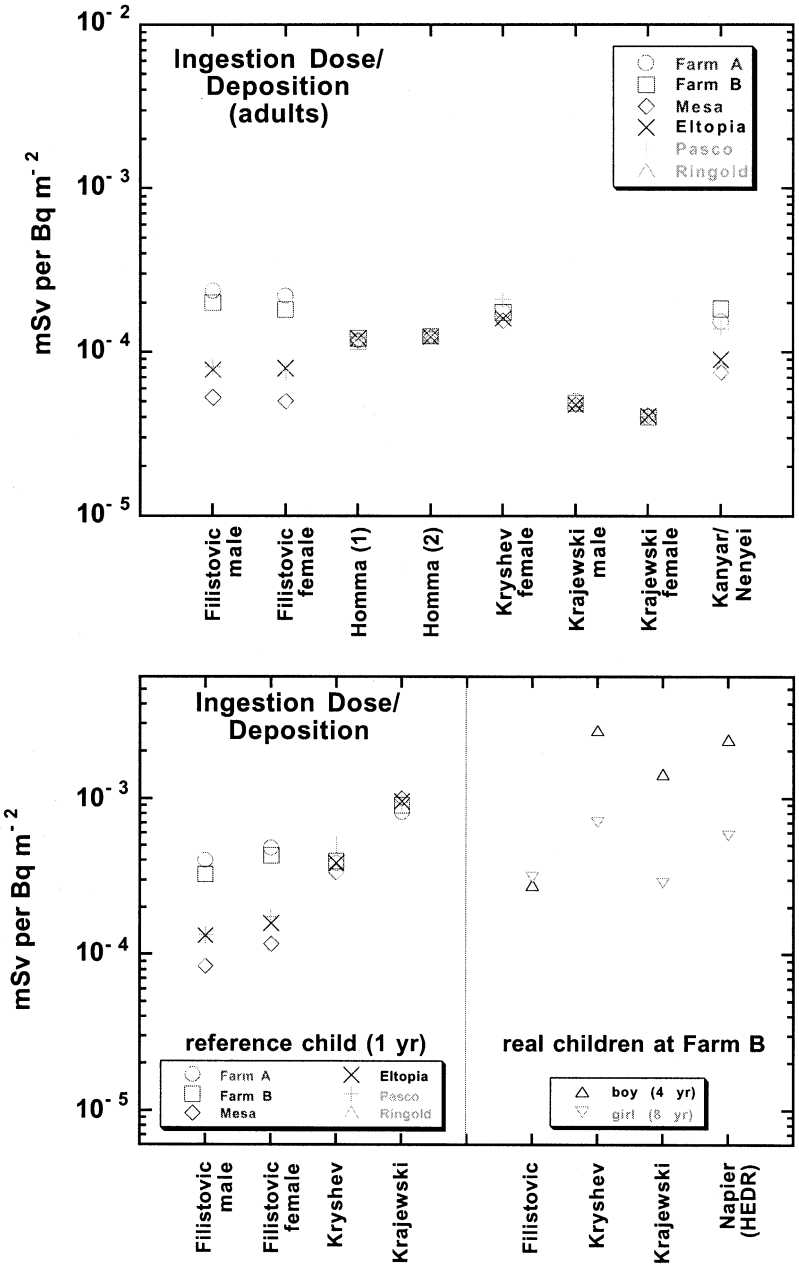

FIG. 29. Comparison of model predictions for mean doses to the thyroid from ingestion of ^{131}I for selected real and reference individuals at six sites near Hanford, normalized for predicted mean deposition at each site.

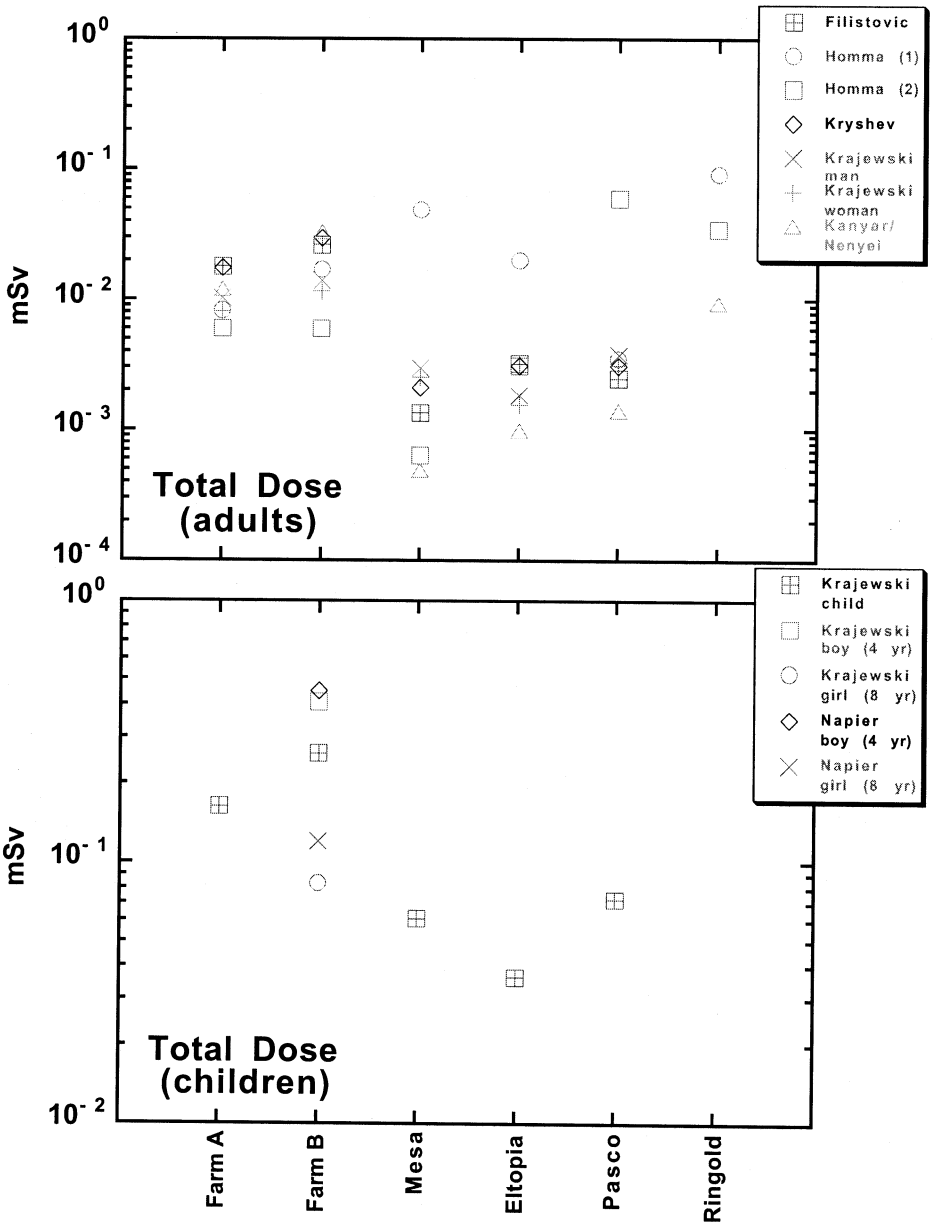

FIG. 30. Comparison of model predictions for mean total dose from ^{131}I for specified adults (top) and children (bottom) at six sites near Hanford. Uncertainties on the model predictions are not shown.

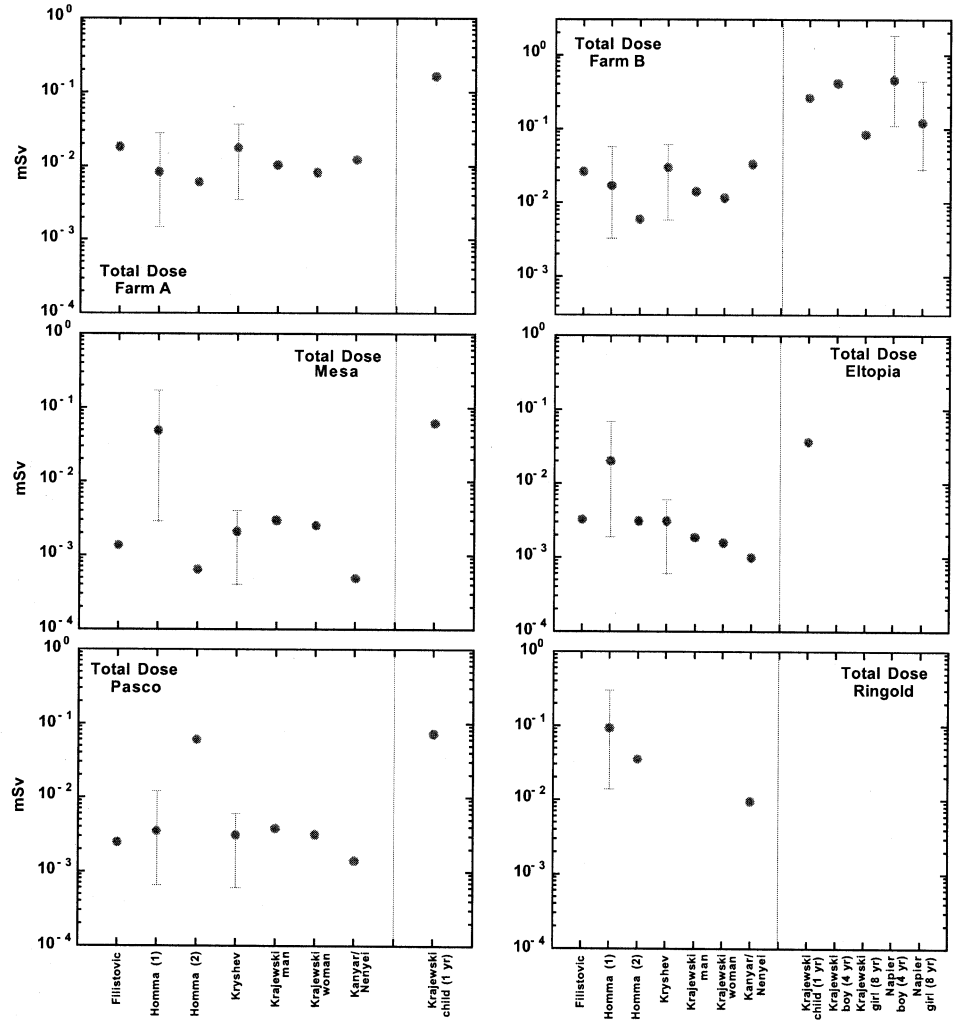

FIG. 31. Comparison of model predictions for mean total dose from ^{131}I for specified individuals at six sites near Hanford. Vertical lines indicate the uncertainties on the model predictions.

REFERENCES

[1] SOLDAT, J.K., Environmental evaluation of an acute release of ^{131}I to the atmosphere, Health Phys. 11 (1965) 1009–1015.

[2] FARRIS, W.T., NAPIER, B.A., IKENBERRY, T.A., SIMPSON, J.C., SHIPLER, D.B., Atmospheric Pathway Dosimetry Report 1944–1992, Hanford Environmental Dose Reconstriction Project, PNWD-2228 HEDR, Battelle, Pacific Northwest Labs, Richland (1994).

[3] SOLDAT, J.K., The relationship between ^{131}I concentrations in various environmental samples, Health Phys. 9 (1963) 1167–1171.

[4] KOCHER, D.C., Dose-rate conversion factors for external exposure to photon and electron radiation from radionuclides occurring in routine releases from nuclear fuel cycle facilities. Health Phys. 38 (1980) 543–633.

[5] ROMANOV, G.N., 'Elimination of Consequences of Radiation Accidents', Guide Book. Moscow, Nuclear Society International (1993).

[6] JACOB, P., ROSENBAUM, H., PETOUSSI, N., ZANKL, M., Calculation of organ doses from environmental gamma rays, Part II. GSF-Bericht 12/90, Forschungszentrum für Umwelt und Gesundheit, Neuherberg, (1990).

[7] JOHNSON, J.R., Radioiodine dosimetry, J. Radioanalytical Chem. 65 (1981) 223–238.

[8] INTERNATIONAL COMMISSION ON RADIOLOGICAL PROTECTION, Limits for intake of radionuclides by workers. ICRP Publication No. 30, Pergamon Press, Oxford (1979).

[9] INTERNATIONAL ATOMIC ENERGY AGENCY, International Basic Safety Standards for Protection against Ionizing Radiation and for the Safety of Radiation Sources, Safety Series No. 115, IAEA, Vienna (1996).

[10] SNYDER, W.S., FORD, M.R., WARNER, G.G., WATSON, S.B., A tabulation of dose equivalent per microcurie-day for source and target organs of an adult for various radionuclides, ORNL-5000, Oak Ridge National Laboratory, (1974).

ANNEX I

SCENARIO DESCRIPTION

I–1. INTRODUCTION

The following set of data and information has been collected to assist the validation of radiological assessment models. The test scenario is an inadvertent acute release of ^{131}I to the environment from the Hanford Purex Chemical Separations Plant stack that occurred on September 2–5 1963. Monitoring data were collected in nine counties in the northwestern US over the two-month period following this release.

Details of the site are given in Section 1 of this report and are not repeated here as a result.

I–2. INPUT INFORMATION

An acute, inadvertent release of ^{131}I from the 60 m stack of a nuclear chemical separations plant (centrally-located on the 1450 km^2 Hanford Site) occurred beginning 2 September 1963. Laboratory analyses of stack effluent samples were made. These were provided as a possible starting point for calculations in Table I–II. The routine program of environmental surveillance was augmented with additional sampling. Measurements of wind velocity and temperature were made routinely at the site meteorology tower. Similar data from additional weather stations within a few hundred kilometres were also made available.

No significant rainfall occurred in the region in the few weeks following the release, and no protective measures were taken following the release. No atmospheric nuclear test explosions occurred in the several month period prior to this event. Routine atmospheric releases of ^{131}I prior to and following this event were of the order of 4×10^9 Bq/month (0.1 Ci/month), or less.

I–2.1. Iodine chemical form

The iodine released was essentially 100% molecular (I_2). It is believed that the iodine quickly partitioned into particulate, reactive gaseous, and organic phases. Equilibrium partitioning between these phases is assumed to be approximately 25% particulate (5–25%), 40% reactive gas (20–60%), and the rest organic (Ramsdell et al., 1994) [1].

I–2.2. Meteorological data

Tabular data of meteorological observations taken at the Hanford Meteorological Station (HMS) are provided in Tables I–III and I–IV and Figure 32. These, and additional data from other nearby stations, were made available in similar format in electronic form (Table I–I).

All meteorological data are hourly observations. The observations were taken at the start of each hour and represent the conditions at that time. Wind speeds and directions, temperatures, and other data recorded represent the conditions at that time only, not an hourly average.

TABLE I–I. ADDITIONAL METEOROLOGICAL DATA AVAILABLE IN ELECTRONIC FORMAT

Station Name	Latitude	Longitude	Meas. Ht.	Sfc Roughness
Hanford, WA	46.563	119.598	30.5	0.05
Walla Walla, WA	46.100	118.283	6.1	0.10
Baker, OR	44.833	117.817	10.4	0.20
Burns, OR	43.583	119.050	20.7	0.10
Dallesport, WA	45.617	121.150	6.1	0.20
Lewiston, ID	46.383	117.017	12.2	0.20
Moses Lake, WA	47.183	119.333	3.7	0.05
Pendleton, OR	45.683	118.850	6.1	0.10
Redmond, OR	44.267	121.150	9.5	0.10
Spokane, WA	47.667	117.333	12.2	0.30
Stampede Pass, WA	47.283	121.333	8.8	1.00
Yakima, WA	46.567	120.533	6.1	0.20
Hanford, WA	46.563	119.598	30.5	0.05

Notes:

(1) All latitudes are north and longitudes are west.
(2) Wind measurement height is in meters
(3) Surface roughness (z_0) is in meters
(4) Release point (PUREX stack) 46.549N, 119.517W
(5) Release height 60.5 m
(6) Stack radius 1.067 m
(7) Stack flow 56.63 m^3/s
(8) Effluent temperature ~25°C
(9) Meteorological data format (1x,i2,i3,i2,1x,2i2,1x,i3,1x,12(2i2,2i1))
(10) The first 3 fields contain the last 2 digits of the year, the day of the year (1-365), and the hour of the observation (0-23). The next 2 fields contain the wind direction (16 pt compass) and wind speed (miles per hour) measured at Hanford at the release height. The next field is the ambient air temperature at the release height in tenths of a degree F (650 = 65.0). Then come 12 fields containing surface level wind, stability, and precipitation data. The data in the 2i2,2i1 groups are, in order, wind direction, wind speed, Pasquill-Gifford-Turner stability class (1-7) in place of (A-G)...1=A, and precipitation class. Precipitation classes are 0 = none, 1 = light liquid precip (rain or drizzle), 2 = moderate liquid precip, 3 = heavy liquid precip, 4 = light frozen precip (snow), 5 = moderate frozen precip, 6 = heavy precip, and 8 and 9 are missing data. We use the US National Weather Service definitions of light (0.1 mm/hour), moderate (3 mm/hour), and heavy (5 mm/hour) to go to precipitation rates. All wind directions are given in a 16 pt compass with 0 or 16 used for north, 4 for east, etc. Calms and variable are indicated by 17 and 18, and 88 and 99 indicate missing data. Wind speeds for all stations except Hanford are in knots (nautical miles per hour). Hanford winds are in miles per hour. The order of the stations in the record is the same as in the list above.
(11) The measurements in the file are hourly averages. The hourly averages are assigned to the beginning of the hour. (Note that the meteorological data in the tables on the following pages are assigned to the end of the hour.)

I–2.3. Measurements of ^{131}I in the environment

Measurements of ^{131}I in samples of vegetation and milk were performed in the area surrounding the Hanford site. The sampling location codes and their geographical positions are given in Table I–V. The system used to define locations of air sample measurements is explained in Section I–2.3.2.

I–2.3.1. Vegetation samples

Increased vegetation sampling was begun on 2 September and continued for the next week. Sampling of grass and milk was extended up to 100 km Southeast of the release point. The

maximum off-site activity concentration in vegetation (of 13 pCi/g) was measured in a sample of green hay from a farm 32 km SSE of the release point where no cattle were being grazed. Maximum on-site vegetation contamination was found within 3 km of the stack.

The values provided in Table I–VI are those historically recorded (with the units updated to modern S.I. usage). The measurements were made and a counting room background was subtracted before the results were recorded. In some instances, this results in a negative value being recorded. This indicates that the value was below the detection level of the instrumentation at the time. That lower limit is not known.

I–2.3.2. Air samples

Twenty-two permanent atmospheric monitoring stations were maintained in the Hanford environs. Equipment installed in these stations included an 'HV-70' brand filter and a caustic scrubber in series. These permanent air sampling stations were supplemented by several temporary caustic scrubber and charcoal cartridge samplers during September 1963. The concentrations provided in Table I–VII are daily values obtained by averaging the result (dividing) evenly over the varying sampling periods, with no decay correction.

The particulate filter was about 99.8% efficient for 3 μm size particles, and the caustic solution was reported to capture "most" of the elemental iodine, but it would have been inefficient with organic forms.

Air sample measurements are provided in Table I–VII. Locations are given notations such as 100 BSE or 200 EWC. These notations refer to positions at the Hanford Site operating areas, in these examples the 100 B and 200 E Areas. These operating areas are shown in Figure 1 of this report. The additional designation refers to locations along the outer fence of these areas; '100 BSE' means that the sampler was located at the eastern end of the southern fence of the 100 B Area, while '200 EWC' indicates that the sampler was located at the centre of the western fence of the 200 E Area. For areas without this type of notation, the sampler can be considered to be near the centre of the designated area. Detailed latitude and longitude descriptors of all sample locations are also provided.

I–2.3.3. Milk samples

Routine milk collection in 1963 included daily to weekly samples from seven local dairy farms, two milk shed composites twice per month, and three commercial brands of milk twice per month. Spot sampling at several other dairy farms brought the total number of farms where milk and grass were sampled up to fifteen during the month of September 1963. Milk measurement data are provided in Table I–VIII.

Darigold creamery processes milk from the east of the Hanford Site; the Twin City Dairy processes milk from both the east and the south of the Hanford Site. The general area of each creamery's collection is represented in Figure 1 of this report; Darigold by the area roughly bounded by Ringold, Eltopia, Pasco, and Riverview, and Twin City by the same area plus the area south of the Yakima River between Kiona and Kennewick in a band no more than 5 km wide.

I–2.3.4. Additional potentially useful tables of data

Tables of daily food consumption rates of green leafy vegetables and fresh milk, and regional agricultural information, was provided to participants as 'potentially useful' for conducting an assessment of the parameters specified above. These data are given in Tables I–IX to I–XXI. The results of contemporaneous measurements of the thyroid burden in the children of Farm B are given in Table I–XXI.

I–3. ASSESSMENT TASKS

Two types of calculational endpoints were suggested: quantities for which measurements exist, and against which model predictions can be tested; and quantities which can only be predicted but not tested (such as radiation dose). The latter were included because they are the most common and useful endpoints in radiological assessments. For all quantities, a 90% confidence level (5% and 95%, respectively, lower and upper bound estimates) was requested to quantify the expected uncertainty in the result. Given the nature of the data provided, only 'subjective' confidence interval information was expected. The arithmetic mean values for the assessment endpoints were requested for specified time periods.

I–3.1. Calculations for model testing

The following endpoints were specified:

(1) The total deposition of ^{131}I (Bq) at the following locations: Farm A, Farm B, Mesa,

(2) The integrated ^{131}I concentrations in milk (Bq d L^{-1}) for the month of September 1963, at Farm A, Farm B, Mesa, Eltopia, Ringold, and Pasco, and the ^{131}I concentration of composite milk samples taken daily from the Twin City Dairy and the Darigold Dairy for September.

(3) The average integrated ^{131}I concentrations in leafy sagebrush; pasture grass; and green alfalfa (Bq d kg^{-1} fresh weight) for the month of September 1963 for the 6 locations.

(4) The integrated ^{131}I intake (Bq) of test persons (woman, man, child) for the month of September 1963, from Darigold and Carnation creameries.

(5) The thyroid burden for a four-year old boy and his 8-year old sister, who were residents of Farm B located 25 km SSE of the point of release, on October 19, 1963. This was the location of the maximum off-site exposure. Milk was obtained from a single cow on the farm maintained for the sole use of the owner's family. Milk consumption estimated by the parents was 1 gallon/day (4 L/d) for the boy and one quart/day (1 L/d) for the girl.

I–3.2. Calculations for comparison of dose predictions

Participants were asked to estimate the mean dose to 'test persons' (20 years old in 1963) at the locations Farm A, Farm B, Mesa, Eltopia, Ringold, and Pasco, from the following pathways:

(1) external exposure due to ^{131}I from the cloud released (mSv);

(2) from the ^{131}I ground deposits in the periods September 2, 1963–September 5, 1963 and September 2, 1963–October 1, 1963;

(3) inhalation from the ^{131}I cloud (mSv);

(4) from ingestion (mSv) for the period between September 2, 1963–September 5, 1963, and September 2, 1963–October 1, 1963.

Participants were also asked to estimate the mean dose to the test persons from all pathways (mSv) for the periods September 2, 1963–September 5, 1963, and September 2, 1963–October 1, 1963.

I–3.3. Dispersion contours (optional)

Participants were given the option of estimating the atmospheric transport within 40 km (25 miles) of the Purex Plant and to derive the estimated maximum concentrations of ^{131}I dispersed in air, deposited on vegetation, and measured in farm milk over the test area. Participants were asked to sketch appropriate contours a map of the test area provided for the following:

Air: 01–0.1; 0.1–1; 1–10 Bq/m^3 at 6 pm on each day from 2–6 September. (Air measurements are based on 24-hour samples.)

Vegetation: 0.01–0.1; 0.1–1; 1–10 Bq/kg at 6 pm on each day from 2–6 September.

Farm Milk: 0.1–1; 1–10; 10–20 Bq/L at 6 pm on each day from 2–6 September

TABLE I–II. HOURLY SOURCE TERM DATA

Date	Time	^{131}I Activity released	
		(Bq)	(Ci)
September 2	12:25 – 16:25	2.04×10^{11}	5.5
September 2	16:25 – 23:30	6.84×10^{11}	18.5
September 2–3	23:30 – 09:10	8.25×10^{11}	22.3
September 3	09:10 – 11:55	1.44×10^{11}	3.9
September 3	11:55 – 15:05	8.51×10^{10}	2.3
September 3	15:10 – 23:30	1.96×10^{11}	5.3
September 3	23:30 – 08:50	8.51×10^{10}	2.3
September 4	08:50 – 15:00	4.81×10^{10}	1.3
September 4–5	15:00 – 09:10	4.07×10^{10}	1.1
September 5	09:10 – 14:45	7.77×10^{9}	0.21
September 5–6	14:45 – 00:30	5.92×10^{9}	0.16
September 6	00:30 – 09:00	6.66×10^{9}	0.18
September 6	09:00 – 14:25	3.52×10^{9}	0.095
September 6–7	14:25 – 09:00	8.51×10^{9}	0.23
September 7	09:00 – 15:20	4.07×10^{9}	0.11
September 7–8	15:20 – 14:00	1.37×10^{10}	0.37
September 8–9	14:00 – 09:00	1.07×10^{10}	0.29
September 9–10	09:00 – 09:15	1.33×10^{10}	0.36
September 10–11	09:15 – 09:00	1.30×10^{10}	0.35
to September 30		2.59×10^{11}	7 ± 2
TOTAL		2.33×10^{12}	72 ± 2

(1) Hourly data from handwritten record by Soldat.
(2) Monthly total (72 Ci) from HW-76525 9, page 3, calculated as monthly average of 2.4 Ci/day times 30 days. Note also that this reference says daily average 12 months prior to this event was 1.3 x 1010 Bq/d (0.36 Ci/d) (essentially same as that seen following return to routine operations in the latter part of the month).

Text cont. on page 72.

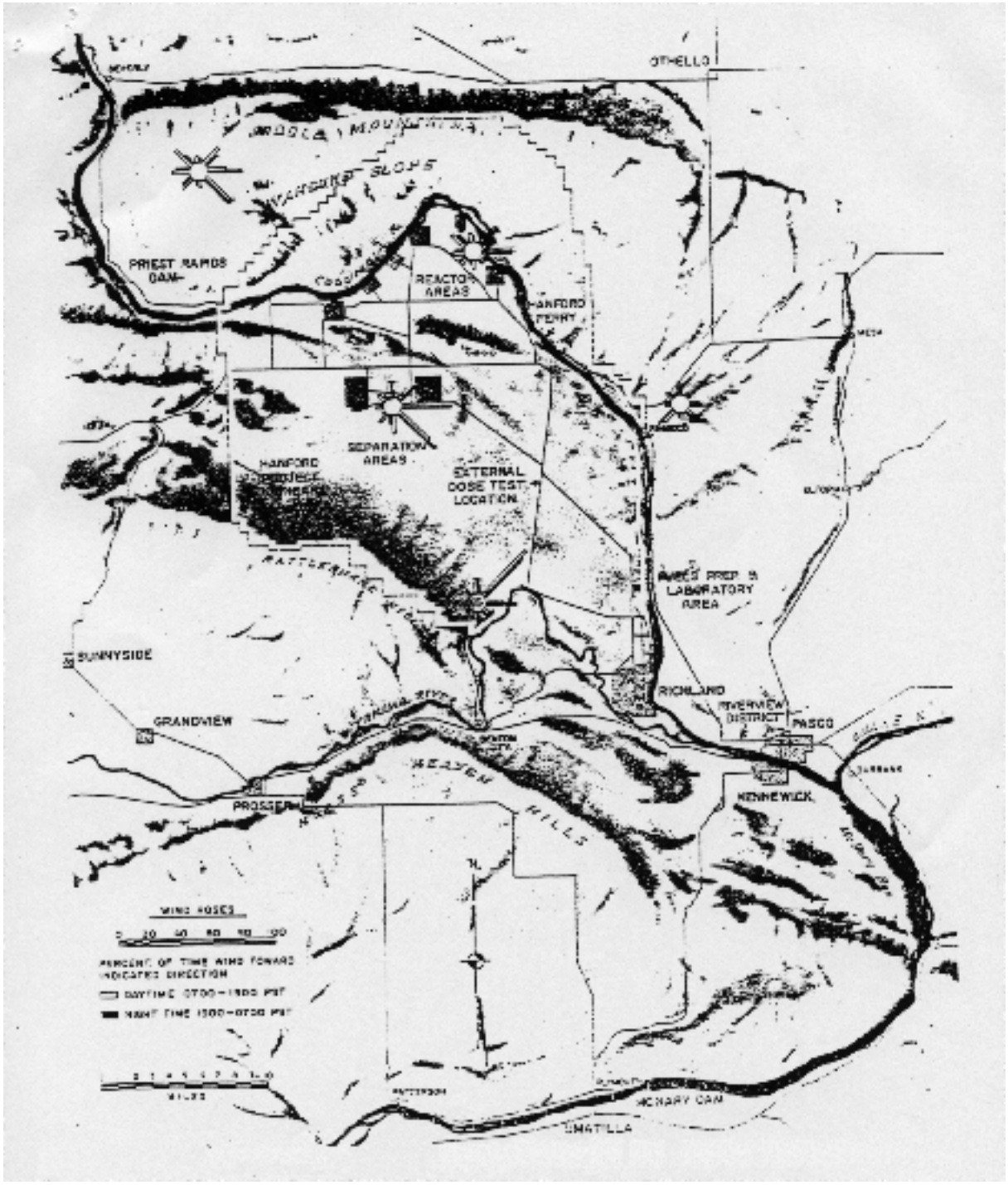

FIG. 32. Features of Hanford Project and Vicinity.

TABLE I–III. METEOROLOGICAL DATA FOR SEPTEMBER 2–5, 1963: SURFACE OBSERVATIONS MADE AT THE HANFORD METEOROLOGICAL STATION (HMS)[a]

Day and hour	Sea leve pressure (millibars)[b]	Dew point (ºF)[c]	Wind direction	Wind speed (mph)[d]	Pressure (in Hg)[e]	Dry bulb temperature (ºF)[c]	Wet bulb temperature (°F)[c]	Relative humidity (%)	Solar radiation (langleys)[f]
September 2, 1963									
1 am	134	47	WNW	9	29.17	64	55	54	0
2 am	136	46	WSW	11	29.17	64	54	51	0
3 am	142	46	WSW	10	29.19	61	53	57	0
4 am	146	46	W	8	29.20	61	53	58	0
5 am	149	49	WNW	10	29.21	63	55	60	3
6 am	156	48	WNW	6	29.23	63	55	59	24
7 am	160	48	W	5	29.24	63	55	52	50
8 am	163	50	NW	7	29.25	71	59	47	76
9 am	165	50	NE	7	29.25	74	60	43	97
10 am	167	49	E	3	29.26	76	60	39	104
11 am	163	49	NNE	6	29.25	78	61	36	126
12 pm	160	48	NNW	8	29.24	81	61	32	123
1 pm	156	47	NNE	3	29.23	82	61	29	112
2 pm	153	47	NE	6	29.22	83	62	29	96
3 pm	149	47	SE	2	29.21	83	62	28	67
4 pm	145	46	S	1	29.20	83	61	27	46
5 pm	145	46	NNW	1	29.20	83	61	27	20
6 pm	145	46	ESE	7	29.20	81	61	29	2
7 pm	147	46	SE	3	29.20	76	59	34	0
8 pm	155	45	ESE	10	29.22	73	57	37	0
9 pm	157	44	NW	9	29.23	70	56	40	0
10 pm	164	46	NW	7	29.25	68	56	45	0
11 pm	164	46	W	9	29.25	65	54	50	0
12 am	166	47	WNW	8	29.26	64	55	54	0

[a] Measurements are 1-hour averages. Times are assigned to the end of the hour.
[b] 1 millibar = 100 Pa
[c] T(°C) = [T(ºF) – 32]/1.8
[d] 1 mile per hour (mph) = 1.609 km h^{-1} or 0.4470 m s^{-1}
[e] 1 in Hg (32ºF) = 3386.38 Pa; 1 in Hg (60ºF) = 3376.85 Pa
[f] 1 langley = 41840.00 J m^{-2}

TABLE I–III. (cont.)

Day and hour	Sea level pressure (millibars)[b]	Dew point (ºF)[c]	Wind direction	Wind speed (mph)[d]	Pressure (in Hg)[e]	Dry bulb temperature (ºF)[c]	Wet bulb temperature (°F)[c]	Relative humidity (%)	Solar radiation (langleys)[f]
September 3, 1963									
1 am	166	48	WNW	7	29.26	64	55	56	0
2 am	170	48	NW	7	29.27	61	54	61	0
3 am	173	44	SSW	2	29.28	58	51	59	0
4 am	177	42	SSE	3	29.28	56	49	60	0
5 am	180	41	SSW	5	29.29	55	48	59	4
6 am	187	43	SSW	5	29.31	59	51	56	24
7 am	188	49	NW	4	29.32	65	56	57	50
8 am	187	50	NW	6	29.32	69	58	51	73
9 am	190	50	NNE	1	29.33	73	59	45	92
10 am	190	50	NNW	4	29.32	76	60	40	108
11 am	186	50	NNW	5	29.31	79	62	36	116
12 pm	179	47	SSE	2	29.29	82	61	29	114
1 pm	176	47	ENE	6	29.28	83	61	28	106
2 pm	169	45	N	4	29.26	86	62	24	92
3 pm	161	43	E	5	29.24	87	62	22	72
4 pm	152	44	NNE	4	29.22	87	62	22	47
5 pm	148	42	SE	4	29.21	87	61	21	20
6 pm	147	41	NNE	3	29.20	84	60	23	2
7 pm	144	40	NNW	4	29.20	78	57	26	0
8 pm	144	40	NW	8	29.20	74	56	30	0
9 pm	147	39	NW	6	29.20	69	53	33	0
10 pm	145	39	W	6	29.20	69	53	33	0
11 pm	148	39	WSW	9	29.20	69	53	33	0
12 am	145	39	WNW	8	29.20	66	52	36	0

[a] Measurements are 1-hour averages. Times are assigned to the end of the hour.
[b] 1 millibar = 100 Pa
[c] T(°C) = [T(ºF) – 32]/1.8
[d] 1 mile per hour (mph) = 1.609 km h^{-1} or 0.4470 m s^{-1}
[e] 1 in Hg (32ºF) = 3386.38 Pa; 1 in Hg (60ºF) = 3376.85 Pa
[f] 1 langley = 41840.00 J m^{-2}

TABLE I–III. (cont.)

Day and hour	Sea level pressure (millibars)[b]	Dew point (ºF)[c]	Wind direction	Wind speed (mph)[d]	Pressure (in Hg)[e]	Dry bulb temperature (ºF)[c]	Wet bulb temperature (°F)[c]	Relative humidity (%)	Solar radiation (langleys)[f]
September 4, 1963									
1 am	145	40	W	8	29.20	67	53	37	0
2 am	144	39	W	8	29.19	66	52	37	0
3 am	141	40	W	8	29.19	66	52	38	0
4 am	136	40	WNW	10	29.18	67	53	37	0
5 am	135	39	W	9	29.17	66	52	37	3
6 am	137	41	NW	3	29.18	64	52	43	24
7 am	141	44	NW	11	29.18	68	55	41	50
8 am	141	44	WNW	4	29.18	74	57	34	72
9 am	141	45	NW	10	29.18	79	59	30	92
10 am	135	42	NNW	7	29.17	82	61	29	108
11 am	128	47	N	6	29.15	84	62	27	114
12 pm	122	47	NNW	5	29.13	86	62	25	114
1 pm	110	44	NW	2	29.10	89	63	21	106
2 pm	102	46	E	2	29.08	93	65	20	90
3 pm	94	45	E	0	29.06	94	65	19	67
4 pm	88	45	ESE	2	29.04	93	64	19	42
5 pm	84	45	SSE	5	29.02	93	64	19	16
6 pm	83	44	ESE	4	29.02	89	63	21	1
7 pm	84	43	SE	2	29.02	81	59	26	0
8 pm	86	43	SSE	10	29.03	80	59	27	0
9 pm	90	41	NW	7	29.04	73	56	31	0
10 pm	92	44	WNW	7	29.05	76	58	33	0
11 pm	91	51	WNW	8	29.05	76	61	42	0
12 am	93	53	WNW	15	29.05	77	62	43	0

[a] Measurements are 1-hour averages. Times are assigned to the end of the hour.
[b] 1 millibar = 100 Pa
[c] T(°C) = [T(ºF) – 32]/1.8
[d] 1 mile per hour (mph) = 1.609 km h^{-1} or 0.4470 m s^{-1}
[e] 1 in Hg (32ºF) = 3386.38 Pa; 1 in Hg (60ºF) = 3376.85 Pa
[f] 1 langley = 41840.00 J m^{-2}

TABLE I–III. (cont.)

Day and hour	Sea level pressure (millibars)[b]	Dew point (ºF)[c]	Wind direction	Wind speed (mph)[d]	Pressure (in Hg)[e]	Dry bulb temperature (ºF)[c]	Wet bulb temperature (°F)[c]	Relative humidity (%)	Solar radiation (langleys)[f]
September 5, 1963									
1 am	95	53	WNW	13	29.06	76	62	46	0
2 am	98	53	WNW	16	29.07	75	62	46	0
3 am	105	53	NW	6	29.09	71	61	52	0
4 am	104	54	WNW	11	29.08	72	61	53	0
5 am	105	53	W	9	29.09	69	59	56	4
6 am	108	53	W	6	29.09	70	60	56	21
7 am	110	54	NW	7	29.10	75	62	48	47
8 am	114	54	NW	5	29.10	78	63	42	74
9 am	114	53	W	0	29.10	82	63	37	94
10 am	108	52	WSW	1	29.09	84	64	33	109
11 am	98	50	WSW	4	29.07	88	65	28	114
12 pm	97	49	SSW	4	29.06	90	64	24	114
1 pm	91	47	W	5	29.05	93	65	21	104
2 pm	85	50	ESE	4	29.03	95	67	22	90
3 pm	77	49	ENE	3	29.01	95	67	21	68
4 pm	74	48	NE	6	29.00	95	66	20	42
5 pm	69	48	SE	6	28.98	93	66	22	16
6 pm	69	45	SE	5	28.98	90	63	21	2
7 pm	74	44	SE	8	28.99	84	61	25	0
8 pm	84	47	WNW	16	29.03	82	61	29	0
9 pm	88	48	NW	18	29.04	80	61	32	0
10 pm	93	49	NW	14	29.05	78	61	36	0
11 pm	98	47	NW	6	29.07	75	59	36	0
12 am	102	46	NW	11	29.08	74	58	38	0

[a] Measurements are 1-hour averages. Times are assigned to the end of the hour.
[b] 1 millibar = 100 Pa
[c] T(°C) = [T(ºF) – 32]/1.8
[d] 1 mile per hour (mph) = 1.609 km h^{-1} or 0.4470 m s^{-1}
[e] 1 in Hg (32ºF) = 3386.38 Pa; 1 in Hg (60ºF) = 3376.85 Pa
[f] 1 langley = 41840.00 J m^{-2}

TABLE I–IV. METEOROLOGICAL DATA FOR SEPTEMBER 2–5, 1963: HANFORD METEOROLOGICAL STATION (HMS) TOWER OBSERVATIONS OF TEMPERATURE AND WIND

Day/ hour	Subsurface temperature (ºF)[a] *Depth (in)*[b]			Air temperature (ºF)[a] *Tower height (ft)*[b]							Wind speed (mph)[c] *Tower height (ft)*[d]						Wind direction (10s of degrees) *Tower height (ft)*[d]		
Sept. 2	-0.5	-15	-36	3	50	100	200	250	300	400	7	50	100	200	300	400	50	200	400
1 am	69.5	–	–	65.0	66.1	65.9	66.6	66.5	66.3	66.0	7	11	13	16	17	19	29	29	29
2 am	68.6	–	–	66.3	66.7	66.5	66.8	66.8	66.7	66.6	9	13	15	19	21	24	27	29	29
3 am	68.0	–	–	60.5	62.0	63.8	66.5	66.7	66.6	66.2	5	10	12	15	15	16	25	27	27
4 am	66.9	–	–	62.6	63.5	64.0	65.3	65.2	65.0	64.8	5	9	12	13	13	15	27	27	27
5 am	66.0	80.4	77.0	62.9	64.3	64.4	64.6	64.5	64.2	63.9	6	9	11	13	15	17	27	29	29
6 am	65.8	–	–	61.5	63.5	63.9	64.5	64.2	64.0	63.9	4	8	10	14	14	16	27	29	29
7 am	65.8	–	–	62.7	63.5	64.0	65.0	65.0	64.5	64.5	2	3	5	8	7	8	27	29	29
8 am	70.0	–	–	68.4	68.0	66.9	66.5	66.2	65.9	65.9	5	6	6	7	7	8	29	32	29
9 am	78.8	–	–	73.0	71.0	69.5	69.3	69.2	68.9	68.2	6	6	7	8	8	8	34	34	34
10 am	88.0	–	–	74.0	73.0	71.2	71.8	70.6	70.6	70.7	4	5	6	6	6	6	34	36	34
11 am	93.0	80.0	77.2	78.1	75.2	74.1	73.9	72.9	72.1	72.4	4	4	4	4	3	3	37	37	37
12 pm	100.0	–	–	78.2	77.1	76.5	76.2	75.5	75.8	76.1	4	4	4	4	4	3	37	37	37
1 pm	106.4	–	–	80.7	79.0	78.1	77.6	77.1	77.3	77.4	6	7	7	7	6	6	37	36	36
2 pm	110.0	–	–	83.0	80.4	78.9	78.5	78.6	78.4	78.5	5	5	6	5	5	4	36	36	34
3 pm	111.4	–	–	83.0	82.0	80.5	80.5	79.9	80.2	80.1	3	3	3	3	3	3	36	2	2
4 pm	108.8	–	–	83.9	83.0	81.4	80.6	80.4	80.3	80.0	2	2	2	3	3	3	2	2	37
5 pm	103.8	79.5	77.5	83.7	82.7	82.2	81.5	81.1	81.0	81.1	2	2	2	2	2	2	37	23	37
6 pm	99.9	–	–	82.8	81.6	81.3	80.7	80.5	80.3	80.1	5	5	6	7	7	7	11	11	9
7 pm	95.5	–	–	78.4	79.1	78.8	78.8	78.3	78.2	77.9	6	6	7	7	8	9	11	14	11
8 pm	85.0	–	–	73.9	75.2	76.5	77.1	76.8	76.7	76.5	5	6	8	10	11	12	14	14	14
9 pm	80.0	–	–	70.7	74.4	76.5	76.5	76.2	76.1	76.0	4	8	10	12	12	14	16	18	16
10 pm	78.1	–	–	68.6	70.9	71.2	72.0	72.0	72.0	73.1	3	7	10	15	16	15	32	32	32
11 pm	74.0	80.0	77.2	64.2	69.4	69.8	70.7	71.5	77.1	72.4	2	7	10	16	16	15	29	32	32
12 am	71.9	–	–	65.0	68.0	68.6	69.7	69.8	70.0	70.5	3	7	11	16	16	20	29	32	32

[a] $T(ºC) = [T(°F) – 32]/1.8$

[b] 1 in = 0.02540 m

[c] 1 mile per hour (mph) = 1.609 km h^{-1} or 0.4470 m s^{-1}

[d] 1 ft = 0.3048 m

TABLE I–IV. METEOROLOGICAL DATA FOR SEPTEMBER 2–5, 1963: HANFORD METEOROLOGICAL STATION (HMS) TOWER OBSERVATIONS OF TEMPERATURE AND WIND (Continued)

Day/ hour	Subsurface temperature (ºF)[a] *Depth (in)*[b]			Air temperature (ºF)[a] *Tower height (ft)*[b]							Wind speed (mph)[c] *Tower height (ft)*[d]						Wind direction (10s of degrees) *Tower height (ft)*[d]		
Sept. 3	-0.5	-15	-36	3	50	100	200	250	300	400	7	50	100	200	300	400	50	200	400
1 am	70.0	–	–	63.0	65.9	66.4	68.0	68.4	69.8	70.5	2	6	10	15	18	17	29	32	32
2 am	68.6	–	–	61.8	65.1	65.3	66.7	67.0	67.7	69.0	2	7	10	16	17	17	32	32	32
3 am	67.7	–	–	60.3	65.0	65.2	65.8	65.7	65.9	66.9	1	4	7	10	12	14	29	32	32
4 am	66.0	–	–	55.2	62.4	63.5	64.3	64.3	64.6	64.9	2	3	2	6	9	12	20	29	29
5 am	64.2	80.0	77.1	54.3	63.7	64.0	64.6	64.3	64.3	64.3	1	1	1	2	4	6	20	29	29
6 am	62.8	–	–	54.8	61.6	61.7	63.1	63.3	63.1	63.5	1	4	3	3	5	5	20	29	29
7 am	63.0	–	–	61.0	62.3	62.5	63.5	63.9	64.0	64.1	1	3	4	5	6	7	27	27	29
8 am	68.8	–	–	66.0	65.7	64.9	64.5	64.0	64.2	64.2	5	5	5	5	5	6	32	29	29
9 am	77.0	–	–	70.3	67.8	67.2	67.5	67.5	67.1	66.3	3	3	3	3	3	3	34	34	34
10 am	88.0	–	–	74.8	71.8	72.0	71.9	71.1	70.8	70.3	2	2	2	2	2	2	34	34	36
11 am	92.8	79.8	77.0	78.1	76.2	74.9	75.1	75.0	75.1	75.1	3	3	3	3	2	2	36	36	2
12 pm	101.9	–	–	80.8	79.0	77.9	77.6	76.9	76.8	77.1	4	4	4	4	4	4	5	5	5
1 pm	107.0	–	–	84.0	82.0	80.3	80.1	79.5	79.2	79.1	4	4	4	5	5	5	5	5	5
2 pm	110.5	–	–	86.1	84.0	82.3	81.6	81.4	81.0	81.0	5	5	5	6	6	6	2	5	5
3 pm	111.2	–	–	86.7	86.3	85.0	84.0	83.4	83.9	84.0	4	4	4	5	5	5	11	11	7
4 pm	110.0	–	–	86.6	86.1	84.6	84.4	84.4	84.5	84.6	3	4	4	4	4	4	2	2	7
5 pm	106.2	79.0	77.2	87.2	86.8	85.7	85.4	84.3	84.7	84.9	3	3	3	3	4	4	7	9	9
6 pm	100.5	–	–	86.0	86.4	85.1	84.9	84.4	84.6	84.4	1	2	2	3	3	3	32	36	2
7 pm	92.5	–	–	80.9	84.1	83.5	83.6	83.2	83.0	82.7	0	2	3	3	3	3	36	36	2
8 pm	86.0	–	–	74.7	81.6	81.7	82.0	81.8	81.7	81.4	2	6	7	8	7	7	32	36	36
9 pm	80.5	–	–	71.6	80.2	80.5	81.3	80.9	80.9	80.4	2	8	7	7	6	6	32	36	36
10 pm	77.0	–	–	65.2	75.7	76.5	78.9	79.5	79.7	79.5	2	6	8	12	9	8	27	32	34
11 pm	74.2	80.0	77.2	68.8	75.0	75.5	76.8	77.5	78.2	79.0	3	7	8	11	11	10	27	29	32
12 am	72.6	–	–	68.0	73.4	76.5	76.5	76.3	77.0	78.8	3	8	9	12	12	12	27	32	32

[a] $T(ºC) = [T(°F) – 32]/1.8$

[b] 1 in = 0.02540 m

[c] 1 mile per hour (mph) = 1.609 km h^{-1} or 0.4470 m s^{-1}

[d] 1 ft = 0.3048 m

TABLE I–IV. METEOROLOGICAL DATA FOR SEPTEMBER 2–5, 1963: HANFORD METEOROLOGICAL STATION (HMS) TOWER OBSERVATIONS OF TEMPERATURE AND WIND (Continued)

Day/ hour	Subsurface temperature (ºF)[a] *Depth (in)[b]*			Air temperature (ºF)[a] *Tower height (ft)[b]*							Wind speed (mph)[c] *Tower height (ft)[d]*						Wind direction (10s of degrees) *Tower height (ft)[d]*		
Sept. 4	-0.5	-15	-36	3	50	100	200	250	300	400	7	50	100	200	300	400	50	200	400
1 am	70.3	–	–	67.2	71.7	72.2	75.0	77.0	77.8	78.0	2	7	9	15	13	12	27	32	34
2 am	69.6	–	–	67.4	72.2	72.6	73.8	74.9	76.4	76.8	3	8	10	17	15	13	27	32	32
3 am	68.6	–	–	66.3	70.0	72.1	76.4	76.5	76.8	76.7	3	9	12	17	14	12	29	32	34
4 am	68.0	–	–	66.3	70.0	70.6	72.8	74.6	75.4	76.0	3	8	10	17	15	13	27	29	32
5 am	67.6	80.1	77.3	65.4	68.2	69.0	71.4	73.8	74.2	74.6	4	9	11	18	17	15	29	29	32
6 am	66.8	–	–	65.4	68.0	68.5	69.5	69.5	69.8	71.1	2	7	8	13	16	19	29	32	32
7 am	66.6	–	–	65.4	65.9	66.2	66.0	66.1	66.3	68.2	3	5	6	10	12	17	32	32	32
8 am	70.1	–	–	70.5	70.4	68.9	68.9	69.4	69.8	69.5	5	6	6	7	6	6	32	34	34
9 am	79.0	–	–	76.6	76.0	73.4	73.2	73.4	73.1	72.5	7	8	8	9	9	8	32	32	32
10 am	86.0	–	–	81.0	78.9	77.2	77.1	76.8	76.4	76.1	6	8	8	9	9	9	32	32	32
11 am	93.6	79.8	77.6	83.1	81.1	80.0	79.4	78.9	78.8	78.7	3	4	4	5	5	5	34	34	34
12 pm	102.1	–	–	85.3	83.3	82.6	82.5	81.9	82.0	82.0	3	3	3	3	3	3	2	36	36
1 pm	110.0	–	–	90.0	87.7	86.2	86.6	85.7	85.8	85.8	3	3	3	3	3	3	5	5	2
2 pm	114.0	–	–	90.9	90.1	88.7	88.9	88.4	88.5	88.6	3	3	3	3	3	2	23	25	27
3 pm	115.8	–	–	92.0	92.1	90.9	90.7	89.5	89.4	89.9	3	3	3	4	3	3	16	16	16
4 pm	114.2	–	–	94.3	93.7	92.3	91.8	91.1	91.6	92.1	3	3	3	4	3	3	14	14	14
5 pm	110.0	79.0	77.0	93.0	93.2	91.7	92.2	91.4	91.3	91.6	5	5	5	6	6	6	14	14	14
6 pm	103.8	–	–	91.6	92.3	91.3	91.2	90.7	90.5	90.4	5	5	6	6	6	6	14	14	14
7 pm	95.9	–	–	85.4	88.6	88.2	88.3	88.0	87.9	87.5	3	7	7	7	7	7	11	14	14
8 pm	89.0	–	–	80.4	86.1	87.4	87.5	87.3	87.5	87.5	4	9	9	9	7	6	14	14	14
9 pm	84.3	–	–	75.1	82.0	84.1	85.7	85.5	85.7	86.5	2	6	7	8	8	8	20	18	16
10 pm	80.3	–	–	75.8	82.1	83.0	84.0	83.6	84.1	84.7	2	7	9	12	13	13	29	32	32
11 pm	78.5	80.0	78.5	77.4	79.8	80.5	82.2	82.3	82.3	82.3	4	10	12	16	18	20	29	29	29
12 am	77.2	–	–	75.8	78.7	78.7	78.8	78.8	78.9	79.1	5	10	12	15	17	21	29	29	29

[a] $T(ºC) = [T(°F) - 32]/1.8$

[b] 1 in = 0.02540 m

[c] 1 mile per hour (mph) = 1.609 km h^{-1} or 0.4470 m s^{-1}

[d] 1 ft = 0.3048 m

TABLE I–IV. METEOROLOGICAL DATA FOR SEPTEMBER 2–5, 1963: HANFORD METEOROLOGICAL STATION (HMS) TOWER OBSERVATIONS OF TEMPERATURE AND WIND (Continued)

Day/ hour	Subsurface temperature (ºF)[a] *Depth (in)*[b]			Air temperature (ºF)[a] *Tower height (ft)*[b]							Wind speed (mph)[c] *Tower height (ft)*[d]						Wind direction (10s of degrees) *Tower height (ft)*[d]		
Sept. 5	-0.5	-15	-36	3	50	100	200	250	300	400	7	50	100	200	300	400	50	200	400
1 am	76.1	–	–	76.4	77.2	77.1	78.0	78.0	78.3	79.6	10	15	18	23	25	27	29	32	29
2 am	75.6	–	–	75.3	76.0	76.0	76.8	76.7	76.9	77.3	11	17	18	24	25	27	32	32	32
3 am	75.2	–	–	73.5	74.5	74.5	74.9	74.9	74.6	75.3	6	10	12	18	20	21	29	32	32
4 am	74.0	–	–	72.5	74.1	74.2	74.4	74.1	74.0	73.9	5	10	12	15	16	18	32	32	29
5 am	72.3	80.4	77.0	70.1	73.6	73.6	74.4	74.9	75.1	75.1	4	10	13	15	16	18	29	29	29
6 am	71.0	–	–	69.3	71.0	71.2	73.4	73.2	73.5	73.8	4	9	11	17	18	19	27	29	29
7 am	71.0	–	–	72.8	73.2	72.2	72.8	72.9	72.7	72.7	4	7	8	11	12	14	29	32	29
8 am	75.5	–	–	76.5	75.8	74.6	74.6	74.8	74.3	73.3	4	6	7	8	8	8	32	32	32
9 am	84.0	–	–	80.4	79.1	77.3	77.1	76.9	76.8	76.2	3	4	4	5	4	4	32	34	32
10 am	93.0	–	–	83.0	82.0	80.6	80.2	79.8	79.4	79.1	1	1	1	2	2	2	25	34	34
11 am	98.1	80.2	76.8	87.6	84.6	83.3	83.1	82.8	82.6	82.6	2	2	2	2	2	2	25	25	27
12 pm	107.0	–	–	89.3	87.1	86.1	85.9	85.6	85.6	85.0	3	3	4	4	4	4	25	25	25
1 pm	113.0	–	–	92.9	90.1	88.9	88.0	87.5	87.8	88.1	4	4	4	5	5	5	20	20	20
2 pm	116.5	–	–	93.5	90.7	89.7	89.4	88.5	88.2	88.6	6	6	6	6	6	6	11	11	11
3 pm	116.5	–	–	95.0	93.2	91.9	90.5	90.3	90.3	90.6	4	5	5	5	5	5	9	9	9
4 pm	114.7	–	–	94.6	93.6	92.1	91.2	91.0	91.3	91.2	4	5	5	5	5	5	5	5	7
5 pm	110.0	79.9	76.8	93.6	93.6	92.6	92.6	91.7	91.8	92.1	5	5	5	5	5	5	11	11	11
6 pm	104.0	–	–	92.1	92.4	91.6	91.5	91.1	90.9	90.9	5	8	8	8	8	8	14	14	14
7 pm	96.0	–	–	84.1	88.0	88.0	88.3	88.7	88.5	88.4	4	9	9	9	9	9	14	14	14
8 pm	90.0	–	–	85.1	87.2	86.6	86.3	85.8	85.8	85.7	5	10	11	13	14	15	32	32	32
9 pm	86.2	–	–	81.0	81.8	81.5	82.3	82.5	83.1	83.7	11	15	18	23	25	24	32	32	32
10 pm	83.8	–	–	79.1	79.6	79.3	79.8	79.3	79.6	80.3	10	15	17	21	24	25	32	32	32
11 pm	81.2	80.9	77.0	76.6	77.8	77.9	78.8	78.4	78.7	79.0	6	10	12	16	20	24	29	29	29
12 am	78.2	–	–	73.6	76.8	76.9	77.5	77.6	77.9	78.0	3	9	10	13	16	20	32	32	32

[a] T(ºC) = [T(°F) –32]/1.8

[b] 1 in = 0.02540 m

[c] 1 mile per hour (mph) = 1.609 km h^{-1} or 0.4470 m s^{-1}

[d] 1 ft = 0.3048 m

TABLE I–V. SAMPLING LOCATION CODES

Locations	North Latitude			West Longitude		
	Deg	Min	Sec	Deg	Min	Sec
ROUTE 2N, MILE 3	46	36	55	119	25	16
ROUTE 2N, MILE 5	46	38	7	119	27	3
ROUTE 2N, MILE 7	46	39	30	119	28	34
ROUTE 2N, MILE 9	46	40	39	119	30	28
ROUTE 2S, MILE 1	46	34	10	119	22	46
ROUTE 2S, MILE 3	46	32	24	119	22	45
ROUTE 2S, MILE 5	46	30	37	119	23	3
ROUTE 4S, MILE 13	46	28	11	119	22	44
ROUTE 4S, MILE 15	46	26	59	119	20	56
ROUTE 4S, MILE 17	46	25	45	119	19	9
ROUTE 4S, MILE 19	46	24	31	119	17	25
ROUTE 4S, MILE 21	46	22	49	119	16	58
Y BARRICADE	46	28	56	119	23	30
200E - GATE HOUSE	46	32	42	119	32	12
ERC GATE (ERC INTERSECTION)	46	22	14	119	26	39
ERC GATE + 1 MILE	46	22	55	119	26	3
ERC GATE + 2 MILES (TO ROUTE 10 + 4S)	46	23	3	119	24	45
ERC GATE + 3 MILES	46	23	56	119	24	32
ERC GATE + 4 MILES (TO RT10 +4S)	46	24	50	119	24	22
ERC GATE + 5 MILES	46	25	44	119	24	9
ERC GATE + 6 MILES (TO RT10 +4S)	46	26	38	119	23	58
ERC GATE + 7 MILES	46	27	32	119	23	48
ERC GATE + 8 MILES (TO RT 10 +4S)	46	28	27	119	23	38
ERC GATE + 9 MILES	46	29	21	119	23	24
ERC GATE + 10 MILES	46	30	14	119	23	7
ROUTE 10 + ROUTE 4S INTERSECTION	46	28	40	119	23	30
ROUTE 11A + ROUTE 3 INTERSECTION	46	34	48	119	36	17
ROUTE 11A + ROUTE 4S INTERSECTION	46	34	48	119	33	12
ROUTE 11A + ROUTE 6 INTERSECTION	46	34	47	119	39	43
ROUTE 11A , FROM ROUTE 3 TO ROUTE 6, MILE	46	34	49	119	36	53
ROUTE 11A , FROM ROUTE 3 TO ROUTE 6, MILE	46	34	49	119	37	29
ROUTE 11A, FROM ROUTE 3 TO ROUTE 6, MILE	46	34	49	119	38	6
ROUTE 11A, FROM ROUTE 3 TO ROUTE 6, MILE	46	34	48	119	38	42
ROUTE 11A, FROM ROUTE 4S TO ROUTE 6, MILE	46	34	49	119	33	49
ROUTE 11A, FROM ROUTE 4S TO ROUTE 6, MILE	46	34	49	119	34	24
ROUTE 11A, FROM ROUTE 4S TO ROUTE 6, MILE	46	34	49	119	35	0
ROUTE 4S, 3 MILES SOUTH OF Y BARRICADE	46	26	26	119	20	8
ROUTE 4S, 5 MILES SOUTH OF Y BARRICADE	46	25	11	119	18	22
ROUTE 4S, 7 MILES SOUTH OF Y BARRICADE	46	23	50	119	16	58
ROUTE 4S, 9 MILES SOUTH OF Y BARRICADE	46	22	1	119	16	58
ROUTE 4S, 11 MILES SOUTH OF Y BARRICADE	46	20	12	119	16	57
ROUTE 4S, 13 MILES SOUTH OF Y BARRICADE	46	18	20	119	17	10
ROUTE 4S, 15 MILES SOUTH OF Y BARRICADE	46	16	48	119	18	18
ROUTE 4S, 17 MILES SOUTH OF Y BARRICADE	46	15	33	119	16	46
ROUTE 4S, 19 MILES SOUTH OF Y BARRICADE	46	14	43	119	14	58
ROUTE 4S, 21 MILES SOUTH OF Y BARRICADE	46	13	55	119	12	53
200E - 1	46	33	32	119	31	13
200E - 4	46	34	9	119	30	50
200E -7	46	33	27	119	31	41
200 - 8	46	33	28	119	30	49
200 - 10	46	33	7	119	32	8
200 - 12	46	33	10	119	30	52

TABLE I–V. (cont.)

Locations	North Latitude			West Longitude		
	Deg	Min	Sec	Deg	Min	Sec
ROUTE 4S, MILE 1	46	33	53	119	33	14
ROUTE 4S, MILE 3	46	32	36	119	32	26
ROUTE 4S, MILE 4	46	32	36	119	31	14
ROUTE 4S, MILE 5	46	32	28	119	30	3
A ZONE	46	33	23	119	37	35
B ZONE	46	33	25	119	32	4
Farm A	46	16	45	119	28	29
NEW PASCO BRIDGE TO PROSSER, MILE 2	46	13	30	119	9	59
NEW PASCO BRIDGE TO PROSSER, MILE 4	46	13	15	119	12	16
NEW PASCO BRIDGE TO PROSSER, MILE 6	46	14	20	119	14	27
NEW PASCO BRIDGE TO PROSSER, MILE 8	46	14	50	119	16	43
NEW PASCO BRIDGE TO PROSSER, MILE 10	46	15	19	119	18	60
NEW PASCO BRIDGE TO PROSSER, MILE 12	46	15	41	119	21	17
NEW PASCO BRIDGE TO PROSSER, MILE 14	46	15	50	119	23	29
NEW PASCO BRIDGE TO PROSSER, MILE 16	46	15	37	119	25	46
NEW PASCO BRIDGE TO PROSSER, MILE 18	46	15	7	119	27	59
NEW PASCO BRIDGE TO PROSSER, MILE 20	46	15	13	119	30	17
NEW PASCO BRIDGE TO PROSSER, MILE 22	46	15	57	119	32	28
NEW PASCO BRIDGE TO PROSSER, MILE 24	46	15	47	119	34	30
NEW PASCO BRIDGE TO PROSSER, MILE 26	46	15	0	119	36	43
NEW PASCO BRIDGE TO PROSSER, MILE 28	46	14	9	119	38	47
NEW PASCO BRIDGE TO PROSSER, MILE 30	46	13	17	119	40	50
PROSSER, EAST OF CITY LIMITS	42	12	49	119	43	6
Farm J	46	17	13	119	33	11
Farm B	46	20	58	119	22	23
Farm G	46	21	33	119	14	46
Farm Z	46	25	10	119	12	6
Farm N	46	33	55	119	6	45
Farm T	46	15	9	119	10	51
RADAR HILL	46	43	13	119	10	27
RADAR HILL TO PASCO, MILE 2	46	41	25	119	10	25
RADAR HILL TO PASCO, MILE 4	46	39	36	119	10	24
RADAR HILL TO PASCO, MILE 6	46	37	48	119	10	25
RADAR HILL TO PASCO, MILE 8	46	36	9	119	10	26
RADAR HILL TO PASCO, MILE 10	46	34	54	119	11	27
RADAR HILL TO PASCO, MILE 12	46	33	28	119	12	57
RADAR HILL TO PASCO, MILE 14	46	31	60	119	14	6
RADAR HILL TO PASCO, MILE 18	46	29	17	119	12	14
RADAR HILL TO PASCO, MILE 20	46	27	53	119	11	41
RADAR HILL TO PASCO, MILE 22	46	26	3	119	11	42
RADAR HILL TO PASCO, MILE 24	46	24	10	119	11	43
RADAR HILL TO PASCO, MILE 26	46	22	20	119	11	47
RADAR HILL TO PASCO, MILE 28	46	20	25	119	11	48
RADAR HILL TO PASCO, MILE 30	46	18	46	119	11	16
RADAR HILL TO PASCO, MILE 32	46	17	3	119	11	17
RADAR HILL TO PASCO, MILE 34	46	15	17	119	10	42
RADAR HILL TO PASCO, MILE 36	46	14	22	119	9	27
RADAR HILL TO PASCO, MILE 38	46	14	21	119	7	5
Farm K	46	32	8	119	14	54
Farm H	46	15	12	119	13	39
PUREX STACK	46	33	0	119	31	6
MET TOWER	46	33	47	119	35	55

TABLE I–V. (cont.)

Locations	North Latitude			West Longitude		
	Deg	Min	Sec	Deg	Min	Sec
100 BSE	46	37	56	119	38	7
100-F	46	38	59	119	26	42
100-K	46	38	41	119	35	44
100-D	46	41	8	119	31	32
100-HE	46	41	38	119	29	0
200 ESE	46	32	33	119	30	52
200 EWC	46	33	2	119	33	9
200 EEC	46	33	2	119	30	52
200E SEMI	46	33	24	119	31	35
REDOX	46	32	3	119	37	7
200 WEC	46	33	15	119	36	29
200 WWC	46	33	6	119	38	14
300-A	46	22	13	119	16	37
HANFORD	46	35	0	119	22	30
WHITE BLUFFS	46	39	42	119	28	30
BYERS LANDING	46	22	11	119	15	32
700-A	46	16	42	119	16	30
1100-A	46	19	21	119	17	0
BENTON CITY	46	18	0	119	30	0
PASCO	46	13	0	119	2	0
KENNEWICK	46	11	0	119	4	0
ELTOPIA	46	27	28	119	1	3
MESA	46	34	30	119	0	0
RINGOLD	46	30	0	119	15	10

Carnation (composite - physically in Prosser)
Darigold (composite - physically in Kennewick)
Twin City (composite - physically in Pasco)

TABLE I–VI. MEASURED CONCENTRATIONS OF ^{131}I IN VEGETATION SAMPLES

Farm	Collection site	County	Date	Vegetation type	Concentration of ^{131}I	
					pCi g^{-1}	Bq kg^{-1}
	Route 2N, Mile 3		9/2/63	leafy sage	0.666	24.64
	Route 2N, Mile 5		9/2/63	bare sage stems	-0.792	-29.3
	Route 2N, Mile 7		9/2/63	bare sage stems	-0.38	-14.06
	Route 2N, Mile 9		9/2/63	leafy sage	-0.664	-24.57
	Route 2S, Mile 1		9/2/63	leafy sage	0.218	8.07
	Route 2S, Mile 3		9/2/63	leafy sage	2.29	84.73
	Route 2S, Mile 5		9/2/63	leafy sage	-0.335	-12.4
	Route 4S, Mile 13		9/2/63	bare sage stems	0.251	9.29
	Route 4S, Mile 15		9/2/63	leafy sage	-1.52	-56.24
	Route 4S, Mile 17		9/2/63	leafy sage	-0.96	-35.52
	Route 4S, Mile 19		9/2/63	leafy sage	-2.34	-86.58
	Route 4S, Mile 21		9/2/63	leafy sage	1.49	55.13
	Y Barricade		9/2/63	leafy sage	-0.582	-21.53
	200E - Gate House		9/3/63	leafy sage	8.74	323.38
	ERC Intersection		9/3/63		5	185
	ERC Intersection to Route 10 + Route 4S, Mile 2		9/3/63		0.534	19.76
	ERC Intersection to Route 10 + Route 4S, Mile 4		9/3/63		5.83	215.71
	ERC Intersection to Route 10 + Route 4S, Mile 6		9/3/63		6	222
	ERC Intersection to Route 10 + Route 4S, Mile 8		9/3/63		1.15	42.55
	Route 10 + Route 4S Intersection		9/3/63		0.917	33.93
	Route 11A + Route 3 Intersection		9/3/63	dry cheat grass	3.91	144.67
	Route 11A + Route 4S Intersection		9/3/63	leafy sage	2.33	86.21
	Route 11A + Route 6 Intersection		9/3/63	leafy sage	-0.064	-2.37
	Route 11A, from Route 3 to Route 6, Mile 0.5		9/3/63	half dry grass	0.322	11.91
	Route 11A, from Route 3 to Route 6, Mile 1		9/3/63	dry cheat grass	1.44	53.28
	Route 11A, from Route 3 to Route 6, Mile 1.5		9/3/63	dry cheat grass	0.956	35.37
	Route 11A, from Route 3 to Route 6, Mile 2		9/3/63	dry cheat grass	2.05	75.85
	Route 11A, from Route 4S to Route 6, Mile 0.5		9/3/63	leafy sage	3.66	135.42
	Route 11A, from Route 4S to Route 6, Mile 1		9/3/63	dry cheat grass	14.3	529.1
	Route 11A, from Route 4S to Route 6, Mile 1.5		9/3/63	dry cheat grass	5.3	196.1
	Route 4S, 3 Miles South of Y Barricade		9/3/63	leafy sage	7.72	285.64
	Route 4S, 5 Miles South of Y Barricade		9/3/63	leafy sage	91.3	3378.1
	Route 4S, 7 Miles South of Y Barricade		9/3/63	leafy sage	18.7	691.9
	Route 4S, 9 Miles South of Y Barricade		9/3/63	leafy sage	14	518

TABLE I–VI. (cont.)

Farm	Collection site	County	Date	Vegetation type	Concentration of ^{131}I	
					pCi g^{-1}	Bq kg^{-1}
	Route 4S, 11 Miles South of Y Barricade		9/3/63	leafy sage	7.41	274.17
	Route 4S, 13 Miles South of Y Barricade		9/3/63	leafy sage	12	444
	Route 4S, 15 Miles South of Y Barricade		9/3/63	leafy sage	5.64	208.68
	Route 4S, 17 Miles South of Y Barricade		9/3/63	leafy sage	1.17	43.29
	Route 4S, 19 Miles South of Y Barricade		9/3/63	leafy sage	0.765	28.31
	Route 4S, 21 Miles South of Y Barricade		9/3/63	leafy sage	0.316	11.69
	Y Barricade		9/3/63	leafy sage	13.9	514.3
	100 B Gate		9/4/63	bare sage stems	6.53	241.61
	100 D Gate		9/4/63	leafy sage	0.094	3.48
	100 F Gate		9/4/63	leafy sage	0.099	3.66
	100 H Gate		9/4/63	bare sage stems	0.375	13.88
	100 K Gate		9/4/63	leafy sage	0.696	25.75
	200E - 1		9/4/63	leafy sage	11.1	410.7
	200E - 4		9/4/63	leafy sage	6.3	233.1
	200E - 7		9/4/63	leafy sage	4.2	155.4
	200E - 8		9/4/63	leafy sage	44	1628
	200E - 10		9/4/63	leafy sage	22.4	828.8
	200E - 12		9/4/63	leafy sage	125	4625
	Route 4S, Mile 1		9/4/63	leafy sage	19.5	721.5
	Route 4S, Mile 3		9/4/63	leafy sage	7.67	283.79
	Route 4S, Mile 4		9/4/63	leafy sage	246	9102
	Route 4S, Mile 5		9/4/63	leafy sage	63.7	2356.9
	A Zone		9/6/63		6.01	222.37
	B Zone		9/6/63		67.2	2486.4
	614 Building - Byers		9/7/63	leafy weeds	0.809	29.93
	A Zone		9/13/63		3.29	121.73
	B Zone		9/13/63		87.2	3226.4
	A Zone		9/20/63		1.28	47.36
	B Zone		9/20/63		30.8	1139.6
	A Zone		9/27/63		1.36	50.32
	B Zone		9/27/63		10.2	377.4

TABLE I–VI. (cont.)

Farm	Collection site	County	Date	Vegetation type	Concentration of ^{131}I	
					pCi g^{-1}	Bq kg^{-1}
Farm A	Benton City	Benton	9/3/63	half dry grass	1.04	38.48
	New Pasco Bridge to Prosser, Mile 2	Benton	9/3/63	dry grass	-0.741	-27.42
	New Pasco Bridge to Prosser, Mile 4	Benton	9/3/63	dry grass	0.376	13.91
	New Pasco Bridge to Prosser, Mile 6	Benton	9/3/63	dry grass	3.08	113.96
	New Pasco Bridge to Prosser, Mile 8	Benton	9/3/63	leafy sage	2.49	92.13
	New Pasco Bridge to Prosser, Mile 10	Benton	9/3/63	leafy sage	2.15	79.55
	New Pasco Bridge to Prosser, Mile 12	Benton	9/3/63	green hay	13	481
	New Pasco Bridge to Prosser, Mile 14	Benton	9/3/63	leafy sage	4.06	150.22
	New Pasco Bridge to Prosser, Mile 16	Benton	9/3/63	leafy sage	1.97	72.89
	New Pasco Bridge to Prosser, Mile 18	Benton	9/3/63	half dry grass	1.8	66.6
	New Pasco Bridge to Prosser, Mile 20	Benton	9/3/63	dry grass	0.735	27.2
	New Pasco Bridge to Prosser, Mile 22	Benton	9/3/63	leafy sage	1.16	42.92
	New Pasco Bridge to Prosser, Mile 24	Benton	9/3/63	green grass	0.649	24.01
	New Pasco Bridge to Prosser, Mile 26	Benton	9/3/63	green grass	1.29	47.73
	New Pasco Bridge to Prosser, Mile 28	Benton	9/3/63	green grass	0.37	13.69
	New Pasco Bridge to Prosser, Mile 30	Benton	9/3/63	green grass	0.621	22.98
	Prosser, East of City Limits	Benton	9/3/63	green grass	0.405	14.99
Farm A	Benton City	Benton	9/4/63	pasture grass	1.53	56.61
Farm A	Benton City	Benton	9/5/63	pasture grass	1.39	51.43
Farm A	Benton City	Benton	9/6/63	pasture grass	1.78	65.86
Farm J		Benton	9/7/63	pasture grass	1.6	59.2
Farm M		Benton	9/7/63	pasture grass	1.36	50.32
	614 Building - Benton City	Benton	9/7/63	leafy weeds	1.53	56.61
	614 Building - Kennewick	Benton	9/7/63	leafy weeds	0.598	22.13
Farm A	Benton City	Benton	9/7/63	pasture grass	2.61	96.57
Farm A	Benton City	Benton	9/8/63	pasture grass	1.04	38.48
Farm A	Benton City	Benton	9/9/63	pasture grass	0.344	12.73
Farm A	Benton City	Benton	9/10/63	pasture grass	0.387	14.32
Farm M		Benton	9/11/63	pasture grass	0.054	2
Farm A	Benton City	Benton	9/11/63	pasture grass	0.049	1.81
Farm A	Benton City	Benton	9/12/63	pasture grass	0.376	13.91
Farm B	Twin Bridge	Benton	9/12/63	pasture grass	0.938	34.71
Farm A	Benton City	Benton	9/13/63	pasture grass	0.119	4.4

TABLE I–VI. (cont.)

Farm	Collection site	County	Date	Vegetation type	Concentration of ^{131}I	
					pCi g^{-1}	Bq kg^{-1}
Farm B	Twin Bridge	Benton	9/13/63	pasture grass	0.24	8.88
Farm B	Twin Bridge	Benton	9/13/63	pasture grass	1.15	42.55
Farm A	Benton City	Benton	9/14/63	pasture grass	0.201	7.44
Farm A	Benton City	Benton	9/16/63	pasture grass	0.175	6.48
Farm B	Twin Bridge	Benton	9/16/63	pasture grass	0.391	14.47
Farm A	Benton City	Benton	9/17/63	pasture grass	0.371	13.73
Farm B	Twin Bridge	Benton	9/17/63	pasture grass	0.327	12.1
Farm A	Benton City	Benton	9/18/63	pasture grass	0.359	13.28
Farm B	Twin Bridge	Benton	9/18/63	pasture grass	0.994	36.78
Farm A	Benton City	Benton	9/19/63	pasture grass	0.368	13.62
Farm B	Twin Bridge	Benton	9/19/63	pasture grass	0.356	13.17
Farm A	Benton City	Benton	9/20/63	pasture grass	0.195	7.22
Farm B	Twin Bridge	Benton	9/20/63	pasture grass	0.495	18.32
Farm A	Benton City	Benton	9/23/63	weeds	0.223	8.25
Farm B	Twin Bridge	Benton	9/23/63	pasture grass	0.552	20.42
Farm A	Benton City	Benton	9/24/63	weeds	0.295	10.92
Farm B	Twin Bridge	Benton	9/24/63	weeds	0.839	31.04
Farm A	Benton City	Benton	9/25/63	pasture grass	0.612	22.64
Farm B	Twin Bridge	Benton	9/25/63	pasture grass	0.575	21.28
Farm A	Benton City	Benton	9/26/63	pasture grass	1.11	41.07
Farm B	Twin Bridge	Benton	9/26/6	pasture grass	1.02	37.74
Farm A	Benton City	Benton	9/27/63	pasture grass	0.311	11.51
Farm B	Twin Bridge	Benton	9/27/63	pasture grass	0.59	21.83
Farm A	Benton City	Benton	9/30/63	alfalfa	0.236	8.73
Farm B	Twin Bridge	Benton	9/30/63	pasture grass	0.374	13.84
Farm G	Byers Landing	Franklin	9/3/63	pasture grass	0.3	11.1
Farm Z	Eltopia	Franklin	9/3/63	pasture grass	0.093	3.44
Farm N	Mesa	Franklin	9/3/63	pasture grass	0.264	9.77
Farm T	Pasco	Franklin	9/3/63	pasture grass	0.468	17.32

TABLE I–VI. (cont.)

Farm	Collection site	County	Date	Vegetation type	Concentration of ^{131}I	
					pCi g^{-1}	Bq kg^{-1}
Farm T	Pasco	Franklin	9/3/63	pasture grass	0.616	22.79
	Pasco	Franklin	9/3/63	leafy sage	0.146	5.4
	Radar Hill	Franklin	9/3/63	leafy sage	0.259	9.58
	Radar Hill to Pasco, Mile 2	Franklin	9/3/63	leafy sage	-0.076	-2.81
	Radar Hill to Pasco, Mile 4	Franklin	9/3/63	green hay	0.263	9.73
	Radar Hill to Pasco, Mile 6	Franklin	9/3/63	green alfalfa	0.264	9.77
	Radar Hill to Pasco, Mile 8	Franklin	9/3/63	green grass	0.235	8.7
	Radar Hill to Pasco, Mile 10	Franklin	9/3/63	leafy sage	0.234	8.66
	Radar Hill to Pasco, Mile 12	Franklin	9/3/63	leafy sage	0.0676	2.5
	Radar Hill to Pasco, Mile 14	Franklin	9/3/63	half dry grass	-0.465	-17.21
	Radar Hill to Pasco, Mile 18	Franklin	9/3/63	green hay	0.732	27.08
	Radar Hill to Pasco, Mile 20	Franklin	9/3/63	leafy sage	-0.161	-5.96
	Radar Hill to Pasco, Mile 22	Franklin	9/3/63	leafy sage	0.477	17.65
	Radar Hill to Pasco, Mile 24	Franklin	9/3/63	green clover	0.489	18.09
	Radar Hill to Pasco, Mile 26	Franklin	9/3/63	leafy sage	0.074	2.74
	Radar Hill to Pasco, Mile 28	Franklin	9/3/63	leafy sage	0.127	4.7
	Radar Hill to Pasco, Mile 30	Franklin	9/3/63	leafy sage	0.355	13.14
	Radar Hill to Pasco, Mile 32	Franklin	9/3/63	leafy sage	0.37	13.69
	Radar Hill to Pasco, Mile 34	Franklin	9/3/63	dry rye heads	-0.414	-15.32
	Radar Hill to Pasco, Mile 36	Franklin	9/3/63	leafy sage	0.152	5.62
	Radar Hill to Pasco, Mile 38	Franklin	9/3/63	leafy sage	-0.249	-9.21
Farm K	Ringold	Franklin	9/3/63	pasture grass	1.25	46.25
Farm H	Riverview	Franklin	9/3/63	pasture grass	0.495	18.32
Farm G	Byers Landing	Franklin	9/4/63	pasture grass	0.18	6.66
Farm Z	Eltopia	Franklin	9/4/63	pasture grass	0.174	6.44
Farm Z	Eltopia	Franklin	9/4/63	hay	-0.0104	-0.38
Farm T	Pasco	Franklin	9/4/63	pasture grass	0.365	13.51
Farm K	Ringold	Franklin	9/4/63	pasture grass	0.204	7.55
Farm N	Mesa	Franklin	9/5/63	pasture grass	0.245	9.07
Farm T	Pasco	Franklin	9/5/63	pasture grass	0.537	19.87
Farm K	Ringold	Franklin	9/5/63	pasture grass	0.504	18.65
Farm H	Riverview	Franklin	9/5/63	pasture grass	2.68	99.16

TABLE I–VI. (cont.)

Farm	Collection site	County	Date	Vegetation type	Concentration of ^{131}I	
					pCi g^{-1}	Bq kg^{-1}
Farm T	Pasco	Franklin	9/6/63	pasture grass	0.278	10.29
Farm K	Ringold	Franklin	9/6/63	pasture grass	0.083	3.07
	614 Building - Pasco	Franklin	9/7/63	leafy weeds	0.57	21.09
Farm T	Pasco	Franklin	9/7/63	pasture grass	0.323	11.95
Farm K	Ringold	Franklin	9/7/63	pasture grass	0.461	17.06
Farm T	Pasco	Franklin	9/8/63	pasture grass	0.61	22.57
Farm K	Ringold	Franklin	9/8/63	pasture grass	0.433	16.02
Farm T	Pasco	Franklin	9/9/63	pasture grass	0.184	6.81
Farm K	Ringold	Franklin	9/9/63	pasture grass	0.466	17.24
Farm H	Riverview	Franklin	9/9/63	pasture grass	0.792	29.3
Farm T	Pasco	Franklin	9/10/63	pasture grass	0.177	6.55
	Pasco	Franklin	9/10/63	clover	0.579	21.42
Farm K	Ringold	Franklin	9/10/63	pasture grass	0.13	4.81
Farm G	Byers Landing	Franklin	9/11/63	pasture grass	0.261	9.66
Farm Z	Eltopia	Franklin	9/11/63	pasture grass	0.195	7.22
Farm N	Mesa	Franklin	9/11/63	pasture grass	0.118	4.37
Farm T	Pasco	Franklin	9/11/63	pasture grass	0.11	4.07
Farm K	Ringold	Franklin	9/11/63	pasture grass	0.374	13.84
Farm T	Pasco	Franklin	9/12/63	pasture grass	0.327	12.1
Farm K	Ringold	Franklin	9/12/63	pasture grass	0.259	9.58
Farm T	Pasco	Franklin	9/13/63	pasture grass	0.0534	1.98
Farm K	Ringold	Franklin	9/13/63	pasture grass	0.0134	0.5
Farm T	Pasco	Franklin	9/14/63	pasture grass	0.129	4.77
Farm T	Pasco	Franklin	9/16/63	pasture grass	0.0935	3.46
Farm K	Ringold	Franklin	9/16/63	pasture grass	0.081	3
Farm G	Byers Landing	Franklin	9/17/63	pasture grass	0.251	9.29
Farm T	Pasco	Franklin	9/17/63	pasture grass	0.128	4.74
Farm T	Pasco	Franklin	9/18/63	pasture grass	0.225	8.33
Farm Z	Eltopia	Franklin	9/19/63	pasture grass	0.204	7.55
Farm N	Mesa	Franklin	9/19/63	pasture grass	0.191	7.07
Farm T	Pasco	Franklin	9/19/63	pasture grass	0.297	10.99
Farm K	Ringold	Franklin	9/19/63	pasture grass	0.154	5.7

TABLE I–VI. (cont.)

Farm	Collection site	County	Date	Vegetation type	Concentration of ^{131}I	
					pCi g^{-1}	Bq kg^{-1}
Farm H	Riverview	Franklin	9/19/63	pasture grass	0.902	33.37
Farm T	Pasco	Franklin	9/20/63	pasture grass	0.279	10.32
Farm K	Ringold	Franklin	9/20/63	pasture grass	0.103	3.81
Farm T	Pasco	Franklin	9/23/63	weeds & alfalfa	-0.014	-0.52
Farm K	Ringold	Franklin	9/23/63	weeds	0.319	11.8
Farm T	Pasco	Franklin	9/24/63	weeds	0.31	11.47
Farm K	Ringold	Franklin	9/24/63	pasture grass	0.407	15.06
Farm G	Byers Landing	Franklin	9/25/63	alfalfa	0.185	6.85
Farm Z	Eltopia	Franklin	9/25/63	alfalfa	0.161	5.96
Farm N	Mesa	Franklin	9/25/63	alfalfa	0.359	13.28
Farm T	Pasco	Franklin	9/25/63	weeds	0.217	8.03
Farm K	Ringold	Franklin	9/25/63	pasture grass	0.47	17.39
Farm H	Riverview	Franklin	9/25/63	weeds	0.317	11.73
Farm T	Pasco	Franklin	9/26/63	alfalfa	0.095	3.52
Farm K	Ringold	Franklin	9/26/63	pasture grass	0.178	6.59
Farm T	Pasco	Franklin	9/27/63	pasture grass	0.101	3.74
Farm K	Ringold	Franklin	9/27/63	pasture grass	0.315	11.66
Farm T	Pasco	Franklin	9/30/63	pasture grass	0.203	7.51

TABLE I–VII. OBSERVED ^{131}I MEASUREMENTS IN AIR ($\times 10^{-2}$ Bq/m^3)

Location:	100 BSE	100-F	100-K	100-D	100 HE	200 ESE	200 EWC	200 EEC	200E SEMI	REDOX	200 WEC	200 WWC	300-A	HANFORD	WHITE BLUFFS	BYERS LANDING	700-A	1100-A	BENTON CITY	PASCO	KENN
Date																					
26-8-63	0.0	0.059	0.015	-0.041	0.044	0.17	0.16	0.663	0.26	0.637	0.11	0.12	-0.0074	0.0	0.0	0.19	0.056	0.067	0.067	0.019	0.081
27-8-63	3.15	0.078	0.27	0.056	0.11	7.281	0.078	31.52	0.404	0.637	0.11	0.12	1.17	0.096	0.13	0.19	0.056	0.067	0.067	0.019	0.081
28-8-63	3.15	0.078	0.27	0.056	0.11	7.281	0.078	31.52	0.404	1.61	0.067	5.511	1.17	0.096	0.13	0.19	0.422	0.29	0.21	0.096	0.23
29-8-63	3.15	0.078	0.27	0.056	0.11	7.281	0.078	31.52	0.404	1.61	0.067	5.511	1.17	0.096	0.13	0.19	0.422	0.29	0.21	0.096	0.23
30-8-63	3.15	0.078	0.27	0.056	0.11	7.281	0.078	31.52	0.404	1.61	0.067	5.511	1.17	0.096	0.13	0.511	0.422	0.29	0.21	0.096	0.23
31-8-63	3.15	0.078	0.27	0.056	0.11	7.281	0.078	31.52	0.404	1.61	0.067	5.511	1.17	0.096	0.13	0.511	0.422	0.29	0.21	0.096	0.23
1-9-63	3.15	0.078	0.27	0.056	0.11	7.281	0.078	31.52	0.404	1.61	0.067	5.511	1.17	0.096	0.13	0.511	0.422	0.29	0.21	0.096	0.23
2-9-63	3.15	0.078	0.27	0.056	0.11	7.281	0.078	31.52	0.404	1.61	0.067	5.511	1.17	0.096	0.13	0.511	0.422	0.29	0.21	0.096	0.23
3-9-63	3.15	1.17	0.27	1.29	1.044	194.74	8.456	269.27	17.24	13.46	0.10	5.511	0.31	1.75	0.774	0.511	0.422	0.29	0.21	0.096	0.23
4-9-63	3.15	1.17	0.27	1.29	1.044	12.54	0.796	8.341	0.426	1.29	0.10	0.548	0.31	1.75	0.774	0.374	0.878	0.37	0.526	0.31	0.37
5-9-63	0.593	0.13	0.16	0.14	0.13	12.54	0.796	8.341	0.426	1.29	0.10	0.548	0.31	0.15	0.13	0.374	0.878	0.37	0.526	0.31	0.37
6-9-63	0.593	0.13	0.16	0.14	0.13	12.54	0.796	8.341	0.426	1.29	0.10	0.548	0.31	0.15	0.13	0.12	0.878	0.37	0.526	0.31	0.37
7-9-63	0.593	0.13	0.16	0.14	0.13	12.54	0.796	8.341	0.426	1.29	0.10	0.548	0.31	0.15	0.13	0.12	0.878	0.37	0.526	0.31	0.37
8-9-63	0.593	0.13	0.16	0.14	0.13	12.54	0.796	8.341	0.426	1.29	0.10	0.548	0.31	0.15	0.13	0.063	0.093	0.37	0.022	0.070	0.096
9-9-63	0.593	0.13	0.16	0.14	0.13	12.54	0.796	8.341	0.426	1.29	0.10	0.548	0.31	0.15	0.13	0.063	0.093	0.37	0.022	0.070	0.096
10-9-63	0.20	0.048	0.13	0.059	0.011	0.30	0.17	0.941	0.493	1.29	0.10	0.548	0.041	0.074	0.089	0.063	0.093	0.37	0.022	0.070	0.096
11-9-63	0.20	0.048	0.13	0.059	0.011	0.30	0.17	0.941	0.493	0.063	0.17	0.28	0.041	0.074	0.089	0.063	0.063	0.015	0.044	-0.022	0.030
12-9-63	0.20	0.048	0.13	0.059	0.011	0.30	0.17	0.941	0.493	0.063	0.17	0.28	0.041	0.074	0.089	0.063	0.063	0.015	0.044	-0.022	0.030
13-9-63	0.20	0.048	0.13	0.059	0.011	0.30	0.17	0.941	0.493	0.063	0.17	0.28	0.041	0.074	0.089	0.28	0.063	0.015	0.044	-0.022	0.030
14-9-63	0.20	0.048	0.13	0.059	0.011	0.30	0.17	0.941	0.493	0.063	0.17	0.28	0.041	0.074	0.089	0.28	0.063	0.015	0.044	-0.022	0.030
15-9-63	0.20	0.048	0.13	0.059	0.011	0.30	0.17	0.941	0.493	0.063	0.17	0.28	0.041	0.074	0.089	0.28	0.063	0.015	0.044	-0.022	0.030
16-9-63	0.20	0.048	0.13	0.059	0.011	0.30	0.17	0.941	0.493	0.063	0.17	0.28	0.041	0.074	0.089	0.28	0.063	0.015	0.044	-0.022	0.030
17-9-63	0.070	0.059	0.067	0.16	0.074	0.16	0.074	0.493	0.770	0.063	0.17	0.28	0.570	0.067	0.052	0.28	0.063	0.015	0.044	-0.022	0.030
18-9-63	0.070	0.059	0.067	0.16	0.074	0.16	0.074	0.493	0.770	0.496	0.096	0.24	0.570	0.067	0.052	0.28	0.13	0.18	0.078	0.11	0.067
19-9-63	0.070	0.059	0.067	0.16	0.074	0.16	0.074	0.493	0.770	0.496	0.096	0.24	0.570	0.067	0.052	0.28	0.13	0.18	0.078	0.11	0.067
20-9-63	0.070	0.059	0.067	0.16	0.074	0.16	0.074	0.493	0.770	0.496	0.096	0.24	0.570	0.067	0.052	0.28	0.13	0.18	0.078	0.11	0.067
21-9-63	0.070	0.059	0.067	0.16	0.074	0.16	0.074	0.493	0.770	0.496	0.096	0.24	0.570	0.067	0.052	0.28	0.13	0.18	0.078	0.11	0.067
22-9-63	0.070	0.059	0.067	0.16	0.074	0.16	0.074	0.493	0.770	0.496	0.096	0.24	0.570	0.067	0.052	0.28	0.13	0.18	0.078	0.11	0.067
23-9-63	0.070	0.059	0.067	0.16	0.074	0.16	0.074	0.493	0.770	0.496	0.096	0.24	0.570	0.067	0.052	0.28	0.13	0.18	0.078	0.11	0.067
24-9-63	0.16	0.063	0.11	0.081	0.10	0.530	0.27	0.667	0.36	0.496	0.096	0.24	0.14	0.085	0.070	0.28	0.13	0.18	0.078	0.11	0.067
25-9-63	0.16	0.063	0.11	0.081	0.10	0.530	0.27	0.667	0.36	2.71	0.067	0.419	0.14	0.085	0.070	0.28	0.093	0.037	0.078	0.037	0.011
26-9-63	0.16	0.063	0.11	0.081	0.10	0.530	0.27	0.667	0.36	2.71	0.067	0.419	0.14	0.085	0.070	0.11	0.093	0.037	0.093	0.037	0.011
27-9-63	0.16	0.063	0.11	0.081	0.10	0.530	0.27	0.667	0.36	2.71	0.067	0.419	0.14	0.085	0.070	0.033	0.093	0.037	0.093	0.037	0.011
28-9-63	0.16	0.063	0.11	0.081	0.10	0.530	0.27	0.667	0.36	2.71	0.067	0.419	0.14	0.085	0.070	0.033	0.093	0.037	0.093	0.037	0.011
29-9-63	0.16	0.063	0.11	0.081	0.10	0.530	0.27	0.667	0.36	2.71	0.067	0.419	0.14	0.085	0.070	0.033	0.093	0.037	0.093	0.037	0.011
30-9-63	0.16	0.063	0.11	0.081	0.10	0.530	0.27	0.667	0.36	2.71	0.067	0.419	0.14	0.085	0.070	0.033	0.093	0.037	0.093	0.037	0.011

TABLE I–VIII. MEASURED CONCENTRATIONS OF ^{131}I IN MILK SAMPLES

Farm or Dairy	Collection site	County	Date	Concentration of ^{131}I	
				pCi g^{-1}	Bq kg^{-1}
Farm A	Benton City	Benton	9/4/63	64.8	2.40
Farm L	Kiona	Benton	9/4/63	10.3	0.38
Farm A	Benton City	Benton	9/5/63	117	4.33
Twin City	Prosser - Benton City	Benton	9/5/63	3.1	0.11
Farm A	Benton City	Benton	9/6/63	113	4.18
Farm A	Benton City	Benton	9/7/63	96.7	3.58
Farm J		Benton	9/7/63	91	3.37
Farm M		Benton	9/7/63	56.6	2.09
Twin City	Prosser - Benton City	Benton	9/7/63	58.7	2.17
Farm A	Benton City	Benton	9/8/63	77.7	2.87
Farm L	Kiona	Benton	9/8/63	< 4.2	< 0.16
Farm A	Benton City	Benton	9/9/63	69.4	2.57
Farm A	Benton City	Benton	9/10/63	33.8	1.25
Farm A	Benton City	Benton	9/11/63	29.4	1.09
Farm A	Benton City	Benton	9/12/63	22.9	0.85
Farm B	1 Mile North of Twin Bridges	Benton	9/12/63	136	5.03
Farm A	Benton City	Benton	9/13/63	19.6	0.73
Farm B	1 Mile North of Twin Bridges	Benton	9/13/63	119	4.40
Farm A	Benton City	Benton	9/14/63	16.1	0.60
Farm B	1 Mile North of Twin Bridges	Benton	9/14/63	95.1	3.52
Farm A	Benton City	Benton	9/16/63	24.5	0.91
Farm B	1 Mile North of Twin Bridges	Benton	9/16/63	48.4	1.79
Farm A	Benton City	Benton	9/17/63	22	0.81
Farm B	1 Mile North of Twin Bridges	Benton	9/17/63	65.2	2.41
Twin City	Prosser - Benton City	Benton	9/17/63	19.7	0.73
Farm A	Benton City	Benton	9/18/63	19.5	0.72
Farm B	1 Mile North of Twin Bridges	Benton	9/18/63	43.4	1.61
Farm A	Benton City	Benton	9/19/63	20.2	0.75
Farm B	1 Mile North of Twin Bridges	Benton	9/19/63	54.4	2.01
Farm A	Benton City	Benton	9/20/63	19.2	0.71
Farm B	1 Mile North of Twin Bridges	Benton	9/20/63	51.9	1.92
Farm A	Benton City	Benton	9/23/63	19.2	0.71
Farm B	1 Mile North of Twin Bridges	Benton	9/23/63	38.7	1.43
Farm A	Benton City	Benton	9/24/63	14.3	0.53
Farm B	1 Mile North of Twin Bridges	Benton	9/24/63	31.3	1.16
Farm A	Benton City	Benton	9/25/63	11.4	0.42
Farm B	1 Mile North of Twin Bridges	Benton	9/25/63	32.9	1.22
Farm A	Benton City	Benton	9/26/63	9.4	0.35
Farm B	1 Mile North of Twin Bridges	Benton	9/26/63	25.8	0.95
Farm A	Benton City	Benton	9/27/63	9.8	0.36
Farm B	1 Mile North of Twin Bridges	Benton	9/27/63	25.8	0.95
Farm A	Benton City	Benton	9/30/63	10.7	0.40
Farm B	1 Mile North of Twin Bridges	Benton	9/30/63	29.1	1.08
Darigold		composite	9/16/63	8	0.30
Lucerne		composite	9/16/63	< 1.2	< 0.04
Twin City		composite	9/16/63	12.3	0.46
Darigold		composite	9/26/63	1.9	0.07
Lucerne		composite	9/26/63	3.8	0.14
Twin City		composite	9/26/63	4.1	0.15
Farm T	Pasco	Franklin	9/3/63	< 2.0	< 0.07
Farm Z	Eltopia	Franklin	9/4/63	9.9	0.37
Farm G	Byers Landing	Franklin	9/4/63	10.2	0.38
Farm K	Ringold	Franklin	9/4/63	16.1	0.60
Farm T	Pasco	Franklin	9/4/63	18.9	0.70
Farm H	Riverview	Franklin	9/5/63	40	1.48
Farm K	Ringold	Franklin	9/5/63	30.4	1.12

TABLE I–VIII. (cont.)

Farm or Dairy	Collection site	County	Date	Concentration of ^{131}I	
				pCi g^{-1}	Bq kg^{-1}
Farm N	Mesa	Franklin	9/5/63	3.6	0.13
Farm T	Pasco	Franklin	9/5/63	22.8	0.84
Twin City	Columbia Basin	Franklin	9/5/63	4	0.15
Farm K	Ringold	Franklin	9/6/63	36.1	1.34
Farm T	Pasco	Franklin	9/6/63	17.2	0.64
Farm K	Ringold	Franklin	9/7/63	32.9	1.22
Farm T	Pasco	Franklin	9/7/63	14.4	0.53
Farm K	Ringold	Franklin	9/8/63	27.5	1.02
Farm T	Pasco	Franklin	9/8/63	17.3	0.64
Twin City	Columbia Basin	Franklin	9/8/63	18.1	0.67
Farm K	Ringold	Franklin	9/9/63	89.2	3.30
Farm T	Pasco	Franklin	9/9/63	37.1	1.37
Farm K	Ringold	Franklin	9/10/63	23.2	0.86
Farm T	Pasco	Franklin	9/10/63	20.8	0.77
Farm Z	Eltopia	Franklin	9/11/63	10.1	0.37
Farm G	Byers Landing	Franklin	9/11/63	28.6	1.06
Farm H	Riverview	Franklin	9/11/63	37	1.37
Farm K	Ringold	Franklin	9/11/63	14.9	0.55
Farm N	Mesa	Franklin	9/11/63	34.2	1.27
Farm T	Pasco	Franklin	9/11/63	13.8	0.51
Farm K	Ringold	Franklin	9/12/63	12.2	0.45
Farm T	Pasco	Franklin	9/12/63	14.3	0.53
Farm K	Ringold	Franklin	9/13/63	8.2	0.30
Farm T	Pasco	Franklin	9/13/63	19.8	0.73
Farm T	Pasco	Franklin	9/14/63	8.3	0.31
Farm K	Ringold	Franklin	9/16/63	5.8	0.21
Farm T	Pasco	Franklin	9/16/63	4.2	0.16
Farm G	Byers Landing	Franklin	9/17/63	36.8	1.36
Farm K	Ringold	Franklin	9/17/63	32.3	1.20
Farm T	Pasco	Franklin	9/17/63	4.7	0.17
Twin City	Columbia Basin	Franklin	9/17/63	18.7	0.69
Farm K	Ringold	Franklin	9/18/63	8.3	0.31
Farm T	Pasco	Franklin	9/18/63	5.2	0.19
Farm Z	Eltopia	Franklin	9/19/63	7.1	0.26
Farm H	Riverview	Franklin	9/19/63	12.3	0.46
Farm K	Ringold	Franklin	9/19/63	12.3	0.46
Farm N	Mesa	Franklin	9/19/63	19	0.70
Farm T	Pasco	Franklin	9/19/63	7	0.26
Farm K	Ringold	Franklin	9/20/63	31	1.15
Farm T	Pasco	Franklin	9/20/63	6.2	0.23
Farm K	Ringold	Franklin	9/23/63	11.4	0.42
Farm T	Pasco	Franklin	9/23/63	3	0.11
Farm K	Ringold	Franklin	9/24/63	14.2	0.53
Farm T	Pasco	Franklin	9/24/63	3.8	0.14
Farm Z	Eltopia	Franklin	9/25/63	8.4	0.31
Farm G	Byers Landing	Franklin	9/25/63	12.3	0.46
Farm H	Riverview	Franklin	9/25/63	7.4	0.27
Farm K	Ringold	Franklin	9/25/63	8.7	0.32
Farm N	Mesa	Franklin	9/25/63	17.3	0.64
Farm T	Pasco	Franklin	9/25/63	5.4	0.20
Farm K	Ringold	Franklin	9/26/63	14.2	0.53
Farm T	Pasco	Franklin	9/26/63	8	0.30
Farm K	Ringold	Franklin	9/27/63	10.6	0.39
Farm T	Pasco	Franklin	9/27/63	5.5	0.20
Farm K	Ringold	Franklin	9/30/63	4.8	0.18
Farm T	Pasco	Franklin	9/30/63	5.2	0.19

TABLE I–IX. AVERAGE DAILY CONSUMPTION OF LEAFY GREEN VEGETABLES AND FRESH MILK BY AGE GROUP IN THE SPRING OF 1965

Age group	Leafy green vegetables (g)	Fresh milk (g)	Number of observations
Males			
< 1	0 (0)[a]	588 (478)	8
1-4	9 (16)	453 (250)	52
5-9	15 (22)	678 (314)	72
10-14	18 (29)	725 (388)	99
15-19	32 (39)	755 (564)	84
> 20	47 (60)	377 (370)	534
Females			
< 1	0 (0)	550 (498)	14
1-4	5 (13)	549 (273)	44
5-9	18 (20)	635 (301)	71
10-14	22 (32)	588 (328)	79
15-19	29 (44)	523 (403)	88
> 20	50 (63)	260 (257)	608

[a] Mean (standard deviation).

I–4. AGRICULTURAL DATA

The following information was taken from the *"1963 United States Census of Agriculture, Volume 1 Part 46 – Washington"*, published by the U.S. Department of Commerce, Bureau of the Census. The information is not specific to eastern Washington State. It was provided to give the participants with a general idea of the nature of agricultural practices at the time of the release.

TABLE I–X. LETTUCE, COMMERCIAL CROP: ACREAGE AND PRODUCTION IN WASHINGTON STATE, EARLY FALL 1963

Production measure	Quantities
Acreage	1 000 acres (400 ha)
Production	165 000 cwt (7500 tonnes)

TABLE I–XI. TOTAL ACREAGE, YIELD, PRODUCTION OF HAY IN WASHINGTON STATE IN 1963

Production measure	Quantities
Area Harvested	854 000 acres (346 000 ha)
Total production	1 976 000 tons (1 796 000 tonnes)
Production kept on farms	1 304 000 tons (1 185 000 tonnes)
Production sold	672 000 tons (615 000 tonnes)

TABLE I–XII. ACREAGE AND PRODUCTION OF ALFALFA AND ALFALFA MIXTURES, CLOVER, TIMOTHY, AND MIXTURES OF CLOVER AND GRASSES IN WASHINGTON STATE IN 1963

Production measure	Quantities
Alfalfa and alfalfa mixtures	
Area harvested	444 000 acres (180 000 ha)
Production	1 243 000 tons (1 130 000 tonnes)
Clover, timothy, and mixtures of clover and grasses	
Area harvested	238 000 acres (96 000 ha)
Production	476 000 tons (433 000 tonnes)
Wild hay	
Area harvested	43 000 acres (17 400 ha)
Production	54 000 tons (49 000 tonnes)

TABLE I–XIII. FEED (INCLUDING PASTURE) CONSUMED BY LIVESTOCK AND POULTRY, EXPRESSED IN FEED UNIT)[a] 1950–1962

Intake	Quantity
Milk cows (per head)	7405
Other dairy cattle (per head)	4474
Milk cows (per 100 pounds milk produced)	110

[a] A feed unit is the equivalent of pound of corn in feeding value.

TABLE I–XIV. MILK COWS RATIONS: CONCENTRATES AND ROUGHAGE FED PER COW AND DAIRY PASTURE IN WASHINGTON STATE IN 1963

Intake information	Quantities
Grain and other concentrates fed during calendar year	
per cow	2 490 lb (1130 kg)
per 100 pounds (45 kg) of milk produced	28 lb (12.7 kg)
Roughage fed during winter feeding period beginning in october:[a]	
Hay, per cow	2.7 tons (2.45 tonnes)
All roughage, per cow, hay equivalent[b]	3.6 tons (3.26 tonnes)
Condition of dairy pasture feed percent of normal: [c]	89%

[a] Average for the October-May feeding period as reported by dairy correspondents.
[b] In computing hay equivalents, 3 tons of silage are considered equal to 1 ton of hay.
[c] Seasonal average condition for April 1-Oct. 1 period.

TABLE I–XV. MILK COW RATIONS: INDIVIDUAL FEEDS AS PERCENTAGE OF TOTAL CONCENTRATE RATIONS FED TO MILK

Feed constituents	Percentage
Corn	3
Oats	3
Barley	4
Commercial mixed feeds	79
Miscellaneous other	11

TABLE I–XVI. MILK, MILKFAT, AND BUTTER PRODUCTION ON FARMS: NUMBER OF PRODUCING COWS, YIELD PER COW, AND TOTAL QUANTITY PRODUCED IN WASHINGTON STATE

Production information	Quantities
Number of milk cows on farms[a]	222 000
Production of milk per milk cow[b]	8960 lb (4060 kg)
Production of milk fat per milk cow	349 lb (158 kg)
Percentage of fat in milk	3.90%
Total milk production on farms:	994 000 tons (900 000 tonnes)
Total milkfat production on farms:	39 000 tons (35 000 tonnes)
Butter churned on farms	400 000 lb (180 000 kg)

[a] Estimated average number during year, heifers not freshened excluded.
[b] Excludes milk sucked by calves.

TABLE I–XVII. MILK: QUANTITIES USED AND MARKETED BY FARMERS IN WASHINGTON STATE IN 1963

Production information	Quantities
Milk used on farms where produced	
Fed to calves[a]	24 500 tons (22 000 tonnes)
Consumed as fluid milk or cream	28 500 tons (26 000 tonnes)
Used for farm churned butter	4 500 tons (4 100 tonnes)
Total utilized on farms	57 500 tons (52 000 tonnes)
Milk marketed by farmers:	
Whole milk delivered to plants and dealers	905 000 tons (822,000 tonnes)
Farm skimmed cream	15 000 tons (13 600 tonnes)
Retailed by farmers as milk and cream[b]	17 000 tons (15 500 tonnes)
Combined milk and cream marketing	937 000 tons (852,000 tonnes)

[a] Excludes milk sucked by calves.
[b] Sales by producer-distributors and other farmers on own routes or at farm.

TABLE I–XVIII. FARM DAIRY PRODUCTS: QUANTITY SOLD, AND FARM USE IN WASHINGTON STATE IN 1963

Production information	Quantities
Deliveries to plants, dealers, etc. at wholesale	
Whole milk sold	905 000 tons (822,000 tonnes)
Farm separated milkfat cream sold	630 tons (573 tonnes)
Milk and cream retailed by farmers	16 000 000 quarts (15 000 000 L) milk equivalent

TABLE I-XIX. DAIRY PRODUCTS: ANNUAL PER CAPITA CIVILIAN CONSUMPTION, IN THE UNITED STATES IN 1963

Intake	Quantity
Butter[a]: (per capita)	6.7 lb (3.0 kg)
Cheese[b]:(per capita)	9.3 lb (4.2 kg)
Condensed and evaporated milk[c]: (per capita)	11.7 lb (5.3 kg)
Ice cream (product weight) (per capita)	18.1 lb (8.2 kg)
Dry whole milk (per capita)	0.19 lb (86 g)
Non-fat dry milk (per capita)	5.6 lb (2.5 kg)

[a] Includes both farm and factory-made butter.
[b] Includes all kinds of cheese except cottage, pot, and bakers' cheese, and full-skim American.
[c] The evaporated milk is unskimmed, unsweetened, case goods. The condensed milk is unsweetened (plain condensed) unskimmed, bulk goods, and sweetened condensed milk is unskimmed, case, and bulk goods.

TABLE I–XX. ASSUMED[a] MILK COW FEEDING REGIMES DEVELOPED FROM PRECEEDING DATA (FOR EARLY AUTUMN SEASON)

Intake	Quantity
Private Milk Cows	
Pasture grass (dry wt.)	9 kg/day
Grain supplement	1 kg/day
Commercial Dairy Cattle	
Pasture grass (dry wt)	8.5 kg/day
Grain supplement	1.5 kg/day
Alfalfa hay	1.0 kg/day

[a] Beck et al. 1992. PNL-7227 HEDR Hanford Environmental dose Reconstruction Project.

TABLE I–XXI. HUMAN IODINE-131 THYROID BURDEN MEASUREMENTS AT FARM B, 19 OCTOBER 1963

Person measured	Activity measured
4-year-old boy	73 pCi (2.7 Bq)
8-year-old girl	Below detection limit of 30 pCi (1 Bq)

Reference

[1] RAMSDELL, J.V. JR., SIMONEN, C.A., BURK, K.W., Regional Atmiospheric Code for Hanford Emission Tracking (RATCHET), PNWD-2224 HEDR, Pacific Northwest Laboratory, Richland, Wasington (1994).

Annex II

INDIVIDUAL EVALUATIONS OF MODEL PERFORMANCE

This annex contains the model predictions and descriptions provided by the exercise participants. These contributions have not been edited by the IAEA Secretariat or the Working Group Chairman, but are provided in the form in which they were submitted. The contributions are presented in alphabetical order of the name of the first author.

II–1. LIETDOS-FILTSEG

Used by the Institute of Physics, Lithuania
V. Filistovic, T. Nedveckaite

II–1.1. MODEL DESCRIPTION

II–1.1.1. Name of model, model developer, model users

The version of LIETDOS-FILTSEG (FILTSEG segmental model developed in connection with continuous, routine or accident release of radionuclides, the part of LIETDOS database) used in the HANFORD test scenario was developed by V. Filistovic and T. Nedveckaite. FILTSEG is still under development. The user is Radiation Protection Department (Institute of Physics) and Radiation Protection Center (Lithuanian Republic Ministry of Health).

II–1.1.2. Important model characteristics

FILTSEG is based upon segmental diffusion-convection model of radionuclide (^{131}I) transfer in air. It is run in combination with the time-dependent compartmental model using differential equations and transfer factors to simulate the transport of radionuclide through agricultural ecosystems to human. It is used together with subroutine APSVITA to estimate frequency distribution of thyroid equivalent dose with consideration of regional stable iodine deficiency and application of Monte Carlo procedure. Dose is calculated also from immersion into the plume and external irradiation from ground surface.

II–1.1.3. Past experiences using FILTSEG model

Preliminary calibrations or a calculation has not been performed. FILTSEG thyroid equivalent dose evaluation model and subroutine APSVITA was used for dose evaluation of Lithuanian inhabitants after the Chernobyl accident. Some results of these investigations is described in the following publications:

(1) Styra, T. Nedveckaite, V. Filistovic (1992) *Iodine isotopes and radiation safety*. Sankt-Peterburg: Gidrometeoizdat, p.251 (in Russian)

(2) Nedveckaite T., Filistovic V. (1995) Estimates of thyroid equivalent dose in Lithuania following the Chernobyl accident. Health Phys. **69**: 265-268.

II–1.1.4. Descriptions of procedures, equations and parameters used in model

II–1.1.4.1. Atmospheric diffusion model

The atmospheric diffusion model, imported into LIETDOS-FILTSEG, is dynamic diffusion-convection approach (Figure 33) and considers non-steady state conditions.

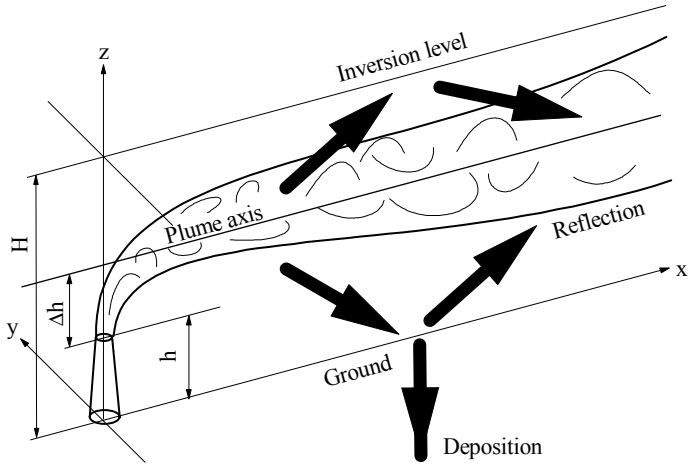

FIG. 33. Model to simulate the behaviour of plume emitted from stack-height source.

Imported segment method (Zanetti, 1986) breaks the plume into independent segments whose initial features and dynamics are a function of local time varying emissions and meteorological conditions. In this formulation plume is described by a series of segments (Figure 34).

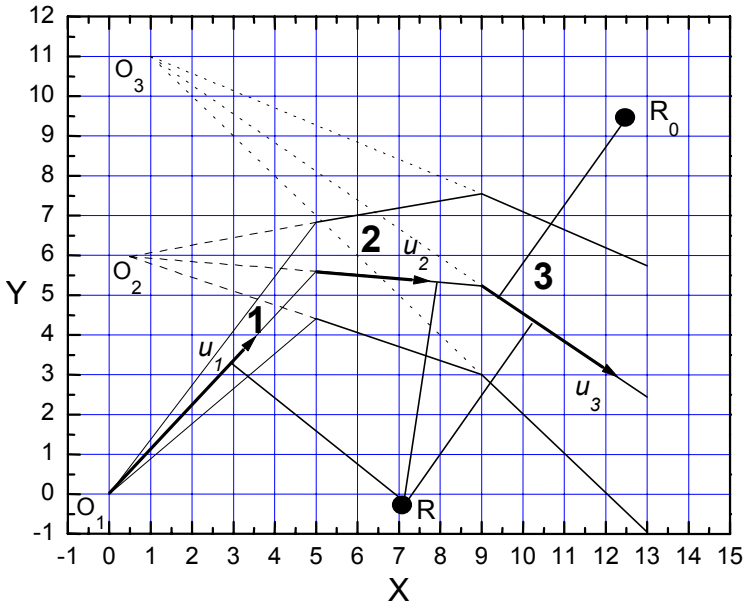

FIG. 34. Schematics of a segmented plume. O_1 is the plume emission point; O_2, O_3 are the imagine emission points for evaluation plume depletion in segment 2 and 3, respectively; u_i are the mean wind speed vectors in i-th segment (i = 1,2,3); R, R_0 – some receptor points in witch concentration are evaluated.

To attain segment steady state formulation diffusion-convection equation, governing the concentration $C_{a,i}(x,y,z)$ of the gaseous reactive (i = r), gaseous organic (i = o) or particulate (i = p) radioiodine, has been written as follows:

$$u\frac{\partial C_{a,i}}{\partial x} - v_g\frac{\partial C_{a,i}}{\partial z} = K_x\frac{\partial^2 C_{a,i}}{\partial x^2} + K_y\frac{\partial^2 C_{a,i}}{\partial y^2} + K_z\frac{\partial^2 C_{a,i}}{\partial z^2} - \lambda_r C_{a,i},$$

where:

x, y, z	=	downwind, crosswind and vertical distance coordinates, respectively (m)
u	=	mean wind velocity (m s^{-1})
v_g	=	gravitational deposition velocity (m s^{-1})
λ_r	=	radioactive decay constant (s^{-1})
K_x, K_y, K_z	=	diffusivities in the x-, y- and z-direction, respectively (m^2 s)

The boundary conditions are:

$$C_{a,i}(x,y,z) \quad as \quad x \to \pm\infty \quad y \to \pm\infty$$

$$\frac{\partial C_{a,i}}{\partial z} = 0 \quad at \quad z = H$$

$$K_z\frac{\partial C_{a,i}}{\partial z} = \left(v_d - v_g\right)C_{a,i} \quad at \quad z = 0$$

$$C_{a,i}(x,y,z) = \frac{f_i Q}{u(h')}\delta(y)\delta(z-h') \quad at \quad x = 0$$

where:

h	=	h + Δh
f_i	=	scenarios partitioning coefficients between the gaseous reactive (i=r), gaseous organic (i=o) and particulate (i=p) fractions (f_r = 0.45; f_o = 0.35; f_p = 0.25)
H	=	height of the inversion layer base (m)
h	=	height (m)
Δh	=	plume rise (m)
Q	=	^{131}I emission rate (Bq s^{-1})

The eddy diffusivities are evaluated from the dispersion coefficients by the relationships:

$$K_y = \frac{\sigma_y^2 u}{2x}; \quad K_z = \frac{\sigma_z^2 u}{2x};$$

Pasquill-Gifford six stability classes together with wind speed data at the release height of the plume was derived from Hanford scenarios. Vertical and horizontal dispersion coefficients were calculated according (Jones, 1980). The effective plume rise (Δh), due to stock gas speed and temperature, and wind speed changes has been evaluated by using Bosanquet formula (Juda and Chrosciel, 1974):

$$\Delta h = 3.55 \frac{\sqrt{V_v v_s}}{u} \left[1.311 - \frac{0.615}{\sqrt{\left(\frac{v_s}{u}\right)^2 + 0.57}} \right]$$

where:

(h	=	plume rise (m)
V_v	=	volumetric gas exit velocity ($m^3\ s^{-1}$)
v_s	=	gas exit velocity ($m\ s^{-1}$)
u	=	mean wind speed ($m\ s^{-1}$)

The solution of the diffusion-convection differential equation, subject to boundary conditions, was obtained using modified Green's functions (Astarita *et al*., 1979). Simulation procedure requires selection of the time step Δt during which segments constituting the plume at any given time are generated. In the present study Δt was as large as 1 h in line with meteorological measurements.

FILTSEG computer software has been developed to calculate hourly radioiodine air activity concentrations, deposition, grass and milk activities over the entire study region. Distributions of time-dependent radioiodine deposition in test area are presented in Figure 35.

II–1.1.4.2. Total dry deposition, D_d

Total dry deposition was calculated as a sum of gaseous reactive, gaseous organic and particulate radioiodine deposition:

$$D_d = \int_o^{t_e} \left[v_{d,r} C_{a,r}(t) + v_{d,o} C_{a,o}(t) + v_{d,p} C_{a,p}(t) \right] dt$$

where:

D_d	=	total ^{131}I dry deposition ($Bq\ m^{-2}$)
$C_{a,r}$, $C_{a,o}$, $C_{a,p}$	=	gaseous reactive, gaseous organic and particulate ^{131}I concentration in air, respectively ($Bq\ m^{-3}$)
$v_{d,r}$, $v_{d,o}$, $v_{d.p}$	=	gaseous reactive, gaseous organic and particulate ^{131}I dry deposition velocity, respectively ($m\ s^{-1}$)
t_e	=	exposure time period (s).

II–1.1.4.3. Grass activity, $C_v(t)$

The time dependent concentration of grass activity at the time t was calculated as a sum of concentrations of gaseous reactive, gaseous organic and particulate radioiodine due to deposition:

$$C_v(t) = C_{v,r}(t) + C_{v,o}(t) + C_{v,p}(t)$$

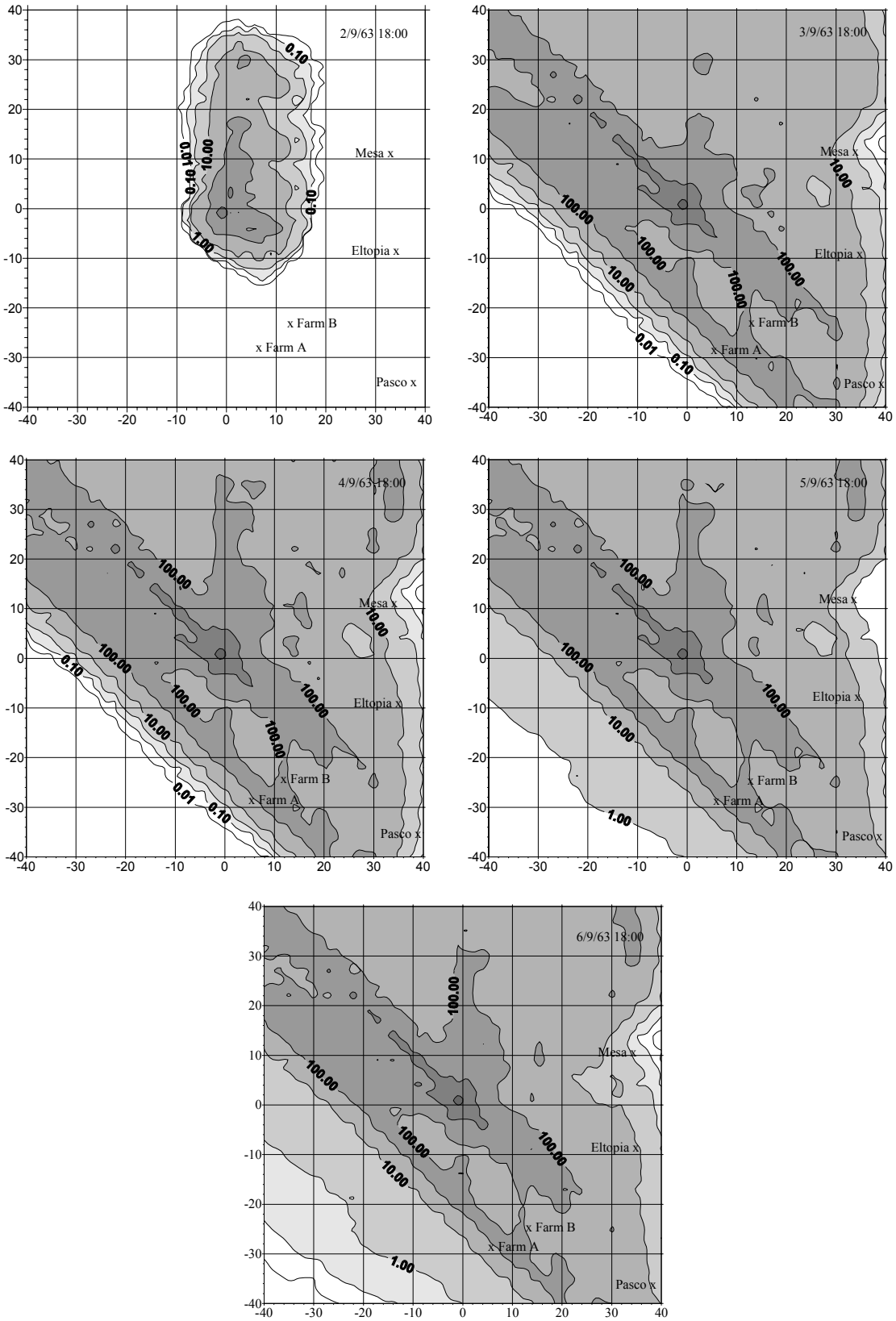

FIG. 35. Distribution of time-dependent ^{131}I deposition (Bq m^{-2}) after the Hanford accident.

$C_{v,r}$, $C_{v,o}$, $C_{v,p}$ were evaluated from equations:

$$\frac{dC_{v,r}(t)}{dt} = \frac{R_d v_{d,r}}{Y} C_{a,r}(t) - (\lambda_r + \lambda_w) C_{v,r}(t);$$
$$\frac{dC_{v,o}(t)}{dt} = \frac{R_d v_{d,o}}{Y} C_{a,o}(t) - (\lambda_r + \lambda_w) C_{v,o}(t);$$
$$\frac{dC_{v,p}(t)}{dt} = \frac{R_d v_{d,p}}{Y} C_{a,p}(t) - (\lambda_r + \lambda_w) C_{v,p}(t)$$

where:

$C_{v,r}$, $C_{v,o}$, $C_{v,p}$	=	gaseous reactive, gaseous organic and particulate ^{131}I concentration in pasture vegetation, respectively (Bq kg^{-1})
$C_{a,r}$, $C_{a,o}$, $C_{a,p}$	=	gaseous reactive, gaseous organic and particulate ^{131}I concentration in air, respectively (Bq m^{-3})
$v_{d,r}$, $v_{d,o}$, $v_{d.p}$	=	gaseous reactive, gaseous organic and particulate ^{131}I dry deposition velocity, rspectively (m s^{-1})
R_d	=	interception factor (1)
Y	=	yield of pasture (kg m^{-2})
λ_r	=	radioactive decay constant (s^{-1})
λ_w	=	activity weathering constant (s^{-1}).

II–1.1.4.4. Milk activity, C_M

Time-dependent radioiodine activity concentration in milk was calculated as follows:

$$C_M(t) = fQ_F F_m \exp(-\lambda_r t_f) C_v(t)$$

where:

C_M	=	^{131}I activity concentration in milk (Bq L^{-1})
C_v	=	^{131}I activity concentration in pasture vegetation (Bq kg^{-1})
f	=	fraction of contaminated forage that reflects periods with different shares of contaminated forage (1)
Q_F	=	cow's total consumption (kg/d^{-1})
t_f	=	time interval between milk-production and consumption (s^{-1})
F_m	=	amount of cattle's daily intake of radionuclide that appears in each litre of milk (dL^{-1}).

II–1.1.4.5. The doses estimation by LIETDOS-FILTSEG

II–1.1.4.5.1. The mean external dose from the cloud for an adult, H_{cloud}

The mean external dose for an adult from cloud is given as follows:

$$H_{cloud} = H^0{}_{cloud} \int_0^{t_e} C_a(t) dt$$

where:

t_e	=	exposure time period (s)
C_a	=	^{131}I activity concentration in air (Bq m^{-3})
H^0_{cloud}	=	dose-rate conversion factor for ^{131}I (1.354(10^{-9} Sv d^{-1} Bq^{-1} m^3 to thyroid and 3.715(10^{-9} Sv d^{-1} Bq^{-1} m^3 to body surface; Kocher, 1980).

II–1.1.4.5.2. The mean external dose from the ground-surface for an adult, H_{ground}

The mean external dose for an adult from contaminated ground is given as follows:

$$H_{ground} = H^0{}_{ground} \int_0^{t_e} D(t)dt$$

where:

H_{ground}	=	maximal (without shielding) dose 1 m above ground (Sv)
t_e	=	exposure time period (s)
C_a	=	^{131}I activity concentration in air (Bq m^{-3})
H^0_{ground}	=	dose-rate 1 m above ground per unit of activity deposition for ^{131}I (2.8712(10^{-11} Sv d^{-1} Bq^{-1} m^2 to thyroid and 7.622(10^{-11} Sv d^{-1} Bq^{-1} m^2 to body surface; Kocher, 1980)

II–1.1.4.6. The inhalation (H_{inh}) and the ingestion (H_{ing}) thyroid dose

Thyroid doses were estimated using the ICRP three-compartment cyclic model (Johnson, 1981) and reference men data (ICRP publ. 23, 1975). The modified ICRP cyclic model (Figure 36) applied consideration of stable iodine deficiency and Monte Carlo methods to generate frequency distributions of thyroid doses to infant, children, teenage and adult thyroid gland by means of computer program APSVITA (Nedveckaite and Filistovic, 1995).

The individual inhalation thyroid dose was given as:

$$H_{inh} = H^0{}_{inh} v_{inh} \int_0^{t_e} C_a(t)dt$$

where:

H_{inh}	=	inhalation thyroid dose (Sv)
H^0_{inh}	=	inhalation thyroid dose conversion factor for ^{131}I (3.7(10^{-7} Sv Bq^{-1}; Johnson, 1981)
v_{inh}	=	inhalation rate (23 m^3 d^{-1} for adult; ICRP publ. 23, 1975)
C_a	=	^{131}I activity concentration in air (Bq m^{-3})
t_e	=	exposure time period (s).

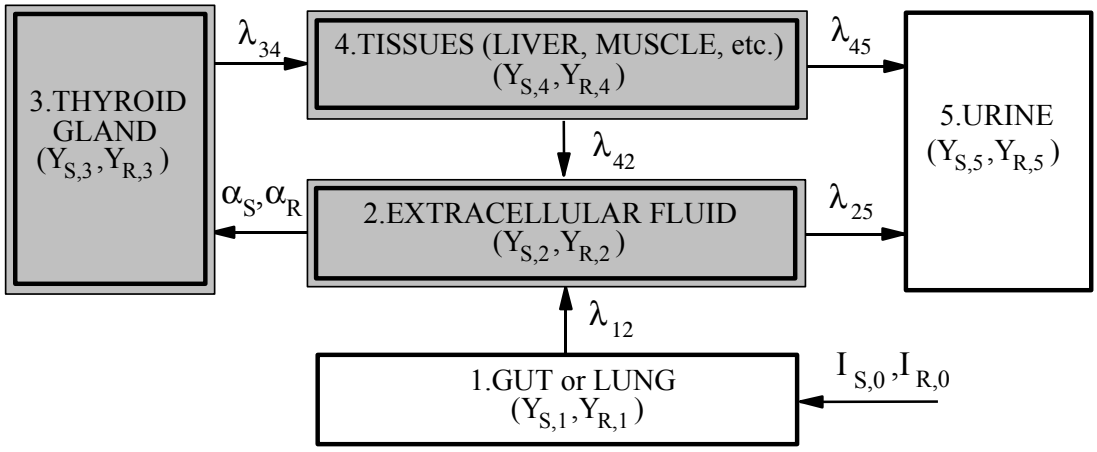

FIG. 36. Modified ICRP three-compartment cyclic model of iodine kinetics in the human body: $Y_{S,i}$ and $Y_{R,i}$ (I=1,...,4) are the content of stable and radioactive iodine in gut (lung), extracellular fluid, thyroid gland, tissues and urine, respectively; λ_{ij} (i, j = 1,...,5) are the rate constants for transfer of iodine from compartment i to j; $I_{S,0}$, $I_{R,0}$ are the intake rate of stable and radioactive iodine, respectively; ($_S$ is the uptake rate of stable iodine to the thyroid gland; ($_R = (\alpha_S/Y_{S,2})\cdot Y_{R,2}$.

The individual ingestion thyroid dose was estimated as an integral of the resultant dose rate over a indicated period of time t_e:

$$H_{ing} = \frac{E_{eff,\beta} + E_{eff,\gamma}}{m_T} \int_0^{t_e} Y_{R,3}(t)dt$$

where:

$E_{eff,\beta}$, $E_{eff,\gamma}$	=	effective energy per beta or gamma disintegration absorbed in thyroid tissue (J Bq^{-1} s^{-1})
m_T	=	thyroid mass (0.02 kg for adult man)
$Y_{R,3}(t)$	=	radioiodine activity in thyroid gland (Bq)

The detailed data for thyroid dose calculations are presented in (Nedveckaite and Filistovic, 1995). Numerical solution of differential equations was made using a Monte Carlo procedure as shown in Figure 37.

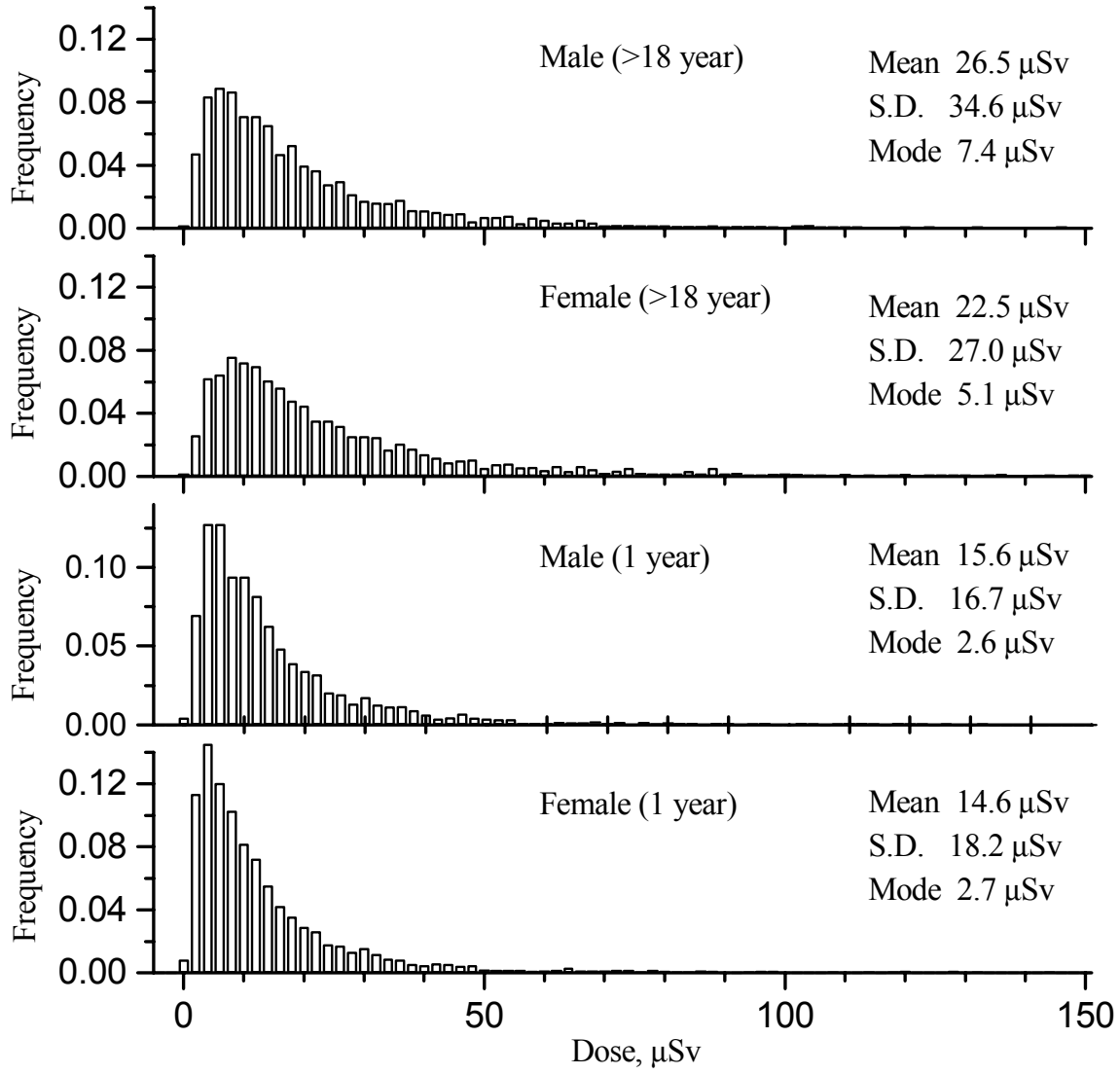

FIG. 37. Adult and infant (Farm A) ingestion thyroid dose frequency distribution.

II–1.2. METHOD USED FOR DERIVING UNCERTAINTY AND ACCURACY ESTIMATES

The uncertainties used in model results, due to uncertainties in model parameter values, has been determined by Monte Carlo sampling from prescribed distributions of model parameters. In specific cases the uncertainty estimates were derived by personal judgement of model parameters uncertainty range, considering experience after the Chernobyl accident. Basically the model at present employs a deterministic approach. This deterministic code was run repeatedly to generate a distribution of predictions in order to obtain 95% confidence interval. Considering that 1000 series of runs were required to obtain all results. The probabilistic FILTSEG code was still under development when these simulations were performed.

Used parameter distribution functions, their mean and standard deviation (S.D.) values are given in Table II–1.I.

TABLE II–1.I. PARAMETER VALUES AND DISTRIBUTIONS USED IN THE HANFORD SCENARIO STUDY

Parameter	Definition	Distribution	Mean	S.D.	Units
Q_i	Release rate	–	Release data	(Constant)	Bq d^{-1}
u_i	Mean wind speed	Log-normal	Meteorology data	0.447	m s^{-1}
φ_i	Mean wind direction	Normal	Meteorology data	$\pi/8$	rad
H_i	Depth of the mixing layer	Log-normal	By Smith/Hosker	$0.1 \cdot H_i$	m
Δh_i	Plume rise	Log-normal	By Bosanquet	$0.2 \cdot \Delta h_i$	m
$\sigma_{z,i}$	Vertical distribution coefficient	Log-normal	By Hosker	$SD(\sigma_{y,i})$ $\sigma_{z,i}/\sigma_{y,i}$	m
$\sigma_{y,i}$	Horizontal distribution coefficient	Log-normal	By Hosker	2 x(tg (ϕ_n/2) ϕ_A=25°,ϕ_B=20°, ϕ_C=15°,ϕ_D=10°, ϕ_E=5°,ϕ_F=1.5°	m
$v_{d,r}$	Reactive iodine gases deposition velocity	Log-normal	0.01	0.002	m s^{-1}
$v_{d,o}$	Organic iodine dry deposition velocity	Log-normal	0.0005	0.0001	m s^{-1}
$v_{d,p}$	Particulate iodine dry deposition velocity	Log-normal	0.001	0.0002	m s^{-1}
h	Stack height	–	65	(Constant)	m
v_s	Gas exit velocity	–	15.74	(Constant)	m s^{-1}
d	Stack inside diameter	–	2.134	(Constant)	m
V_v	Volumetric gas exit velocity	–	56.3	(Constant)	m^3 s^{-1}
T_r	Radioactive iodine half-life	–	8.04	(Constant)	d
λ_w	Weathering loss rate	Log-normal	0.074	0.015	d^{-1}
μ	Pasture absorption coefficient	Log-normal	1.0	0.2μ	m^{-2} kg
Y	Yield of pasture	Triangular	0.519	0.104 (k_{Apex}=0.1)	kg m^{-2}
F_m	Milk transfer coefficient	Log-normal	0.00117	0.00035	d L^{-1}
Q_F	Grass consumption rate	Uniform	60.0	18.0	kg d^{-1}
U_m	Ingestion rate of milk for adult man	Log-normal	0.377	0.370	L d^{-1}
U_l	Ingestion rate of lettuce for adult man	Log-normal	0.047	0.060	kg d^{-1}
s_m	Adult man stable iodine intake rate	Log-normal	200.0	50.0	(g d^{-1}
V_B	Adult man breathing rate	Log-normal	23.0	5.75	$m^3 d^{-1}$
m_T	Adult man thyroid mass	Log-normal	17.5	6.8	g
f_D	Dose transfer factor	Log-normal	$3.7\ 10^{-7}$	$0.9\ 10^{-7}$	Sv Bq^{-1}

II–1.3. THE COMPARISON OF TEST DATA AND MODEL PREDICTIONS

Validity and limitation of developed software are demonstrated through comparison of results obtained using FILTSEG programs and field measurements.

II–1.3.1. Atmospheric radioiodine

The major part of air activity concentration misprediction (Figure 38) may be connected with a lack of knowledge of real gaseous reactive (inorganic), gaseous organic and particulate airborne fraction of radioiodine. Atmospheric monitoring stations maintained in Hanford environment were installed with special equipment. The samples of airborne radioiodine were collected by drawing air through HV-70 brand filter (aerosol radioiodine), caustic scrubber (gaseous reactive radioiodine) and charcoal cartridge (on the assumption organic radioiodine, namely methyl iodide (CH_3I), has been trapped well). In actual fact charcoal coated with thryetilenediamine (TEDA) or $AgNO_3$ are often used for these purposes (von Kienle and Bader, 1980; Naguchi and Murata, 1988; Styra *et al.*, 1995). Charcoal cartridge without mentioned chemical compounds trapped only a minor part of gaseous organic radioiodine. This uncertainty makes further investigation of observed airborne radioiodine and model predictions undetermined.

II–1.3.2. Grass and milk activity concentration

Figures 39 and 40 compare observed and predicted ^{131}I activity concentrations in grass and milk respectively. One general comment on the comparison of observed and predicted grass and milk activity levels are that these results are in rather good agreement with one exception for Mesa location. The major reason for this misprediction is due to used meteorological data, namely, Pasquill-Gifford stability classes and wind direction and speed measured at Hanford at the release height. HMS surface observations as well as detailed HMS tower observations were not used. That is the most possible explanation that observed data was larger as compared to predicted

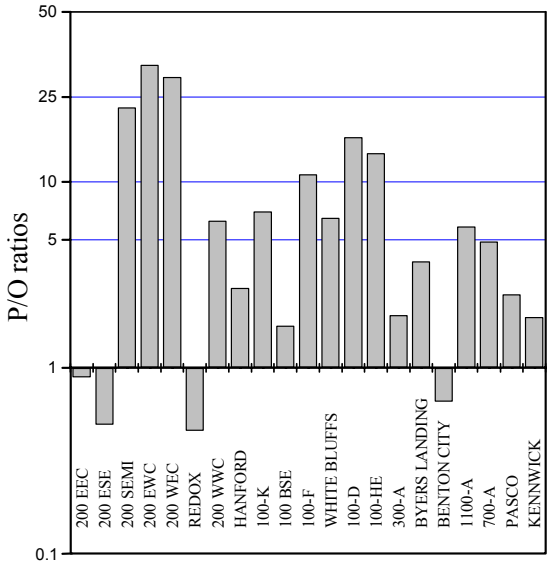

FIG. 38. A comparison of observed and predicted airborne radioiodine activity concentration in the case gaseous organic fraction has been trapped by charcoal. cartridge.

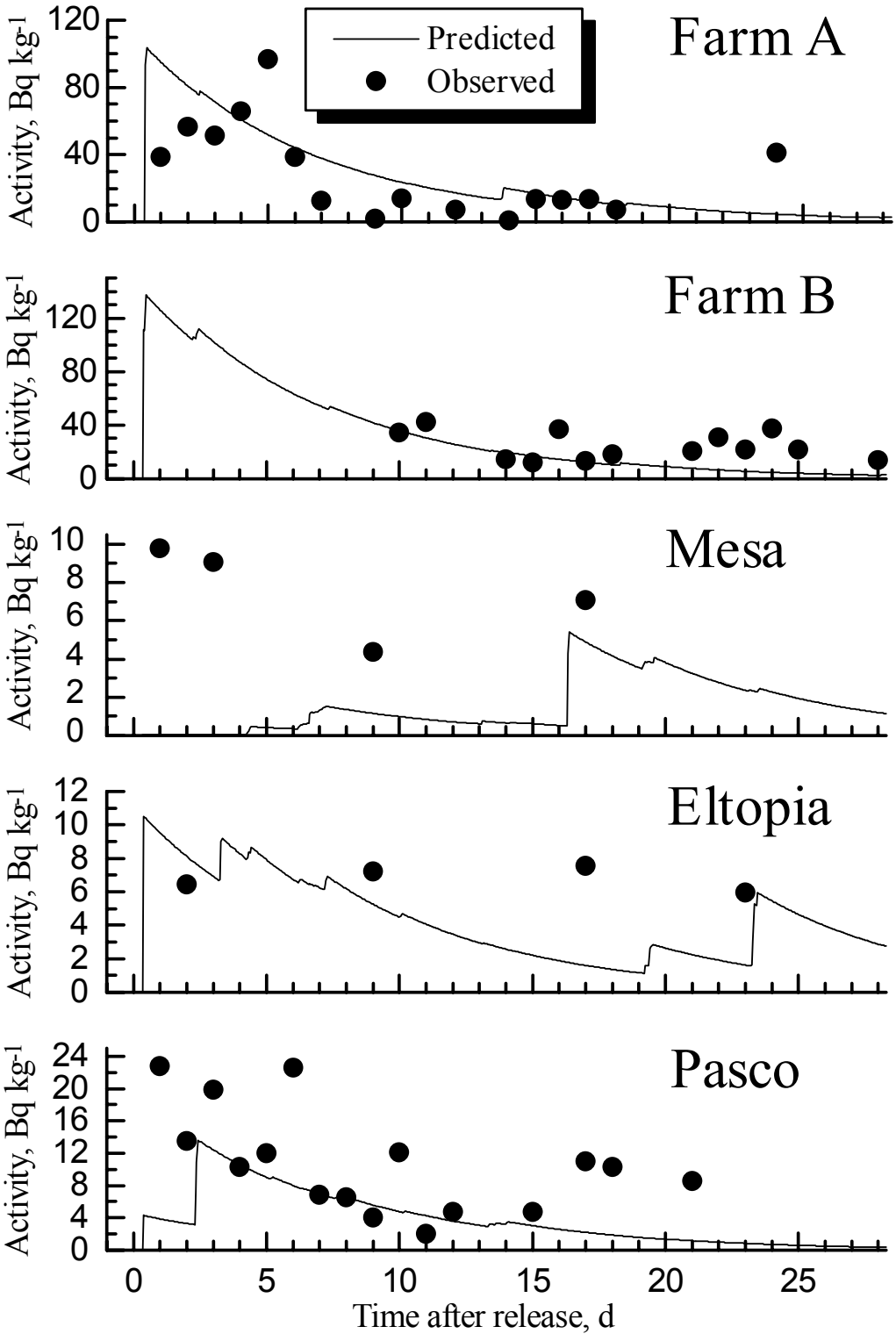

FIG. 39. Predicted and observed ^{131}I activity concentrations in grass.

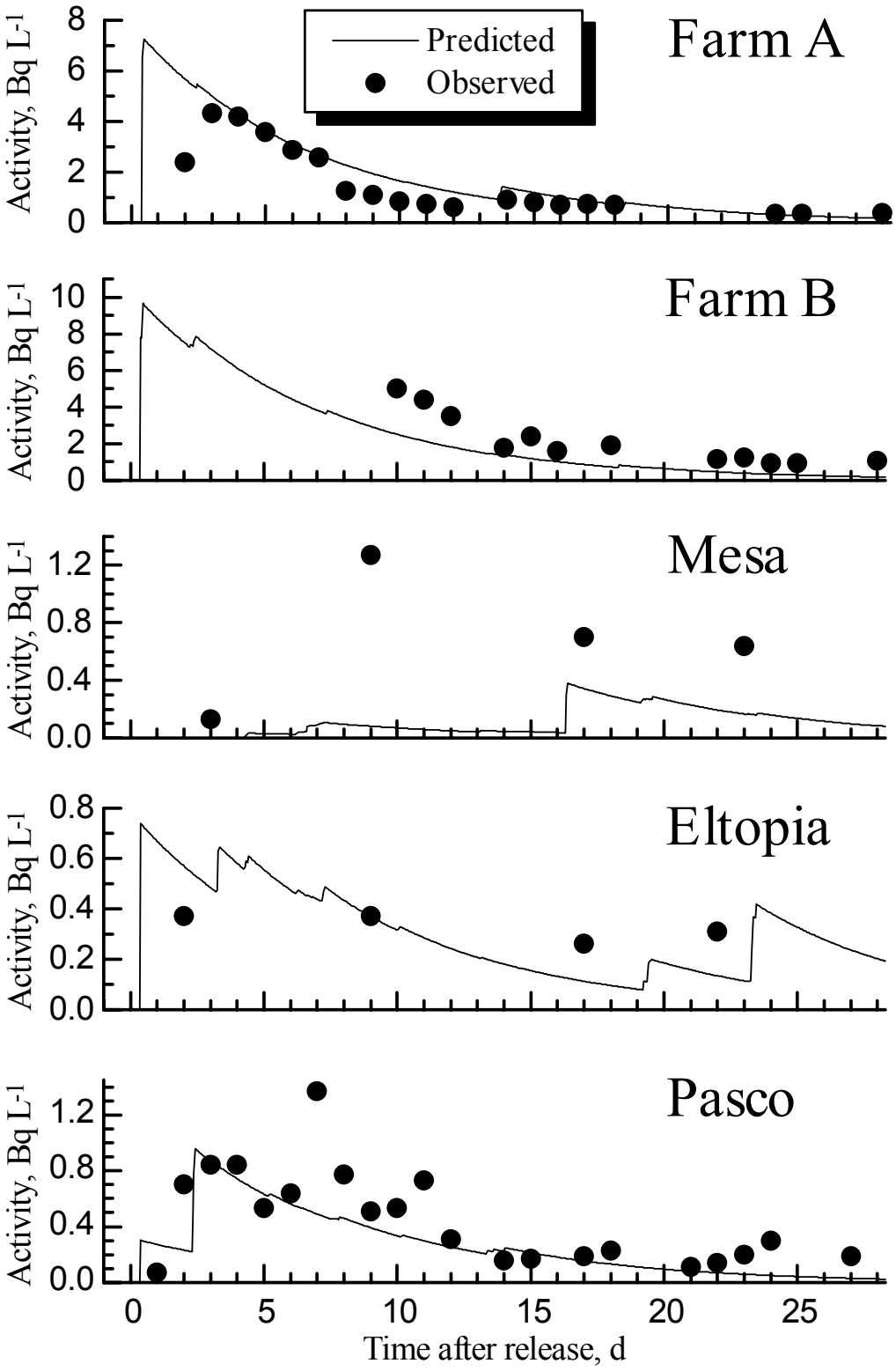

FIG. 40. Predicted and observed ^{131}I activity concentrations in milk.

II–1.4. SUGGESTIONS TO EXTEND CAPABILITY OF FILTSEG MODEL

In general, the predicted results appear to be quite logical and the computer software prepared may prove to be workable in the field of countermeasures available in an early phase of NPP accidents and thyroid dose assessments. The atmospheric behaviour of iodine is of prime consideration to the nuclear industry and is especially important in the case of nuclear accident. In this connection the work is in progress to incorporate following modifications.

— Inclusion into FILTSEG code of stable iodine and radioiodine gas-phase photochemistry. A hybrid stable iodine/radioiodine gas-phase model (Figure 41), including 27 gas-phase reactions (Wayne et al., 1995), and computer software was developed and solved. The work is in progress.

— Description of Hanford scenario stated, that the iodine released as I_2 have been ***quickly*** partitioned into particulate, reactive gaseous, and organic phases. This hypothesis concerning organic phase requires further refinement. Over the past decades, rapid progress has been made in understanding the gas-phase photochemical reactions of radioiodine, concerning the chemical and physical processes occurring in the atmosphere. That is why research on photochemical modelling of atmospheric transformations of radioiodine during transport of radioactive cloud may be performed.

— Inclusion in to FILTSEG a system of programs designed to efficiently evaluate the uncertainty associated with model predictions as a result of uncertainties associated with model parameters.

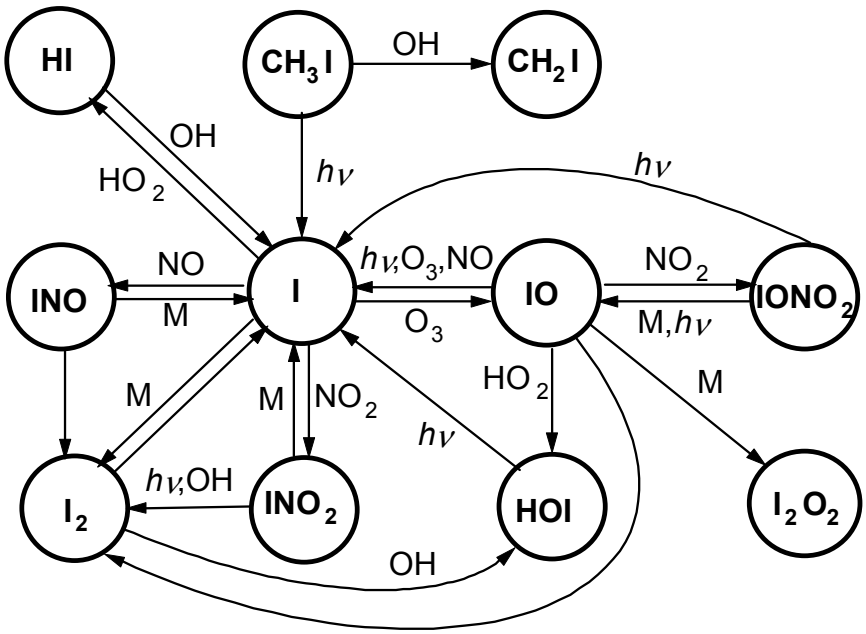

FIG. 41. All important features of the atmospheric iodine model.

References

ASTARITA G., WEI, J., IORIO, G., Theory of dispersion, transformation and deposition of atmospheric pollution using modified Green's functions. Atmospheric environment **13** 239-246 (1979).

INTERNATIONAL COMMISSION ON RADIOLOGICAL PROTECTION, Reference Man Oxford. Pergamon Press; ICRP Publication No. 23, p. 480 (1975).

JOHNSON, J.R., Radioiodine dosimetry. J. Radioanal. Chem. **65**, 223–238 (1981).

JONES, J.A., ESCLOUD: A Computer Program to Calculate the Air Concentration, Deposition Rate and External Dose Rate from a Continuous Discharge of Radioactive Material to Atmosphere. NRPB-R101, p. 39 (1980).

JUDA, J., CHROSCIEL, S., *Atmospheric Protection*. Warszaw. Scientific-Technical Press, p. 448 (in Polish) (1974).

VON KIENLE, H., BADER, E., *Active charcoal and its industrial application*. Stuttgart. Ferdinand Enke Press, p. 213 (in Germany) (1980).

KOCHER, D.C., Dose-rate conversion factors for external exposure to photon and electron radiation from radionuclides occurring in routine releases from nuclear fuel cycle facilities. Health Phys. **38**, 543–633 (1980).

NAGUCHI, H., MURATA, M., Physiochemical Speciation of Airborne ^{131}I in Japan from Chernobyl. J. Environ. Radioactivity **7**, 65–74 (1988).

NEDVECKAITE, T., FILISTOVIC, V., Estimates of thyroid equivalent doses in Lithuania following the Chernobyl accident. Health Phys. **69**, 265–268 (1995).

STYRA, NEDVECKAITE, T., FILISTOVIC, V., *Iodine isotopes and radiation safety*. Sankt-Peterburg: Gidrometeoizdat, p.251 (in Russian) (1992).

ZANETTI, P., New mixed segment-puff approach for dispersion modelling. Atmospheric Environment **20**, 1121–1130 (1986).

WAYNE, R.P., et al., Halogen oxides: radicals, sources and reservoirs in the laboratory and in the atmosphere. Atmospheric Environment **29,** 2675–2881 (1995).

II–2. OSCAAR

Used by Japan Atomic Energy Research Institute, Japan
T. Homma, Y. Inoue, K. Tomita

II–2.1. GENERAL MODEL DESCRIPTION

II–2.1.1. Name of model, model developer and model user

Model name: OSCAAR (Off-Site Consequence Analysis code for Atmospheric Releases in reactor accidents).

Model developer: Toshimitsu Homma and Orihiko Togawa, JAERI

Model user: JAERI Environmental Assessment Laboratory

II–2.1.2. Intended purpose of the model in radiation assessment

OSCAAR has been developed within the research activities on probabilistic safety assessment (PSA) at the Japan Atomic Energy Research Institute (Homma *et al.*, 1990). OSCAAR is primarily designed for use in PSA of nuclear reactors in Japan. OSCAAR calculations, however, can be used for a wide variety of applications including siting, emergency planning, and development of design criteria, and in the comparative risk studies of different energy systems.

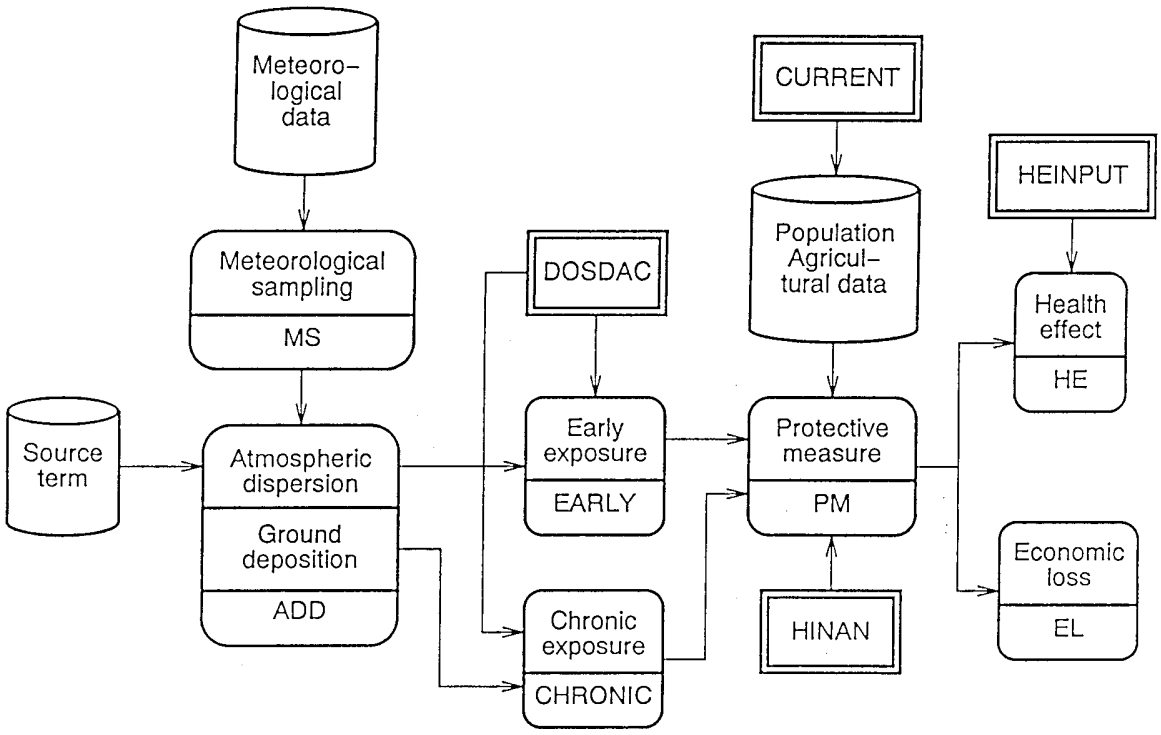

FIG. 42. Schematic representation of the OSCAAR code system.

Figure 42 shows a schematic representation of the OSCARR code system. OSCAAR consists of a series of interlinked modules and data files that are used to calculate the atmospheric dispersion and deposition of selected radionuclides for all sampled weather conditions, and the subsequent dose distributions and health effects in the exposed population. OSCAAR can consider the countermeasures which might be taken to reduce the dose received by the exposed population. Several stand-alone computer codes and databases can also be used to prepare, in advance, necessary input data files for OSCAAR, such as dose conversion factors, population and agricultural product distributions, and lifetime risks for exposed population. The principal endpoints of OSCAAR can be roughly divided into health effects, effects of countermeasures and economic impacts.

II–2.1.3. Model type

For the validation of OSCAAR, the CHRONIC module has been applied to the Chernobyl scenario (Scenario A4) of BIOMOVS Phase I, which starts with daily concentrations of I-131 in air and requests the prediction of concentrations of I-131 in vegetation and milk for several locations in the northern hemisphere (Peterson et al., 1996). In the Hanford test scenario we can examine the performance of other OSCAAR modules such as ADD, EARLY, and CHRONIC by implementing atmospheric dispersion and deposition calculations, food chain transport analysis, and dose calculations. ADD implements a Gaussian multi-puff trajectory model for calculating time-integrated air concentrations and surface contamination. CHRONIC uses time-dependent analytical equations for estimating the radionuclide transport in the food chain.

II–2.1.4. Method used for deriving uncertainty estimates

OSCAAR has been coupled with the uncertainty and sensitivity analysis techniques to quantify uncertainty associated with accident consequence assessment and to identify uncertain processes and important parameters contributed to consequences. Among a number of techniques available for propagating parameter uncertainties through complex models, a Monte Carlo method has been implemented to perform uncertainty and sensitivity analyses of OSCAAR. The software package PREP/SPOP is used to allow for an automatic performance of all necessary steps in uncertainty and sensitivity analysis. The different sampling schemes, such as pure random, Latin hypercube (LHS) and quasi-random sampling, are allowed to be used in PREP(Homma and Saltelli, 1992). SPOP performs the uncertainty and sensitivity analyses on the output of the model. SPOP includes several parametric and non-parametric techniques, based on regression-correlation measures, as well as some “two-sample” tests (Saltelli and Homma, 1992). Variance-based methods are also available for ascertaining if a subset of input may account for the output variance without any linearity assumptions (Homma and Saltelli, 1996).

II–2.2. DETAILED MODEL DESCRIPTION

II–2.2.1. Method

II–2.2.1.1. Atmospheric dispersion and deposition

A multi-puff trajectory model is incorporated in the current version of the OSCAAR atmospheric dispersion and deposition module, ADD. OSCAAR-ADD originally has two

kinds of grid systems for input meteorological information. The first large system is a synoptic scale Eulerian grid which has numerically analyzed wind data at standard constant pressure levels such as 950 hPa, 850 hPa and 700 hPa, provided by the Japan Meteorological Agency. The second system is a meso scale grid defined by users for surface wind and atmospheric stability data. In this test scenario, only the second system is used to calculate the transport and diffusion conditions of each released puff.

Plume rise is calculated from meteorological conditions at the release height and the vertical momentum flux using the formula for vertical jets given by Briggs (1969 and 1975). The mixing height is determined as a function of stability. Within the mixing layer a power-law wind profile is used to determine the average advecting wind over the depth of vertical distribution of activity in each puff. Each puff is assumed to have a Gaussian distribution of concentrations and to be reflected from the ground surface. The diffusion parameters, σ_y and σ_z depend on the distance traveled by the puff and the prevailing atmospheric stability.

Depletion by radioactive decay, dry and wet deposition is considered along the trajectory of each puff in ADD. The effective dry deposition velocity and washout coefficient are assumed to take account of speciation of released iodine. ADD originally can handle the spatial and temporal distribution of rainfall to predict wet deposition. Hourly precipitation data at Hanford site, however, is assumed over the whole area in this calculation.

Hourly air concentrations and surface contamination at receptor points are calculated by summing the contributions from puffs in ADD. Those hourly predictions as well as the time-integrated ones are transferred to the dose calculation modules, EARLY and CHRONIC. The main assumptions in ADD are summarized in Table II–2.I and parameters used in atmospheric dispersion and deposition calculations are given in Table II–2.II.

II–2.2.2. Dose calculations

Two kinds of modules are used to convert the predicted spatial and temporal distributions of activity in the atmosphere and on the ground to distributions of dose in population. The EARLY module calculates early exposure which occurs during and shortly after plume passage. External irradiation from material in the passing cloud (cloudshine), internal irradiation following inhalation of the material, and external irradiation from the deposited material (groundshine) are taken into account in EARLY within several hours to several weeks since the accident occurs. The cloudshine is basically calculated with the submersion model, but the finite cloud model based on isotropic puff assumptions (Healy and Baker, 1968) is used to estimate the irradiation at the places close to the source.

The CHRONIC module calculates the long-term groundshine dose, internal doses via inhalation of radionuclides resuspended from the ground, and internal doses via ingestion of contaminated foodstuffs. The migration of deposited material into soil as well as the radioactive decay is taken into account for the calculation of the long-term groundshine doses. The food chain model in CHRONIC is an extension of the methodology used in WASH-1400 (USNRC, 1975) and is available for important Japanese crops. It can reflect their seasonal dependence in probabilistic assessments.

CHRONIC derives the human intake of I-131 through the pasture-cow-milk pathway by:

$$I = U_m e^{-\lambda t_m} \int D \frac{r}{Y_v} e^{-(\lambda+\lambda_w)t} Q_F F_m(t) dt \quad (1)$$

where:

D = total deposition (Bq/m^2);
r/Y_V = mass interception fraction (m^2/kg-dw);
$\_w$ = environmental loss constant (day^{-1}) (T_w = ln 2/$\_w$) ;
Q_F = daily intake of a dairy cow (kg-dw/day);
F_m = fraction of daily intake of radioiodine secreted per liter of milk by Lengemann (1966): 0.0091 exp(0.021t) [1 - exp(-0.292t)], transfer rate;
t_m = time between milk secretion and milk consumption (day);
U_m = milk consumption rate (L/day).

CHRONIC does not treat deposition of activity as a function of time, while ADD calculates hourly time-integrated air concentrations and deposition of activity. The human intake of radionuclides for each spatial grid element is calculated from the amount of activity deposited, the concentration of activity in foods for unit deposition, and the consumption rate. Table II–2.III gives the main parameter values used in food chain transport calculations. CHRONIC does not explicitly calculate the concentration of activity in forage. In this scenario, however, the time-integrated concentration of I-131 in pasture grass was estimated from the following equation:

$$C_V = D \frac{r}{Y_V} \int_0^{t_e} e^{-(\lambda+\lambda_w)t} dt \quad (2)$$

where t_e is the time period during which vegetation is exposed to contamination. Since we use the mass interception fraction on a dry weight basis, the moisture content of pasture grass is assumed to be 10% to 75% in the comparison with the measured concentrations of I-131 in pasture.

CHRONIC also does not have the function of predicting the thyroid burdens of I-131. For the comparison with the measurements, however, we used a three compartment model with biokinetic data for iodine for 5 and 10 years old given in ICRP Publication 56 (1989) to estimate the thyroid burdens for a four year-old boy and his eight year-old sister.

II–2.2.3. Dosimetry data

The internal dose conversion factors and the external dose rate conversion factors can be used in the EARLY and CHRONIC modules to determine the dose in different organs following an intake of radionuclides and exposure to external irradiation, respectively. A computer code system DOSDAC calculates these quantities from most updating data, such as radioactive decay data, atomic, anatomical and metabolic data and generates the dose conversion factors required for OSCAAR.

Estimates of the internal dose factors resulting from inhalation and ingestion of various radionuclides are made by the methods in the ICRP Publication 30 (1979) in the DOSDAC system. For external exposure the method of Kocher (1980) is used to compute the dose-rate conversion factors which concept is based on the idealized assumptions that the source region

can be regarded as effectively infinite or semi-infinite in extent and that the radionuclide concentration is uniform throughout the source region. The breathing rate for the adult test persons and dose and dose-rate conversion factors for I-131 for thyroid in this calculation are given in Table II–2.IV. In this calculation we did not consider any reduction of either external exposure due to the shielding by buildings or inhalation exposure due to the filtering by the buildings.

II–2.3. RESULTS AND DISCUSSION

Two sets of calculations were performed using the different meteorological data sets for the puff advection. Both results are given in Tables II–2.V and II–2.VI, respectively. In the first approach, both hourly meteorological data at the release height of Hanford and the meso scale wind and stability fields interpolated from data at the surrounding 12 surface meteorological stations were used in the puff advection calculations. The expected uncertainties in the predicted results were estimated using parameter uncertainty analysis with a Monte Carlo technique (Homma and Saltelli, 1993). The statistical information of the parameter values in the atmospheric dispersion and deposition model given in Table II–2.II was taken according to expert judgment. The parameter values and distributions in the food-chain transport parameters given in Table II–2.III were taken from a U.S. extensive review of the literature (Hoffman and Baes, 1979). The mean and subjective confidence levels in Table II–2.V are based on a sample of 100 Monte Carlo simulations.

For investigating the effect of meteorological input data on the estimated deposition pattern, we used only hourly meteorological data at the release height in the puff advection calculations in the second approach. The deterministic calculation was performed to estimate the concentration of I-131 in milk and the resultant doses at each location using the mean values of the uncertain parameters in Tables II–2.II and II–2.III.

II–2.3.1. Air concentration

The predicted I-131 air concentrations by OSCAAD-ADD were compared with air measurements for twenty-one locations provided in the table of the scenario. The observed data are assumed to indicate both particulate and elemental iodine, and to be 65% of total iodine. Figure 43(a) shows the correlation between observed and predicted time-integrated I-131 concentrations in air by the first approach. It shows that the model tends to overestimate the predictions of I-131 air concentrations at the entire region. Figure 43(b) shows the distribution of predicted to observed (P/O) ratios for the time-integrated I-131 concentrations in air for those locations except Byers Landing[1]. Since the spatial and temporal variations of air concentrations of I-131 show complicated pattern (see Figures 49(a) to 49(d)), the ADD transport and dispersion calculations made using wind data at the release height and wind fields by simple interpolation of the surrounding surface wind data indicate limited capabilities. While ADD predicts well in the north part of the release point, the high overpredictions are found to the west close to the release point and the northeast and east of the release point, in particular, such as White Bluffs, 100-F and Hanford along the Columbia River.

Figures 44(a) and 44(b) show the correlation and P/O ratio charts by the second approach. They indicate that the model also tends to overestimate the predictions of I-131 air concentrations at the entire region. In particular, the high overprediction is found at Pasco.

[1] The latitude and longitude of Byers Landing provided in the scenario does not seem to correspond to the location of Byers Landing in the map.

This is due to the fact that the released puffs during the nighttime of September 2 transported to the southeast direction and contributed to the deposition at Pasco. The spatial and temporal variations of air concentrations of I-131 shown in Figures 50(a) to 50(d) indicate the different pattern from those by the first approach. Figure 45 shows the comparison of I-131 time-integrated air concentrations at different farms between the two approaches.

II–2.3.2. Concentrations in milk

The predictions of I-131 time-integrated concentrations in milk at six locations are given in Figure 46 in the form of boxplots in which those measurements for four locations are also included. The boxplots show the 1th, 5th, 25th, 50th (median), 75th, 95th, and 99th percentile of the predicted values. Additionally, the mean of the predictions is shown by the square symbol as well as the minimum and maximum predictions. Observed monthly integrals of I-131 in milk at Farm A, Farm B, Pasco (Farm T) and Ringold (Farm K) were estimated using the simple linear interpolation for those times when no measurements were taken. The predictions of I-131 concentrations in milk seem to be in better agreement with measurements at Farm A, Farm B and Pasco except at Ringold. This may be mainly due to the overpediction of total deposition of I-131 in the case of Ringold.

II–2.3.3. Concentrations in pasture grass

As described above, OSCAAR originally does not have the function of predicting the contamination of radionuclides on pasture grass. However, in order to examine the performance of predicting the deposition of I-131, we compared the predicted I-131 concentrations in pasture grass using equation (2) with the measurements. Since measured concentrations on pasture are fresh weight as collected, the moisture content of the pasture to be assumed becomes very important. The boxplots for the time-integrated concentrations in pasture grass at six locations are given in Figure 47 together with those measurements. Observed monthly integrals of I-131 in pasture grass at Farm A, Farm B, Pasco (Farm T) and Ringold (Farm K) given in this figure were estimated using the simple linear interpolation. In the case of Farm B, the measured concentrations in pasture can be used only from September 12. The monthly integral of I-131 in pasture grass at Farm B was estimated by assuming that the fraction of activity before 12th was the same as that for Farm A. The observed values for three locations except Ringold fall within the subjective confidence interval of the prediction.

II–2.3.4. Thyroid burden

Figure 48 shows the boxplots of predicted I-131 thyroid burdens for a four-year old boy and his 8-year old sister located at Farm B on October 19 together with those measurements. The metabolic mode used in this analysis underestimates the transfer of iodine to the thyroid, but these measurements fall within a 90% confidence interval. These underpredictions may be due to the assumption that the thyroid burden was estimated at 46 days after instantaneous intake of iodine.

II–2.3.5. Dose to individuals

The mean doses to the thyroid of test persons and their confidence levels from various pathways are given in Table II–2.V. Apparently the ingestion dose mainly from contaminated milk is the most contributor to the total dose.

II–2.4. SENSITIVITY ANALYSIS

For each of the endpoins the SA measures in SPOP were applied to examine the sensitivity of the uncertainty in the predictions to the uncertainties in input parameters. Table II–2.VII shows the standardized rank regression coefficients (SRRCs) for those parameters for each endpoint at Farm B. The table also shows the R^2 values, which indicates a reasonably linear relationship between the ranks of the output and the ranks of the input parameter values. The parameter uncertainties which contribute most to the uncertainty in the predicted milk concentration are found to be the deposition velocity of elemental iodine, feed to milk transfer factor, and mass interception fraction of iodine for pasture grass.

II–2.5. CONCLUSIONS

The Hanford test scenario provides a good opportunity to evaluate the performance of OSCAAR. Although it is difficult to perform a model validation over the entire set of conditions to which accident consequence assessment codes like OSCAAR may be applied, the Hanford test scenario is valuable because we can start with source terms and examine atmospheric dispersion and deposition calculations, food chain transport analysis, and dose calculations. The OSCAAR food chain model performs relatively well when the predictions of deposition are well. Since the spatial and temporal variations of air concentrations of I-131, on the other hand, show a complicated pattern, the atmospheric transport and dispersion calculations made using wind data at the release height and wind fields by simple interpolation of the surrounding surface wind data indicate limited capabilities. The Monte Carlo based uncertainty and sensitivity method has been successfully demonstrated in the dose reconstruction scenario. The method presented here also allows determination of the parameters that have a most important impact in accident consequence assessments.

TABLE II–2.I. MAIN ASSUMPTIONS USED IN OSCAAR-ADD

Features	Descriptions
Receptor points	32 angular segments and 21 distance bands and calculation points in the scenario.
Source term	Hourly source term data in the test scenario.
Meteorological data	Hourly data at the release height of Hanford and at 12 surface stations including Hanford surface observations.
Wind and atmospheric stability field	Two-dimensional rectangular grid that has 16×16 grid points (30.48 km spacing). Simple $1/r^2$ interpolation of surface observations.
Wind power-law profile	Power-law exponent values for surface roughness, 0.10 m as a function of Pasquill stability class by Irwin (1978).
Precipitation	Hourly precipitation data at Hanford site is used for calculating wet deposition at all receptor points.
Mixing Height	Spatially varying as a function of stability.
Plume rise	Formulas for vertical jets by Briggs (1969, 1975).
Diffusion parameters	Vertical and horizontal dispersion coefficients as a function of distance by Eimutis and Konicek (1972).
Dry deposition	Dry deposition velocity (m/sec).
Wet deposition	Washout rate (1/sec) recommended by Brenk and Vogt (1981).

Text cont. on page 112.

TABLE II–2.II. PARAMETER VALUES USED IN ATMOSPHERIC DISPERSION AND DEPOSITION MODULE, ADD

Variable	Description	Distribution	Mean	μ *	σ *	Units
h	Stack height	constant	60.5	–	–	m
r_0	Internal stack radius	constant	1.067	–	–	m
D	Internal stack diameter ($D = 2r_0$)	constant	2.134	–	–	m
F_s	Volumetric stack flow velocity	constant	56.63	–	–	m^3/s
W_0	Efflux speed of gases from stack ($W_0 = F_s/\pi/r_0^2$)	constant	15.83	–	–	m/s
p	Wind profile power-law exponent (z_0 = 0.10 m):					
	A	constant	0.08	–	–	–
	B		0.09	–	–	
	C		0.11	–	–	
	D		0.16	–	–	
	E		0.32	–	–	
	F		0.54	–	–	
α_p	Scaling factor for wind profile power-law exponent	normal	1.0	1.0	0.15	–
Hm	Mixing height:					
	A	constant	1600	–	–	m
	B		1200	–	–	
	C		800	–	–	
	D		560	–	–	
	E		320	–	–	
	F		200	–	–	
α_h	Scaling factor for mixing height	normal	1.0	1.0	0.21	–
α_y	Scaling factor for sigma-y	log-normal	1.0	0.0	0.13	–
α_z	Scaling factor for sigma-z	log-normal	1.0	0.0	0.13	–
fc	Fraction of iodine chemical form:					
	reactive gas	constant	40	–	–	%
	particulate		25	–	–	
	organic		35	–	–	
Vg	Dry deposition velocity for iodine:					
	reactive gas	log-normal	1×10^{-2}	-2.0	0.61	m/s
	particulate		1×10^{-3}	-3.0	0.43	
	organic		1×10^{-4}	-4.0	0.43	
Λ	Washout rate: $=aI^b$					
	I: rainfall rate (mm/h)					
	a: reactive gas		8×10^{-5}	–	–	s^{-1}
	particulate		1.2×10^{-4}	–	–	
	organic		1×10^{-6}	–	–	
	b		0.6	–	–	–

* μ and σ are the mean and standard deviation, respectively, of the normally distributed parameters. If the parameter, *x* is log-normally distributed, μ and σ refer to those of the log-transformed parameters ($\log_{10}(x)$).

TABLE II–2.III. PARAMETER VALUES USED IN FOOD CHAIN TRANSPORT CALCULATIONS

Variable	Description	Distribution	Mean	μ *	σ *	Units
r/Y_V	Mass interception fraction for pasture grass	log-normal	2.0	0.26	0.19	m^2/kg-dw
T_W	Weathering half-life	log-normal	10.4	1.0	0.13	days
t_e	Time period during which vegetation is exposed to contamination	constant	30.0	–	–	day
f_w	Water content in pasture grass	uniform	0.1–0.75			–
Q_F	Daily intake of a dairy cow	normal	9.0	9.0	2.3	kg-dw/day
F_m	Fraction of daily intake of radioiodine secreted per liter of milk	log-normal	0.0091	-2.04	0.24	$liter^{-1}$
t_m	Time between milk secretion and milk consumption	normal	2.0	2.0	0.86	days
U_m	Milk consumption rate:					
	Test persons	log-normal	0.315	-0.65	0.36	liter/day
	Man		0.377	-0.57	0.36	
	Woman		0.260	-0.73	0.36	
	Child		0.497	-0.36	0.21	
	Farm B Boy	constant	4.0			
	Farm B Girl	constant	1.0			
t_l	Time delay from harvest to leafy vegetables to human consumption	constant	5.0	–	–	day
U_l	Consumption rate of leafy vegetables:					
	Test persons	constant	0.049	–	–	kg-fw/day
	Man		0.047	–	–	
	Woman		0.050	–	–	
	Child		0.0072	–	–	

TABLE II–2.IV. PARAMETER VALUES USED IN DOSE CALCULATIONS

Variable	Description	Distribution	Mean	μ *	σ *	Units
B_r	Breathing rate for adults	constant	2.66×10^{-4}	–	–	m^3/s
DF_c	Dose rate conversion factor for thyroid for immersion in I-131 contaminated air	constant	5.65×10^{-7}	–	–	Sv/yr per Bq/m^3
DF_g	Dose rate conversion factor for thyroid for exposure 1 m above I-131 contaminated ground surface	constant	1.32×10^{-8}	–	–	Sv/yr per Bq/m^2
DF_{ihn}	Committed dose equivalent in thyroid per intake of unit I-131 by inhalation	constant	2.67×10^{-7}	–	–	Sv/Bq
DF_{ing}	Committed dose equivalent in thyroid per intake of unit I-131 by ingestion	constant	4.35×10^{-7}	–	–	Sv/Bq

* μ and σ are the mean and standard deviation, respectively, of the normally distributed parameters. If the parameter, x is log-normally distributed, μ and σ refer to those of the log-transformed parameters ($\log_{10}(x)$).

TABLE II–2.V. RESULTS OF APPROACH 1 (USING MULT-STATION METEOROLOGICAL DATA)

Item		Farm A	Farm B	Mesa	Ringold	Pasco	Eltopia
Total deposition (Bq/m^2)	Upper	114.	283.	1070.	1540.	37.9	222.
	Mean	61.1	132.	356.	720.	24.9	140.
	Lower	13.1	26.5	40.8	143.	8.44	45.2
Integrated concentrations in milk (Bq d/l)	Upper	198.	397.	1080.	2360.	64.9	382.
	Mean	58.9	127.	337.	678.	24.6	138.
	Lower	6.29	13.3	17.8	60.8	3.44	16.5
Integrated concentrations in grass (Bq d/kg f.w.)	Upper	1060.	2590.	7350.	13400.	396.	2240.
	Mean	455.	977.	2530.	5260.	185.	1030.
	Lower	75.9	13.1	172.	675.	42.4	173.
Item		Carnation			Darigold		
		Man	Woman	Child	Man	Woman	Child
Human intake (Bq)	Upper	17.2	15.6	21.3	26.6	21.1	22.1
	Mean	5.04	3.72	6.23	7.00	4.86	8.66
	Lower	0.48	0.421	0.647	0.574	0.681	0.918
Item		Farm B					
		Boy			Girl		
Thyroid burden (Bq)	Upper	3.18			1.46		
	Mean	1.01			0.467		
	Lower	0.106			0.0491		
Item		Farm A	Farm B	Mesa	Ringold	Pasco	Eltopia
Cloud exposure (mSv)	Upper	4.5E-7	7.5E-7	4.5E-6	4.6E-6	2.6E-7	1.3E-6
	Mean	2.3 E-7	4.5E-7	1.7E-6	2.5E-6	1.2E-7	7.0E-7
	Lower	4.1E-8	9.4E-8	4.7E-8	6.2E-7	6.8E-9	2.4E-8
Ground exposure (mSv) 9/2–10/1	Upper	4.8E-5	1.2E-4	4.5E-4	6.4E-4	1.6E-5	9.3E-5
	Mean	2.6E-5	5.5E-5	1.5E-4	3.0E-4	1.0E-5	5.9E-5
	Lower	5.5E-6	1.1E-5	1.7E-5	6.0E-5	3.5E-6	1.9E-5
Inhalation dose (mSv)	Upper	1.8E-3	3.0E-3	1.8E-2	1.8E-2	1.0E-3	5.3E-3
	Mean	9.3E-4	1.8E-3	6.7E-3	9.7E-3	4.9E-4	2.8E-3
	Lower	1.6E-4	3.7E-4	1.9E-4	2.4E-3	2.7E-5	9.5E-5
Ingestion dose (mSv)	Upper	2.7E-2	5.6E-2	1.5E-1	3.0E-1	1.1E-2	6.8E-2
	Mean	7.2E-3	1.6E-2	4.2E-2	8.2E-2	3.0E-3	1.7E-2
	Lower	6.8E-4	1.2E-3	1.7E-3	5.8E-3	3.0E-4	1.3E-3
Total dose (mSv) 9/2–10/1	Upper	2.8E-2	5.7E-2	1.7E-1	3.0E-1	1.2E-2	6.9E-2
	Mean	8.2E-3	1.7E-2	4.9E-2	9.2E-2	3.5E-3	2.0E-2
	Lower	1.5E-3	3.3E-3	2.9E-3	1.4E-2	6.5E-4	1.9E-3

TABLE II–2.VI. RESULTS OF APPROACH 2 (USING SITE METEOROLOGICAL DATA)

Item	Farm A	Farm B	Mesa	Eltopia	Pasco	Ringold
Total deposition (Bq/m^2)	43.1	43.3	4.69	22.5	430.	257.
Integrated concentrations in milk (Bq d/l)	42.2	42.4	4.59	22.0	421.	252.
Item	Carnation			Darigold		
	Man	Woman	Child	Man	Woman	Child
Human intake (Bq)	9.24	6.61	11.4	13.0	9.27	16.1
Item	Farm B					
	Boy			Girl		
Thyroid burden (Bq)	0.287			0.135		
Item	Farm A	Farm B	Mesa	Eltopia	Pasco	Ringold
Cloud exposure (mSv)	1.4E-7	1.4E-7	1.5E-8	7.5E-8	1.4E-6	8.6E-7
Ground exposure (mSv) 9/2–10/1	1.4E-5	1.4E-5	1.6E-6	7.5E-6	1.4E-4	8.6E-5
Inhalation dose (mSv)	5.6E-4	5.6E-4	6.0E-5	3.0E-4	5.6E-2	3.4E-3
Ingestion dose (mSv)	5.4E-3	5.4E-3	5.8E-4	2.8E-3	5.4E-2	3.2E-2
Total dose (mSv) 9/2–10/1	6.0E-3	6.0E-3	6.4E-4	3.1E-3	6.0E-2	3.5E-2

TABLE II–2.VII. STANDARDIZED RANK REGRESSION COEFFICIENTS FOR UNCERTAIN PARAMETERS FOR DIFFERENT OUTPUT VARIABLES AT FARM B

Parameter	Deposition	Grass	Milk	Total dose
α_p	0.03	0.03	0.03	0.02
α_h	-0.22	-0.19	-0.16	-0.16
α_y	0.09	0.03	0.05	0.06
α_z	0.07	0.04	0.07	0.06
Vg(G)	0.92	0.67	0.62	0.44
Vg(P)	0.06	0.08	0.05	0.04
Vg(O)	0.03	-0.02	-0.02	-0.01
r/YV	–	0.50	0.43	0.29
Tw	–	0.12	0.15	0.15
fw	–	0.40	–	–
Qf	–	–	0.24	0.20
Fm	–	–	0.49	0.39
Tm	–	–	–	-0.08
Um	–	–	–	0.60
R^2	0.89	0.91	0.92	0.92

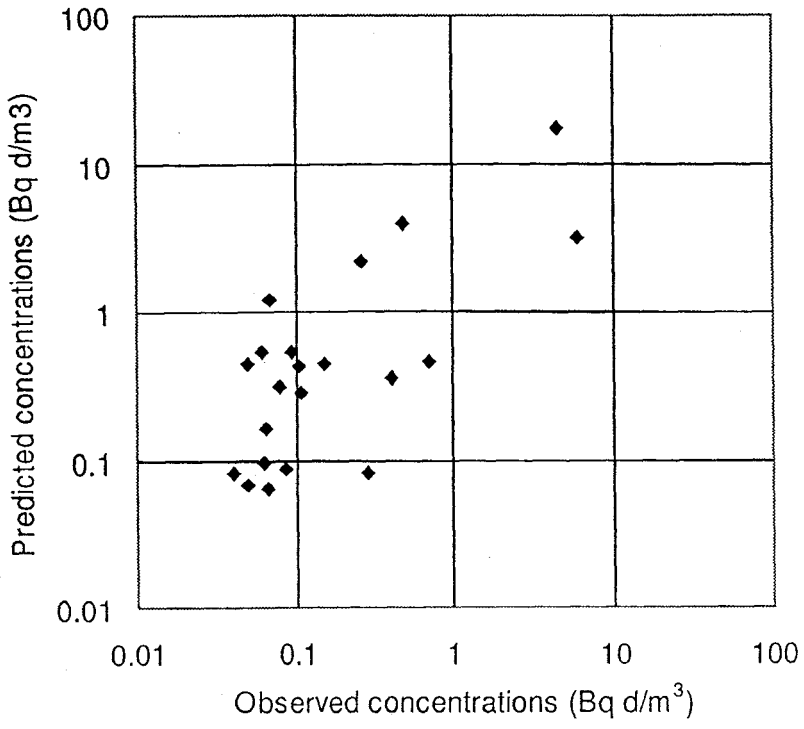

FIG. 43(a) Correlation between observed and predicted time-integrated I-131 concentrations in air.

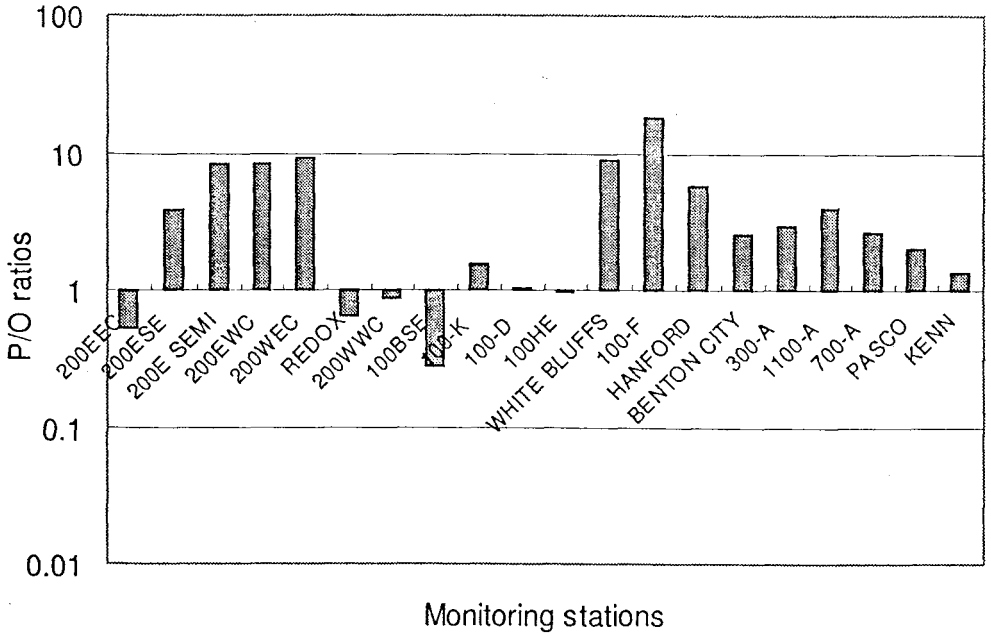

FIG. 43(b) P/O ratios of the time-integrated I-131 concentrations in air.

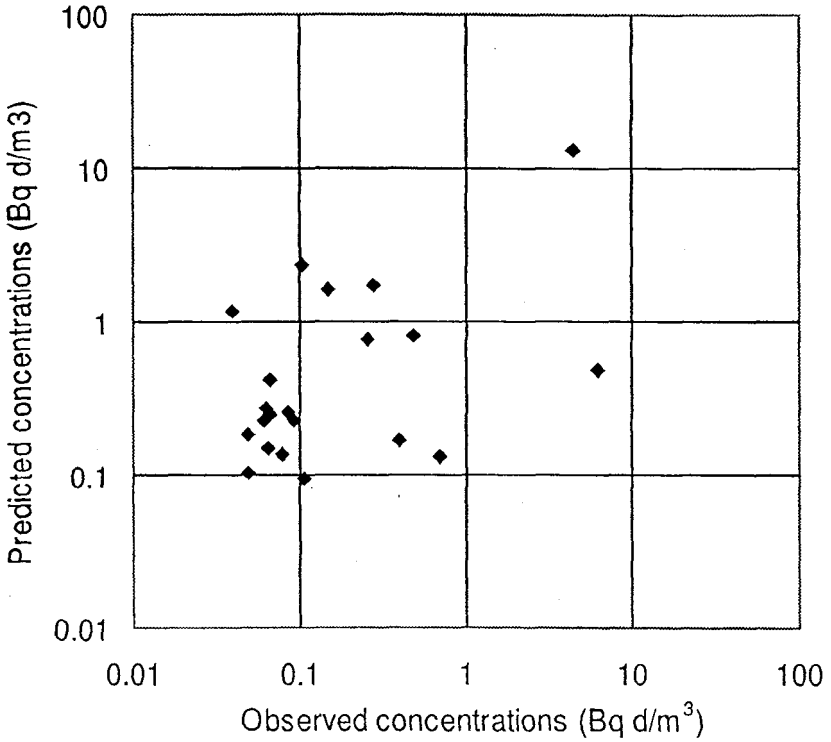

FIG. 44(a) Correlation between observed and predicted time-integrated I-131 concentrations in air.

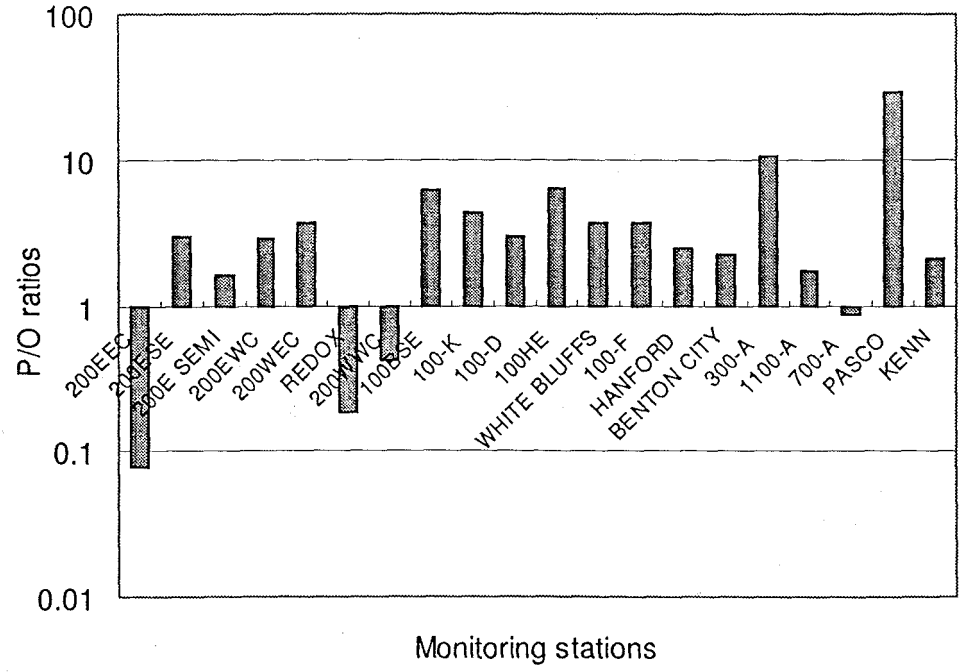

FIG. 44(b) P/O ratios of the time-integrated I-131 concentrations in air.

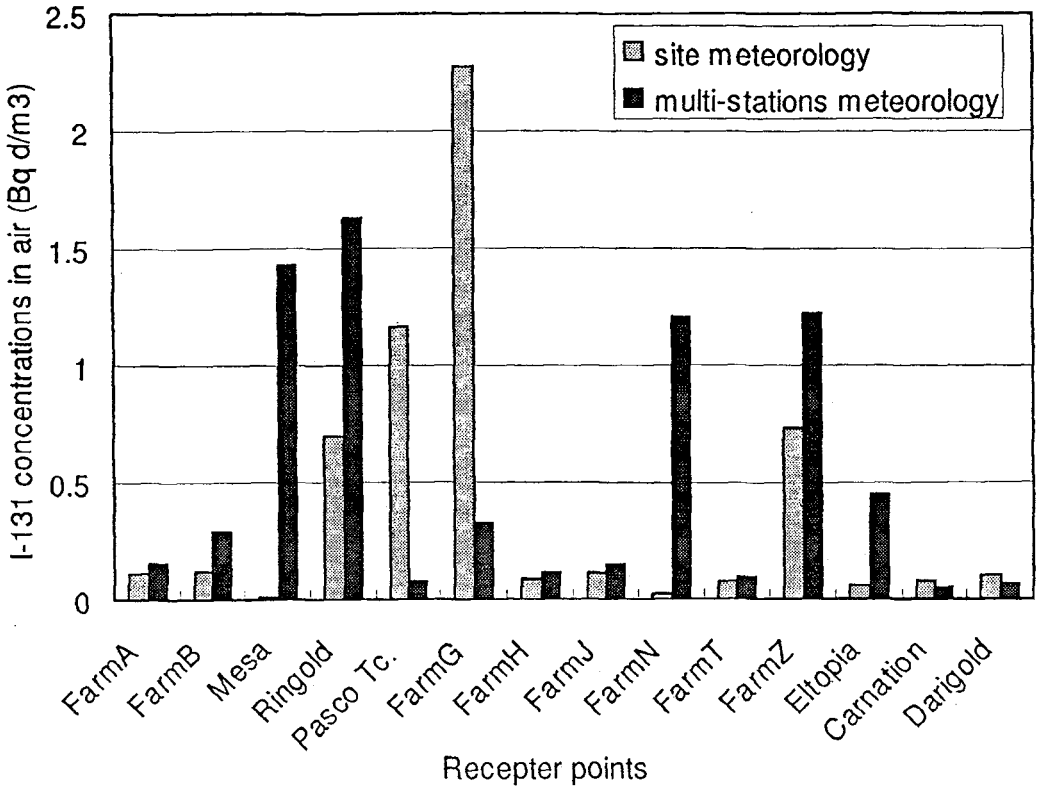

FIG. 45. Comparisons of I-131 time-integrated air concentrations between using two different meteorological data sets.

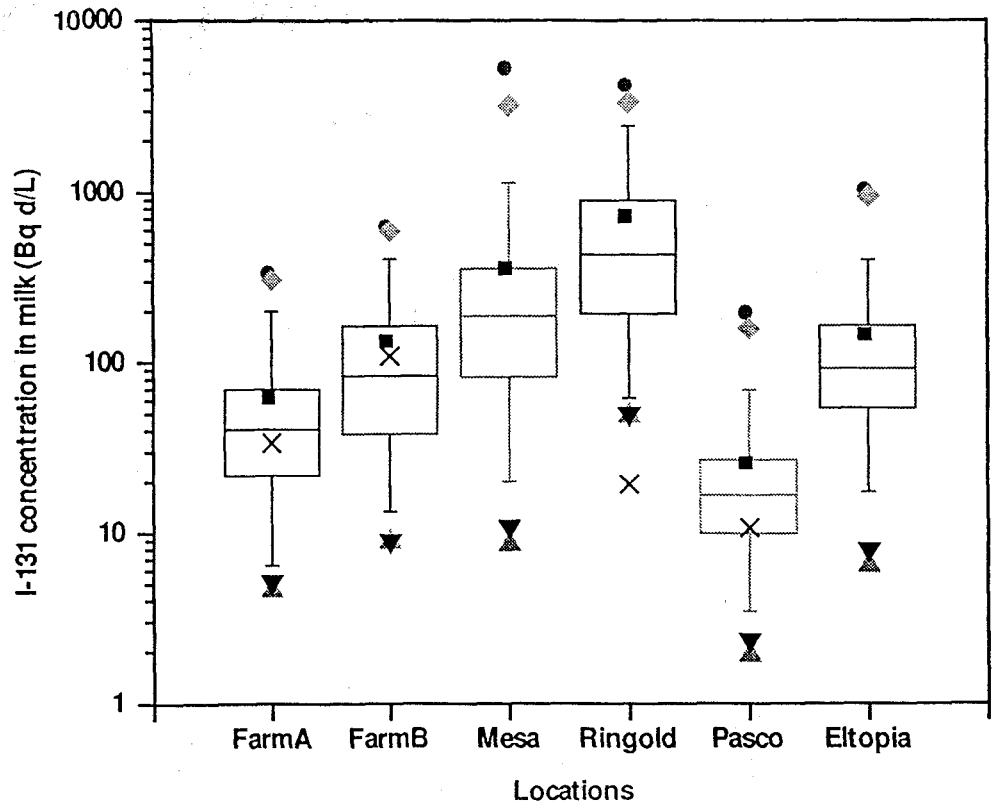

FIG. 46. Boxplots of I-131 concentrations in milk at several locations.

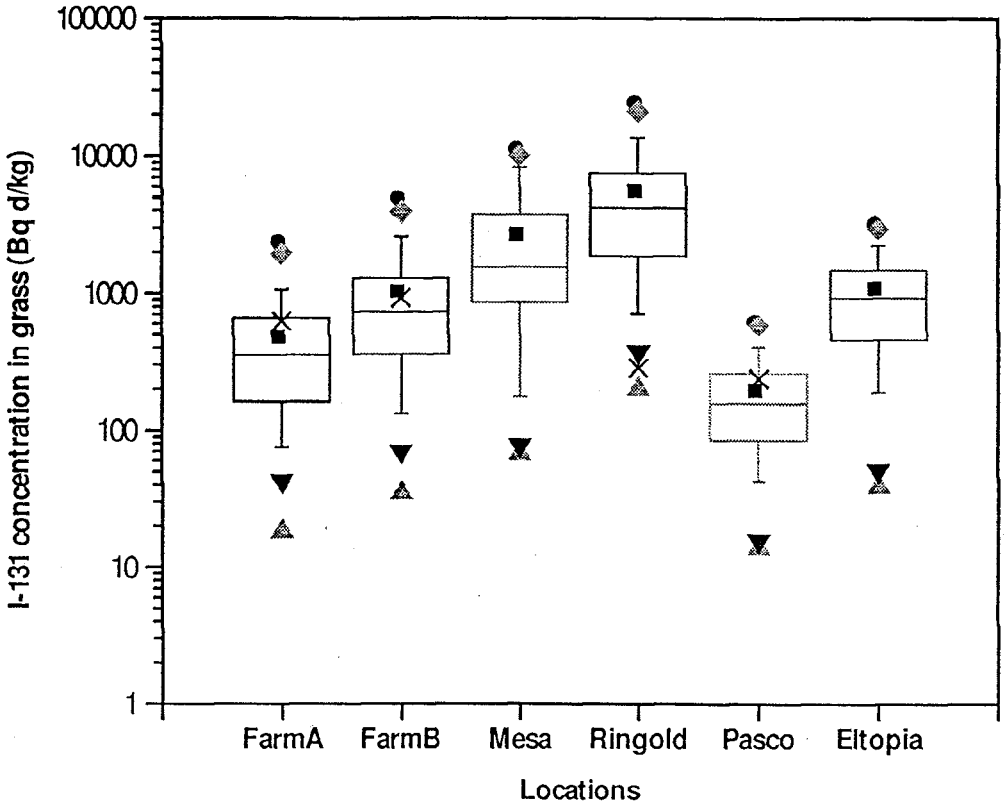

FIG. 47. Boxplots of I-131 concentrations in grass at several locations.

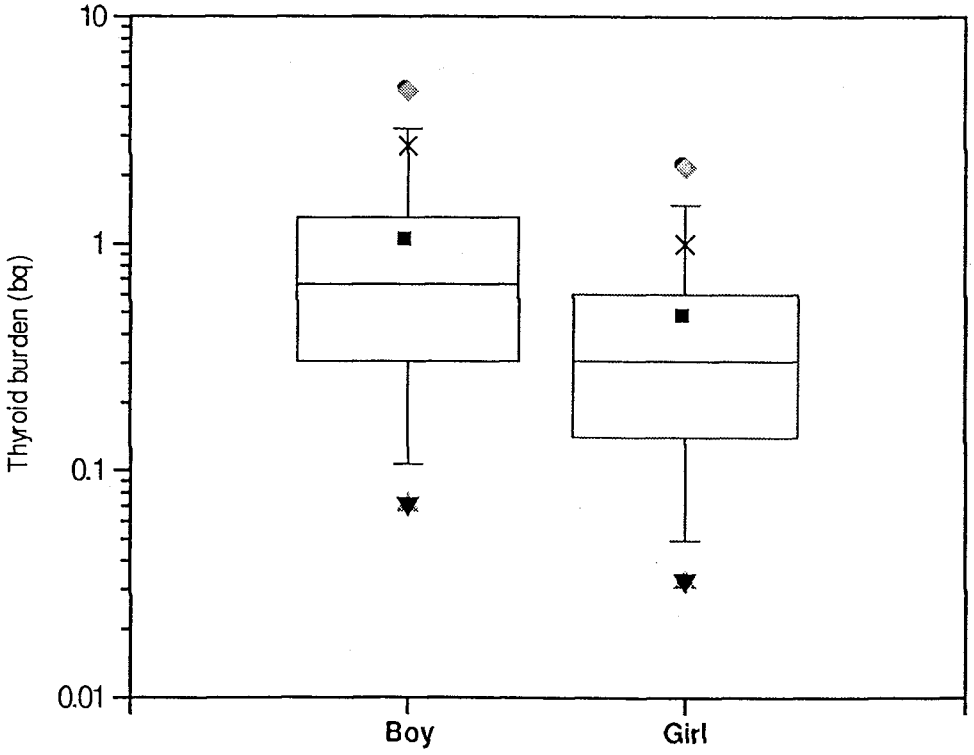

FIG. 48. Boxplots of I-131 thyroid burdens for a 4 year old boy and his 8 year old sister.

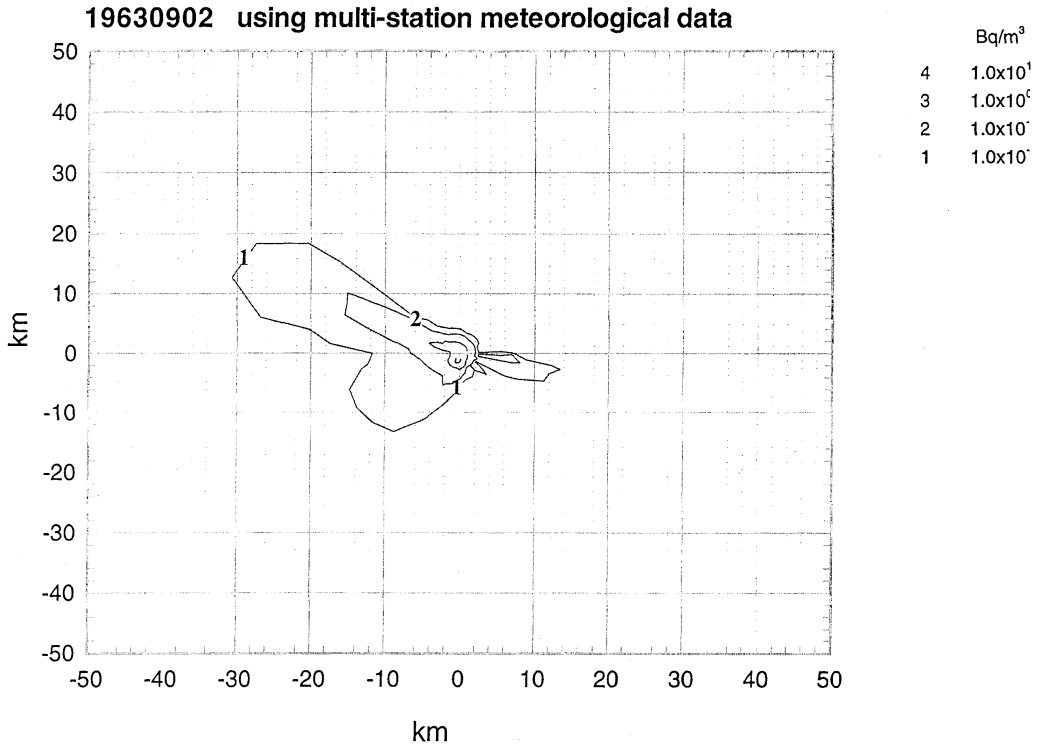

FIG. 49(a) Daily concentration in air of ^{131}I.

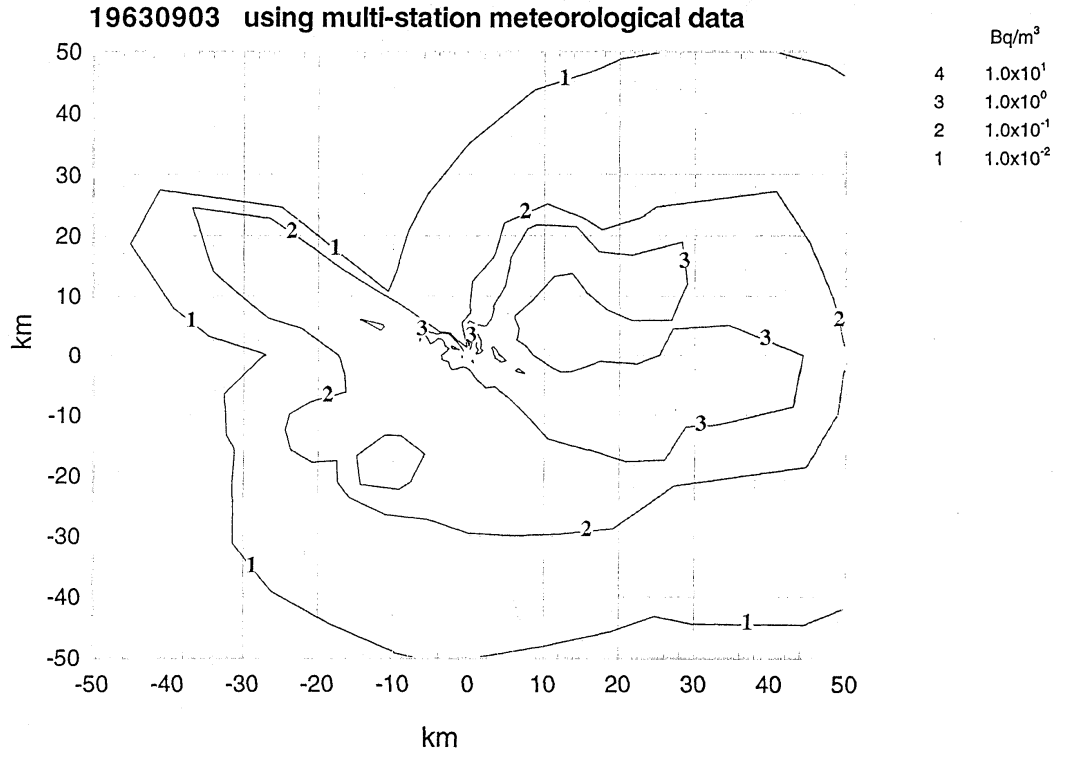

FIG. 49(b) Daily concentration in air of ^{131}I.

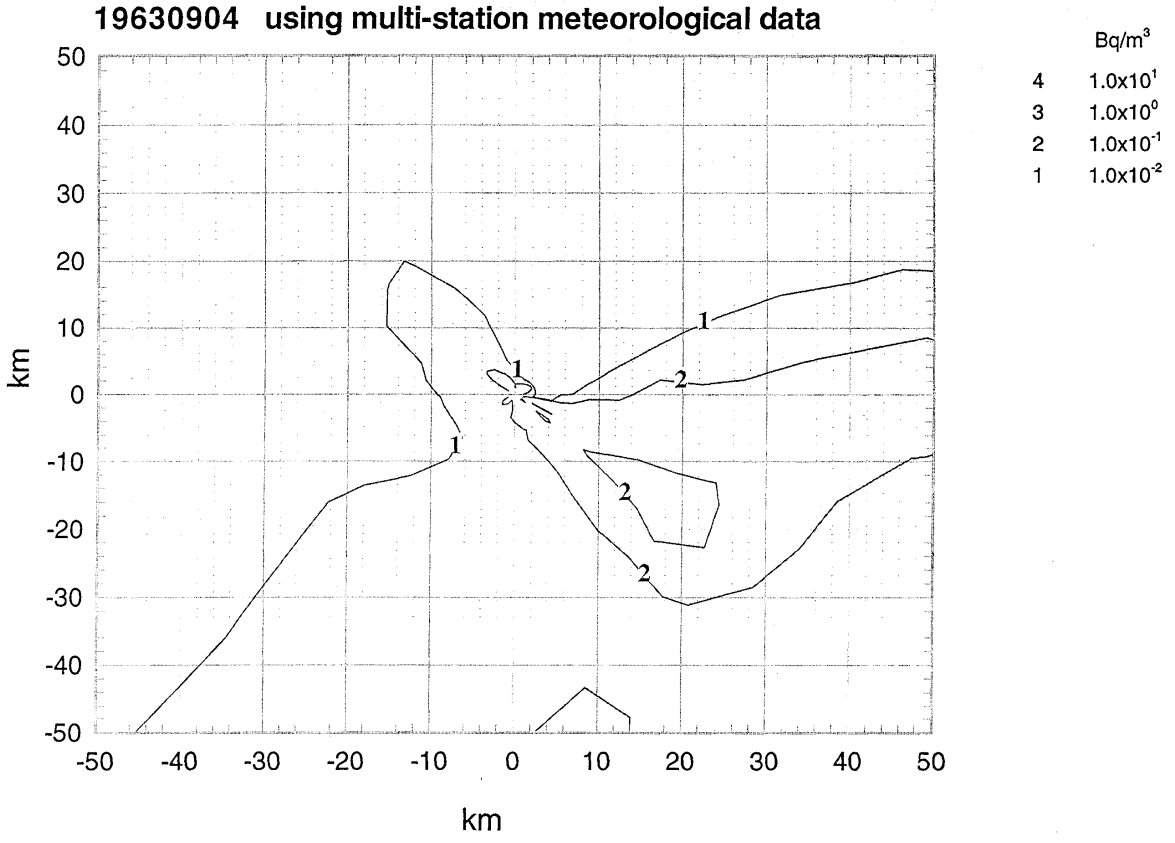

FIG. 49(c) Daily concentration in air of ^{131}I.

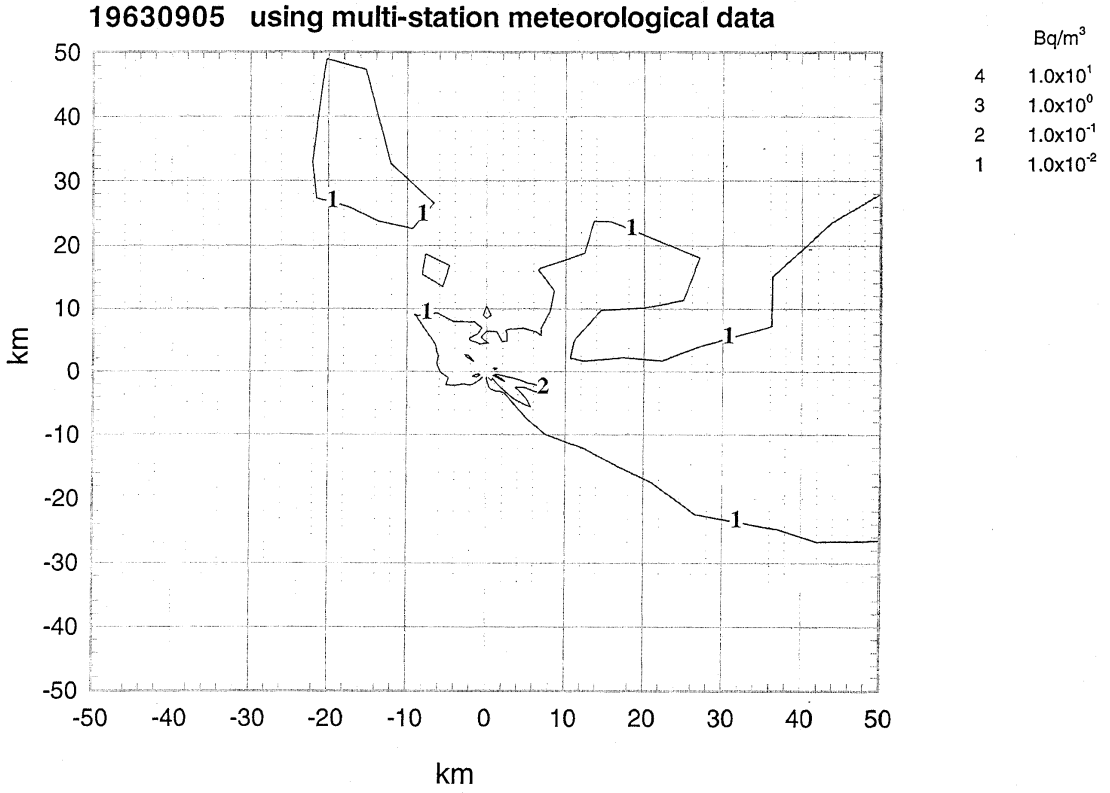

FIG. 49(d) Daily concentration in air of ^{131}I.

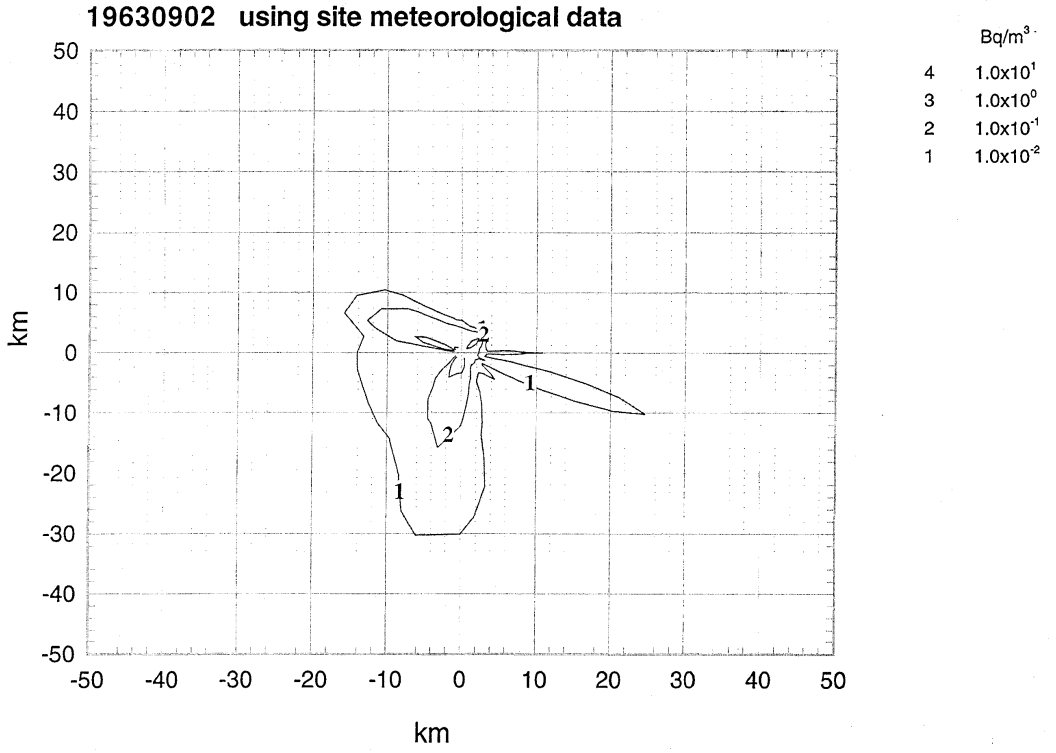

FIG. 50(a) Daily concentration in air of ^{131}I.

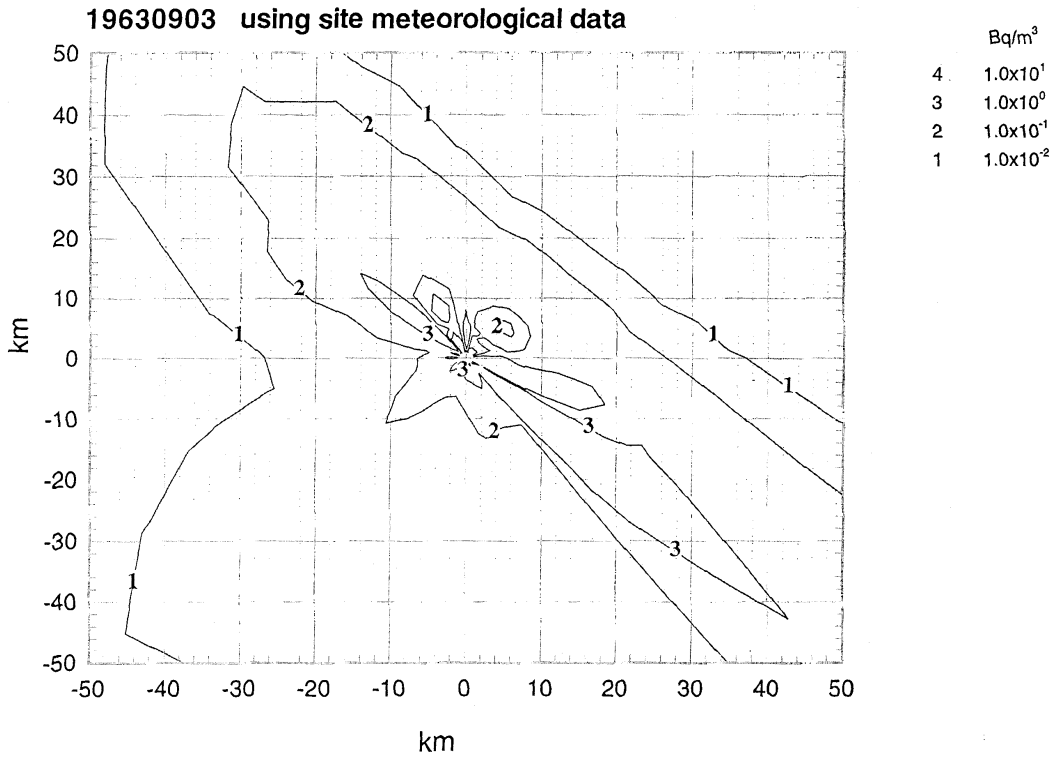

FIG. 50(b) Daily concentration in air of ^{131}I.

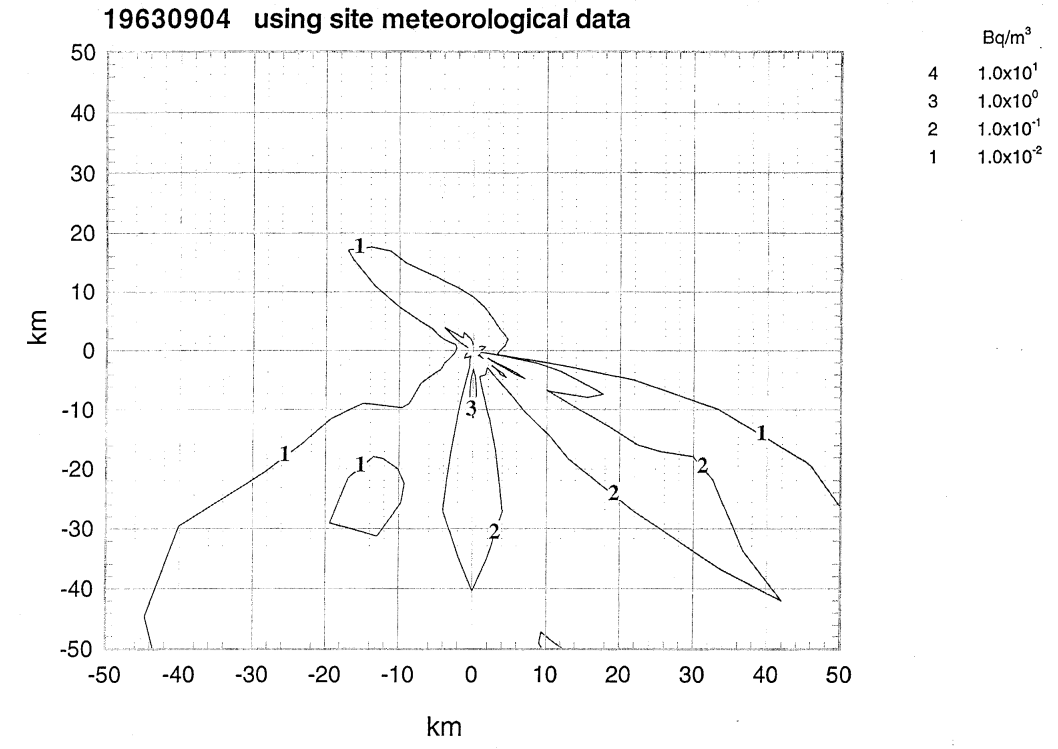

FIG. 50(c) Daily concentration in air of ^{131}I.

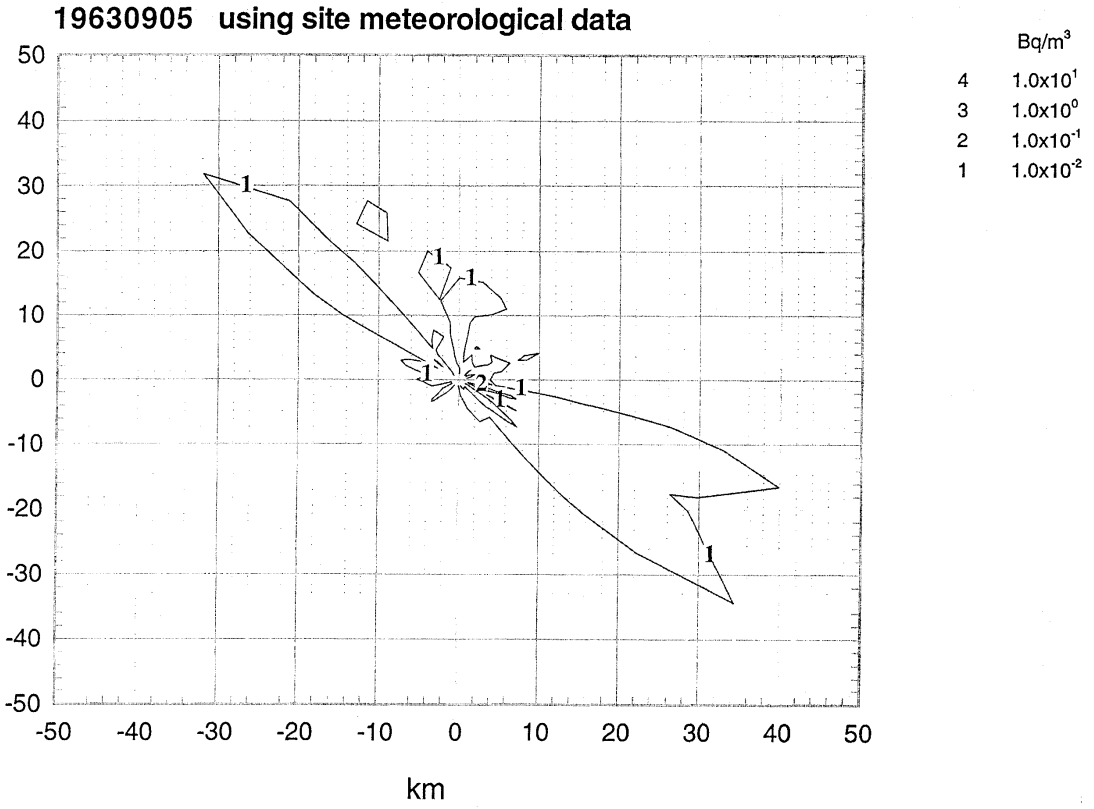

FIG. 50(d) Daily concentration in air of ^{131}I.

ACKNOWLEDGEMENT

We would like to extend thanks to Messrs. N. Kurosawa and S. Matsuoka of Visible Information Center Inc. for technical assistance of producing air concentration graphs and contours from the outputs of OSCAAR.

References

BRENK, H.D., VOGT, K.J., The calculation of wet deposition from radioactive plumes. *Nuclear Safety* 22: 362–371 (1981).

BRIGGS, G.A., Plume rise. USAEC Critical Review Series, TID-25075, U.S. Atomic Energy Commission, Washington, D.C. (1969).

BRIGGS, G.A., Plume rise predictions. in *Lectures on Air Pollution and Environmental Impact Analyses*, American Meteorological Society, Boston, Massachusetts, pp. 59–111 (1975).

EIMUTIS, E.C., KONICEK, M.G., Derivations of continuous functions for the lateral and vertical atmospheric dispersion coefficients. *Atmospheric Environment* 6: 859–863 (1972).

HEALY, J.W., BAKER, R.E., Radioactive cloud-dose calculations. in *Meteorology and Atomic Energy 1968*, TID-24190, U.S. Atomic Energy Commission, Washington, D.C. (1968).

HOMMA, T., TOGAWA, O., IIJIMA, T., Development of accident consequence assessment code at JAERI, EUR-13013/2, p.1049-1063, CEC, Brussels (1990).

HOMMA, T., SALTELLI, A., LISA package user guide Part I, PREP Preparation of input sample for Monte Carlo simulations, EUR 13922 EN, CEC, Luxembourg (1992).

HOMMA, T., SALTELLI, A., Importance measures in global sensitivity analysis of nonlinear models. *Reliability Engineering and System Safety*, 52: 1–17 (1996).

ICRP. Limits for the intake of radionuclides by workers. ICRP Publication 30 Part 1, *Annals of the ICRP*, 2 (3/4) (1979).

ICRP, Age-dependent doses to members of the public from intake of radionuclides: Part1. ICRP Publication 56, *Annals of the ICRP*, 20 (2) (1989).

IRWIN, J.S., A theoretical variation of the wind profile power-law exponent as a function of surface roughness and stability. *Atmospheric Environment* 13: 191–194 (1978).

KOCHER, D.C., Dose-rate conversion factors for external exposure to photons and electron radiation from radionuclides occurring in routine releases from nuclear fuel cycle facilities. *Health Physics*, 38: 543–621 (1980).

LENGEMANN, F.W., Predicting the total projected intake of radioiodine from milk by man – I. The situation where no counter measures are taken. *Health Physics*, 12: 825–830 (1966).

PETERSON, S-R., HOFFMAN, F.O., KÖHLER, H., Summary of the BIOMOVS A4 scenario: Testing models of the air-pasture-cow milk pathway using Chernobyl fallout data, *Health Physics,* 71: 149–159 (1996).

USNRC, Reactor Safety Study, Appendix VI, Calculation of reactor accident consequences, WASH-1400, U.S. Nuclear Regulatory Commission, Washington, D.C. (1975).

II–3. TAM DYNAMIC

Used by the University of Veszprém, Department of Radiochemistry, Hungary
B. Kanyár, Á. Nényei,

II–3.1. METHOD USED FOR DERIVING UNCERTAINTY ESTIMATES

Monte Carlo method. The distributions of the parameters were three angular and normal ones. The values and ranges of the transport coefficients in the cow were mainly assessed by personal judgment, taking into consideration that the F_m (milk transfer) should be 0.008 d/l in steady state.

The I-131 kinetics in the pasture-cow-milk pathway was modelled by a linear compartmental system given in Figure 51. The parameters (mainly not given in the scenario description) are in Table II–3.I.

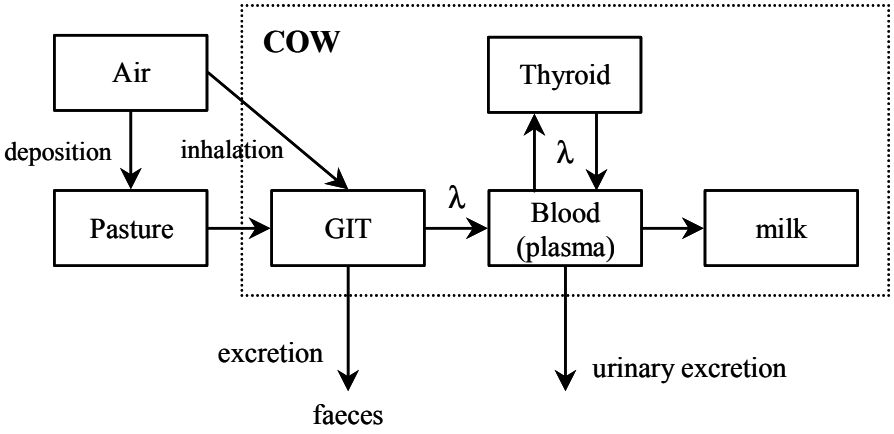

FIG. 51. Compartmental system used to modelling the I-131 kinetics in the pasture-cow-milk pathway.

Dose assessments were provided in the following:

— *External dose from the cloud:* Time integrated concentration in air times the external rate constant for the effective dose by gamma (Skin beta dose was negligable.). The reduction factor (defined by occupancy and shielding) was 0.3.

— *Ground exposure:* By daily deposition and surface external dose factor, meanwhile the reduction factor was 0.3.

— *Inhalation dose (committed equivalent dose, tissue dose to thyroid):* From the time integrated concentration in air, inhalation rate (adult man: 23 m3 d-1) and inhalation dose factor for adults. Reduction factor: 0.4.

— *Ingested dose* (committed equivalent dose, tissue dose to the thyroid): As the product of the contamination of the milk and vegetation, the ingestion rate and the dose factor to the thyroid, in case of adults.

TABLE II–3.I. PARAMETERS, MAINLY OF THE "COW SYSTEM"

Parameter	Mean value	Minimum	Maximum
Effective dry deposition rate (m/d)	715	300	1000
Interception factor for pasture	0.4	0.2	0.7
Interception factor for leafy vegetables	0.6	0.4	1.0
Yield of pasture (kg/m^2, dry w.)	0.5	0.2	0.7
Yield of vegetables (kg/m^2, fresh w.)	1.7	1.0	2.3
Wheathering rate constant (1/d)	0.07	0.03	0.15
Cow: inhal.rate (m^3/d)	120	70	160
excretion conct.to faeces (1/d)	0.5	0.1	2.0
transport coeff. from GIT to blood (1/d)	10	3	20
tr.coeff. from blood to thyroid (1/d)	3.5	1.5	8.0
from blood to milk (1/d)	0.5	0.15	1.5
from blood to urine (1/d)	3.7	1.5	10
from thyroid to blood (1/d)	0.12	0.03	0.3
daily milk production (liter/d)	11	6	16

Dose factors were driven from:

P.Jacob, H.Rosenbaum, N.Petoussi, M.Zankl: Calculation of Organ Doses from Environmental Gamma Rays, Part II., GSF-Bericht 12/90, 1990.

International BSS 1995, IAEA Vienna, 1996.

II–3.2. RESULTS OF THE SIMULATIONS

Deposition of Hanford I-131

	$\bar{X}$ ($Bq\ m^{-2}$)	95% Confidence Interval	
		Lower Bound	Upper Bound
Total Deposition:			
Farm A	78	35	167
Farm B	179	113	268
Mesa	6.5	4.1	8.6
Eltopia	11	8.8	3
Pasco	10	5.1	15
Ringold	43	34	60

($\bar{X}$ denotes the arithmetic mean for the location and the time period specified)

I-131 Concentrations in Milk

	$\bar{X}$ (Bq d/l)	95% Confidence Interval	
		Lower Bound	Upper Bound
Monthly Integrals – Milk[1]:			
Farm A	49	14	105
Farm B	129	39	210
Mesa	1.9	0.71	3.5
Eltopia	3.8	1.8	6.4
Pasco	5.7	2.0	9.8
Ringold	14	4.9	26

[1] Please calculate the contamination of whole, unprocessed milk.

I-131 Concentrations in Milk (cont.)

	$\overline{X}$	95% Confidence Interval	
	(Bq d/l)	Lower Bound	Upper Bound
Daily Averages – Milk[1]:	Twin City	Darigold	
September 4	0.087	< 0.001	
5	0.16	0.0076	
6	0.17	0.024	
7	0.20	0.033	
8	0.22	0.037	
9	0.24	0.039	
10	0.26	0.043	
11	0.27	0.050	
12	0.27	0.056	
13	0.27	0.061	
14	0.26	0.064	
15	0.26	0.068	
16	0.25	0.069	
17	0.24	0.069	
18	0.24	0.068	
19	0.22	0.068	
20	0.21	0.069	
21	0.20	0.062	
22	0.20	0.059	
23	0.18	0.055	
24	0.17	0.052	
25	0.17	0.049	
26	0.15	0.045	
27	0.14	0.041	
28	0.13	0.039	
29	0.12	0.037	
30	0.10	0.035	

($\overline{X}$ denotes the arithmetic mean for the location and the time period specified)
[1] Please calculate the contamination of whole, unprocessed milk.

I-131 Concentrations in Vegetation

	$\overline{X}$	95% Confidence Interval	
	(Bq d/kg f.w.)	Lower Bound	Upper Bound
Monthly Integral: Leafy Sage			
Farm A	270	140	400
Farm B	710	360	1100
Mesa	11	5.7	17
Eltopia	22	12	35
Pasco	31	16	48
Ringold	77	39	120
Monthly Integral: Hay			
Farm A	1100	610	1600
Farm B	2400	1300	4000
Mesa	33	18	48
Eltopia	67	38	110
Pasco	99	53	160
Ringold	230	140	320
Monthly Integral: Grass – Silage[2]			
Farm A	≈ mean of the leafy veg. and hay for fresh w.		
Farm B			
Mesa			
Eltopia			
Pasco			
Ringold			

I-131 Concentrations in Vegetation (cont.)

	$\bar{X}$ (Bq d/kg f.w.)	95% Confidence Interval Lower Bound	Upper Bound
Monthly Integral: Grass – Silage[2]			
Farm A	≈ mean of the leafy veg. and hay for fresh w.		
Farm B			
Mesa			
Eltopia			
Pasco			
Ringold			

($\bar{X}$ denotes the arithmetic mean for the location and the time period specified)
[2] Includes grasses, alfalfa, clover, rye, and straw.

Human I-131 Intake

	$\bar{X}$ (Bq)	95% Confidence Interval Lower Bound	Upper Bound
Monthly Averages: Carnation			
Man	29	12	49
Woman	37	13	57
Child	35	13	59
Monthly Averages: Darigold			
Man	0.96	0.37	1.6
Woman	1.2	0.48	2.0
Child	1.2	0.45	2.1
Thyroid Burden October 19, 1963:			
Farm B Boy	2.5	0.6	5.0
Farm B Girl	0.52	0.20	1.5

External Dose from Hanford I-131

	$\bar{X}$ (nSv)	95% Confidence Interval Lower Bound	Upper Bound
Cloud Exposure:			
Farm A	0.047	0.021	0.095
Farm B	0.11	0.05	0.20
Mesa	0.0039	0.0016	0.0089
Eltopia	0.0065	0.0031	0.012
Pasco	0.0059	0.0028	0.011
Ringold	0.026	0.013	0.050
Ground Exposure: 2–5 September 1963			
Farm A	2.5		
Farm B	5.7		
Mesa	0.21		
Eltopia	0.39		
Pasco	0.32		
Ringold	1.4		
Ground Exposure: 2 September – 1 October 1963			
Farm A	8.0		
Farm B	18		
Mesa	0.65		
Eltopia	1.1		
Pasco	1.0		
Ringold	4.4		

Inhalation Dose from Hanford I-131 (committed equivalent dose to thyroid)

	$\overline{X}$	95% Confidence Interval	
	(nSv)	Lower Bound	Upper Bound
Inhalation from Cloud:			
Farm A	150	65	320
Farm B	330	130	650
Mesa	12	4	25
Eltopia	20	8	45
Pasco	19	7	42
Ringold	81	36	170

Ingestion Dose from Hanford I-131 (committed equivalent dose to thyroid)

	$\overline{X}$	95% Confidence Interval	
	(mSv)	Lower Bound	Upper Bound
2 September – 1 October 1 1963:			
Farm A	0.012		
Farm B	0.033		
Mesa	0.00049		
Eltopia	0.00099		
Pasco	0.0014		
Ringold	0.0035		

Total Dose from Hanford I-131

	$\overline{X}$	95% Confidence Interval	
	(mSv)	Lower Bound	Upper Bound
2–5 September 1963:			
Farm A	0.0019		
Farm B	0.0056		
Mesa	0.000043		
Eltopia	0.000074		
Pasco	0.000086		
Ringold	0.00011		
2 September – 1 October 1963:			
Farm A	0.012		
Farm B	0.033		
Mesa	0.00049		
Eltopia	0.00099		
Pasco	0.0014		
Ringold	0.0095		

II–4. CLRP

Used by the Central Laboratory for Radiological Protection,
Department of Radiation Hygiene, Poland
P. Krajewski

II–4.1. MODEL DESCRIPTION

II–4.1.1. Model Name: CLRP — Concentration Levels Rapid Predictions

II–4.2. IMPORTANT MODEL CHARACTERISTICS

II–4.2.1. Intended purpose of the model in radiation assessment

The model CLRP was created in 1989 as a part of research project "LONG-LIVED POST-CHERNOBYL RADIOACTIVITY AND RADIATION PROTECTION CRITERIA FOR RISK REDUCTION" performed in co-operation with U.S. Environmental Protection Agency. The aim of this project was to examine the fate of long-lived radionuclides in the terrestrial ecosystem [1, 2]. Following the next years the model was intensively developed and extended for another radionuclides especially for iodine [3].

The aim of this code is to simulate the transport of radionuclides through environment to humans body due to examine the fate of some radionuclides in the ecosystem. The Input Parameters Data Base of the code has been created that allows to evaluate the radiological impact for: I, Cs, Ru, Te, Sr. One is able to set up to 20 radionuclides of 44 elements.

All dynamic processes are described by differential formulas and are solved numerically. Radionuclides concentrations in the particular components of terrestrial ecosystem e.g. soil, vegetation, animal tissues and animal products are calculated as a function of time following calculated deposition from the atmosphere. The model considers seasonal changes in the biomass of vegetation and animal diets, also specific ploughing and crop-harvest dates. Human dietary data are included to permit calculation of time -dependent radionuclide ingestion rates as well as critical organ content of radionuclide for seven different age group of population.

Program enables to calculate doses from the following pathways: external (cloud, ground exposure); internal (inhalation, ingestion) and is designed to make able the simulation of many different radiological situations (chronic or acute releases) and dose affecting countermeasures as some diet components ban, buildings shielding as well as stable iodine prophylactics.

During the 1989–1995 period the CLRP code performance for ^{137}Cs was check out in a frame of the International IAEA programme" Validation of models for the transfer of Radionuclides in Terrestrial, Urban and Aquatic Environment and Acquisition of Data for that Purpose" on he base of two "blind" scenarios CB and S [4].

Since 1995 the validation of the CLRP v.4.4 for 137Cs and 131 I has started in a frame of International Programme: BIOMOVS II - BIOspheric MOdel Validation Study, PHASE II in the Working Group: Effect of Modellers Interpretation on Model Uncertainties Biomovs II.

The CLRP code was qualified as one of the three codes that have taken part in this programme. Final results of BIOMOVS II programme were presented and published.

All dynamic processes are described by exponential formulas and are solved numerically.

The new version of the computer code CLRP (Concentration Levels Rapid Predictions) has been written in the Visual Basic Language for Excel 7.0 for Windows 95 as an Ad-In application and consists with dialogs and programs that enable to communicate with one Scenario File simultaneously. Scenario File comprises a set of worksheets of Excel 7.0- one pair of worksheets for particular component input and prediction data. More detailed information one can find in [5].

II–4.2.2. Method used for deriving uncertainty estimates

The uncertainty estimates given for the HANFORD scenario were derived by personal judgement of the range of uncertainty of some model parameters. Item yield of the grass, cow diet, human diet, iodine retention of the cow and human. For all parameters log-normal distribution was assumed with uncertainty factor (1.5– 3). Then CLRP code calculates overall uncertainty range using error propagation method. Unhomogeneity of deposition for the same location was taken in to account only for doses uncertainty estimation.

II–4.3. DESCRIPTION OF PROCEDURES AND PARAMETERS

The aim of this work was to perform the dose reconstruction for the specified locations namely: Farm A (BENTON CITY), Farm B (TWIN BRIDGES), Farm N (Mesa), Farm Z (Eltopia), Farm T (Pasco) in the Hanford region. Due to close vicinity specified locations to release point (Purex stack) and complicated pattern of mass air transport the time dependent I-131 air concentrations changed to 4 orders of magnitude depending on locations. See Figure 52 below. Therefore, the doses reconstruction procedure had to use extensively all available measurements data starting from milk contamination to air measurements for particular location. In another words the task consisted with few steps that were performed for each location as follow:

(1) comparison consistency of milk and grass pasture measurements.

(2) deposition reconstruction based on vegetation measurements

(3) air concentration reconstruction based on vegetation and air measurement.

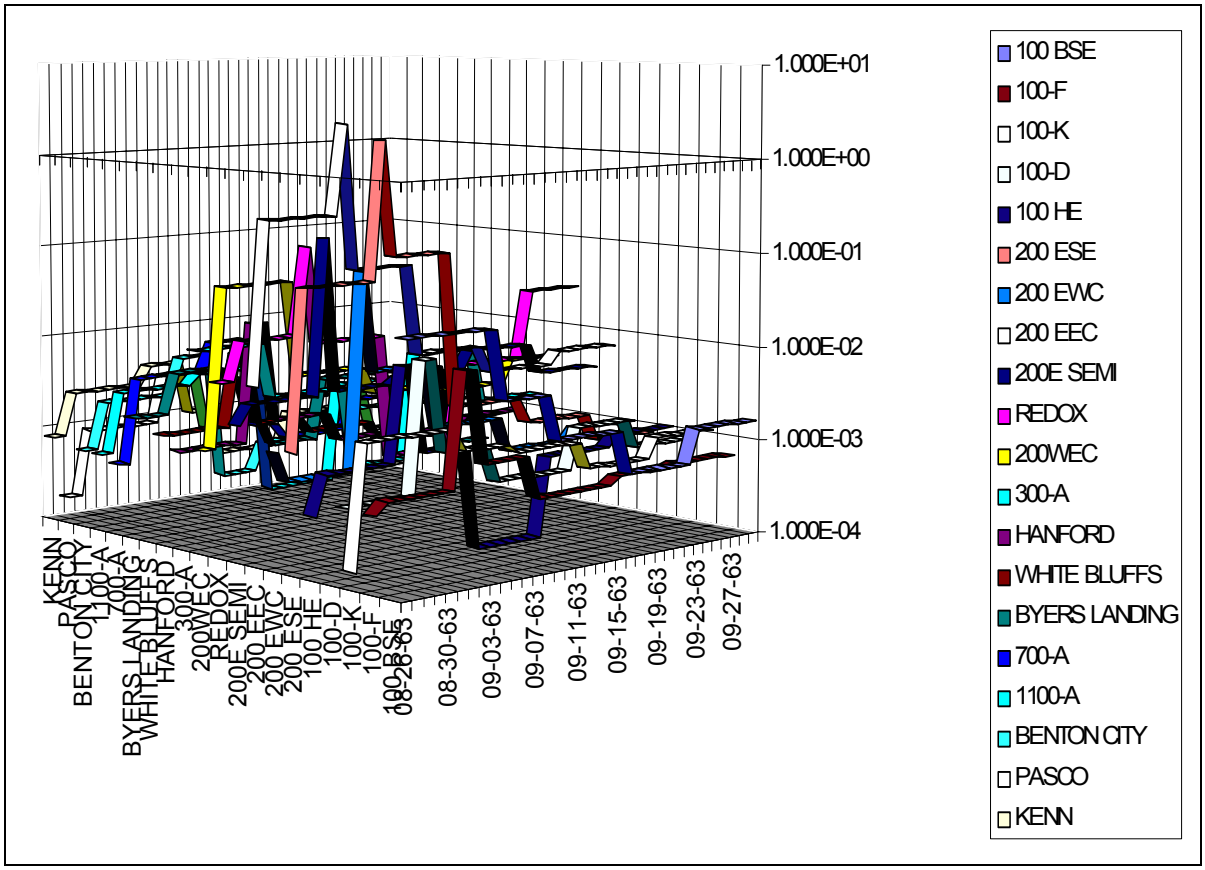

FIG. 52. I-131 air concentrations measured by Hanford sampling stations.

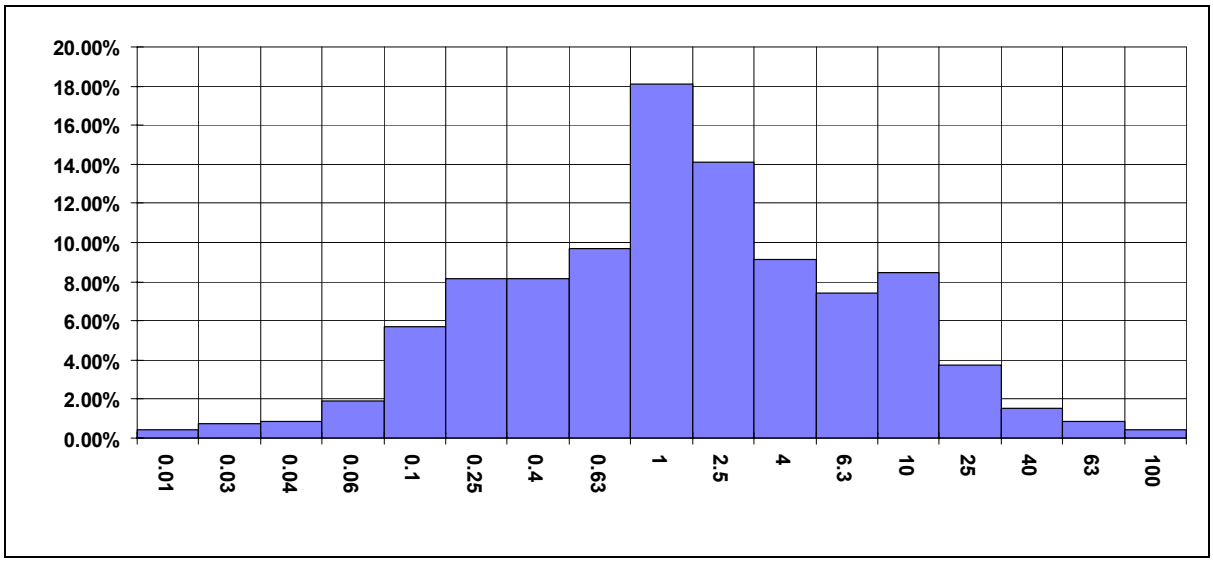

FIG. 53. I-131 particulate distribution (mean of particle diameter = 6.016μm).

II–4.3.1. I-131 air concentration

For each location several runs of the code were performed for different air concentration pattern up to get satisfactory agreement between measured and predicted data for pasture and milk. For some location air measurement data performed by closest air sampling station were used for another plume dispersion model was applied.

For all locations the same dry deposition velocity for aerosol fraction was used equal to 1.610^{-3} [m/s]. The assumed distribution of I-131 bound to aerosol fraction is presented Figure 53.

Iodine form was assumed as it was suggested in the scenario e.g. 25% particulate, 40% I_2, and rest 35% organic. For I_2 deposition velocity equal to 0.01 m/s was taken.

II–4.3.2. Pasture grass

Pasture grass yield was equal to 0.7 kg/m^2 f.w. with dry matter contents 20%. This value was evaluated from scenario on base of Washington Hay production data Table II–4.2: Area (Production = 1, 976, 000 tons) /(Area Harvested = 346,000ha) tat gives 0.519 hay/m^2.

Assuming three cuts of hay and 80% dry matter contents of hay one can get (0.519/3*(80%)/(20%)) values equal to 0.7 kg/m^2 . This value seems to be lower than grass yield in some European countries (1–1.5).

For pasture grass monthly integrals for August-63, September-63, October-63 and Total integral where calculated.

II–4.3.3. Hay, silage

Hay and silage(alfalfa) monthly integrals were calculated assuming constant harvest during September 1963. These estimations may be very confused as no indication in the scenario about of accurate terms of harvest in specified locations. Normally harvest term for alfalfa is at the beginning of September (second cut), and for hay in the middle of September (third cut).

In addition there is no indication in he scenario about composition of silage e.g. what is percentage of another uncontaminated components e.g. grains, straw etc.

II–4.3.4. Sage

Sage was modelled as continuous vegetation of the yield equal to 1.5 kg/m^2 and 20% dry matter contents. It would be appreciable to have in the scenario any indication about this plant (leaf area index for instance) as quite high contamination of that plan was measured along the rout 4S in 3 September 1963 and measurements data of that plant might be deposition pattern indicator in the Hanford area.

II–4.3.5. Milk

I-131 concentration in milk was calculated assuming cow diet equal to 45 kg/per day f.w. of the pasture during the period September 1963. This value was withdrawn from scenario as 9kg/day d.w. assuming 20% of dray matter contents. This value seems to be lower by factor two fold comparing with the cow diet in some countries 70-90 kg/par day of f.w.

Milk retention was calculated on the iodine metabolism function in cow that gives equilibrium factor for I-131 equivalent to 1.68 10^{-3} [d/L]. This factor is 4 fold lower than 9.910^{-3} [d/L] recommended by Ng (1982) but in good agreement with values obtained by Dreicer and Clusek 1988 (1.3 ± 0.410^{-3} [d/L]).

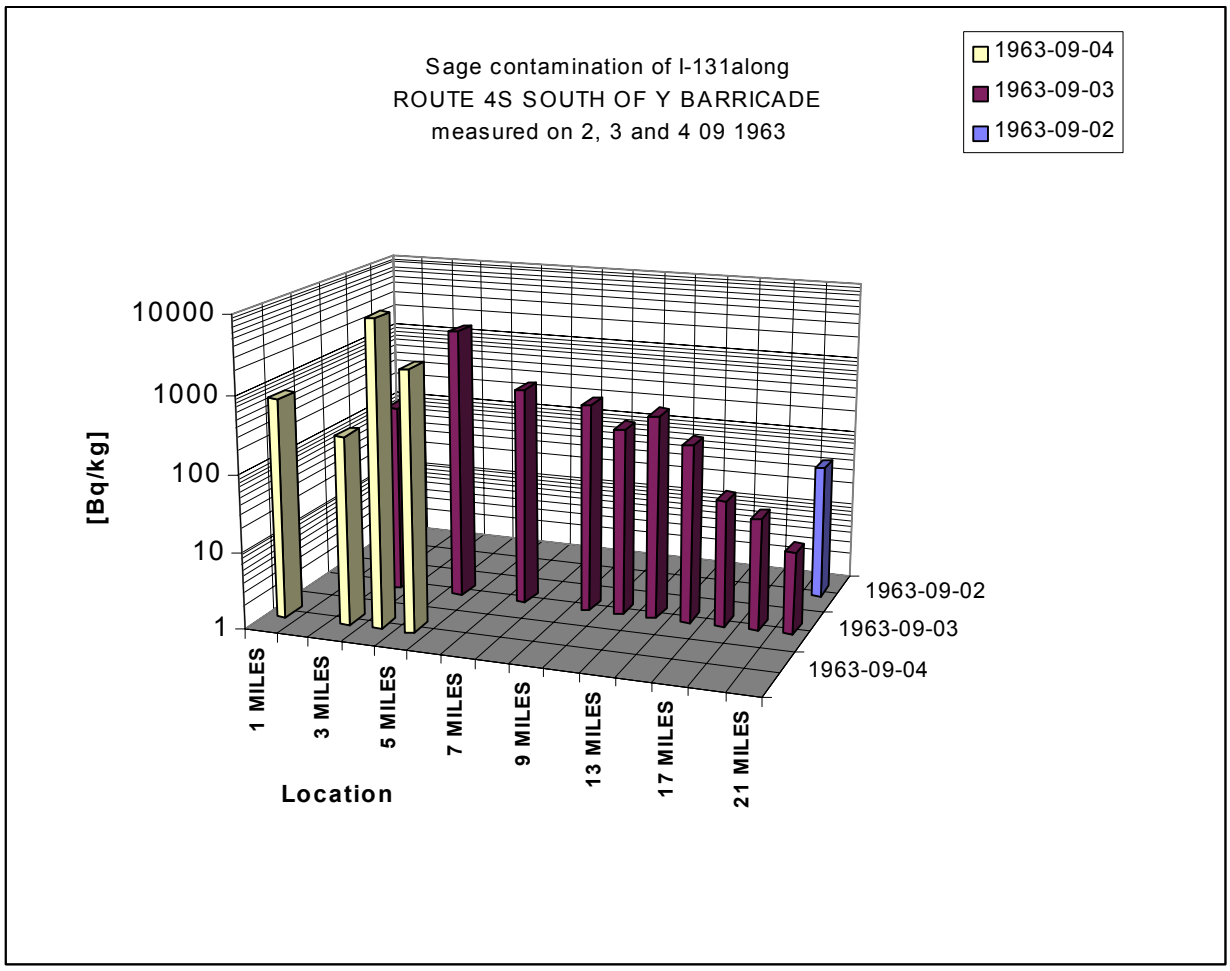

FIG. 54. Sage contamination at the Hanford Site.

II–4.3.6. Intake

Intake of iodine ^{131}I was calculated assuming daily consumption rate for milk and milk products and selected leafy vegetables Table II–4.I.

TABLE II–4.I. DAILY CONSUMPTION RATE FOR ADULT AND CHILD ONE YEAR OLD

Age group	Component Row Products Names	Delay between production and delivery	Food processing factor	Period I from 02 - I to 01 - IV	Period II from 02 – IV to 30 - IV	Period III from 01 - V to 31 - VII	Period VI from 01 - VIII to 15 - IX	Period V from 16 - IX to 30 - XI	Period VI from 01 – XII to 31 - XII
Man	lettuce	03	0.57	0.00	0.00	0.00	0.03	0.03	0.00
(Test person)	spinach	03	0.57	0.00	0.00	0.00	0.03	0.00	0.00
	dairy	01	1.00	0.40	0.40	0.40	0.40	0.40	0.40
Child 1 y old	dairy	01	1.00	1.00	1.00	1.00	1.00	1.00	1.00

II–4.3.7. Thyroid

Thyroid burden was calculated base on iodine metabolism model in man developed by J.R. Johnson; "Radioiodine dosimetry"; *Journal of Radioanalytical Chemistry*, Vol 65, 1981 pp. 223-238. Example of model parameters for 10 years old child is presented below (Table II–4.II). Based on thyroid burden prediction the effective dose from ingestion was calculated.

For adult man, adult women and child 1 year old.

Iodine metabolism model used in the girl 8 years old thyroid burden calculations was for child 10 years old (Table II–4.II).

TABLE II–4.II. METABOLIC PARAMETERS OF IODINE USED IN THE CALCULATION OF THE THYROID BURDEN DOR DIFFERENT AGE GROUPS. JOHNSON J.R, RADIOIODINE DOSIMETRY, *J. RADIOANAL. CHEM 65 (1981)*

Compartment	Age group							
	Child 3 m	Child 1 y	Child 2 y	Child 5 y	Child 10 y	Child 15 y	Ref. woman	Ref. Man
Daily intake of stable iodine mg	10.0	20.6	31.1	62.8	116.0	168.0	166.0	200.0
Body mass [kg]	3.51	7.2	10.9	22	40.5	58.9	58	70
Intake/kg body mass [mg/kg]	2.8	2.9	2.9	2.9	2.9	2.9	2.9	2.9
Thyroid mass [g]	1.63	2.12	2.65	4.39	7.87	12.1	17	20
Iodine concentration in thyroid [mg/g]	184	142	113	226	470	686	588	600
Thyroidal daily uptake [mg]	3.3	6.7	10.1	20.4	37.6	54.7	53.9	65.0
Inorganic compartment content [mg]	5.1	10	16	32	59	85	84	100
Organic compartment content [mg]	56	120	170	350	650	940	930	1100
Thyroid iodine content [mg]	300	300	300	990	3700	8300	10000	12000
Uptake of iodine from Gut, Lung rate constant l_1 [d^{-1}]	192	192	192	192	192	192	192	192
Thyroid rate constant l_3 [d^{-1}]	0.011	0.022	0.034	0.021	0.010	0.007	0.005	0.005
Excretion of iodine from the inorganic compartment to urine compartment l_5 [d^{-1}]	1.92	1.92	1.92	1.92	1.92	1.92	1.92	1.92
Excretion of iodine from the organic compartment to inorganic compartment l_4 [d^{-1}]	0.053	0.053	0.053	0.053	0.053	0.053	0.053	0.053
Excretion of iodine from the organic compartment to urine compartment l_6 [d^{-1}]	0.005	0.005	0.005	0.005	0.005	0.005	0.005	0.005

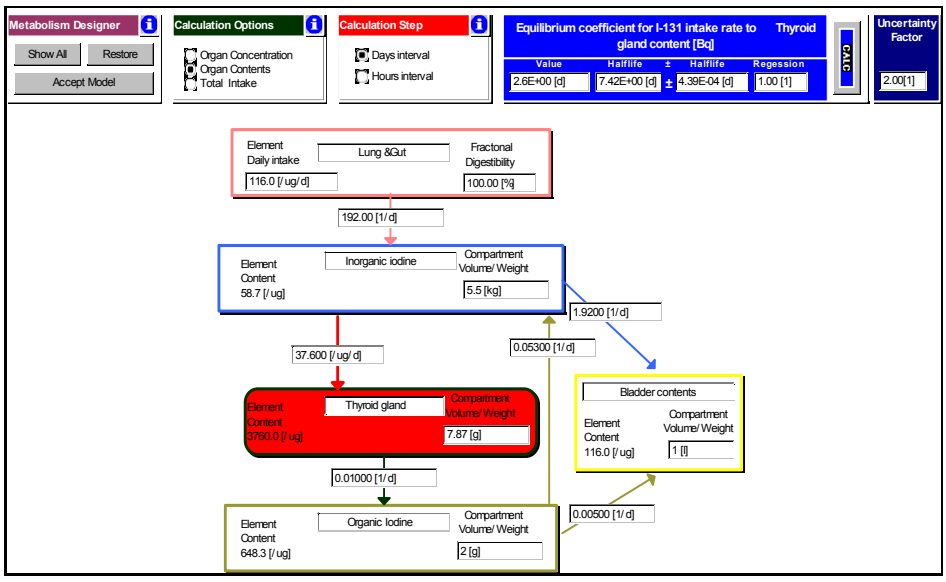

FIG. 55. iodine metabolism model for child 10 years old (print out from the CLRP interactive dialog).

II–4.3.8. Dose calculation

Parameters used for dose calculation are presented on the Figure 55 (printout from the CLRP interactive dialog). For the test person "rural habit" was assumed with about 10 hours (40% of 24 hours) spending outdoor. Shielding and filtration factors for small concrete house were assumed Figure 56.

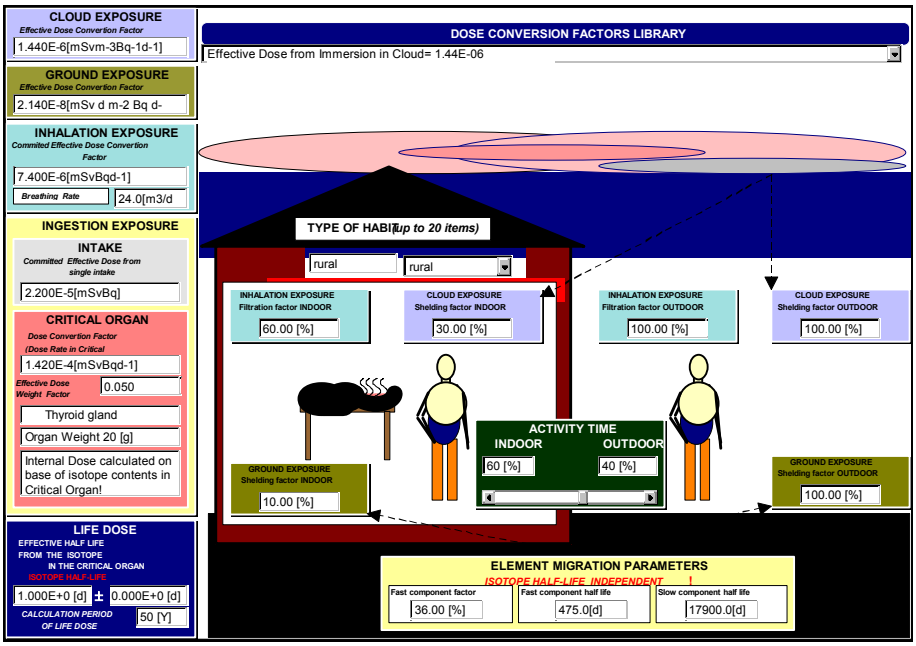

FIG. 56. Doses calculation parameters for test person.

TABLE II–4.III. DOSE CONVERSION FACTORS USED IN CALCULATION GSF-REPORT 12/90 (EXTERNAL), BSS 115 (INTERNAL), ORNL-5000 (IN ORGAN)

Effective dose Cloud **[man]** [mSv/d/Bq/m^3]	Effective dose Water **[man]** [mSv/d/Bq/m^3]	Effective dose Ground **[man]** [mSv/d/Bq/m^3]	Effective dose Inhalation **[man]** [mSv/Bq]	Effective dose Ingestion **[man]** [mSv/Bq]	Dose rate in Crit. organ **[man]** [mSv/Bq/d]
1.440E-06	3.150E-09	2.136E-08	7.400E-06	2.200E-05	1.420E-04
Effective dose Cloud **[woman]** [mSv/d/Bq/m^3]	Effective dose Water **[woman]** [mSv/d/Bq/m^3]	Effective dose Ground **[woman]** [mSv/d/Bq/m^3]	Effective dose Inhalation **[woman]** [mSv/Bq]	Effective dose Ingestion **[woman]** [mSv/Bq]	Dose rate in Crit. organ **[woman]** [mSv/Bq/d]
1.440E-06	3.150E-09	2.136E-08	7.400E-06	2.200E-05	1.700E-04
Effective dose Cloud **[ch15y]** [mSv/d/Bq/m3]	Effective dose Water **[ch15y]** [mSv/d/Bq/m3]	Effective dose Ground **[ch15y]** [mSv/d/Bq/m3]	Effective dose Inhalation **[ch15y]** [mSv/Bq]	Effective dose Ingestion **[ch15y]** [mSv/Bq]	Dose rate in Crit. organ **[ch15y]** [mSv/Bq/d]
1.440E-06	3.150E-09	2.136E-08	1.100E-05	3.400E-05	2.380E-04
Effective dose Cloud **[ch10y]** [mSv/d/Bq/m3]	Effective dose Water **[ch10y]** [mSv/d/Bq/m3]	Effective dose Ground **[ch10y]** [mSv/d/Bq/m3]	Effective dose Inhalation **[ch10y]** [mSv/Bq]	Effective dose Ingestion **[ch10y]** [mSv/Bq]	Dose rate in Crit. organ **[ch10y]** [mSv/Bq/d]
1.608E-06	*3.150E-09*	2.352E-08	1.900E-05	5.200E-05	3.590E-04
Effective dose Cloud **[ch 5y]** [mSv/d/Bq/m3]	Effective dose Water **[ch 5y]** [mSv/d/Bq/m3]	Effective dose Ground **[ch 5y]** [mSv/d/Bq/m3]	Effective dose Inhalation **[ch 5y]** [mSv/Bq]	Effective dose Ingestion **[ch 5y]** [mSv/Bq]	Dose rate in Crit. organ **[ch 5y]** [mSv/Bq/d]
1.608E-06	*3.150E-09*	2.352E-08	3.700E-05	1.000E-04	6.270E-04
Effective dose Cloud **[ch 1y]** [mSv/d/Bq/m3]	Effective dose Water **[ch 1y]** [mSv/d/Bq/m3]	Effective dose Ground **[ch 1y]** [mSv/d/Bq/m3]	Effective dose Inhalation **[ch 1y]** [mSv/Bq]	Effective dose Ingestion **[ch 1y]** [mSv/Bq]	Dose rate in Crit. organ **[ch 1y]** [mSv/Bq/d]
1.824E-06	*3.150E-09*	2.880E-08	7.200E-05	1.800E-04	1.290E-03

TABLE II–4.IV. INHALATION RATES FOR INHALATION DOSE CALCULATION

Adult man	Adult woman	Child 15 y old	Child 10 y old	Child 5 y old	Child 1 y old
24 m^3 per day	21 m^3 per day	18 m^3 per day	15 m^3 per day	10 m^3 per day	4 m^3 per day

The effective doses considering both external (Cloud, Ground) and internal (Inhalation, Ingestion) pathways were calculated. Additionally the doses to thyroid from inhalation and ingestion are reported

II–4.4. DATA EVALUATION

The reconstruction of I-131 concentrations in air and a comparison of pasture grass and milk predictions with measurements data and reconstructed thyroid burden, are presented for the specified locations namely: Farm A, Farm B, Mesa, Eltopia and Pasco. The integrated values for the components specified in Scenario and calculated doses are presented for each location. Table II–4.V provides a summary of the calculated doses for each specified location.

TABLE II–4.V. SUMMARY OF CALCULATED EFFECTIVE DOSES

Location	Adult man (Test person)			One year child old		
	Effective Doses [mSv]			Effective Doses [mSv]		
	Average	95% confidence interval		Average	95% confidence interval	
		Lower Bound	Upper Bound		Lower Bound	Upper Bound
Farm A	5.81E-04	1.94E-04	1.74E-03	8.19E-03	2.73E-03	2.46E-02
Farm B	8.08E-04	2.70E-04	2.42E-03	1.31E-02	4.36E-03	3.92E-02
Mesa	1.70E-04	5.65E-05	5.09E-04	3.05E-03	1.02E-03	9.14E-03
Eltopia	1.08E-04	3.61E-05	3.25E-04	1.82E-03	6.08E-04	5.47E-03
Pasco	2.16E-04	7.22E-05	6.47E-04	3.64E-03	1.21E-03	1.09E-02
Location	Boy (4 years old)			Girl (8 years old)		
	Average	95% confidence interval		Average	95% confidence interval	
		Lower Bound	Upper Bound		Lower Bound	Upper Bound
Farm B	2.06E-02	6.86E-03	6.21E-02	4.29E-03	1.43E-03	1.29E-02

The Reliability Index was used as a statistically meaningful interpretation that model is accurate within a factor of RI with observed data [7]. The RI is defined by:

$$RI = \exp\left(\sqrt{\left[\frac{1}{n}\sum_{i=1}^{n}\left(\ln O_i - \ln P_i\right)^2\right]}\right)$$

where:

$O_1, O_2, \ldots, O_n$ – a set of observations corresponding to
$P_1, P_2, \ldots, P_n$ – a set of model predictions

One can conceive of a “reasonably accurate model” as one whose predictions are usually within a factor of 2 or 3 of corresponding information. RI gives direct information about to relative errors to be expected in comparing model predictions with observations.

II–4.4.1. Farm A

Table II–4.VI and Figure 57 provide details of the reconstructed ^{131}I concentrations in air at Farm A. The comparison of predicted and observed data of I-131 concentration in pasture grass (Table II–4.VII and Figure 58) shows much wider scatter of observed values comparing with 95% uncertainty bound of model prediction. The observed decrease of I-131 concentration in grass for the period (9–16 September) was not predicted by model as well as elevated level of I-131 on 25–27 September. Except former case, the observed I-131 milk concentration reflect grass contamination pattern with time (Table II–4.VIII and Figure 59). Nevertheless, the RI values for milk equal to 1.6 indicates that the model would appear to be quite accurate, particularly in view of dose calculation.

The predicted daily intakes and the thyroid burden for a person at Farm A are given in Figure 60, and a summary of predicted I-131 concentrations and doses are given in Tables II–4.IX and II–4.X.

II–4.4.2. Farm B

The reconstructed concentrations of I-131 in air at Farm B are given in Table II–4.XI and Figure 61. The comparison of predicted and observed data of I-131 concentration in pasture grass (Table I–4.XII and Figure 62) and I-131 concentration in milk (Table II–4.XIII and Figure 63) shows pretty good agreement: RI for grass equal to 1.7, RI for milk equal to 1.24. Predicted thyroid burden for Girl 8 year old (consumption rate:1L of milk per day) on 19-October-63 was equal to1.32 against measured values 1Bq (Figure 64). Predicted thyroid burden for Boy 2 year old (consumption rate:4L of milk per day) on 19-October-63 was equal to 4.4 against measured values 2.7Bq (Figure 65). Base on these sparse data, one can't evaluate the model performance in prediction of thyroid burden. A summary of the predicted I-131 concentrations and doses is given in Tables II–4.XIV to II–4.XVI.

II–4.4.3. MESA

The reconstructed concentrations of ^{131}I in air at Mesa are given in Table II–4.XVII and Figure 66. The comparison of predicted and observed data of I-131 concentration in pasture grass (Table II–4.XVIII and Figure 67) and I-131 concentration in milk (Table II–4.XIX and Figure 68) show better prediction for grass (RI = 1.2) than for milk (RI=2.7), but sparse data, unable to evaluate the model performance. A summary of the predicted ^{131}I concentrations and doses at Mesa is given in Tables II–4.XX and II–4.XXI.

II–4.4.4. ELTOPIA

The reconstructed concentrations of ^{131}I in air at Eltopia are given in Table II–4.XXII and Figure 69. The comparison of predicted and observed data of I-131 concentration in pasture grass (Table II–4.XXIII and Figure 70) and I-131 concentration in milk (Table II–4.XXIV and Figure 71) show model as a good predictor both for grass (RI = 1.5) and for milk (RI=1.2), but sparse data, make difficult to evaluate the general model performance. A summary of predicted concentrations and doses at Eltopia is given in Tables II–4.XXV to II–4.XXVI.

II–4.4.5. PASCO

The reconstructed concentrations of ^{131}I in air at Pasco are given in Table II–4.XXVII and Figure 72. The comparison of predicted and observed data of I-131 concentration in pasture grass (Table II–4.XXVIII and Figure 73) shows wide scatter of observed values comparing with 95% uncertainty bound of model prediction. The RI equal to 1.8 indicates that the model would appear to be quite accurate, but comparison of predicted and observed data of I-131 concentration in milk (Table II–4.XXIX and Figure 74) shows not predicted decrease of I-131 concentration in milk for the period (14–30 September 1963). This phenomena is not supported by grass observation. The RI values for milk equal to 2.3 gives acceptable factor of accuracy. A summary of the predicted ^{131}I concentrations and doses are Pasco is given in Tables II–4.XXX and II–4.XXXI.

II–4.5. GENERAL COMMENTS

In the dose reconstruction task an uncertainty of measurements data is essential. It would be valuable to add some information in the Hanford scenario about method of measurement vegetation (pasture grass) and method to measurement thyroid burden of boy and girl because of very low level measured I-131 thyroid content (1 Bq ??).

Total effective dose equivalent for all locations calculated for test person fit in a range 3×10^{-5} – 3×10^{-3} mSv. Hanford I-131 release in the 2-4 September 1963 was about of 2.66 10^{12} Bq ; (BIOMOVS II Technical Report No. 7, August 1996, Hanford Scenario description), and that the total Hanford release from 1945 to 1972 was $2.73\text{x}10^{16}$ Bq [6]. Therefore, comparing single release to the total, it gives factor 10^4, that yealds to the raft estimation of effective dose equivalent from total release of Hanford in a range 0.3÷30 mSv.

It gives effective dose less than 1 mSv per year that fulfilled even recent dose limit recommendation.

II–4.6. RESULTS OF PREDICTIONS FOR SPECIFIED LOCATIONS

II–4.6.1. Farm A (Benton City)

II–4.6.1.1. ^{131}I air concentration

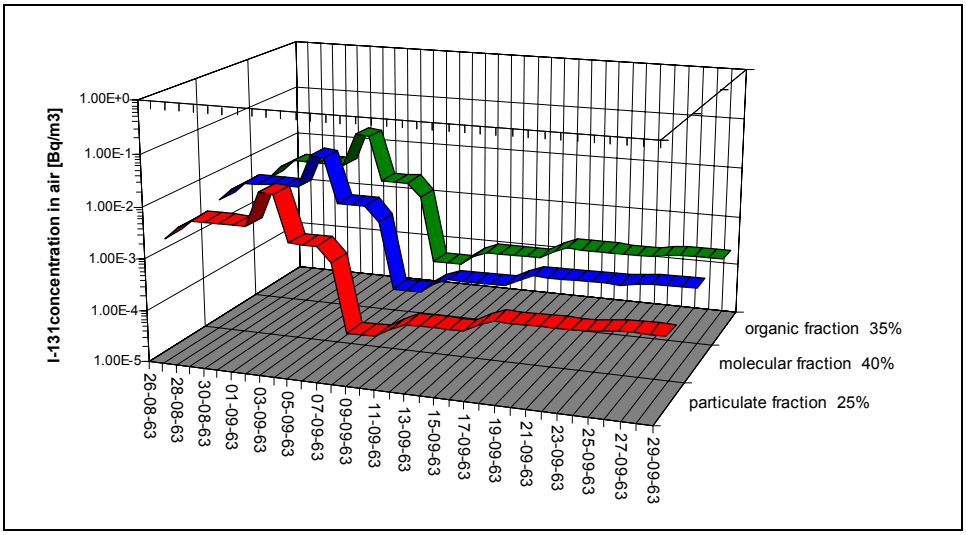

FIG. 57. Reconstruction of ^{131}I concentration in Air for Farm A. (Based on measurements of stations BENTON CITY, REDOX)

TABLE II–4.VI. RECONSTRUCTION OF ^{131}I CONCENTRATION IN AIR FOR FARM A (Based on measurements of stations BENTON CITY, REDOX)

Date	^{131}I in air [Bq m^{-3}]	Iodine-131 form distribution			Atmospheric conditions			Log normal distribution of aerosol fraction		High of mixing layer
		Particulate	I_2	Organic CH_3I	Wind speed [m s^{-1}]	Rain intensity [mm h^{-1}]	Precipit-ation [mm d^{-1}]	Mean [μ]	Standard deviation [μ]	[km]
26-08-63	6.37E-03	25.0%	40.0%	35.0%	4.00	0.00	0.00	6.00	25.00	1.0
27-08-63	1.12E-02	25.1%	40.1%	35.1%	4.00	0.00	0.00	6.00	25.00	1.0
28-08-63	1.61E-02	25.0%	40.0%	35.0%	4.00	0.00	0.00	6.00	25.00	1.0
29-08-63	1.61E-02	25.0%	40.0%	35.0%	4.00	0.00	0.00	6.00	25.00	1.0
30-08-63	1.61E-02	25.0%	40.0%	35.0%	4.00	0.00	0.00	6.00	25.00	1.0
31-08-63	1.61E-02	25.0%	40.0%	35.0%	4.00	0.00	0.00	6.00	25.00	1.0
1-09-63	1.61E-02	25.0%	40.0%	35.0%	4.00	0.00	0.00	6.00	25.00	1.0
2-09-63	7.54E-02	24.9%	39.9%	35.0%	4.00	0.00	0.00	6.00	25.00	1.0
3-09-63	7.18E-02	25.1%	40.0%	35.0%	4.00	0.00	0.00	6.00	25.00	1.0
4-09-63	9.08E-03	25.0%	40.0%	35.0%	4.00	0.00	0.00	6.00	25.00	1.0
5-09-63	9.08E-03	25.0%	40.0%	35.0%	4.00	0.00	0.00	6.00	25.00	1.0
6-09-63	9.08E-03	25.0%	40.0%	35.0%	4.00	0.00	0.00	6.00	25.00	1.0
7-09-63	4.65E-03	24.9%	40.0%	35.1%	4.00	0.00	0.00	6.00	25.00	1.0
8-09-63	2.20E-04	25.0%	40.0%	35.0%	4.00	0.00	0.00	6.00	25.00	1.0
9-09-63	2.20E-04	25.0%	40.0%	35.0%	4.00	0.00	0.00	6.00	25.00	1.0
10-09-63	2.20E-04	25.0%	40.0%	35.0%	4.00	0.00	0.00	6.00	25.00	1.0
11-09-63	3.30E-04	25.0%	40.0%	35.2%	4.00	0.00	0.00	6.00	25.00	1.0
12-09-63	4.40E-04	25.0%	40.0%	35.0%	4.00	0.00	0.00	6.00	25.00	1.0
13-09-63	4.40E-04	25.0%	40.0%	35.0%	4.00	0.00	0.00	6.00	25.00	1.0
14-09-63	4.40E-04	25.0%	40.0%	35.0%	4.00	0.00	0.00	6.00	25.00	1.0
15-09-63	4.40E-04	25.0%	40.0%	35.0%	4.00	0.00	0.00	6.00	25.00	1.0
16-09-63	4.40E-04	25.0%	40.0%	35.0%	4.00	0.00	0.00	6.00	25.00	1.0
17-09-63	6.10E-04	24.9%	40.0%	35.1%	4.00	0.00	0.00	6.00	25.00	1.0
18-09-63	7.80E-04	25.0%	40.0%	35.0%	4.00	0.00	0.00	6.00	25.00	1.0
19-09-63	7.80E-04	25.0%	40.0%	35.0%	4.00	0.00	0.00	6.00	25.00	1.0
20-09-63	7.80E-04	25.0%	40.0%	35.0%	4.00	0.00	0.00	6.00	25.00	1.0
21-09-63	7.80E-04	25.0%	40.0%	35.0%	4.00	0.00	0.00	6.00	25.00	1.0
22-09-63	7.80E-04	25.0%	40.0%	35.0%	4.00	0.00	0.00	6.00	25.00	1.0
23-09-63	7.80E-04	25.0%	40.0%	35.0%	4.00	0.00	0.00	6.00	25.00	1.0
24-09-63	7.80E-04	25.0%	40.0%	35.0%	4.00	0.00	0.00	6.00	25.00	1.0
25-09-63	8.55E-04	25.0%	40.0%	35.0%	4.00	0.00	0.00	6.00	25.00	1.0
26-09-63	9.30E-04	24.9%	40.0%	35.1%	4.00	0.00	0.00	6.00	25.00	1.0
27-09-63	9.30E-04	24.9%	40.0%	35.1%	4.00	0.00	0.00	6.00	25.00	1.0
28-09-63	9.30E-04	24.9%	40.0%	35.1%	4.00	0.00	0.00	6.00	25.00	1.0
29-09-63	9.30E-04	24.9%	40.0%	35.1%	4.00	0.00	0.00	6.00	25.00	1.0
30-09-63	9.30E-04	25.1%	40.0%	35.1%	4.00	0.00	0.00	6.00	25.00	1.0

II–4.6.1.2. ^{131}I concentration in pasture grass

TABLE II–4.VII. COMPARISON OF PREDICTED AND MEASURED ^{131}I CONCENTRATION IN PASTURE GRASS FOR FARM A

Date	Predicted values [Bq kg^{-1} fresh weight]			Observed values [Bq kg^{-1} fresh weight]	Predicted/ observed P/O
	Daily averages	95% confidence interval		Measured single values	
		Lower limit	Upper Limit		
04-09-63	5.75E+01	2.73E+01	1.21E+02	5.66E+01	1.03
05-09-63	5.36E+01	2.54E+01	1.13E+02	5.14E+01	1.05
06-09-63	5.01E+01	2.37E+01	1.06E+02	6.59E+01	0.77
07-09-63	4.57E+01	2.16E+01	9.64E+01	9.66E+01	0.48
08-09-63	4.03E+01	1.91E+01	8.50E+01	3.85E+01	1.06
09-09-63	3.56E+01	1.68E+01	7.50E+01	1.27E+01	2.83
10-09-63	3.14E+01	1.49E+01	6.63E+01	1.43E+01	2.22
11-09-63	2.78E+01	1.32E+01	5.87E+01	1.81E+00	15.50
12-09-63	2.46E+01	1.17E+01	5.20E+01	1.39E+01	1.79
13-09-63	2.19E+01	1.04E+01	4.62E+01	4.40E+00	5.03
14-09-63	1.95E+01	9.22E+00	4.11E+01	7.44E+00	2.64
16-09-63	1.54E+01	7.32E+00	3.26E+01	6.48E+00	2.41
17-09-63	1.39E+01	6.57E+00	2.93E+01	1.37E+01	1.02
18-09-63	1.25E+01	5.92E+00	2.64E+01	1.33E+01	0.95
19-09-63	1.13E+01	5.36E+00	2.39E+01	1.36E+01	0.84
20-09-63	1.03E+01	4.87E+00	2.17E+01	7.22E+00	1.44
25-09-63	6.70E+00	3.18E+00	1.42E+01	2.26E+01	0.30
26-09-63	6.27E+00	2.97E+00	1.32E+01	4.11E+01	0.15
27-09-63	5.89E+00	2.79E+00	1.24E+01	1.15E+01	0.52

Reliability Index RI for period 4-09-27-09 = 2.8,
Logtransformer values correlation coefficient r^2=0.12,
Linear relationship for Ln(P)=0.26*ln(O)+ 2.3

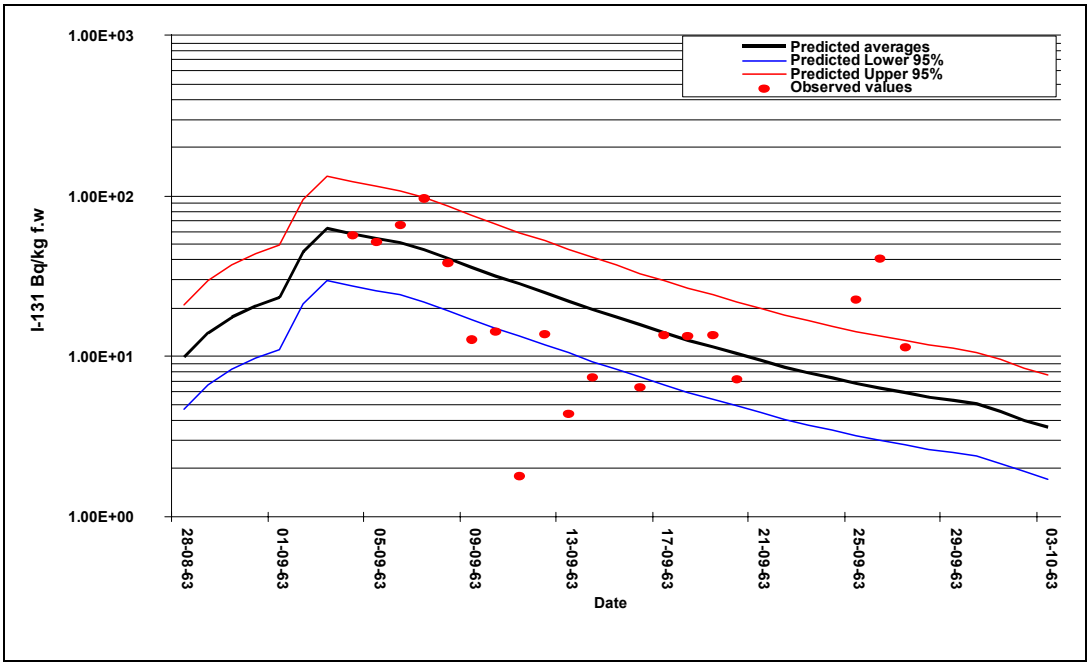

FIG. 58. Comparison of predicted and measured data of ^{131}I concentration in pasture grass for Farm A.

II–4.6.1.3. ^{131}I concentration in milk

TABLE II–4.VIII. COMPARISON OF PREDICTED AND MEASURED ^{131}I CONCENTRATION IN MILK FOR FARM A

Date	Predicted values [Bq L^{-1}]			Observed values [Bq L^{-1}]	Predicted/ observed P/O
	Daily averages	95% confidence interval		Measured single values	
		Lower limit	Upper Limit		
3-09-63	2.69E+00	1.41E+00	5.15E+00	2.40E+00	1.12
4-09-63	3.26E+00	1.70E+00	6.23E+00	4.33E+00	0.75
5-09-63	3.40E+00	1.77E+00	6.50E+00	4.18E+00	0.81
6-09-63	3.34E+00	1.75E+00	6.40E+00	3.58E+00	0.93
7-09-63	3.18E+00	1.66E+00	6.09E+00	2.87E+00	1.11
8-09-63	2.94E+00	1.54E+00	5.62E+00	2.57E+00	1.14
9-09-63	2.66E+00	1.39E+00	5.09E+00	1.25E+00	2.13
10-09-63	2.38E+00	1.24E+00	4.55E+00	1.09E+00	2.18
11-09-63	2.12E+00	1.11E+00	4.06E+00	8.50E-01	2.49
12-09-63	1.88E+00	9.84E-01	3.61E+00	7.30E-01	2.58
13-09-63	1.67E+00	8.75E-01	3.21E+00	6.00E-01	2.79
15-09-63	1.32E+00	6.92E-01	2.53E+00	9.10E-01	1.46
16-09-63	1.18E+00	6.17E-01	2.26E+00	8.10E-01	1.46
17-09-63	1.06E+00	5.51E-01	2.02E+00	7.20E-01	1.47
18-09-63	9.46E-01	4.94E-01	1.81E+00	7.50E-01	1.26
19-09-63	8.52E-01	4.46E-01	1.63E+00	7.10E-01	1.20
22-09-63	6.38E-01	3.33E-01	1.22E+00	7.10E-01	0.90
23-09-63	5.83E-01	3.04E-01	1.12E+00	5.30E-01	1.10
24-09-63	5.34E-01	2.79E-01	1.02E+00	4.20E-01	1.27
25-09-63	4.92E-01	2.57E-01	9.41E-01	3.50E-01	1.41
26-09-63	4.56E-01	2.38E-01	8.72E-01	3.60E-01	1.27
29-09-63	3.75E-01	1.96E-01	7.16E-01	4.00E-01	0.94

Reliability Index RI for period 4-09-29-09 = 1.6,
Logtransformer values correlation coefficient r^2=0.78,
Linear relationship for Ln(P)=0.82*ln(O)+ 0.29

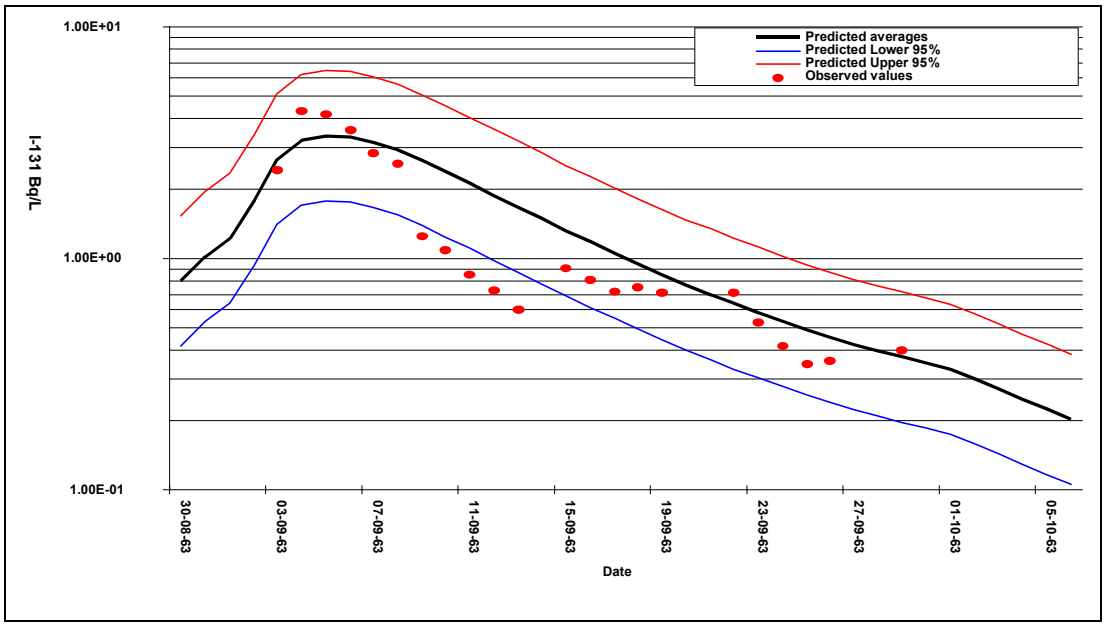

FIG. 59. Comparison of predicted and measured ^{131}I concentration in MILK for FARM A.

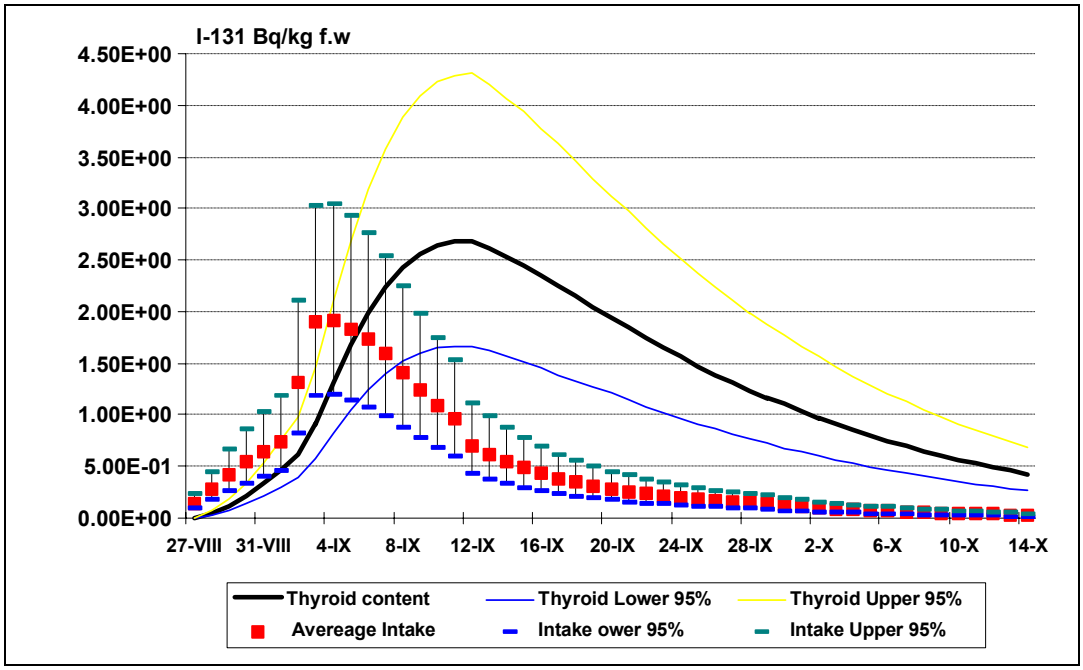

FIG. 60. I-131 daily intakes and thyroid burden of "TEST PERSON" for Farm A.

II–4.6.1.4. Predictions summary

TABLE II–4.IX. PREDICTIONS OF ^{131}I ACTIVITY IN PARTICULAR COMPONENTS FOR FARM A

Integrated air concentration [Bqm^{-3}d]	2.90E-01		
Total deposition [Bq m^{-2}]	Average	95% confidence interval	
		Lower Bound	Upper Bound
	2.00E+02	1.80E+02	2.20E+02
Milk integrals (August–October) [Bqkg^{-1}d]	Average	95% confidence interval	
		Lower Bound	Upper Bound
	4.60E+01	2.40E+01	8.70E+01
Leafy sage integrals (August–October) [Bq kg^{-1} d wet weight]	Average	95% confidence interval	
		Lower Bound	Upper Bound
	4.80E+02	2.40E+02	9.70E+02
Hay integrals (August–October) [Bq kg^{-1} d]	Average	95% confidence interval	
		Lower Bound	Upper Bound
	2.20E+03	1.00E+03	4.50E+03
Pasture grass integrals for period specified [Bq kg^{-1} d wet weight]	Average	95% confidence interval	
		Lower Bound	Upper Bound
August-63	6.96E+01	3.29E+01	1.47E+02
September-63	6.93E+02	3.28E+02	1.46E+03
October-63	4.78E+01	2.26E+01	1.01E+02
Total integral (August–October)	8.10E+02	3.84E+02	1.71E+03
Silage integrals (August–October) [Bq kg^{-1} d wet weight]	Average	95% confidence interval	
		Lower Bound	Upper Bound
	1.20E+02	5.80E+01	2.60E+02
Human intake (August–October) [Bq]	Average	95% confidence interval	
		Lower Bound	Upper Bound
	2.20E+01	1.40E+01	3.50E+01

TABLE II–4.X. DOSES FOR FARM A

Adult man (test person)						
Pathway	Effective Doses [mSv]			Doses to Thyroid [mSv]		
	Average	95% confidence interval		Average	95% confidence interval	
		Lower Bound	Upper Bound		Lower Bound	Upper Bound
External from cloud	2.44E-07	8.13E-08	7.32E-07	–	–	–
External from ground	2.37E-05	7.90E-06	7.11E-05	–	–	–
Inhalation	5.18E-05	1.73E-05	1.55E-04	1.04E-03	3.46E-04	3.10E-03
Ingestion[1]	5.05E-04	1.69E-04	1.52E-03	1.01E-02	3.37E-03	3.03E-02
Total effective dose	5.81E-04	1.94E-04	1.74E-03	–	–	–
Adult woman						
Pathway	Effective Doses [mSv]			Doses to Thyroid [mSv]		
	Average	95% confidence interval		Average	95% confidence interval	
		Lower Bound	Upper Bound		Lower Bound	Upper Bound
External from cloud	2.44E-07	8.13E-08	7.32E-07	–	–	–
External from ground	2.37E-05	7.90E-06	7.11E-05	–	–	–
Inhalation	4.54E-05	1.51E-05	1.36E-04	9.08E-04	3.02E-04	2.72E-03
Ingestion	4.01E-04	1.34E-04	1.21E-03	8.02E-03	2.67E-03	2.41E-02
Total effective dose	4.70E-04	1.57E-04	1.41E-03	–	–	–
One year child old						
Pathway	Effective Doses [mSv]			Doses to Thyroid [mSv]		
	Average	95% confidence interval		Average	95% confidence interval	
		Lower Bound	Upper Bound		Lower Bound	Upper Bound
External from cloud	3.08E-07	1.03E-07	9.24E-07	–	–	–
External from ground	3.19E-05	1.06E-05	9.57E-05	–	–	–
Inhalation	8.41E-06	2.80E-06	2.52E-05	1.68E-04	5.60E-05	5.04E-04
Ingestion	8.15E-03	2.72E-03	2.45E-02	1.63E-01	5.43E-02	4.89E-01
Total effective dose	8.19E-03	2.73E-03	2.46E-02	–	–	–

[1] Calculated from thyroid gland content of ^{131}I

II–4.6.2. Farm B (Twin Bridge)

II–4.6.2.1. ^{131}I air concentration

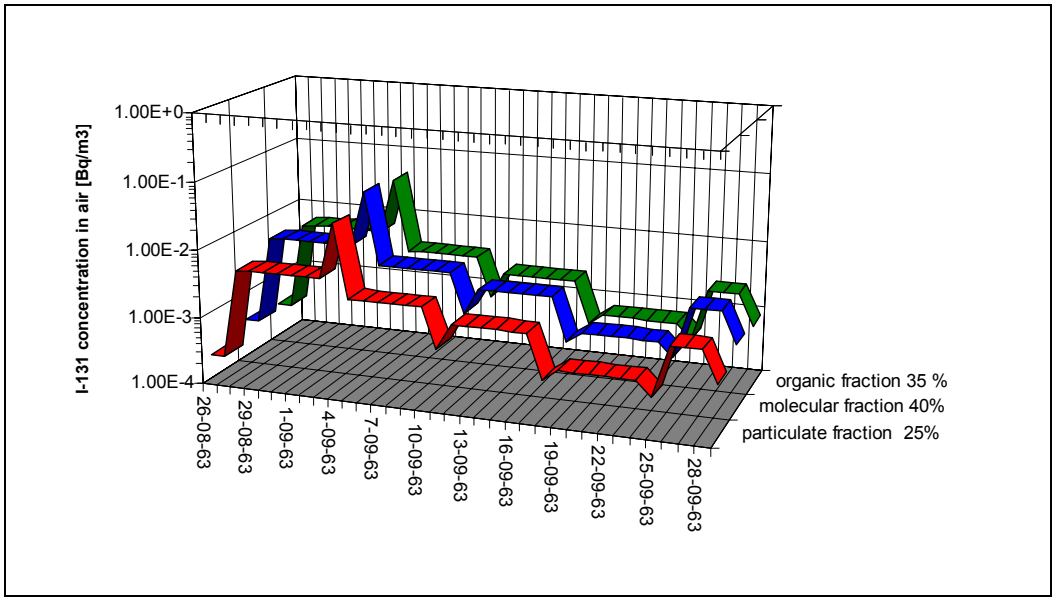

FIG. 61. Revised Reconstruction of I-131 concentration in air for Farm B.
(based on data of REDOX/3, 200WEC/5,1100-A, 200 EEC/5, 300-A &Dispersion Plume Model)

TABLE II–4.XI. RECONSTRUCTION OF ^{131}I CONCENTRATION IN AIR FOR FARM B (based on data of REDOX/3, 200WEC/5, 1100-A, 200 EEC/5,300-A &Dispersion Plume Model)

Date	^{131}I in air [Bq m^{-3}]	Iodine-131 form distribution			Atmospheric conditions			Log normal distribution of aerosol fraction		High of mixing layer
		Particulate	I_2	Organic CH_3I	Wind speed [m s^{-1}]	Rain intensity [mm h^{-1}]	Precipit-ation [mm d^{-1}]	Mean [μ]	Standard deviation [μ]	[km]
26-08-63	8.92E-04	25.0%	40.0%	35.0%	4.00	0.00	0.00	6.00	25.00	1.0
27-08-63	8.92E-04	25.1%	40.1%	35.1%	4.00	0.00	0.00	6.00	25.00	1.0
28-08-63	1.84E-02	25.0%	40.0%	35.0%	4.00	0.00	0.00	6.00	25.00	1.0
29-08-63	1.95E-02	25.0%	40.0%	35.0%	4.00	0.00	0.00	6.00	25.00	1.0
30-08-63	1.95E-02	25.0%	40.0%	35.0%	4.00	0.00	0.00	6.00	25.00	1.0
31-08-63	1.95E-02	25.0%	40.0%	35.0%	4.00	0.00	0.00	6.00	25.00	1.0
1-09-63	1.95E-02	25.0%	40.0%	35.0%	4.00	0.00	0.00	6.00	25.00	1.0
2-09-63	1.95E-02	24.9%	39.9%	35.0%	4.00	0.00	0.00	6.00	25.00	1.0
3-09-63	1.95E-02	25.1%	40.0%	35.0%	4.00	0.00	0.00	6.00	25.00	1.0
4-09-63	1.30E-01	25.0%	40.0%	35.0%	4.00	0.00	0.00	6.00	25.00	1.0
5-09-63	1.06E-02	25.0%	40.0%	35.0%	4.00	0.00	0.00	6.00	25.00	1.0
6-09-63	1.06E-02	25.0%	40.0%	35.0%	4.00	0.00	0.00	6.00	25.00	1.0
7-09-63	1.06E-02	24.9%	40.0%	35.1%	4.00	0.00	0.00	6.00	25.00	1.0
8-09-63	1.06E-02	25.0%	40.0%	35.0%	4.00	0.00	0.00	6.00	25.00	1.0
9-09-63	1.06E-02	25.0%	40.0%	35.0%	4.00	0.00	0.00	6.00	25.00	1.0
10-09-63	1.06E-02	25.0%	40.0%	35.0%	4.00	0.00	0.00	6.00	25.00	1.0
11-09-63	2.72E-03	25.0%	40.0%	35.2%	4.00	0.00	0.00	6.00	25.00	1.0
12-09-63	6.50E-03	25.0%	40.0%	35.0%	4.00	0.00	0.00	6.00	25.00	1.0
13-09-63	6.50E-03	25.0%	40.0%	35.0%	4.00	0.00	0.00	6.00	25.00	1.0
14-09-63	6.50E-03	25.0%	40.0%	35.0%	4.00	0.00	0.00	6.00	25.00	1.0
15-09-63	6.50E-03	25.0%	40.0%	35.0%	4.00	0.00	0.00	6.00	25.00	1.0
16-09-63	6.50E-03	25.0%	40.0%	35.0%	4.00	0.00	0.00	6.00	25.00	1.0
17-09-63	6.50E-03	24.9%	40.0%	35.1%	4.00	0.00	0.00	6.00	25.00	1.0
18-09-63	1.47E-03	25.0%	40.0%	35.0%	4.00	0.00	0.00	6.00	25.00	1.0
19-09-63	2.09E-03	25.0%	40.0%	35.0%	4.00	0.00	0.00	6.00	25.00	1.0
20-09-63	2.09E-03	25.0%	40.0%	35.0%	4.00	0.00	0.00	6.00	25.00	1.0
21-09-63	2.09E-03	25.0%	40.0%	35.0%	4.00	0.00	0.00	6.00	25.00	1.0
22-09-63	2.09E-03	25.0%	40.0%	35.0%	4.00	0.00	0.00	6.00	25.00	1.0
23-09-63	2.09E-03	25.0%	40.0%	35.0%	4.00	0.00	0.00	6.00	25.00	1.0
24-09-63	2.09E-03	25.0%	40.0%	35.0%	4.00	0.00	0.00	6.00	25.00	1.0
25-09-63	1.27E-03	25.0%	40.0%	35.0%	4.00	0.00	0.00	6.00	25.00	1.0
26-09-63	7.20E-03	24.9%	40.0%	35.1%	4.00	0.00	0.00	6.00	25.00	1.0
27-09-63	7.20E-03	24.9%	40.0%	35.1%	4.00	0.00	0.00	6.00	25.00	1.0
28-09-63	7.20E-03	24.9%	40.0%	35.1%	4.00	0.00	0.00	6.00	25.00	1.0
29-09-63	2.46E-03	24.9%	40.0%	35.1%	4.00	0.00	0.00	6.00	25.00	1.0
30-09-63	2.46E-03	25.1%	40.0%	35.1%	4.00	0.00	0.00	6.00	25.00	1.0

II–4.6.2.2. ^{131}I concentration in pasture grass

TABLE II–4.XXI. COMPARISON OF PREDICTED AND MEASURED ^{131}I CONCENTRATION IN PASTURE GRASS FOR FARM B

Date	Predicted values [Bq kg^{-1} fresh weight]			Observed values [Bq kg^{-1} fresh weight]	Predicted/ observed P/O
	Daily averages	95% confidence interval		Measured single values	
		Lower limit	Upper Limit		
12-09-63	4.02E+01	2.00E+01	8.08E+01	3.47E+01	1.16
13-09-63	3.76E+01	1.87E+01	7.57E+01	5.14E+01	0.73
16-09-63	3.15E+01	1.57E+01	6.34E+01	1.45E+01	2.17
17-09-63	3.00E+01	1.49E+01	6.04E+01	1.21E+01	2.48
18-09-63	2.70E+01	1.34E+01	5.44E+01	3.68E+01	0.73
19-09-63	2.46E+01	1.22E+01	4.95E+01	1.32E+01	1.86
20-09-63	2.25E+01	1.12E+01	4.52E+01	1.83E+01	1.23
23-09-63	1.75E+01	8.71E+00	3.52E+01	2.04E+01	0.86
25-09-63	1.48E+01	7.37E+00	2.98E+01	2.13E+01	0.70
26-09-63	1.56E+01	7.76E+00	3.14E+01	3.77E+01	0.41
27-09-63	1.63E+01	8.11E+00	3.28E+01	2.18E+01	0.75
30-09-63	1.51E+01	7.49E+00	3.03E+01	1.38E+01	1.09
Reliability Index RI for period 4-09-30-09 = 1.7, Logtransformer values correlation coefficient r^2=0.05, Linear relationship for Ln(P)=0.18*ln(O)+ 2.6					

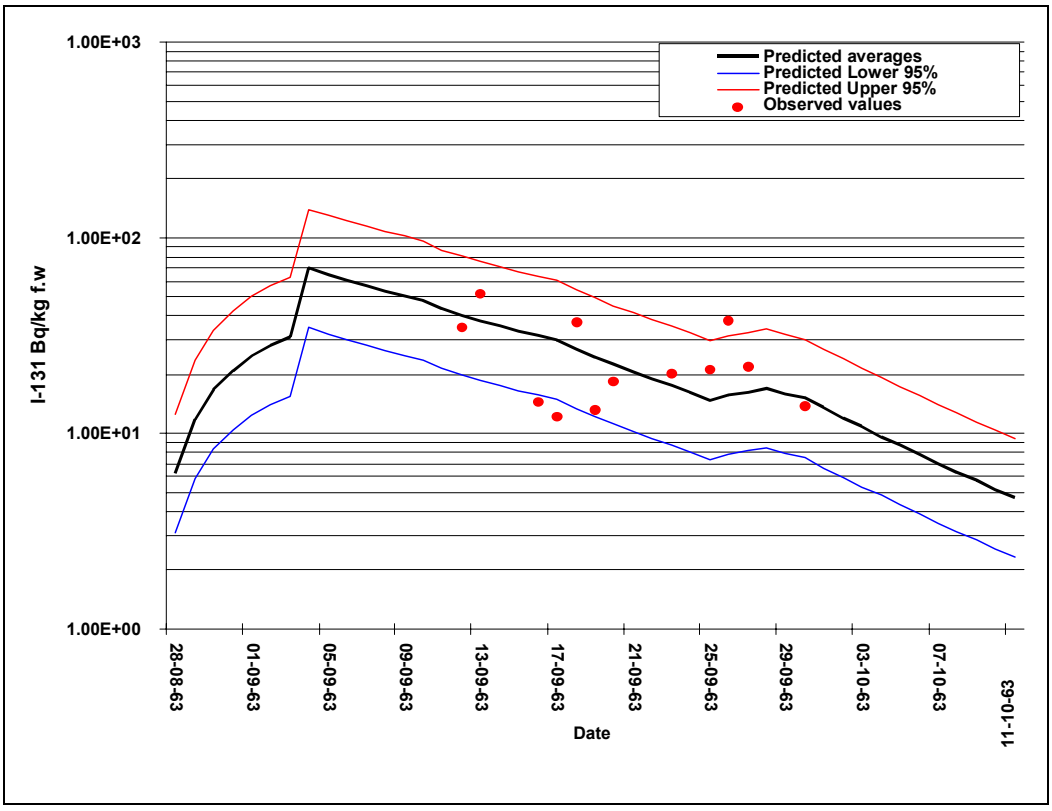

FIG. 62. Comparison of predicted and measured data of I-131 concentration in pasture grass for Farm B (revised prediction).

II–4.6.2.3. ^{131}I concentration in milk

TABLE II–4.XIII. COMPARISON OF PREDICTED AND MEASURED ^{131}I CONCENTRATION IN MILK FOR FARM B

Date	Predicted values [Bq L^{-1}]			Observed values [Bq L^{-1}]	Predicted/ observed P/O
	Daily averages	95% confidence interval		Measured single values	
		Lower limit	Upper Limit		
11-09-63	3.05E+00	1.85E+00	5.03E+00	5.03E+00	0.61
12-09-63	2.83E+00	1.72E+00	4.67E+00	4.40E+00	0.64
13-09-63	2.64E+00	1.60E+00	4.35E+00	3.52E+00	0.75
15-09-63	2.31E+00	1.40E+00	3.81E+00	1.79E+00	1.29
16-09-63	2.18E+00	1.32E+00	3.59E+00	2.41E+00	0.90
17-09-63	2.06E+00	1.25E+00	3.40E+00	1.61E+00	1.28
18-09-63	1.93E+00	1.17E+00	3.18E+00	2.01E+00	0.96
19-09-63	1.77E+00	1.08E+00	2.92E+00	1.92E+00	0.92
22-09-63	1.37E+00	8.32E-01	2.26E+00	1.43E+00	0.96
23-09-63	1.26E+00	7.66E-01	2.08E+00	1.16E+00	1.09
24-09-63	1.16E+00	7.07E-01	1.92E+00	1.22E+00	0.95
25-09-63	1.07E+00	6.51E-01	1.77E+00	9.50E-01	1.13
26-09-63	1.03E+00	6.24E-01	1.69E+00	9.50E-01	1.08
29-09-63	1.05E+00	6.39E-01	1.73E+00	1.08E+00	0.97
Reliability Index RI for period 4-09-30-09 = 1.25, Logtransformer values correlation coefficient r^2=0.88, Linear relationship for Ln(P)=0.67*ln(O)+ 0.14					

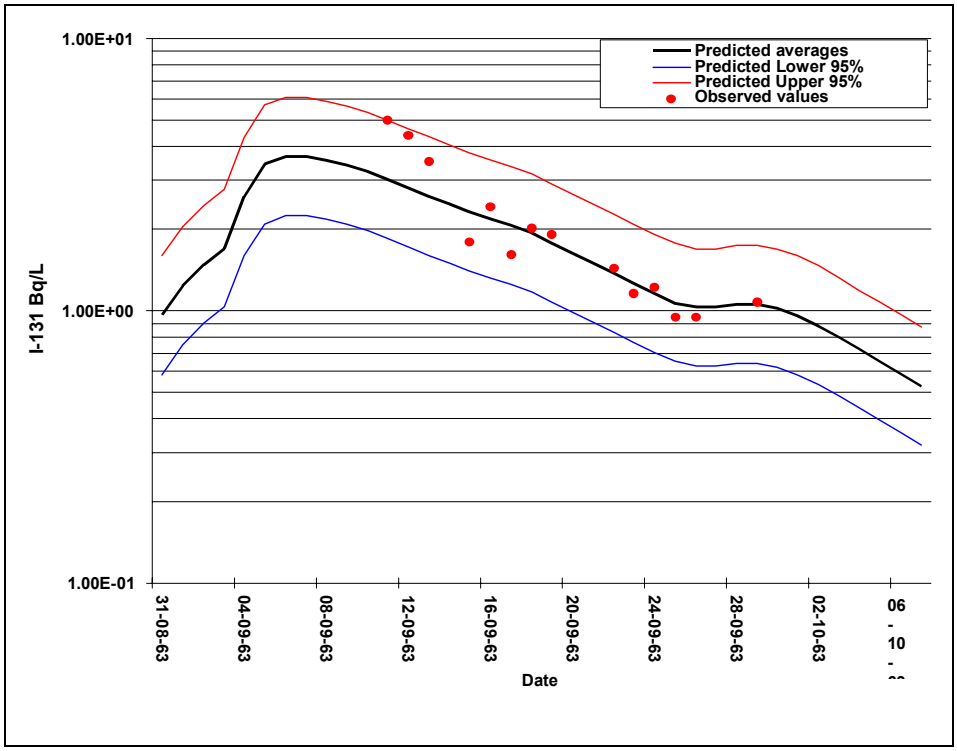

FIG. 63. Comparison of predicted and measured data of I-131 concentration in MILK for Farm B (revised prediction).

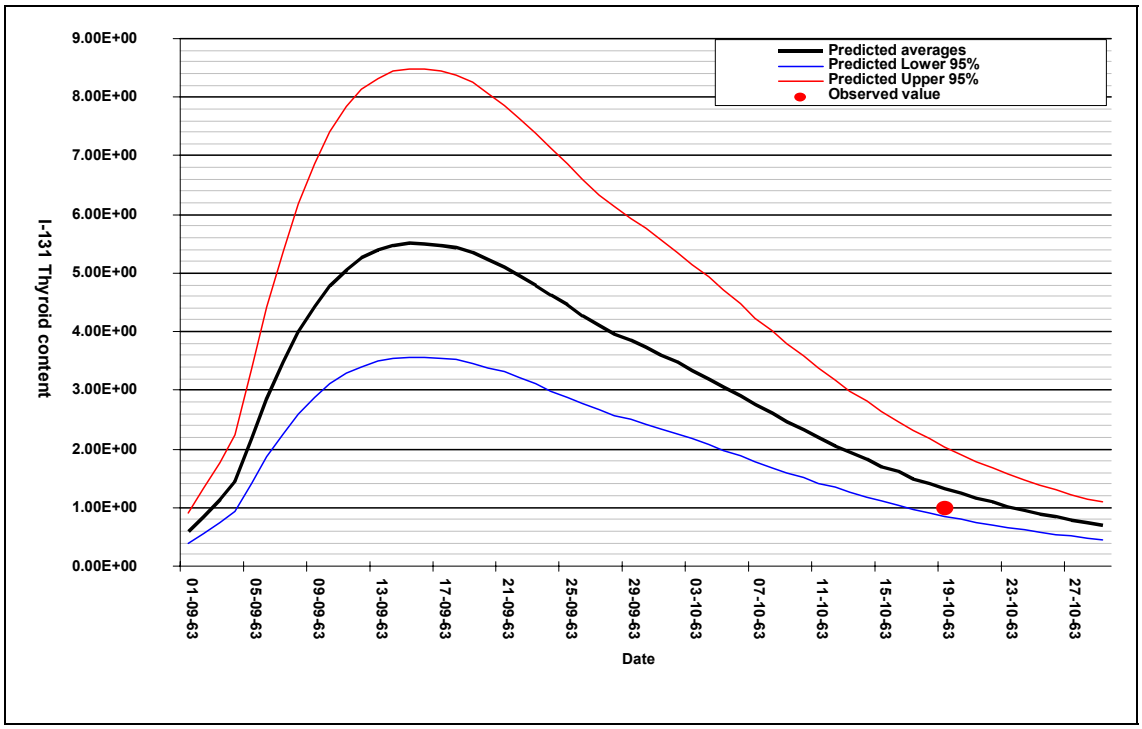

FIG. 64. I-131 thyroid burden of "girl 8 year old" from Farm B (1 L of Milk per day) (revised prediction) Predicted value on 19-10-63 = 1.32 <0.9 ÷2>Bq against measured value 1 Bq.

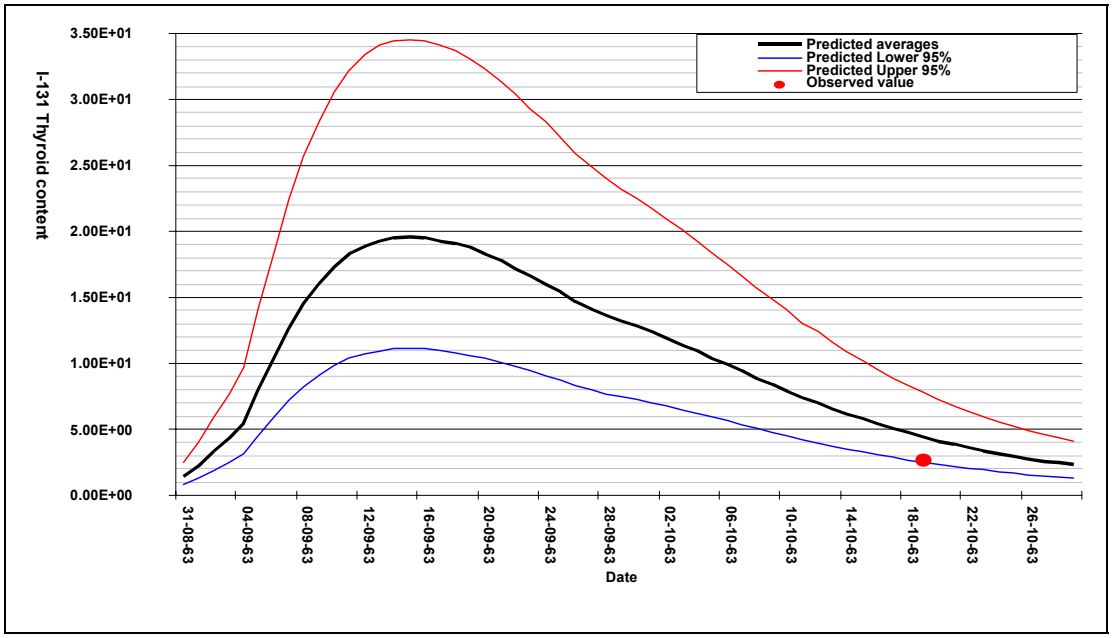

FIG. 65. I-131 thyroid burden of "boy 2 years old" from Farm B (4 L of Milk per day) (revised prediction) Predicted value on 19-10-63 = 4.4 <2.5÷7.8> Bq against measured value 2.7 Bq.

II–4.6.2.4. Predictions summary

TABLE II–4.XIV. PREDICTIONS OF ^{131}I ACTIVITY IN PARTICULAR COMPONENTS FOR FARM B

Integrated air concentration [Bqm^{-3}d]	4.14E-01		
Total deposition [Bq m^{-2}]	Average	95% confidence interval	
		Lower Bound	Upper Bound
	2.87E+02	2.58E+02	3.18E+02
Milk integrals (August–October) [Bqkg^{-1}d]	Average	95% confidence interval	
		Lower Bound	Upper Bound
	7.67E+01	4.65E+01	1.26E+02
Leafy sage integrals (August–October) [Bq kg^{-1} d wet weight]	Average	95% confidence interval	
		Lower Bound	Upper Bound
	7.99E+02	3.96E+02	1.61E+03
Hay integrals (August–October) [Bq kg^{-1} d]	Average	95% confidence interval	
		Lower Bound	Upper Bound
	3.12E+03	1.48E+03	6.59E+03
Pasture grass integrals for period specified [Bq kg^{-1} d wet weight]	Average	95% confidence interval	
		Lower Bound	Upper Bound
August-63	5.72E+01	2.84E+01	1.15E+02
September-63	9.82E+02	4.88E+02	1.98E+03
October-63	1.37E+02	6.81E+01	2.76E+02
Total integral (August–October)	1.18E+03	5.85E+02	2.37E+03
Silage integrals (August–October) [Bq kg^{-1} d wet weight]	Average	95% confidence interval	
		Lower Bound	Upper Bound
	2.74E+02	1.30E+02	5.78E+02
Human intake (August–October) [Bq]	Average	95% confidence interval	
		Lower Bound	Upper Bound
	2.77E+01	1.66E+01	4.43E+01

TABLE II–4.XV. DOSES FOR FARM B

Adult man (test person)						
Pathway	Effective Doses [mSv]			Doses to Thyroid [mSv]		
	Average	95% confidence interval		Average	95% confidence interval	
		Lower Bound	Upper Bound		Lower Bound	Upper Bound
External from cloud	3.46E-07	1.15E-07	1.04E-06	–	–	–
External from ground	3.37E-05	1.12E-05	1.01E-04	–	–	–
Inhalation	7.36E-05	2.45E-05	2.21E-04	1.47E-03	4.90E-04	4.42E-03
Ingestion[1]	7.00E-04	2.34E-04	2.10E-03	1.40E-02	4.67E-03	4.20E-02
Total effective dose	8.08E-04	2.70E-04	2.42E-03	–	–	–
Adult woman						
Pathway	Effective Doses [mSv]			Doses to Thyroid [mSv]		
	Average	95% confidence interval		Average	95% confidence interval	
		Lower Bound	Upper Bound		Lower Bound	Upper Bound
External from cloud	3.46E-07	1.15E-07	1.04E-06	–	–	–
External from ground	3.37E-05	1.12E-05	1.01E-04	–	–	–
Inhalation	6.44E-05	2.15E-05	1.93E-04	1.29E-03	4.30E-04	3.86E-03
Ingestion	5.75E-04	1.92E-04	1.73E-03	1.15E-02	3.83E-03	3.45E-02
Total effective dose	6.73E-04	2.25E-04	2.03E-03	–	–	–
One year child old						
Pathway	Effective Doses [mSv]			Doses to Thyroid [mSv]		
	Average	95% confidence interval		Average	95% confidence interval	
		Lower Bound	Upper Bound		Lower Bound	Upper Bound
External from cloud	4.37E-07	1.46E-07	1.31E-06	–	–	–
External from ground	4.54E-05	1.51E-05	1.36E-04	–	–	–
Inhalation	1.19E-05	3.97E-06	3.57E-05	2.38E-04	7.94E-05	7.14E-04
Ingestion	1.30E-02	4.34E-03	3.90E-02	2.60E-01	8.67E-02	7.80E-01
Total effective dose	1.31E-02	4.35E-03	3.92E-02	–	–	–

[1] Calculated from thyroid gland content of ^{131}I

TABLE II–4.XVI. DOSES FOR FARM B (MONITORING CHILDREN)

Boy (4 years old)						
Pathway	Effective Doses [mSv]			Doses to Thyroid [mSv]		
	Average	95% confidence interval		Average	95% confidence interval	
		Lower Bound	Upper Bound		Lower Bound	Upper Bound
External from Cloud	3.87E-07	1.29E-07	1.16E-06	–	–	–
External from Ground	3.70E-05	1.23E-05	1.11E-04	–	–	–
Inhalation	1.53E-04	5.10E-05	4.59E-04	3.06E-03	1.02E-03	9.18E-03
Ingestion	2.05E-02	6.80E-03	6.15E-02	4.09E-01	1.36E-01	1.23E+00
Total Effective Dose	2.06E-02	6.86E-03	6.21E-02	–	–	–
Girl (8 years old)						
Pathway	Effective Doses [mSv]			Doses to Thyroid [mSv]		
	Average	95% confidence interval		Average	95% confidence interval	
		Lower Bound	Upper Bound		Lower Bound	Upper Bound
External from Cloud	3.87E-07	1.29E-07	1.16E-06	–	–	–
External from Ground	3.70E-05	1.23E-05	1.11E-04	–	–	–
Inhalation	1.18E-04	3.93E-05	3.54E-04	2.36E-03	7.86E-04	7.08E-03
Ingestion	4.14E-03	1.38E-03	1.24E-02	8.27E-02	2.76E-02	2.48E-01
Total Effective Dose	4.29E-03	1.43E-03	1.29E-02	–	–	–

II–4.6.3. Farm N (Mesa)

II–4.6.3.1. ^{131}I air concentration

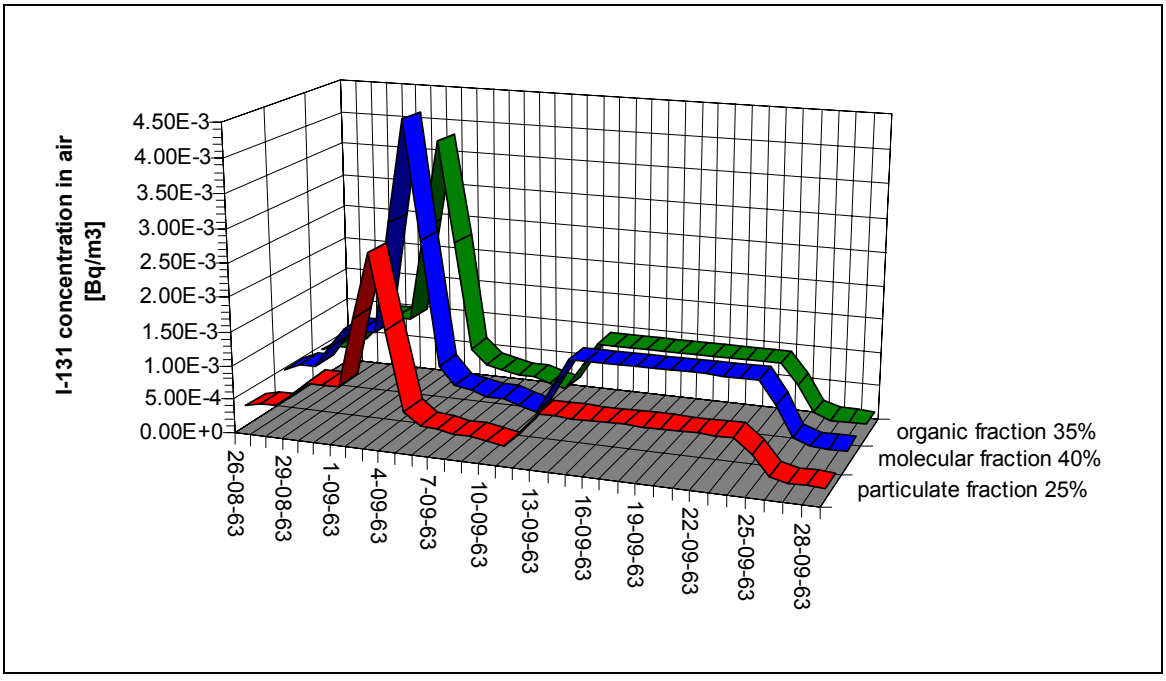

FIG. 66. Reconstruction of I-131 concentration in air for Farm N (MESA). (based on data of stations BYERS LANDING, HANFORD &Dispersion Plume Model)

TABLE II–4.XVII. RECONSTRUCTION OF ^{131}I CONCENTRATION IN AIR FOR FARM N (MESA)
(based on data of stations BYERS LANDING, HANFORD &Dispersion Plume Model)

Date	^{131}I in air [Bq m^{-3}]	Iodine-131 form distribution			Atmospheric conditions			Log normal distribution of aerosol fraction		High of mixing layer
		Particulate	I_2	Organic CH_3I	Wind speed [m s^{-1}]	Rain intensity [mm h^{-1}]	Precipit-ation [mm d^{-1}]	Mean [μ]	Standard deviation [μ]	[km]
26-08-63	1.19E-03	25.0%	40.0%	35.0%	4.00	0.00	0.00	6.00	25.00	1.0
27-08-63	1.43E-03	25.1%	40.1%	35.1%	4.00	0.00	0.00	6.00	25.00	1.0
28-08-63	1.43E-03	25.0%	40.0%	35.0%	4.00	0.00	0.00	6.00	25.00	1.0
29-08-63	2.23E-03	25.0%	40.0%	35.0%	4.00	0.00	0.00	6.00	25.00	1.0
30-08-63	3.03E-03	25.0%	40.0%	35.0%	4.00	0.00	0.00	6.00	25.00	1.0
31-08-63	3.03E-03	25.0%	40.0%	35.0%	4.00	0.00	0.00	6.00	25.00	1.0
1-09-63	3.03E-03	25.0%	40.0%	35.0%	4.00	0.00	0.00	6.00	25.00	1.0
2-09-63	7.17E-03	24.9%	39.9%	35.0%	4.00	0.00	0.00	6.00	25.00	1.0
3-09-63	1.10E-02	25.1%	40.0%	35.0%	4.00	0.00	0.00	6.00	25.00	1.0
4-09-63	6.62E-03	25.0%	40.0%	35.0%	4.00	0.00	0.00	6.00	25.00	1.0
5-09-63	1.98E-03	25.0%	40.0%	35.0%	4.00	0.00	0.00	6.00	25.00	1.0
6-09-63	1.35E-03	25.0%	40.0%	35.0%	4.00	0.00	0.00	6.00	25.00	1.0
7-09-63	1.21E-03	24.9%	40.0%	35.1%	4.00	0.00	0.00	6.00	25.00	1.0
8-09-63	1.07E-03	25.0%	40.0%	35.0%	4.00	0.00	0.00	6.00	25.00	1.0
9-09-63	1.07E-03	25.0%	40.0%	35.0%	4.00	0.00	0.00	6.00	25.00	1.0
10-09-63	8.75E-04	25.0%	40.0%	35.0%	4.00	0.00	0.00	6.00	25.00	1.0
11-09-63	6.85E-04	25.0%	40.0%	35.2%	4.00	0.00	0.00	6.00	25.00	1.0
12-09-63	1.74E-03	25.0%	40.0%	35.0%	4.00	0.00	0.00	6.00	25.00	1.0
13-09-63	2.80E-03	25.0%	40.0%	35.0%	4.00	0.00	0.00	6.00	25.00	1.0
14-09-63	2.80E-03	25.0%	40.0%	35.0%	4.00	0.00	0.00	6.00	25.00	1.0
15-09-63	2.80E-03	25.0%	40.0%	35.0%	4.00	0.00	0.00	6.00	25.00	1.0
16-09-63	2.80E-03	25.0%	40.0%	35.0%	4.00	0.00	0.00	6.00	25.00	1.0
17-09-63	2.80E-03	24.9%	40.0%	35.1%	4.00	0.00	0.00	6.00	25.00	1.0
18-09-63	2.80E-03	25.0%	40.0%	35.0%	4.00	0.00	0.00	6.00	25.00	1.0
19-09-63	2.80E-03	25.0%	40.0%	35.0%	4.00	0.00	0.00	6.00	25.00	1.0
20-09-63	2.80E-03	25.0%	40.0%	35.0%	4.00	0.00	0.00	6.00	25.00	1.0
21-09-63	2.80E-03	25.0%	40.0%	35.0%	4.00	0.00	0.00	6.00	25.00	1.0
22-09-63	2.80E-03	25.0%	40.0%	35.0%	4.00	0.00	0.00	6.00	25.00	1.0
23-09-63	2.80E-03	25.0%	40.0%	35.0%	4.00	0.00	0.00	6.00	25.00	1.0
24-09-63	2.80E-03	25.0%	40.0%	35.0%	4.00	0.00	0.00	6.00	25.00	1.0
25-09-63	1.95E-03	25.0%	40.0%	35.0%	4.00	0.00	0.00	6.00	25.00	1.0
26-09-63	8.45E-04	24.9%	40.0%	35.1%	4.00	0.00	0.00	6.00	25.00	1.0
27-09-63	5.90E-04	24.9%	40.0%	35.1%	4.00	0.00	0.00	6.00	25.00	1.0
28-09-63	5.90E-04	24.9%	40.0%	35.1%	4.00	0.00	0.00	6.00	25.00	1.0
29-09-63	5.90E-04	24.9%	40.0%	35.1%	4.00	0.00	0.00	6.00	25.00	1.0
30-09-63	5.90E-04	25.1%	40.0%	35.1%	4.00	0.00	0.00	6.00	25.00	1.0

II–4.6.3.2. ^{131}I concentration in pasture grass

TABLE II–4.XVIII. COMPARISON OF PREDICTED AND MEASURED ^{131}I CONCENTRATION IN PASTURE GRASS FOR FARM N (MESA)

Date	Predicted values [Bq kg^{-1} fresh weight]			Observed values [Bq kg^{-1} fresh weight]	Predicted/ observed P/O
	Daily averages	95% confidence interval		Measured single values	
		Lower limit	Upper Limit		
3-09-63	8.30E+00	3.93E+00	1.75E+01	9.77E+00	0.85
5-09-63	8.91E+00	4.22E+00	1.88E+01	9.07E+00	0.98
11-09-63	5.50E+00	2.60E+00	1.16E+01	4.37E+00	1.26
19-09-63	6.63E+00	3.14E+00	1.40E+01	7.07E+00	0.94
Reliability Index RI for period 3-09-19-09 = 1.2, Logtransformer values correlation coefficient r^2=0.90, Linear relationship for Ln(P)=0.58*ln(O)+ 0.8					

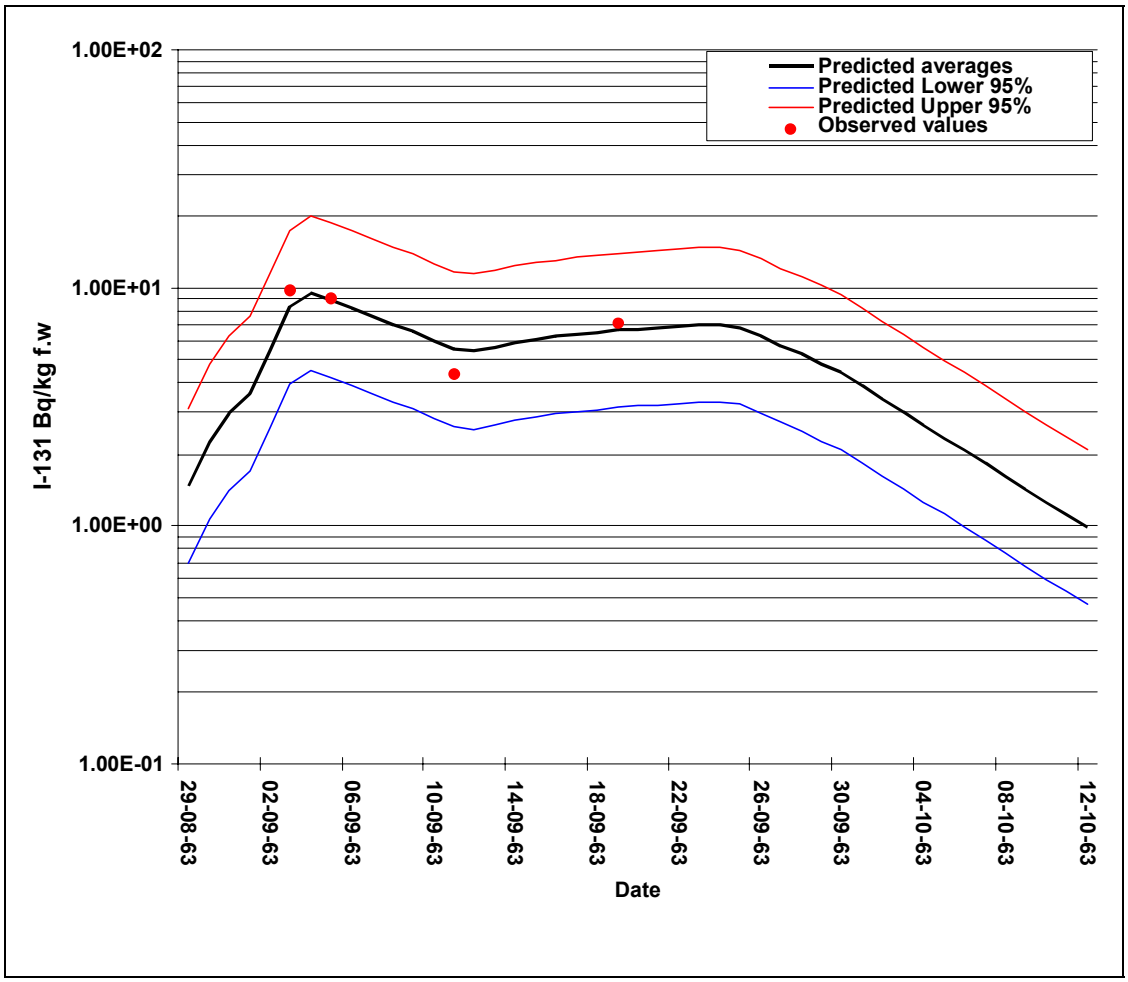

FIG. 67. Comparison of predicted and measured data of I-131 concentration in pasture grass for Farm N (MESA).

II–4.6.3.3. ^{131}I concentration in milk

TABLE II–4.XIX. COMPARISON OF PREDICTED AND MEASURED ^{131}I CONCENTRATION IN MILK FOR FARM N (MESA)

Date	Predicted values [Bq L^{-1}]			Observed values [Bq L^{-1}]	Predicted/ observed P/O
	Daily averages	95% confidence interval		Measured single values	
		Lower limit	Upper Limit		
5-09-63	6.09E-01	3.18E-01	1.17E+00	1.30E-01	4.69
11-09-63	4.15E-01	2.17E-01	7.94E-01	1.27E+00	0.33
19-09-63	4.64E-01	2.42E-01	8.88E-01	7.00E-01	0.66
25-09-63	4.91E-01	2.57E-01	9.39E-01	6.40E-01	0.77
Reliability Index RI for period 5-09÷25-09 = 2.7, Logtransformer values correlation coefficient r^2=0.98, Linear relationship for Ln(P)=- 0.16*ln(O) -0.82					

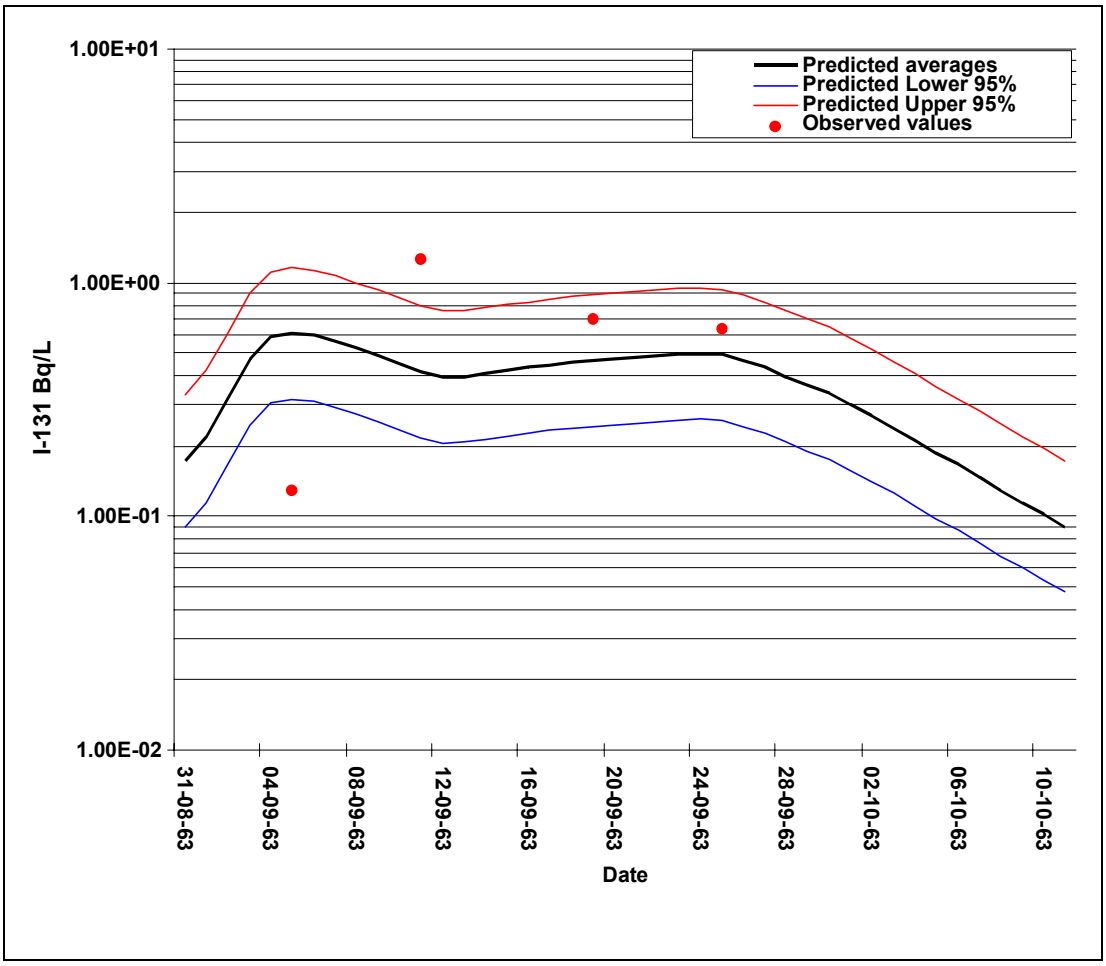

FIG. 68. Comparison of predicted and measured data of I-131 concentration in MILK for Farm N (MESA).

II–4.6.3.4. Predictions summary

TABLE II–4.XX. PREDICTIONS OF ^{131}I ACTIVITY IN PARTICULAR COMPONENTS FOR FARM N (MESA)

Integrated air concentration [Bqm^{-3}d]	8.90E-02		
Total deposition [Bq m^{-2}]	Average	95% confidence interval	
		Lower Bound	Upper Bound
	6.10E+01	5.50E+01	6.80E+01
Milk integrals (August–October) [Bqkg^{-1}d]	Average	95% confidence interval	
		Lower Bound	Upper Bound
	1.30E+01	6.80E+00	2.50E+01
Leafy sage integrals (August–October) [Bq kg^{-1} d wet weight]	Average	95% confidence interval	
		Lower Bound	Upper Bound
	1.50E+02	7.20E+01	2.90E+02
Hay integrals (August–October) [Bq kg^{-1} d]	Average	95% confidence interval	
		Lower Bound	Upper Bound
	4.20E+02	2.00E+02	9.00E+02
Pasture grass integrals for period specified [Bq kg^{-1} d wet weight]	Average	95% confidence interval	
		Lower Bound	Upper Bound
August-63	8.02E+00	3.80E+00	1.70E+01
September-63	1.93E+02	9.15E+01	4.08E+02
October-63	3.26E+01	1.55E+01	6.89E+01
Total integral (August–October)	2.34E+02	1.11E+02	4.94E+02
Silage integrals (August–October) [Bq kg^{-1} d wet weight]	Average	95% confidence interval	
		Lower Bound	Upper Bound
	6.20E+01	2.90E+01	1.30E+02
Human intake (August–October) [Bq]	Average	95% confidence interval	
		Lower Bound	Upper Bound
	5.80E+00	3.60E+00	9.30E+00

TABLE II–4.XXI. DOSES FOR FARM N (MESA)

Adult man (test person)						
Pathway	Effective Doses [mSv]			Doses to Thyroid [mSv]		
	Average	95% confidence interval		Average	95% confidence interval	
		Lower Bound	Upper Bound		Lower Bound	Upper Bound
External from cloud	7.42E-08	2.47E-08	2.23E-07	–	–	–
External from ground	7.19E-06	2.40E-06	2.16E-05	–	–	–
Inhalation	1.58E-05	5.27E-06	4.74E-05	3.16E-04	1.05E-04	9.48E-04
Ingestion[1]	1.47E-04	4.89E-05	4.40E-04	2.93E-03	9.77E-04	8.79E-03
Total effective dose	1.70E-04	5.65E-05	5.09E-04	–	–	–
Adult woman						
Pathway	Effective Doses [mSv]			Doses to Thyroid [mSv]		
	Average	95% confidence interval		Average	95% confidence interval	
		Lower Bound	Upper Bound		Lower Bound	Upper Bound
External from cloud	7.42E-08	2.47E-08	2.23E-07	–	–	–
External from ground	7.19E-06	2.40E-06	2.16E-05	–	–	–
Inhalation	1.38E-05	4.60E-06	4.14E-05	2.76E-04	9.20E-05	8.28E-04
Ingestion	1.26E-04	4.19E-05	3.77E-04	2.51E-03	8.37E-04	7.53E-03
Total effective dose	1.47E-04	4.89E-05	4.40E-04	–	–	–
One year child old						
Pathway	Effective Doses [mSv]			Doses to Thyroid [mSv]		
	Average	95% confidence interval		Average	95% confidence interval	
		Lower Bound	Upper Bound		Lower Bound	Upper Bound
External from cloud	9.38E-08	3.13E-08	2.81E-07	–	–	–
External from ground	9.68E-06	3.23E-06	2.90E-05	–	–	–
Inhalation	2.56E-06	8.53E-07	7.68E-06	5.12E-05	1.71E-05	1.54E-04
Ingestion	3.04E-03	1.02E-03	9.10E-03	6.08E-02	2.03E-02	1.82E-01
Total effective dose	3.05E-03	1.02E-03	9.14E-03	–	–	–

[1] Calculated from thyroid gland content of ^{131}I

II–4.6.4. Farm Z (Eltopia)

II–4.6.4.1. ^{131}I air concentration

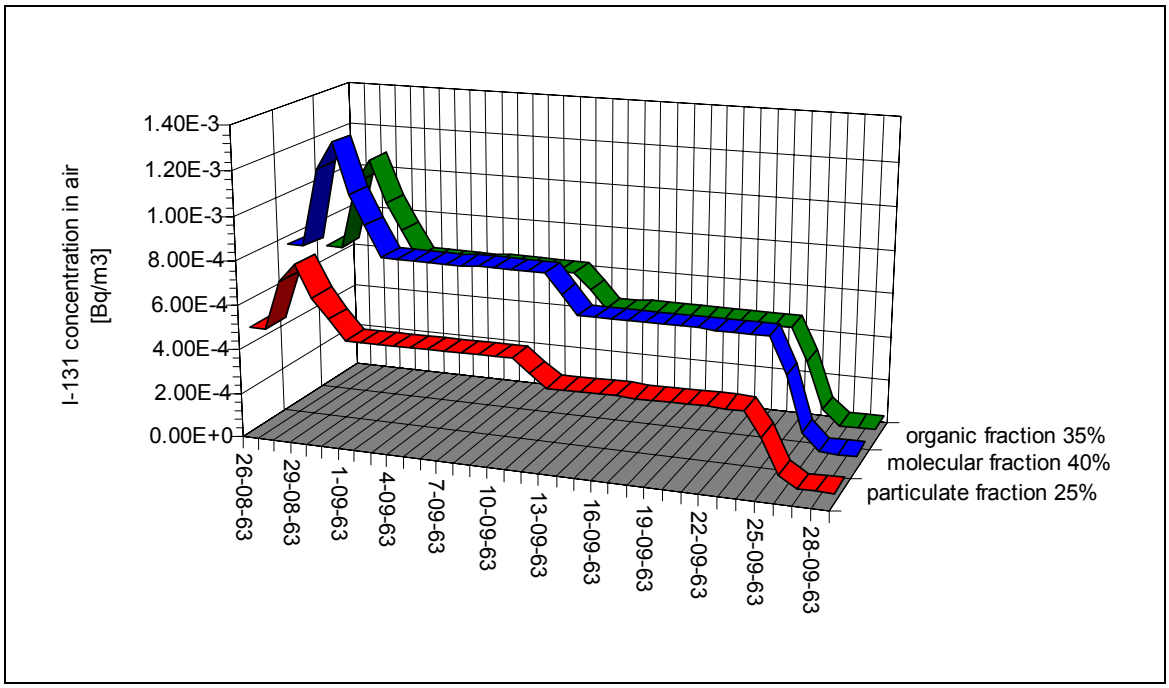

FIG. 69. Reconstruction of I-131 concentration in air for Farm Z (ELTOPIA). (based on data of stations BYERS LANDING & DISPERSION PLUMB MODEL)

TABLE II–4.XXII. RECONSTRUCTION OF ^{131}I CONCENTRATION IN AIR FOR FARM Z (ELTOPIA)
(based on data of stations BYERS LANDING & DISPERSION PLUMB MODEL)

Date	^{131}I in air [Bq m^{-3}]	Iodine-131 form distribution			Atmospheric conditions			Log normal distribution of aerosol fraction		High of mixing layer
		Particulate	I_2	Organic CH_3I	Wind speed [m s^{-1}]	Rain intensity [mm h^{-1}]	Precipit-ation [mm d^{-1}]	Mean [μ]	Standard deviation [μ]	[km]
26-08-63	1.90E-03	25.0%	40.0%	35.0%	4.00	0.00	0.00	6.00	25.00	1.0
27-08-63	1.90E-03	25.1%	40.1%	35.1%	4.00	0.00	0.00	6.00	25.00	1.0
28-08-63	2.80E-03	25.0%	40.0%	35.0%	4.00	0.00	0.00	6.00	25.00	1.0
29-08-63	3.13E-03	25.0%	40.0%	35.0%	4.00	0.00	0.00	6.00	25.00	1.0
30-08-63	2.56E-03	25.0%	40.0%	35.0%	4.00	0.00	0.00	6.00	25.00	1.0
31-08-63	3.15E-03	25.0%	40.0%	35.0%	4.00	0.00	0.00	6.00	25.00	1.0
1-09-63	3.74E-03	25.0%	40.0%	35.0%	4.00	0.00	0.00	6.00	25.00	1.0
2-09-63	3.74E-03	24.9%	39.9%	35.0%	4.00	0.00	0.00	6.00	25.00	1.0
3-09-63	3.74E-03	25.1%	40.0%	35.0%	4.00	0.00	0.00	6.00	25.00	1.0
4-09-63	3.74E-03	25.0%	40.0%	35.0%	4.00	0.00	0.00	6.00	25.00	1.0
5-09-63	3.74E-03	25.0%	40.0%	35.0%	4.00	0.00	0.00	6.00	25.00	1.0
6-09-63	3.74E-03	25.0%	40.0%	35.0%	4.00	0.00	0.00	6.00	25.00	1.0
7-09-63	3.74E-03	24.9%	40.0%	35.1%	4.00	0.00	0.00	6.00	25.00	1.0
8-09-63	3.74E-03	25.0%	40.0%	35.0%	4.00	0.00	0.00	6.00	25.00	1.0
9-09-63	2.79E-03	25.0%	40.0%	35.0%	4.00	0.00	0.00	6.00	25.00	1.0
10-09-63	1.85E-03	25.0%	40.0%	35.0%	4.00	0.00	0.00	6.00	25.00	1.0
11-09-63	1.85E-03	25.0%	40.0%	35.2%	4.00	0.00	0.00	6.00	25.00	1.0
12-09-63	1.63E-03	25.0%	40.0%	35.0%	4.00	0.00	0.00	6.00	25.00	1.0
13-09-63	1.40E-03	25.0%	40.0%	35.0%	4.00	0.00	0.00	6.00	25.00	1.0
14-09-63	1.40E-03	25.0%	40.0%	35.0%	4.00	0.00	0.00	6.00	25.00	1.0
15-09-63	1.40E-03	25.0%	40.0%	35.0%	4.00	0.00	0.00	6.00	25.00	1.0
16-09-63	1.40E-03	25.0%	40.0%	35.0%	4.00	0.00	0.00	6.00	25.00	1.0
17-09-63	1.40E-03	24.9%	40.0%	35.1%	4.00	0.00	0.00	6.00	25.00	1.0
18-09-63	1.40E-03	25.0%	40.0%	35.0%	4.00	0.00	0.00	6.00	25.00	1.0
19-09-63	1.40E-03	25.0%	40.0%	35.0%	4.00	0.00	0.00	6.00	25.00	1.0
20-09-63	1.40E-03	25.0%	40.0%	35.0%	4.00	0.00	0.00	6.00	25.00	1.0
21-09-63	1.40E-03	25.0%	40.0%	35.0%	4.00	0.00	0.00	6.00	25.00	1.0
22-09-63	1.40E-03	25.0%	40.0%	35.0%	4.00	0.00	0.00	6.00	25.00	1.0
23-09-63	1.40E-03	25.0%	40.0%	35.0%	4.00	0.00	0.00	6.00	25.00	1.0
24-09-63	1.40E-03	25.0%	40.0%	35.0%	4.00	0.00	0.00	6.00	25.00	1.0
25-09-63	9.75E-04	25.0%	40.0%	35.0%	4.00	0.00	0.00	6.00	25.00	1.0
26-09-63	3.58E-04	24.9%	40.0%	35.1%	4.00	0.00	0.00	6.00	25.00	1.0
27-09-63	1.65E-04	24.9%	40.0%	35.1%	4.00	0.00	0.00	6.00	25.00	1.0
28-09-63	1.65E-04	24.9%	40.0%	35.1%	4.00	0.00	0.00	6.00	25.00	1.0
29-09-63	1.65E-04	24.9%	40.0%	35.1%	4.00	0.00	0.00	6.00	25.00	1.0
30-09-63	1.65E-04	25.1%	40.0%	35.1%	4.00	0.00	0.00	6.00	25.00	1.0

II–4.6.4.2. ^{131}I concentration in pasture grass

TABLE II–4.XXIII. COMPARISON OF PREDICTED AND MEASURED ^{131}I CONCENTRATION IN PASTURE GRASS FOR FARM Z (ELTOPIA)

Date	Predicted values [Bq kg^{-1} fresh weight]			Observed values [Bq kg^{-1} fresh weight]	Predicted/ observed P/O
	Daily averages	95% confidence interval		Measured single values	
		Lower limit	Upper Limit		
3-09-63	3.99E+00	1.89E+00	8.42E+00	3.44E+00	1.16
4-09-63	4.11E+00	1.95E+00	8.68E+00	6.44E+00	0.64
11-09-63	4.68E+00	2.22E+00	9.88E+00	7.22E+00	0.65
19-09-63	4.25E+00	2.01E+00	8.97E+00	7.55E+00	0.56
Reliability Index RI for period 3-09-19-09 = 1.5, Logtransformer values correlation coefficient r^2=0.44, Linear relationship for Ln(P)=0.13*ln(O)+ 1.2					

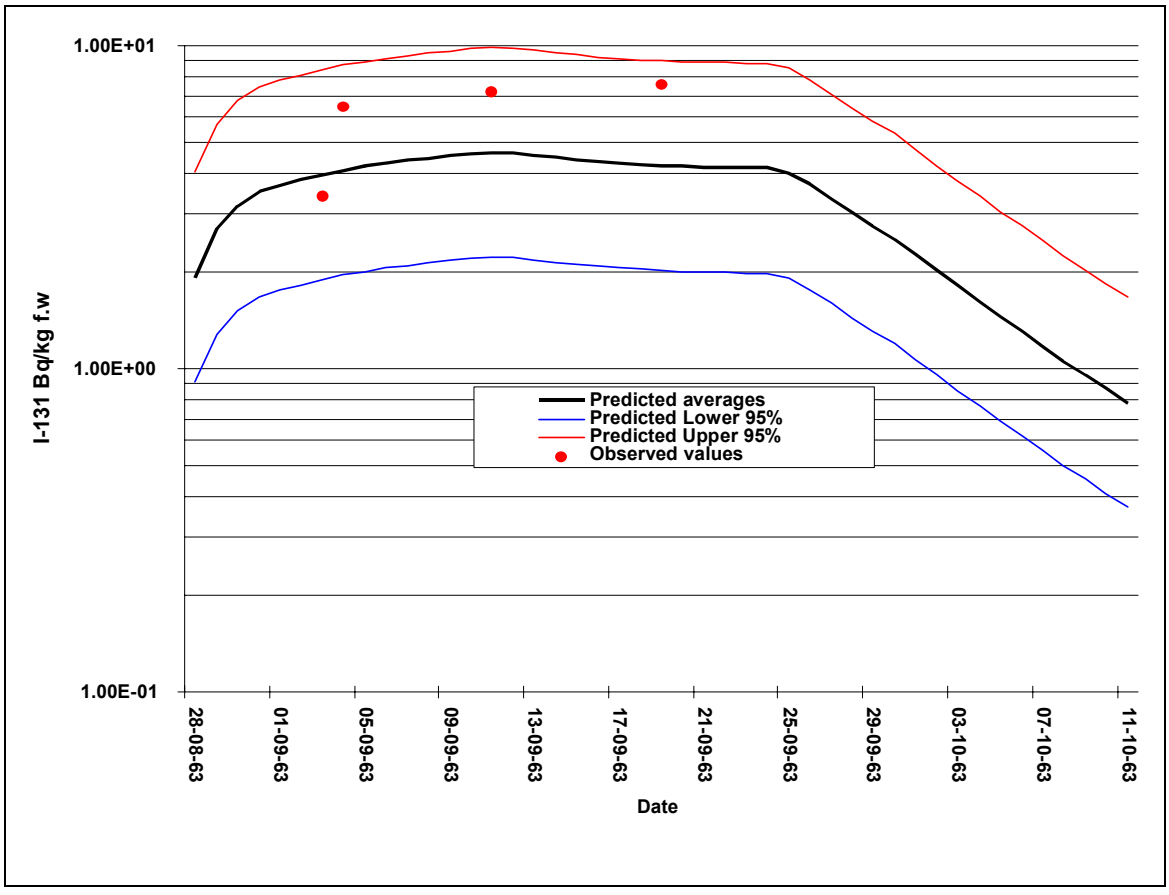

FIG. 70. Comparison of predicted and measured data of I-131 concentration in pasture grass for Farm Z (ELTOPIA)

II–4.6.4.3. ^{131}I concentration in milk

TABLE II–4.XXIV. COMPARISON OF PREDICTED AND MEASURED ^{131}I CONCENTRATION IN MILK FOR FARM Z (ELTOPIA)

Date	Predicted values [Bq kg^{-1} fresh weight]			Observed values [Bq kg^{-1} fresh weight]	Predicted/ observed P/O
	Daily averages	95% confidence interval		Measured single values	
		Lower limit	Upper Limit		
5-09-63	2.82E-01	1.21E-01	6.58E-01	3.70E-01	0.76
11-09-63	3.28E-01	1.41E-01	7.64E-01	3.70E-01	0.89
19-09-63	3.04E-01	1.30E-01	7.08E-01	2.60E-01	1.17
25-09-63	2.91E-01	1.25E-01	6.80E-01	3.10E-01	0.94
Reliability Index RI for period 5-09÷25-09 = 1.2, Logtransformer values correlation coefficient r^2=0.004, Linear relationship for Ln(P)=- 0.02*ln(O) –1.2					

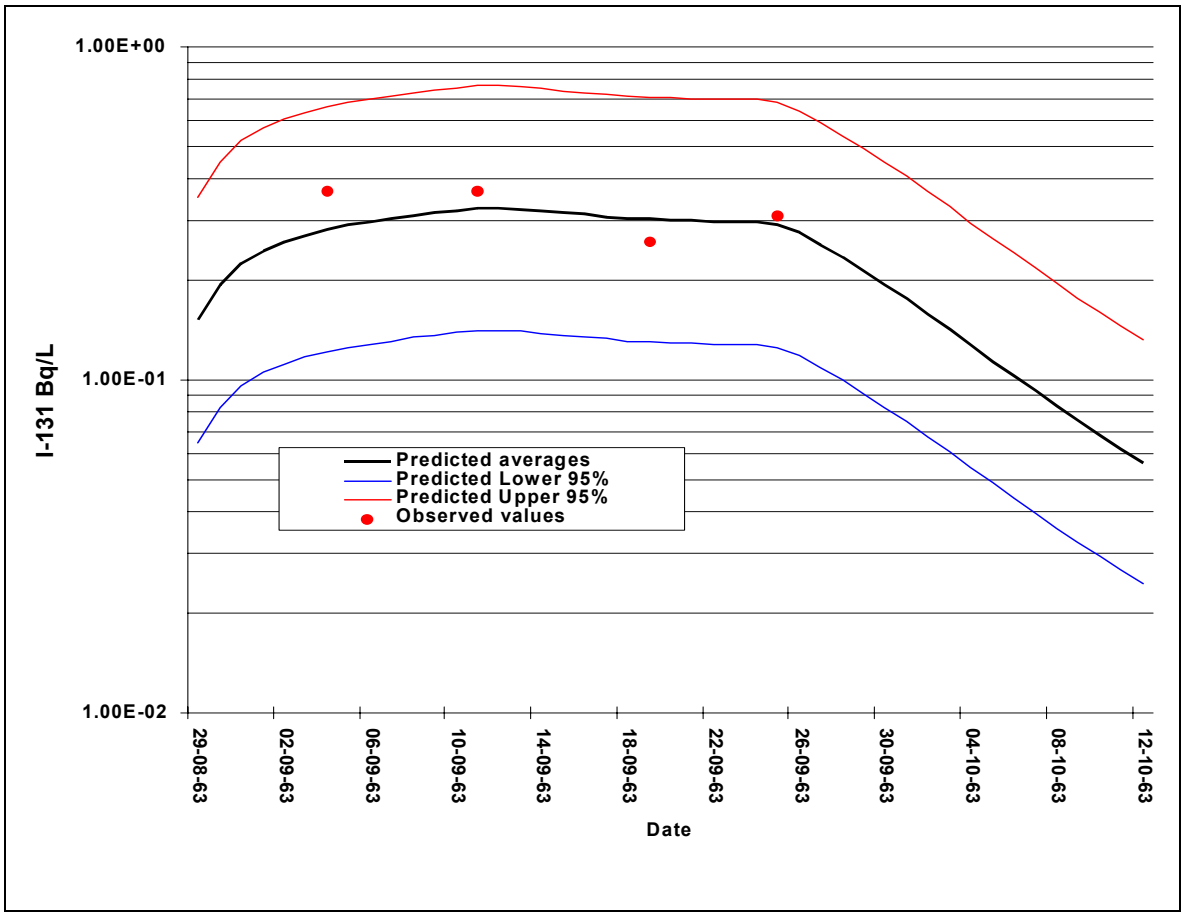

FIG. 71. Comparison of predicted and measured data of I-131 concentration in MILK for Farm Z (ELTOPIA).

II–4.6.4.4. Predictions summary

TABLE II–4.XX.V. PREDICTIONS OF ^{131}I ACTIVITY IN PARTICULAR COMPONENTS FOR FARM Z (ELTOPIA)

Integrated air concentration [Bqm^{-3}d]	7.20E-02		
Total deposition [Bq m^{-2}]	Average	95% confidence interval	
		Lower Bound	Upper Bound
	3.80E+01	1.90E+01	7.60E+01
Milk integrals (August–October) [Bqkg^{-1}d]	Average	95% confidence interval	
		Lower Bound	Upper Bound
	8.00E+00	3.40E+00	1.90E+01
Leafy sage integrals (August–October) [Bq kg^{-1} d wet weight]	Average	95% confidence interval	
		Lower Bound	Upper Bound
	8.70E+01	4.30E+01	1.80E+02
Hay integrals (August–October) [Bq kg^{-1} d]	Average	95% confidence interval	
		Lower Bound	Upper Bound
	2.70E+02	1.30E+02	5.80E+02
Pasture grass integrals for period specified [Bq kg^{-1} d wet weight]	Average	95% confidence interval	
		Lower Bound	Upper Bound
August-63	1.31E+01	1.31E+01	1.31E+01
September-63	1.23E+02	1.23E+02	1.23E+02
October-63	2.39E+01	1.13E+01	5.05E+01
Total integral (August–October)	1.60E+02	1.47E+02	1.86E+02
Silage integrals (August–October) [Bq kg^{-1} d wet weight]	Average	95% confidence interval	
		Lower Bound	Upper Bound
	4.30E+01	2.00E+01	9.10E+01
Human intake (August–October) [Bq]	Average	95% confidence interval	
		Lower Bound	Upper Bound
	4.57E+00	2.21E+00	9.45E+00

TABLE II–4.XXVI. DOSES FOR FARM Z (ELTOPIA)

Adult man (test person)						
Pathway	Effective Doses [mSv]			Doses to Thyroid [mSv]		
	Average	95% confidence interval		Average	95% confidence interval	
		Lower Bound	Upper Bound		Lower Bound	Upper Bound
External from cloud	6.04E-08	2.01E-08	1.81E-07	–	–	–
External from ground	4.48E-06	1.49E-06	1.34E-05	–	–	–
Inhalation	1.28E-05	4.27E-06	3.84E-05	2.56E-04	8.54E-05	7.68E-04
Ingestion[1]	9.10E-05	3.04E-05	2.73E-04	1.82E-03	6.07E-04	5.46E-03
Total effective dose	1.08E-04	3.61E-05	3.25E-04	–	–	–
Adult woman						
Pathway	Effective Doses [mSv]			Doses to Thyroid [mSv]		
	Average	95% confidence interval		Average	95% confidence interval	
		Lower Bound	Upper Bound		Lower Bound	Upper Bound
External from cloud	6.04E-08	2.01E-08	1.81E-07	–	–	–
External from ground	4.48E-06	1.49E-06	1.34E-05	–	–	–
Inhalation	1.12E-05	3.73E-06	3.36E-05	2.24E-04	7.46E-05	6.72E-04
Ingestion	7.75E-05	2.59E-05	2.33E-04	1.55E-03	5.17E-04	4.65E-03
Total effective dose	9.32E-05	3.11E-05	2.80E-04	–	–	–
One year child old						
Pathway	Effective Doses [mSv]			Doses to Thyroid [mSv]		
	Average	95% confidence interval		Average	95% confidence interval	
		Lower Bound	Upper Bound		Lower Bound	Upper Bound
External from cloud	7.63E-08	2.54E-08	2.29E-07	–	–	–
External from ground	6.03E-06	2.01E-06	1.81E-05	–	–	–
Inhalation	2.08E-06	6.93E-07	6.24E-06	4.16E-05	1.39E-05	1.25E-04
Ingestion	1.81E-03	6.05E-04	5.45E-03	3.62E-02	1.21E-02	1.09E-01
Total effective dose	1.82E-03	6.08E-04	5.47E-03	–	–	–

[1] Calculated from thyroid gland content of ^{131}I

II–4.6.5. Farm T (Pasco)

II–4.6.5.1. ^{131} I air concentration

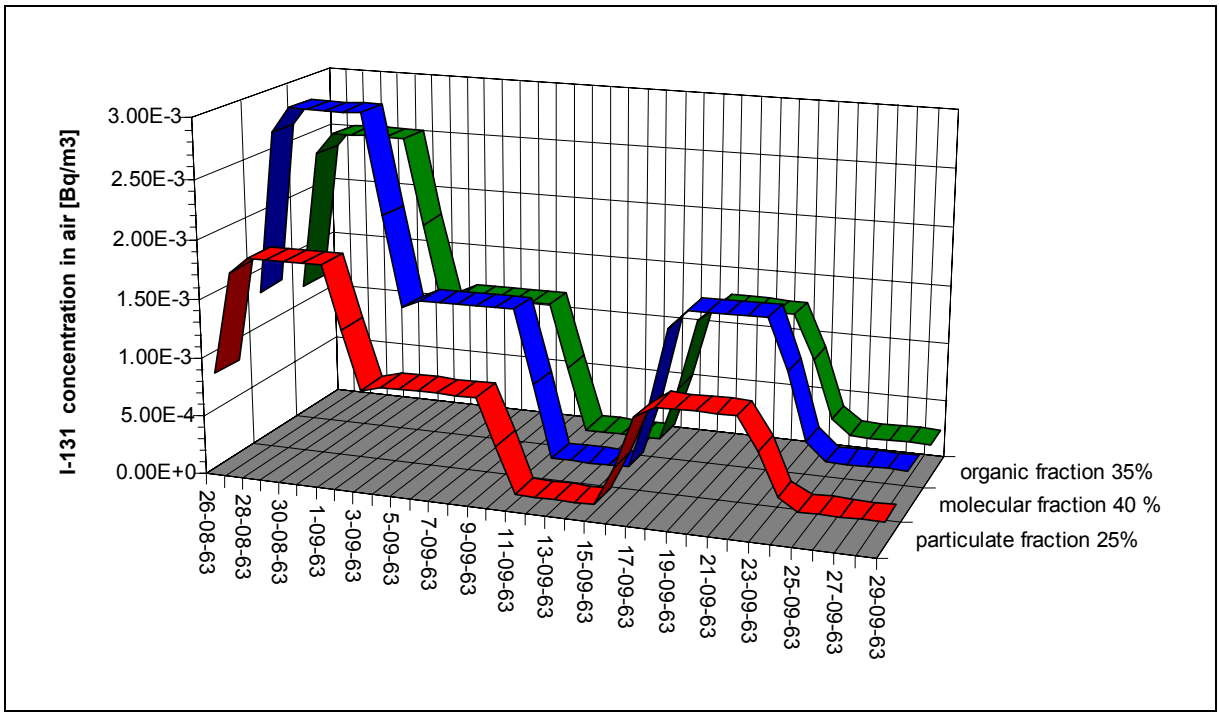

FIG. 72. Reconstruction of I-131 concentration in air for farm PASCO. (based on data of stations 300-A and 1100-A&Dispersion Plume Model)

TABLE II–4.XXVII. RECONSTRUCTION OF ^{131}I CONCENTRATION IN AIR FOR FARM PASCO
(based on data of stations 300-A and 1100-A & Dispersion Plume Model)

Date	^{131}I in air [Bq m^{-3}]	Iodine-131 form distribution			Atmospheric conditions			Log normal distribution of aerosol fraction		High of mixing layer
		Particulate	I_2	Organic CH_3I	Wind speed [m s^{-1}]	Rain intensity [mm h^{-1}]	Precipit-ation [mm d^{-1}]	Mean [μ]	Standard deviation [μ]	[km]
26-08-63	3.26E-03	25.0%	40.0%	35.0%	4.00	0.00	0.00	6.00	25.00	1.0
27-08-63	6.74E-03	25.1%	40.1%	35.1%	4.00	0.00	0.00	6.00	25.00	1.0
28-08-63	7.30E-03	25.0%	40.0%	35.0%	4.00	0.00	0.00	6.00	25.00	1.0
29-08-63	7.30E-03	25.0%	40.0%	35.0%	4.00	0.00	0.00	6.00	25.00	1.0
30-08-63	7.30E-03	25.0%	40.0%	35.0%	4.00	0.00	0.00	6.00	25.00	1.0
31-08-63	7.30E-03	25.0%	40.0%	35.0%	4.00	0.00	0.00	6.00	25.00	1.0
1-09-63	7.30E-03	25.0%	40.0%	35.0%	4.00	0.00	0.00	6.00	25.00	1.0
2-09-63	5.15E-03	24.9%	39.9%	35.0%	4.00	0.00	0.00	6.00	25.00	1.0
3-09-63	3.20E-03	25.1%	40.0%	35.0%	4.00	0.00	0.00	6.00	25.00	1.0
4-09-63	3.40E-03	25.0%	40.0%	35.0%	4.00	0.00	0.00	6.00	25.00	1.0
5-09-63	3.40E-03	25.0%	40.0%	35.0%	4.00	0.00	0.00	6.00	25.00	1.0
6-09-63	3.40E-03	25.0%	40.0%	35.0%	4.00	0.00	0.00	6.00	25.00	1.0
7-09-63	3.40E-03	24.9%	40.0%	35.1%	4.00	0.00	0.00	6.00	25.00	1.0
8-09-63	3.40E-03	25.0%	40.0%	35.0%	4.00	0.00	0.00	6.00	25.00	1.0
9-09-63	3.40E-03	25.0%	40.0%	35.0%	4.00	0.00	0.00	6.00	25.00	1.0
10-09-63	1.84E-03	25.0%	40.0%	35.0%	4.00	0.00	0.00	6.00	25.00	1.0
11-09-63	2.80E-04	25.0%	40.0%	35.2%	4.00	0.00	0.00	6.00	25.00	1.0
12-09-63	2.80E-04	25.0%	40.0%	35.0%	4.00	0.00	0.00	6.00	25.00	1.0
13-09-63	2.80E-04	25.0%	40.0%	35.0%	4.00	0.00	0.00	6.00	25.00	1.0
14-09-63	2.80E-04	25.0%	40.0%	35.0%	4.00	0.00	0.00	6.00	25.00	1.0
15-09-63	2.80E-04	25.0%	40.0%	35.0%	4.00	0.00	0.00	6.00	25.00	1.0
16-09-63	1.60E-03	25.0%	40.0%	35.0%	4.00	0.00	0.00	6.00	25.00	1.0
17-09-63	3.34E-03	24.9%	40.0%	35.1%	4.00	0.00	0.00	6.00	25.00	1.0
18-09-63	3.75E-03	25.0%	40.0%	35.0%	4.00	0.00	0.00	6.00	25.00	1.0
19-09-63	3.75E-03	25.0%	40.0%	35.0%	4.00	0.00	0.00	6.00	25.00	1.0
20-09-63	3.75E-03	25.0%	40.0%	35.0%	4.00	0.00	0.00	6.00	25.00	1.0
21-09-63	3.75E-03	25.0%	40.0%	35.0%	4.00	0.00	0.00	6.00	25.00	1.0
22-09-63	3.75E-03	25.0%	40.0%	35.0%	4.00	0.00	0.00	6.00	25.00	1.0
23-09-63	2.67E-03	25.0%	40.0%	35.0%	4.00	0.00	0.00	6.00	25.00	1.0
24-09-63	1.24E-03	25.0%	40.0%	35.0%	4.00	0.00	0.00	6.00	25.00	1.0
25-09-63	8.85E-04	25.0%	40.0%	35.0%	4.00	0.00	0.00	6.00	25.00	1.0
26-09-63	8.85E-04	24.9%	40.0%	35.1%	4.00	0.00	0.00	6.00	25.00	1.0
27-09-63	8.85E-04	24.9%	40.0%	35.1%	4.00	0.00	0.00	6.00	25.00	1.0
28-09-63	8.85E-04	24.9%	40.0%	35.1%	4.00	0.00	0.00	6.00	25.00	1.0
29-09-63	8.85E-04	24.9%	40.0%	35.1%	4.00	0.00	0.00	6.00	25.00	1.0
30-09-63	8.85E-04	25.1%	40.0%	35.1%	4.00	0.00	0.00	6.00	25.00	1.0

II–4.6.5.2. ^{131}I concentration in pasture grass

TABLE II–4.XXVIII. COMPARISON OF PREDICTED AND MEASURED ^{131}I CONCENTRATION IN PASTURE GRASS FOR FARM T (PASCO)

Date	Predicted values [Bq kg^{-1} fresh weight]			Observed values [Bq kg^{-1} fresh weight]	Predicted/ observed P/O
	Daily averages	95% confidence interval		Measured single values	
		Lower limit	Upper Limit		
3-09-63	1.06E+01	5.01E+00	2.23E+01	4.01E+01	0.26
4-09-63	1.04E+01	4.93E+00	2.20E+01	1.35E+01	0.77
5-09-63	1.03E+01	4.86E+00	2.17E+01	1.99E+01	0.52
6-09-63	1.01E+01	4.80E+00	2.14E+01	1.03E+01	0.98
7-09-63	1.00E+01	4.76E+00	2.12E+01	1.19E+01	0.84
8-09-63	9.95E+00	4.71E+00	2.10E+01	2.26E+01	0.44
9-09-63	9.88E+00	4.68E+00	2.09E+01	6.81E+00	1.45
10-09-63	9.31E+00	4.41E+00	1.97E+01	6.55E+00	1.42
11-09-63	8.30E+00	3.93E+00	1.75E+01	4.07E+00	2.04
12-09-63	7.41E+00	3.51E+00	1.56E+01	1.21E+01	0.61
13-09-63	6.63E+00	3.14E+00	1.40E+01	1.98E+00	3.35
14-09-63	5.94E+00	2.81E+00	1.25E+01	4.77E+00	1.25
16-09-63	5.24E+00	2.48E+00	1.11E+01	3.46E+00	1.52
17-09-63	5.74E+00	2.72E+00	1.21E+01	4.74E+00	1.21
18-09-63	6.31E+00	2.99E+00	1.33E+01	8.33E+00	0.76
19-09-63	6.82E+00	3.23E+00	1.44E+01	1.10E+01	0.62
20-09-63	7.28E+00	3.45E+00	1.54E+01	1.03E+01	0.71
27-09-63	6.10E+00	2.89E+00	1.29E+01	3.74E+00	1.63
30-09-63	5.12E+00	2.43E+00	1.08E+01	7.51E+00	0.68
Reliability Index RI for period 3-09-30-09 = 1.8, Logtransformer values correlation coefficient r^2=0.42, Linear relationship for Ln(P)=0.23*ln(O)+ 1.56					

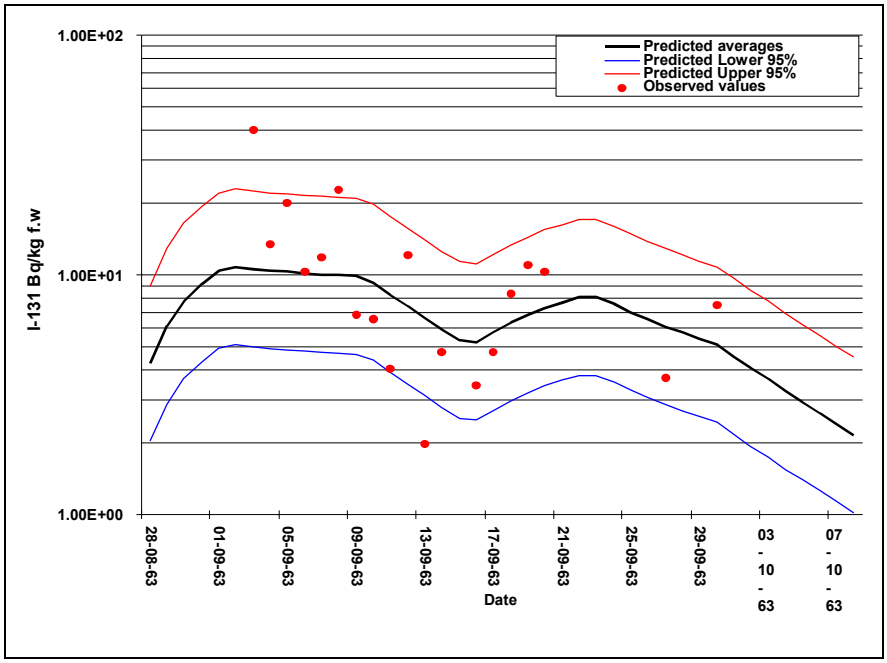

FIG. 73. Comparison of predicted and measured data of I-131 concentration in pasture grass for Farm T (PASCO).

II–4.6.5.3. ^{131}I concentration in milk

TABLE II–4.XXIX. COMPARISON OF PREDICTED AND MEASURED ^{131}I CONCENTRATION IN MILK FOR FARM T (PASCO)

Date	Predicted values [Bq L^{-1}]			Observed values [Bq L^{-1}]	Predicted/ observed P/O
	Daily averages	95% confidence interval		Measured single values	
		Lower limit	Upper Limit		
3-09-63	7.34E-01	3.84E-01	1.40E+00	7.00E-02	10.48
4-09-63	7.33E-01	3.82E-01	1.40E+00	7.00E-01	1.05
5-09-63	7.28E-01	3.81E-01	1.39E+00	8.40E-01	0.87
6-09-63	7.19E-01	3.75E-01	1.38E+00	6.40E-01	1.12
7-09-63	7.11E-01	3.71E-01	1.36E+00	5.30E-01	1.34
8-09-63	7.06E-01	3.69E-01	1.35E+00	6.40E-01	1.10
9-09-63	7.02E-01	3.66E-01	1.34E+00	1.37E+00	0.51
10-09-63	6.76E-01	3.53E-01	1.30E+00	7.70E-01	0.88
11-09-63	6.25E-01	3.26E-01	1.20E+00	5.10E-01	1.22
12-09-63	5.67E-01	2.96E-01	1.08E+00	5.30E-01	1.07
13-09-63	5.11E-01	2.67E-01	9.78E-01	7.30E-01	0.70
14-09-63	4.59E-01	2.40E-01	8.78E-01	3.10E-01	1.48
16-09-63	3.90E-01	2.03E-01	7.47E-01	1.60E-01	2.44
17-09-63	4.01E-01	2.10E-01	7.67E-01	1.70E-01	2.36
18-09-63	4.29E-01	2.24E-01	8.21E-01	1.90E-01	2.26
19-09-63	4.62E-01	2.41E-01	8.85E-01	2.60E-01	1.78
20-09-63	4.95E-01	2.58E-01	9.48E-01	2.30E-01	2.15
23-09-63	5.65E-01	2.95E-01	1.08E+00	1.10E-01	5.14
24-09-63	5.49E-01	2.87E-01	1.05E+00	1.40E-01	3.92
25-09-63	5.20E-01	2.71E-01	9.96E-01	2.00E-01	2.60
26-09-63	4.88E-01	2.54E-01	9.35E-01	3.00E-01	1.63
27-09-63	4.57E-01	2.39E-01	8.76E-01	2.00E-01	2.29
30-09-63	3.82E-01	2.00E-01	7.31E-01	1.90E-01	2.01

Reliability Index RI for period 3-09÷30-09 = 2.3,
Logtransformer values correlation coefficient r^2=0.28,
Linear relationship for Ln(P)=0.16*ln(O) -0.42

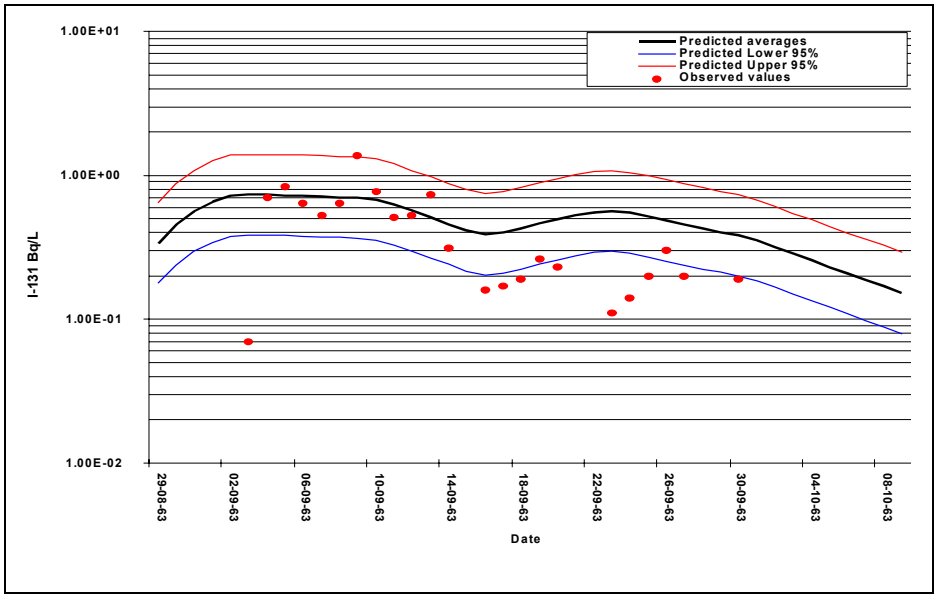

FIG. 74. Comparison of predicted and measured data of I-131 concentration in MILK for Farm T (PASCO).

II–4.6.5.4. Predictions summary

TABLE II–4.XXX. PREDICTIONS OF ^{131}I ACTIVITY IN PARTICULAR COMPONENTS FOR FARM T (PASCO)

Integrated air concentration [Bqm^{-3}d]	1.10E-01		
Total deposition [Bq m^{-2}]	Average	95% confidence interval	
		Lower Bound	Upper Bound
	7.70E+01	6.90E+01	8.50E+01
Milk integrals (August–October) [Bqkg^{-1}d]	Average	95% confidence interval	
		Lower Bound	Upper Bound
	1.70E+01	9.10E+00	3.30E+01
Leafy sage integrals (August–October) [Bq kg^{-1} d wet weight]	Average	95% confidence interval	
		Lower Bound	Upper Bound
	1.70E+02	8.30E+01	3.40E+02
Hay integrals (August–October) [Bq kg^{-1} d]	Average	95% confidence interval	
		Lower Bound	Upper Bound
	6.00E+02	2.90E+02	1.30E+03
Pasture grass integrals for period specified [Bq kg^{-1} d wet weight]	Average	95% confidence interval	
		Lower Bound	Upper Bound
August-63	3.42E+01	3.42E+01	3.42E+01
September-63	2.38E+02	2.38E+02	2.38E+02
October-63	4.87E+01	4.87E+01	4.87E+01
Total integral (August–October)	3.12E+02	1.48E+02	6.59E+02
Silage integrals (August–October) [Bq kg^{-1} d wet weight]	Average	95% confidence interval	
		Lower Bound	Upper Bound
	7.20E+01	3.40E+01	1.50E+02
Human intake (August–October) [Bq]	Average	95% confidence interval	
		Lower Bound	Upper Bound
	7.00E+00	4.40E+00	1.10E+01

TABLE II–4.XXXI. DOSES FOR FARM T (PASCO)

Adult man (test person)						
Pathway	Effective Doses [mSv]			Doses to Thyroid [mSv]		
	Average	95% confidence interval		Average	95% confidence interval	
		Lower Bound	Upper Bound		Lower Bound	Upper Bound
External from cloud	9.30E-08	3.10E-08	2.79E-07	–	–	–
External from ground	9.05E-06	3.02E-06	2.72E-05	–	–	–
Inhalation	1.98E-05	6.60E-06	5.94E-05	3.96E-04	1.32E-04	1.19E-03
Ingestion[1]	1.87E-04	6.25E-05	5.60E-04	3.74E-03	1.25E-03	1.12E-02
Total effective dose	2.16E-04	7.22E-05	6.47E-04	–	–	–
Adult woman						
Pathway	Effective Doses [mSv]			Doses to Thyroid [mSv]		
	Average	95% confidence interval		Average	95% confidence interval	
		Lower Bound	Upper Bound		Lower Bound	Upper Bound
External from cloud	9.30E-08	3.10E-08	2.79E-07	–	–	–
External from ground	9.05E-06	3.02E-06	2.72E-05	–	–	–
Inhalation	1.73E-05	5.77E-06	5.19E-05	3.46E-04	1.15E-04	1.04E-03
Ingestion	1.56E-04	5.20E-05	4.68E-04	3.12E-03	1.04E-03	9.36E-03
Total effective dose	1.82E-04	6.08E-05	5.47E-04	–	–	–
One year child old						
Pathway	Effective Doses [mSv]			Doses to Thyroid [mSv]		
	Average	95% confidence interval		Average	95% confidence interval	
		Lower Bound	Upper Bound		Lower Bound	Upper Bound
External from cloud	1.18E-07	3.93E-08	3.54E-07	–	–	–
External from ground	1.22E-05	4.07E-06	3.66E-05	–	–	–
Inhalation	3.21E-06	1.07E-06	9.63E-06	6.42E-05	2.14E-05	1.93E-04
Ingestion	3.62E-03	1.21E-03	1.09E-02	7.24E-02	2.41E-02	2.17E-01
Total effective dose	3.64E-03	1.21E-03	1.09E-02	–	–	–

[1] Calculated from thyroid gland content of ^{131}I

References

[1] PIETRZAK-FLIS, Z., KRAJEWSKI, P., KRAJEWSKA, G., SUNDERLAND, N.R., Transfer of radiocesium from uncultivated soils to grass after the Chernobyl accident, Science of the Total Environment, No 141, str. 147–153 (1994).

[2] PIETRZAK-FLIS, Z., KRAJEWSKI, P., Radiocesium in diet and man in north-eastern Poland after the Chernobyl accident, Health Physics, **67** 2 (1994).

[3] Application of the CLRP Model For Assessement of Thyroid Content and Commited Dose Equivalent for population of Poland due to Releases Radioactive Iodine ^{131}I To Environment. Verification of Model Prediction on the Basis of Charnobyl Data in Poland. International Symposium on Environmental Impact of Radioactive Releases, MAEA Wiedeñ May 1995. Extended Synopses IAEA-SM-339, pages 214–215.

[4] KRAJEWSKI; P., CLRP model descriptions and individual evaluation of model predictions; w: Validation of multiple pathways assessement models using Chernobyl fallout data of ^{137}Cs in region Central Bohemia (CB) of Czech Republic- Scenario CB-Raport of the first test exercise of the VAMP Multiple Patways Assessement Working Group; IAEA TECDOC-795, Vienna April (1995).

[5] KRAJEWSKI P.; CLRP version 4.2 Manual; BIOMOVS II Technical Report No. 7, August (1996).

[6] HEEB, C.M., GYDESEN, S.P., et al.; "Reconstruction of Radionuclide Releases from The Hanford Site, 1944-1972, Health Phys. Vol.71, No 4, October 1996, Pp.545–567.

[7] WILLIAMS, L.R., LEGGET, R.W., "A measure of model reliability", Health Phys. 46, 85–95 (1984).

II–5. THE "TYPHOON" MODEL

Used by the SPA "Typhoon", Russian Federation
A. Kryshev

II–5.1. MODEL DESCRIPTION

The general scheme of the model is given in Figure 75. The most important feature of the model is that calculations are conducted subsequently from the source, through the atmospheric transfer and deposition, to estimate the human intake, as well as the ingestion, inhalation and external doses to thyroid.

The calculations of the radionuclide air concentrations were performed on the basis of the Pasquill-Gifford model for the dispersion of ^{131}I released from a stack. This model requires information about wind direction, wind velocity at the release location, atmospheric stability, plume height and source release rate, and can provide assessments of air concentrations, depending on the distance from a stack, the roughness of the underlying surface, and the meteorlogical conditions at the time of release.

The air concentration of radioactivity released from a stack can be estimated by the Pasquill-Gifford model from the equation:

$$q_{air} = \frac{Q}{\pi u \sigma_y \sigma_z} \exp(-\frac{y^2}{2\sigma_y^2}) \cdot \exp(-\frac{h^2}{2\sigma_z^2})$$

where q_{air} is the air concentration of released radioactivity at point (x,y,0) in Bq/m^3, Q is the released rate in Bq/s, σ_y, σ_z are the cross-wind and vertical standard deviations of the concentration distributions in m, h is the effective weight in m, equal to the stack height h_s plus the plume rise Δh, u is the average wind speed in m/s.

The following formula for the calculation of Δh was used [1]: $\Delta h=3.75w_0r_0/u+5w_0r_0^2g\Delta T/(Tu^3)$; where w_0 - release velocity at the source exit (m/s), r_0 - inside radius of the release source exit (m), g - free fall acceleration (m/s^2), ΔT - overheating of released gas-air mixture (°C).

The losses by the radioactive decay was taken into account through the correction factor $f_d=\exp(-\lambda_d x/u)$, where λ_d is the decay constant (1/s). The plume depletion by dry deposition and washout was not taken into account.

The land contamination density was determined as a product of the time-integrated ground-level air concentration and the deposition rate v_g:

$$A = q_{air} v_g \Delta t$$

The value of the deposition rate was chosen to be equal to 0.013 m/s with physico-chemical distribution of a released iodine being taken into account. It was considered that 40% of iodine was in form of reactive gas, thus the preferable value for its deposition rate was 0.03 m/s; 25% of iodine was in particulate phase, for it deposition rate was 0.002 m/s, and the remain iodine was in form of an organic compounds, thus its deposition rate was 0.0001 m/s [2].

When calculating the ^{131}I concentrations in vegetation, only the direct initial contamination during deposition of radioactivity for the time of cloud passage over a given point was taken into account. This pathway is most important for the early phase of accident. The radionuclide concentrations in the productive parts of vegetation were calculated by the formula [1]:

$$q_{veg} = R \cdot \exp[-(\lambda_d + \lambda_{env})(t - t_0)] \cdot \frac{1 - \exp[-\mu(t_0 - t_{g.b.})]}{a(t - t_{g.b.})} \cdot A$$

where R is the ratio of the radionuclide concentration in the productive part of the harvest to that in the aboveground biomass (R=1 for a grassland vegetation); λ_{env} is the constant of the radionuclide loss rate from the plant cover under the action of the ecological factors in d^{-1} (λ_{env}=0.05 d^{-1} , that corresponds to the period of 14 days); μ is the empirical constant of retention chosen to be equal to 2.8 m^2/kg, a is the phytomass growth rate chosen to be equal to 6.4×10^{-4} kg $(m^2\ d)^{-1}$ [1]; t_0 is the time of deposition (t_0=0), and $t_{g.b.}$ is the time of the beginning of the growing season (I assumed that t=-180 d); A is density of the land contamination in Bq/m^2.

It was considered that radionuclides were incorporated in the organisms of animals by ingestion of contaminated fodder and by consumption of the small amounts of the contaminated soil particles. The concentrations of ^{131}I in milk were estimated from the equation [1]:

$$q_{milk} = k_r \cdot \{\sum_j m_j q_j(t) + \frac{A}{\rho_s} \exp(-\lambda_d t)[\sum_j m_j g_j + \varphi]\}$$

where q_{milk} is the concentration of radionuclide in milk (Bq/l); k_r is the coefficient of radionuclide transfer from fodder to 1 kg of animal products (in this case k_r=0.01 d/kg [1]); m_j is the daily consumption of the j-th fodder by animal in kg/d; $q_j(t)$ is the concentration of the radionuclide in the j-th fodder; g_j is the fraction of soil in the j-th fodder mass (g_j=0.001 in green fodder); ρ_s is the mass of 1 cm-thick soil layer 1 m^2 in area (for pasture ρ_s=15 kg/m^2); φ is the daily consumption of soil by grazing animals (φ=0.4 kg/d for the milk cattle) [1].

The intake of ^{131}I (in Bq) to a human organism with milk was estimated by the relationship:

$$Q = q_{milk} \cdot m \cdot B$$

where m is the mass of milk consumed for the given period; B is the coefficient of the radionuclide losses by the culinary preparation of foodstuffs (B=1 for fresh milk).

Doses from each pathway was calculated for thyroid of adult man.

Ingestion doses were estimated through the dose transfer coefficients on the basis of the calculated intake of ^{131}I with milk. The only consumption of contaminated fresh milk was considered. The value of the dose transfer coefficient was taken to be equal to 440×10^{-9} Sv/Bq [2].

Inhalation doses were estimated on the basis of calculated air concentrations, with time of the cloud passage over a given point being taken into account. The value of the dose transfer

coefficient was taken to be equal to 2.7×10^{-7} Sv/Bq [2]. The respiration rate was estimated as 2.7×10^{-4} m^3/s.

External doses from the cloud passage and the ground exposure were calculated on the basis of air concentrations and the land contamination densities. The dose coefficient for the cloud exposure was taken as 1.8×10^{-14} Sv*(Bq $s/m^3)^{-1}$, and the dose coefficient for the ground exposure was taken as 3.1×10^{-11} Sv* $(Bq/m^2)^{-1}$ [1].

Total dose from Hanford ^{131}I was estimated with the ingestion, inhalation, and external pathways being taken into account.

II–5.2. RESULTS

The results of calculations on the scenario are presented in Figures 76 to 79 and Tables II–5.I to II–5-XII.

The maximum level of ^{131}I activity in the environmental components were predicted for Farm B location. The minimum levels of ^{131}I were predicted for Mesa and Pasco locations.

The ingestion pathway was predicted to be the most important contibutor to the human thyroid dose. The doses from inhalation were calculated to be of 2 order of magnitude lower than the doses from ingestion.

TABLE II–5.I. DEPOSITION OF HANFORD ^{131}I

Location	A, Bq/m^2	Lower Bound	Upper Bound
Farm A	68	20	116
Farm B	114	34	194
Mesa	9	3	15
Eltopia	13	4	22
Pasco	10	3	17

TABLE II–5.II. ^{131}I CONCENTRATIONS IN VEGETATION (PASTURE GRASS), MONTHLY INTEGRALS

Location	q_{veg}, Bq.d/kg	Lower Bound	Upper Bound
Farm A	1050	315	1785
Farm B	1760	530	2990
Mesa	140	40	240
Eltopia	200	60	340
Pasco	155	45	265

TABLE II–5.III. ^{131}I CONCENTRATIONS IN MILK, MONTHLY INTEGRALS

Location	q_{milk}, Bq.d/L	Lower Bound	Upper Bound
Farm A	105	32	178
Farm B	177	53	300
Mesa	14	4	24
Eltopia	20	6	34
Pasco	16	5	27

TABLE II–5.IV. DAILY AVERAGE MILK CONCENTRATIONS

Day	Twin City, Bq/l	Darigold, Bq/l
September 4	4.4	3.7
5	3.8	3.2
6	3.3	2.8
7	2.8	2.4
8	2.5	2.1
9	2.1	1.8
10	1.9	1.6
11	1.6	1.4
12	1.4	1.2
13	1.2	1.0
14	1.1	0.9
15	0.9	0.78
16	0.8	0.68
17	0.7	0.59
18	0.6	0.51
19	0.5	0.45
20	0.45	0.38
21	0.39	0.34
22	0.34	0.29
23	0.30	0.25
24	0.26	0.22
25	0.22	0.19
26	0.19	0.17
27	0.17	0.14
28	0.15	0.12
29	0.13	0.11
30	0.11	0.09

TABLE II–5.V. HUMAN ^{131}I INTAKE, MONTHLY AVERAGES

Location, group	Q, Bq	Lower Bound	Upper Bound
Twin City			
Man	0.47	0.09	0.85
Woman	0.33	0.07	0.59
Child (7 years old)	0.82	0.16	1.48
Darigold			
Man	0.40	0.08	0.72
Woman	0.28	0.06	0.50
Child (7 years old)	0.70	0.14	1.26

TABLE II–5.VI. THYROID BURDEN

October 19, 1963	Q, Bq	Lower Bound	Upper Bound
Farm B boy	4.7	1.0	8.4
Farm B girl	4.0	0.8	7.2

TABLE II–5.VII. INGESTION DOSE TO THYROID (SEPTEMBER 2–OCTOBER 1, 1963)

Location	D_{ing}, mSv	Lower Bound	Upper Bound
Farm A	0.017	0.004	0.03
Farm B	0.029	0.006	0.052
Mesa	0.002	0.0004	0.0036
Eltopia	0.003	0.0006	0.0054
Pasco	0.003	0.0006	0.0054

TABLE II–5.VIII. INHALATION DOSE TO THYROID

Location	D_{inh}, 10(-5) mSv	Lower Bound	Upper Bound
Farm A	38	11	65
Farm B	64	19	109
Mesa	5.5	1.7	9.3
Eltopia	7.3	2.2	12.4
Pasco	5.6	1.7	9.5

TABLE II–5.IX. EXTERNAL DOSE TO THYROID, CLOUD EXPOSURE

Location	D_{ext}, 10(-8) mSv	Lower Bound	Upper Bound
Farm A	9	3	15
Farm B	16	5	27
Mesa	1.4	0.4	2.4
Eltopia	1.8	0.5	3.1
Pasco	1.5	0.5	2.5

TABLE II–5.X. GROUND EXPOSURE, SEPTEMBER 2–OCTOBER 1, 1963

Location	D_{ext}, 10(-6) mSv	Lower Bound	Upper Bound
Farm A	21	6	36
Farm B	36	11	61
Mesa	3	1	5
Eltopia	4	1	7
Pasco	3	1	5

TABLE II–5.XI. TOTAL DOSE FROM HANFORD ^{131}I (SEPTEMBER 2–OCTOBER 1, 1963)

Location	D_{total}, mSv	Lower Bound	Upper Bound
Farm A	0.0174	0.0035	0.036
Farm B	0.0297	0.0059	0.061
Mesa	0.0021	0.0004	0.004
Eltopia	0.0031	0.0006	0.006
Pasco	0.0031	0.0006	0.006

TABLE II–5.XII. CALCULATIONS ON THE HANFORD SCENARIO PERFORMED BY STUDENTS AT THE DEPARTMENT OF ECOLOGY, INSTITUTE OF ATOMIC POWER ENGINEERING, OBNINSK

Location	Air concentration Bq/m^3	Land contamination Bq/m^2	Concentration in milk Bq/l (t=15 days)
Farm A	1.0	78	2.25
Farm B	6.9		
Mesa	0.07	6.2	0.18
Eltopia	0.01	1.7	0.05
Pasco	0.07	6.4	0.19
	0.08	8.7	0.25
Ringold	0.09	14.1	0.41
Riverview	0.29	36	1.04
Kennewick	0.01	0.93	0.05
Kiona	0.08	25	0.7
White Bluffs	8.9		
Hanford	0.33		
Benton City	0.13		

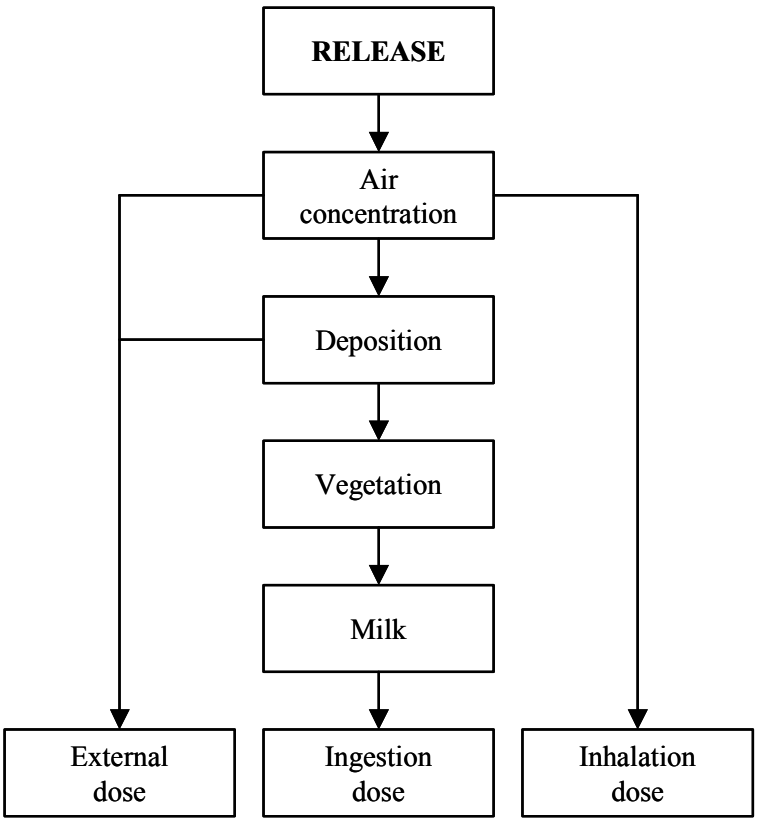

FIG. 75. The scheme of the model.

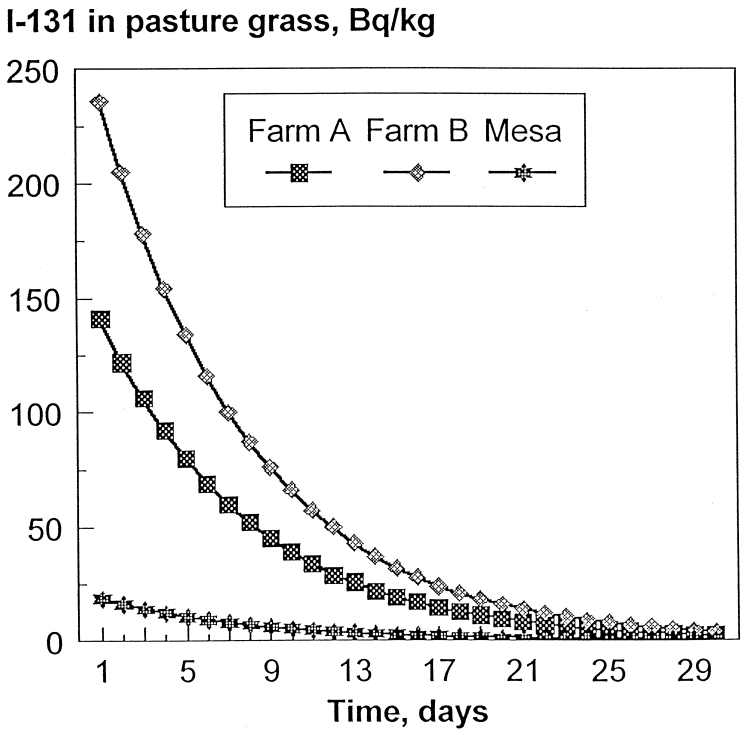

FIG. 76. Concentration of I-131 in pasture.

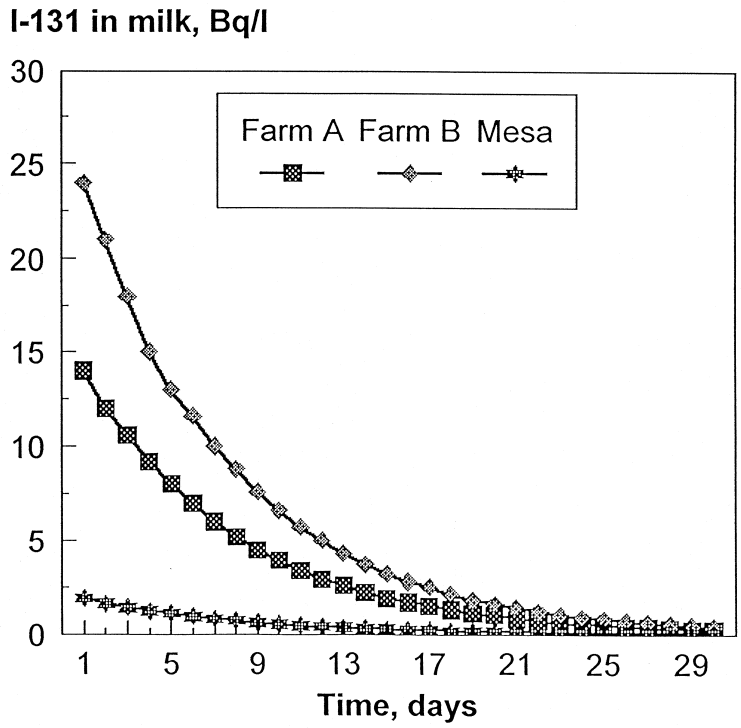

FIG. 77. Concentration of I-131 in milk at Farm A, Farm B and Mesa.

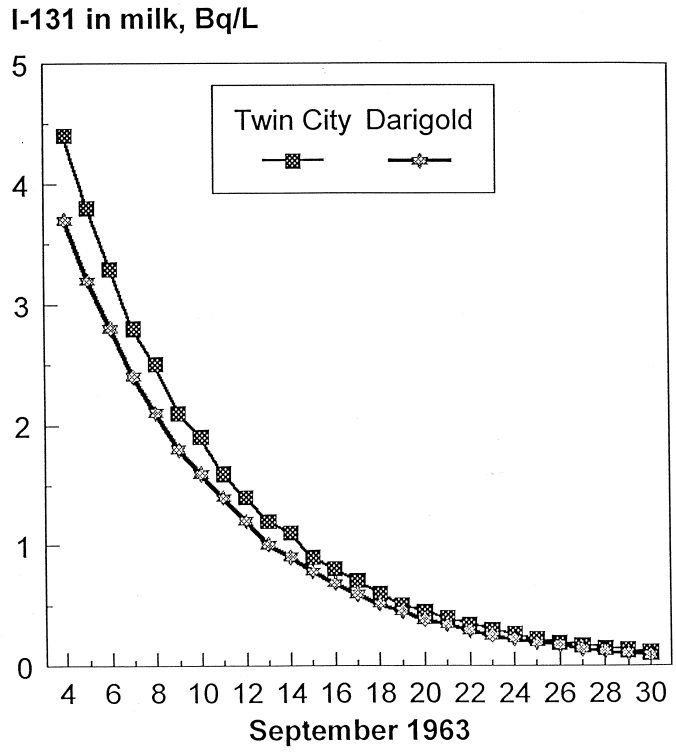

FIG. 78. Concentration of I-131 in milk at Twin City and Darigold.

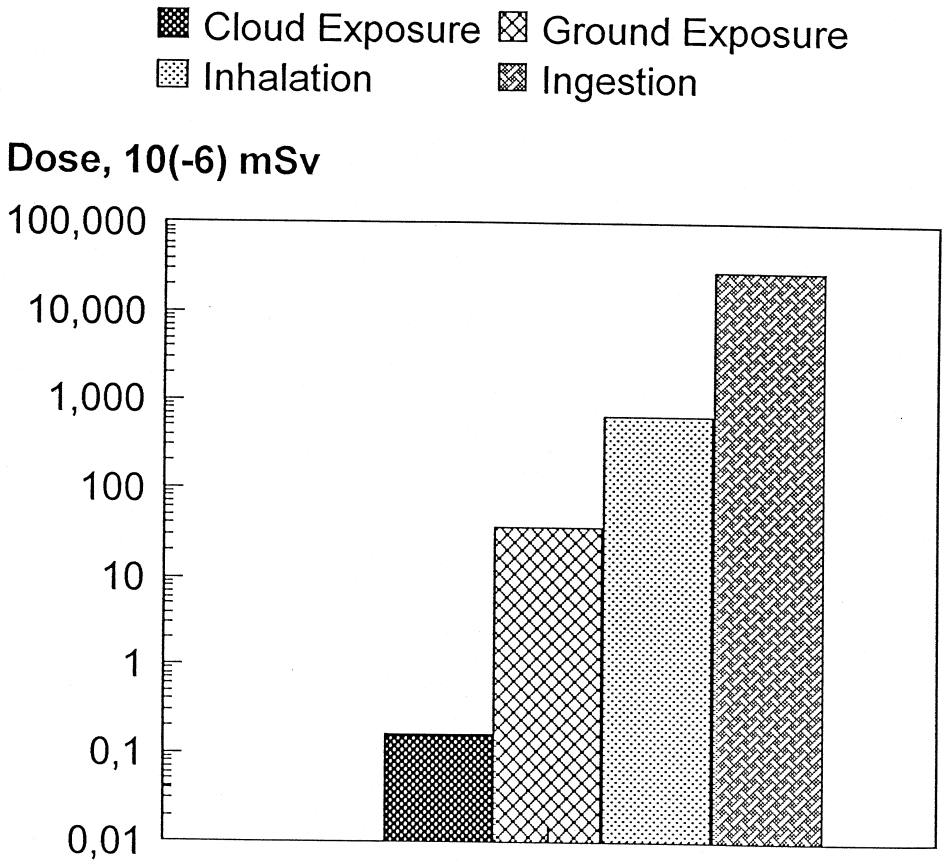

FIG. 79. Doses to thyroid (adult man) from different pathways, Farm B.

References

[1] ROMANOV, G.N., Elimination of Consequences of Radiation Accidents. Guide Book. Nuclear Society International, Moscow (1993).

[2] Handbook on the organization of the environmental control in the areas of NPPs (Ed. by K.P. Makhonko). Leningrad, Gidrometeoizdat (1990) (in Russian).

II–6. ESTIMATIONS PERFORMED AT INSTITUTE FOR ENERGY TECHNOLOGY, NORWAY

Used by the Institute for Energy Technology, Norway
U. Tveten

II–6.1. INTRODUCTION

The calculations described below are performed using a quite simplified approach and a number of approximations. Some of these approximations are also inherent in other calculations of the Hanford scenario, although perhaps not as clearly stated.

II–6.2. RELEASE

The release is given in a Table in the Scenario, but it is given in the form of one value only for rather long time periods, up to almost ten hours in the first phases and even more in the last phases of the release. The only practical way to treat this is to assume that the release has been homogenous over each time period for which there is a value.

The trajectory tracking is done following the front end of the release from each hour, while the concentration calculations are performed assuming that the release is evenly distributed over the whole hour.

II–6.3. TRAJECTORIES

Figure 80 shows the shifting wind directions from 13:00 on the 2nd September to 19:00 on the 3rd September, or actually the distances and directions in which an air package would travel, using the wind direction and wind speed information from the specifications. I have used a transparent version of this figure to be laid on top of the map of the area. When the point representing 13:00, 2 September is positioned to be exactly on the Purex plant, the whole figure shows how a release (or an air parcel) taking place (starting) exactly at that time would move around in the area. As can be seen, there are very drastic wind direction changes over the time period in question, and the travel time and distance of a plume is in most cases very much longer than the shortest distance from the Purex plant to the receptor point.

If the point representing 14:00, 2 September is put on top of the Purex plant, the figure shows the movement of a release taking place at exactly this time etc. This procedure is followed repeatedly hour by hour from 13:00 on the 2nd September to 19:00 on the 3rd September.

This method has been used to identify the release times for which the subsequent trajectories in the area eventually "hit" one of the specified receptor points, and at what time. The method is obviously quite rough, and was used as an experiment.

Figure 81 shows the “trajectory tracking figure” put on top of the map of the area. In this figure the “trajectory tracking figure” shows the trajectory over the area of the release taking place at 15:00 of the 2nd September. This release hits Eltopia at 06:00 on the day after.

The resulting “hit list” is given below:

FARM A:	Air parcel starting at 3 September	04:00	arrives at	16:00	
	"	06:00	"	16:00	
	"	07:00	"	14:00	
	"	08:00	"	15:00	
FARM B:	Air parcel starting at 2 September	13:00	arrives at	01:00	
	Air parcel starting at 3 September	03:00	arrives at	16:00	
	"	04:00	"	16:00	
	"	05:00	"	16:00	
	"	06:00	"	14:00	
	"	07:00	"	11:00	
	"	08:00	"	12:00	
MESA	No hits at all				
ELTOPIA	Air parcels starting at 2 September	15:00 to 18:00	arrive at	06:00	
	Air parcel starting at 2 September	23:00	arrives at	02:00	
	"	24:00	"	06:00	
	Air parcel starting at 3 September	01:00	arrives at	09:00	
PASCO	Air parcel starting at 2 September	14:00	arrives at 3 September		16:00
	"	24:00	"		17:00
	Air parcel starting at 3 September	01:00	"		19:00

II–6.4. CHOICE OF DEPOSITION VELOCITY

According to descriptions, the area, including the area used for grazing, is quite arid, and one should expect a deposition velocity lower than that for traditional pasture.

A deposition velocity value often used for pasture is 0.01 m/s. According to VAMP, IAEA-TECDOC-760 the deposition velocity for mowed grass (a lawn in an urban area) is 0.0026 m/s and for a horizontal smooth surface 0.0007 m/s.

In the present calculations a value of 0.006 m/s has been used, to represent something intermediate between a rich pasture and a lawn.

II–6.5. ATMOSPHERIC DISPERSION CONDITIONS

In the description it is mentioned that the weather during the time period in question was "fairly unstable" and that there was no rain. The wind velocities used are rough averages of day and night time conditions as given in the specifications.

The conditions used are the following:

Day-time:	Stability D, wind speed 4 m/s, mixing height 1000 m.
Night-time:	Stability E, wind speed 2 m/s, mixing height 300 m.

II–6.6. CONCENTRATION CALCULATIONS

The calculations have been carried out with the MACCS computer program developed by USNRC. The program has been used in the constant-weather-option, which is in reality a straight-line Gaussian model with surface depletion and homogenous vertical concentration distribution after the upper part of the plume hits the mixing layer.

Two sets of calculations were carried out with MACCS: day- and night-conditions.

For each set of release - arrival time in the "hit" lists, the distance actually traveled by the air package has been calculated "by hand", using the wind velocities given in the specifications, and the ground concentrations have been taken from the results of the MACCS calculations at the appropriate distances.

Finally the concentrations for all sets of release - arrival "hits" at each of the receptor points have been added.

The calculated cumulative ground concentrations are:

FARM A:	61	Bq/m^2
FARM B:	146	Bq/m^2
MESA:	0	Bq/m^2
ELTOPIA:	229	Bq/m^2
PASCO:	9.2	Bq/m^2

II–6.7. CONCENTRATIONS IN VEGETATION

Lettuce:
Using 1000 acres = 4.047×10^6 m^2 and the total production of lettuce on this area being 7500 tonnes, the yield is 1.9 kg/m^2. With a best-guess-value of interception of 0.8, 1 Bq/m^2 gives 0.42 Bq/kg lettuce. The scenario, however, does not contain a single lettuce-measurement, nor tell where lettuce is produced.

Hay:
Production in Washington State: Upon 854,000 acres (= 3.46×10^9 m^2) the total production of hay is 1.796×10^9 kg, which gives a yield of 0.52 kg/m^2. A best-guess-value for interception on grass of 0.4 is used. Then 1 Bq/m^2 gives 0.77 Bq/kg (grass dryweight, or "hay").

In the following Table is a comparison between my calculation results and a very rough estimate of averages of the measured values given in the scenario.

Receptor point	Measured value (Bq/kg)	Calculated value (Bq/kg)
Farm A	50	45
Farm B	30	110
Mesa	8	0
Eltopia	6	180
Pasco	8	7

For some of the receptor points the agreement is exceptionally good, but for Eltopia it is not good at all. Possible explanations can be found in the following subchapter.

II–6.8. VARIOUS WEAKNESSES OF THESE CALCULATIONS

Radioactive decay of iodine has been taken into account only as long as the material is airborne. By this is meant that radioactive decay is taken into account during atmospheric transport of every release, but not after deposition has taken place. The fact is that iodine deposited in one receptor point can have been brought with several air parcels of very different travel time and deposited at different times of the day/night. For instance, in Eltopia the first deposition took place at 02:00 at night and the last at 09:00 in the forenoon. The summed-up deposited amount consists of the amount of iodine deposited at 02:00 (with no further decay) plus the amount deposited at 09:00 (with all decay till 09:00 taken account of) plus several other "hits". The error introduced in this manner will be insignificant, however.

When the wind directions change as drastically as was the case in the Hanford scenario, the strangest things will happen. The tracing of trajectories has been performed as if every release takes place exactly on the hour. In reality it is distributed over the hour in some unknown fashion (actually the distribution within the time intervals given in the specifications (which are considerably longer than one hour) is not even known). The reasonable assumption is to assume the release to have been even over the whole time period for which one value is given. This means that e.g. the release during the hour following 2 September 14:00 is evenly distributed along the line from 14 to 15 in Figure 80. When the wind shifts 90^0 at 15:00 the whole plume will start to move sideways. None of the simple atmospheric transport programs can handle a situation like this properly. With repeated wind shifts, one will expect real concentrations to be somewhat lower than the calculation result.

The choice of mixing height is very important in a calculation like this, and the specifications really give no clue as to the likely value of this parameter, neither during day nor night conditions. Too high mixing height will result in too low concentrations at the longer distances.

The following of trajectories will only give an approximate idea of exactly where a certain air parcel is at a certain time. The concentration estimated for Eltopia seems to be an overestimation. In this case the trajectory drawing shows that the wind direction changes so sharply that it does not completely reach Eltopia before moving in a completely different direction. It is quite possible that the wind direction shift took place before the plume reached the point at which the vegetation samples were taken and that the concentrations in vegetation could be much higher only a relatively short distance away in a Westerly direction.

The last portion of the release I took into consideration in these calculations took place during the hour following 18:00 on the 3 September, and this release and several preceding it were not followed properly, as I left off drawing trajectories when they went off the sheet upon which I was drawing. This is a rather arbitrary cut-off and quite unscientific. If I wanted to do this once more in a more stringent manner, I would follow the trajectories quite a bit longer, and this might modify my results somewhat.

The basis given for estimating uptake of radioactivity by grazing animals is “hay”, which may not correctly describe the diet of the animals in the area in question. According to verbal and informal information given during the discussions, these animals graze all sorts of wild vegetation rather than pasture grass (or “hay”, which is a very imprecise word, since moisture content may vary considerably), for which neither yield nor interception nor deposition are known.

II–6.9. CONCLUSIONS

It is rather surprising that the very rough approach applied in the present calculations gives such good agreement - and this is not the result of "fudging". I honestly did not even see the measurement values until after I had completed all calculations.

One way in which I intend to utilize the results of this exercise is to throw them in the face of meteorologists who insist that Gaussian methods are absolutely useless.

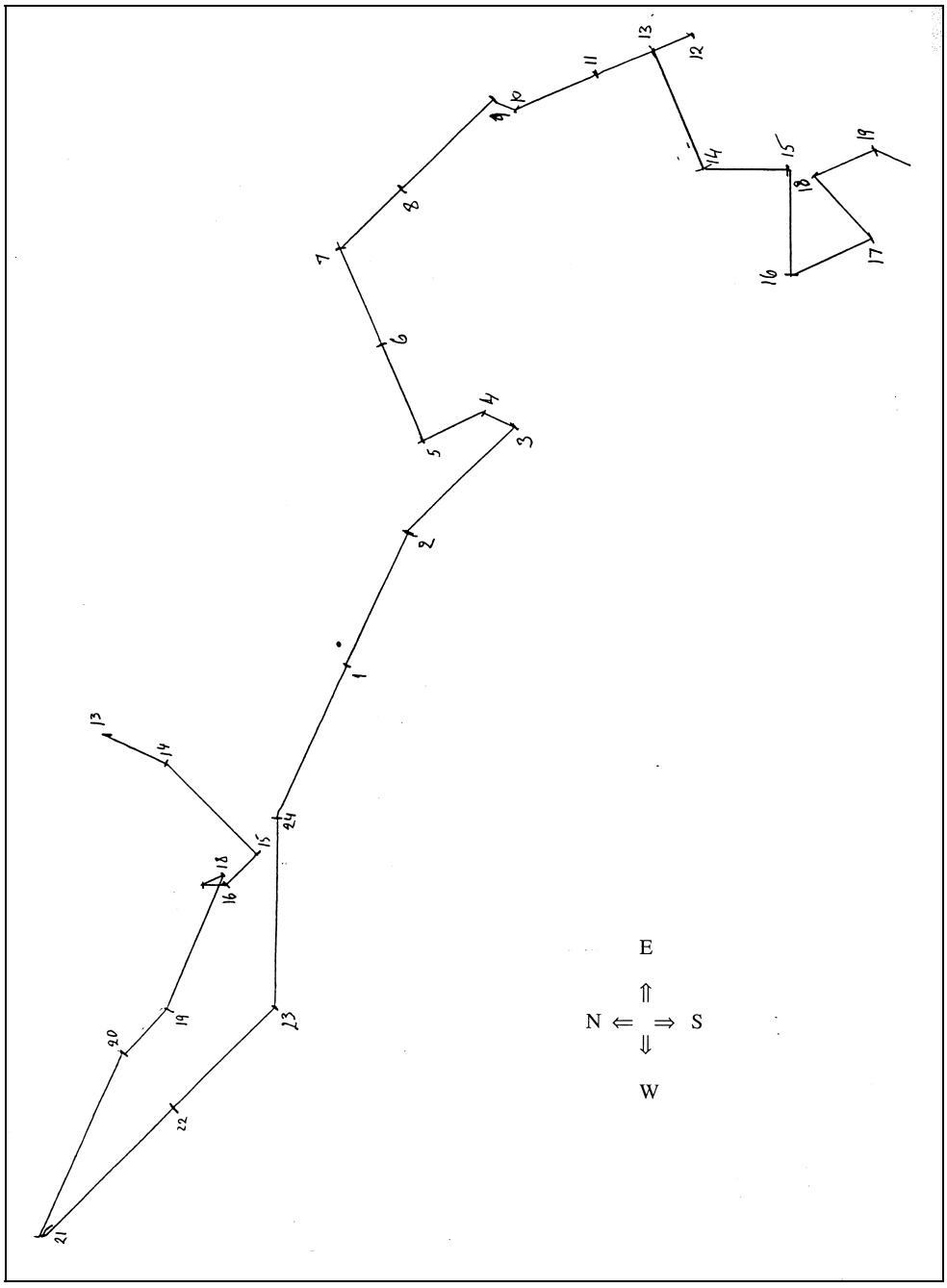

FIG. 80. The "trajectory tracking" figure.

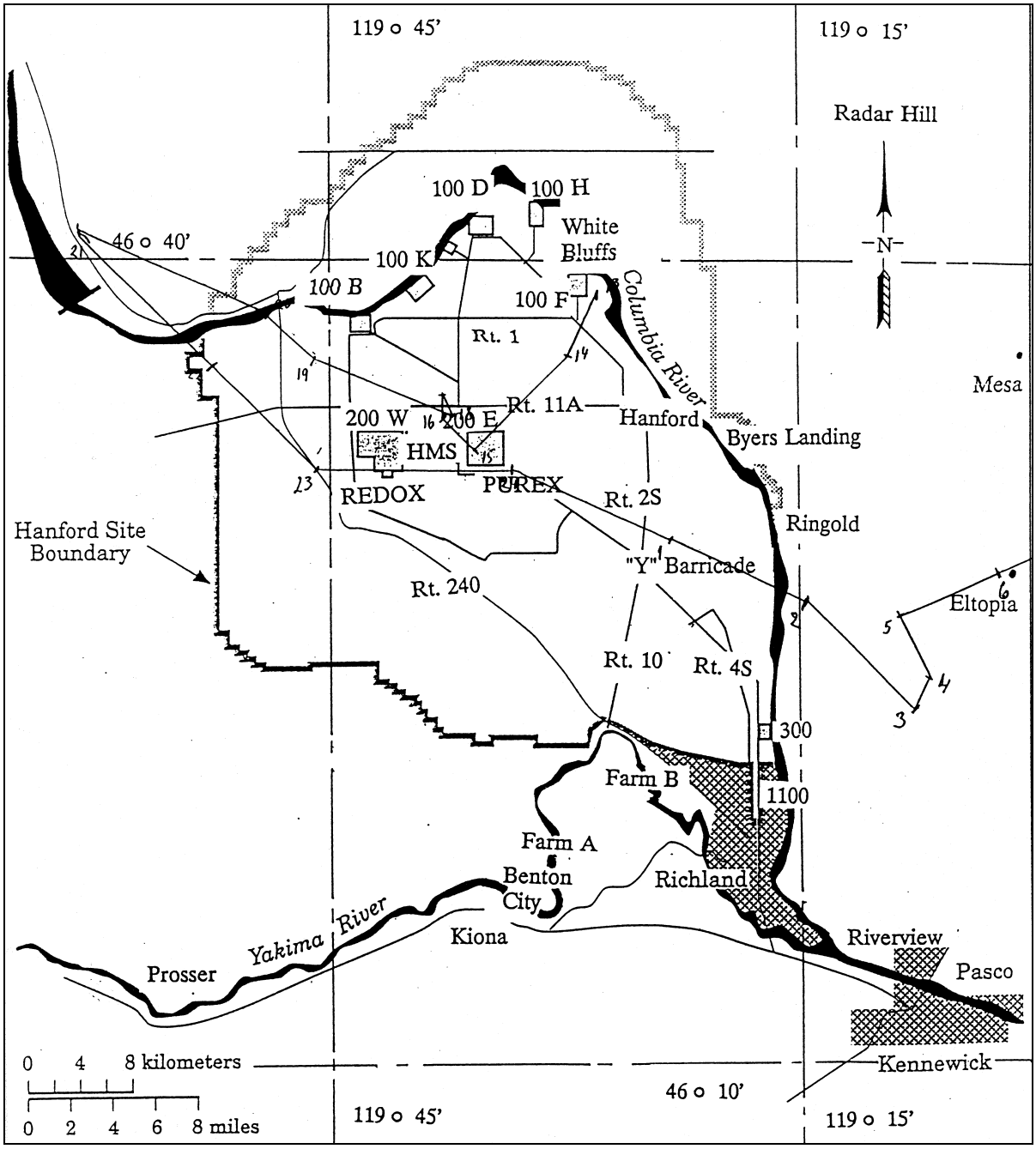

FIG. 81. Example of trajectory over the geographical area.

Annex III

SUMMARY OF MODEL PREDICTIONS

The tables in this annex contains the predictions submitted for each endpoint by the exercise participants. The observations are included, where available, as are the predictions or estimates from measurements provided by the Hanford Environmental Dose Reconstruction Project (HEDR). The tables include columns labelled 'lower' and 'upper', these refer to the 90 or 95% subjective confidence intervals on model predictions. Uncertainties were not available for most observations.

TABLE. III–I. PREDICTED DEPOSITION OF ^{131}I AT SPECIFIED LOCATIONS (Bq m^{-2})

	Farm A	lower	upper	Farm B	lower	upper	Mesa	lower	upper
Napier (HEDR)	96	32	290	190	63	570	19	6	57
Filistovic	66	1.9	970	108.3	5.1	970	17.5	0.9	280
Homma (1)	61.1	13.1	114	132	26.5	283	356	40.8	1070
Homma (2)	43.1			43.3			4.69		
Kryshev	68	20	116	114	34	194	9	3	15
Krajewski	200	180	220	287	258	318	61	55	68
Kanyar/Nenyei	78	35	167	179	113	268	6.5	4.1	8.6
Tveten	61			146			0		

	Eltopia	lower	upper	Pasco	lower	upper	Ringold	lower	upper
Napier (HEDR)	39	13	120	140	47	420			
Filistovic	33.9	2.4	460	27.5	0.5	460			
Homma (1)	140	45.2	222	24.9	8.44	37.9	720	143	1540
Homma (2)	22.5			430			257		
Kryshev	13	4	22	10	3	17			
Krajewski	38	19	76	77	69	85			
Kanyar/Nenyei	11	8.8	13	10	5.1	15	43	34	60
Tveten	229			9.2					

TABLE. III–II. PREDICTED AND OBSERVED CONCENTRATIONS OF ^{131}I IN PASTURE GRASS (FRESH WEIGHT) AT SPECIFIED LOCATIONS (Bq d kg^{-1})

	Farm A	lower	upper	Farm B	lower	upper	Mesa	lower	upper
Observed	600			940			230		
Napier (HEDR)	110	40	270	210	80	550	20	8	52
Filistovic	342	9	5430	627	25	8100	72	3	2000
Homma (1)	455	75.9	1060	977	131	2590	2530	172	7350
Homma (2)	156			156			17.0		
Kryshev	1050	315	1785	1760	530	2990	140	40	240
Krajewski	810	384	1710	1180	585	2370	234	111	494
Tveten	200			570			0		

	Eltopia	lower	upper	Pasco	lower	upper	Ringold	lower	upper
Observed	180			250			290		
Napier (HEDR)	40	15	100	160	62	420			
Filistovic	150	9	2000	155	2	4450			
Homma (1)	1030	173	2240	185	42.4	396	5260	675	13400
Homma (2)	81.5			1560			931		
Kryshev	200	60	340	155	45	265			
Krajewski	160	147	186	312	148	659			
Tveten	890			32					

TABLE. III–III. PREDICTED CONCENTRATIONS OF ^{131}I IN SAGE (FRESH WEIGHT), SILAGE (FRESH WEIGHT) AND HAY (DRY WEIGHT) AT SPECIFIED LOCATIONS (Bq d kg^{-1})

	Farm A	lower	upper	Farm B	lower	upper	Mesa	lower	upper
leafy sage									
Napier (HEDR)	77	28	190	150	56	380	14	6	36
Krajewski	480	240	970	799	396	1610	150	72	290
Kanyar/Nenyei	270	140	400	710	360	1100	11	5.7	17
silage									
Krajewski	120	58.0	260	274	130	578	62	29	130
hay									
Krajewski	2200	1000	4500	3120	1480	6590	420	200	900
Kanyar/Nenyei	1100	610	1600	2400	1300	4000	33	18	48

	Eltopia	lower	upper	Pasco	lower	upper	Ringold	lower	upper
leafy sage									
Napier (HEDR)	28	10	70	110	43	290			
Krajewski	87	43	180	170	83	340			
Kanyar/Nenyei	22	12	35	31	16	48	77	39	120
silage									
Krajewski	43	20	91	72	34	150			
hay									
Krajewski	270	130	580	600	290	1300			
Kanyar/Nenyei	67	38	110	99	53	160	230	140	320

hay (Bq/kg)	Farm A	Farm B	Mesa	Eltopia	Pasco
Estimate of observed	50	30	8	6	8
Tveten	45	110	0	180	7

TABLE. III–IV. PREDICTED AND OBSERVED CONCENTRATIONS OF ^{131}I IN MILK AT SPECIFIED LOCATIONS (Bq d L^{-1})

	Farm A	lower	upper	Farm B	lower	upper	Mesa	lower	upper
Observed	36			110			26		
Napier (HEDR)	23	5	110	46	9	230	5	1	25
Filistovic	24.7	0.92	93	37.8	2.2	135	6.1	0.34	19.6
Homma (1)	58.9	6.29	198	127	13.3	397	337	17.8	1080
Homma (2)	42.2			42.4			4.59		
Kryshev	105	32	178	177	53	300	14	4	24
Krajewski	46	24	87	76.7	46.5	126	13	6.8	25
Kanyar/Nenyei	49	14	105	129	39	210	1.9	0.71	3.5

	Eltopia	lower	upper	Pasco	lower	upper	Ringold	lower	upper
Observed	8.5			11			20		
Napier (HEDR)	10	2	50	35	7	180			
Filistovic	12.5	0.902	36.8	7.5	0.33	31.2			
Homma (1)	138	16.5	382	24.6	3.44	64.9	678	60.8	2360
Homma (2)	22			421			252		
Kryshev	20	6	34	16	5	27			
Krajewski	8	3.4	19	17	9.1	33			
Kanyar/Nenyei	3.8	1.8	6.4	5.7	2	9.8	14	4.9	26

TABLE. III–V. PREDICTED AND OBSERVED CONCENTRATIONS OF ^{131}I IN DAIRY MILK (Bq L^{-1})

	Twin City			Darigold		
	Observed	Kryshev	Kanyar/Nenyei	Observed	Kryshev	Kanyar/Nenyei
1963-09-04		4.4	0.087		3.7	< 0.001
1963-09-05		3.8	0.16		3.2	0.0076
1963-09-06		3.3	0.17		2.8	0.024
1963-09-07		2.8	0.20		2.4	0.033
1963-09-08		2.5	0.22		2.1	0.037
1963-09-09		2.1	0.24		1.8	0.039
1963-09-10		1.9	0.26		1.6	0.043
1963-09-11		1.6	0.27		1.4	0.050
1963-09-12		1.4	0.27		1.2	0.056
1963-09-13		1.2	0.27		1	0.061
1963-09-14		1.1	0.26		0.9	0.064
1963-09-15		0.9	0.26		0.78	0.068
1963-09-16	0.46	0.8	0.25	0.30	0.68	0.069
1963-09-17		0.7	0.24		0.59	0.069
1963-09-18		0.6	0.24		0.51	0.068
1963-09-19		0.5	0.22		0.45	0.068
1963-09-20		0.45	0.21		0.38	0.069
1963-09-21		0.39	0.20		0.34	0.062
1963-09-22		0.34	0.20		0.29	0.059
1963-09-23		0.3	0.18		0.25	0.055
1963-09-24		0.26	0.17		0.22	0.052
1963-09-25		0.22	0.17		0.19	0.049
1963-09-26	0.15	0.19	0.15	0.07	0.17	0.045
1963-09-27		0.17	0.14		0.14	0.041
1963-09-28		0.15	0.13		0.12	0.039
1963-09-29		0.13	0.12		0.11	0.037
1963-09-30		0.11	0.10		0.09	0.035

TABLE. III–VI. PREDICTED INTAKE OF ^{131}I BY HUMANS (Bq)

	Twin City man	lower	upper	woman	lower	upper	child	lower	upper
Kryshev	0.47	0.09	0.85	0.33	0.07	0.59	0.82	0.16	1.48

	Darigold man	lower	upper	woman	lower	upper	child	lower	upper
Homma (1)	7.00	0.574	26.6	4.86	0.681	21.2	8.66	0.918	22.1
Homma (2)	13.0			9.27			16.1		
Kryshev	0.4	0.08	0.72	0.28	0.06	0.5	0.7	0.14	1.26
Kanyar/Nenyei	0.96	0.37	1.6	1.2	0.48	2.0	1.2	0.45	2.1

	Carnation man	lower	upper	woman	lower	upper	child	lower	upper
Homma (1)	5.04	0.480	17.2	3.72	0.421	15.6	6.23	0.647	21.3
Homma (2)	9.24			6.61			11.4		
Kanyar/Nenyei	29	12	49	37	13	57	35	13	59

	Farm A	lower	upper	Farm B	lower	upper
Krajewski	22.0	14.0	35.0	27.7	16.6	44.3

	Mesa	lower	upper	Pasco	lower	upper
Krajewski	5.8	3.6	9.3	7	4.4	11

TABLE. III–VII. PREDICTED AND OBSERVED THYROID BURDENS OF ^{131}I FOR SPCIFIED INDIVIDUALS (Bq)

	Farm B-boy	lower	upper	Farm B-girl	lower	upper
Observed	2.7			1		
Kryshev	4.7	1	8.4	4	0.8	7.2
Krajewski	4.4	2.5	7.8	1.3	0.9	2
Kanyar/Nenyei	2.5	0.6	5.0	0.52	0.20	1.5
Homma (1)	1.01	0.106	3.18	0.467	0.0491	1.46

TABLE. III–VIII. PREDICTED EXTERNAL DOSES FROM CLOUD EXPOSURE (mSv)

	Farm A	lower	upper	Farm B	lower	upper	Mesa	lower	upper
Filistovic-thyroid	8.35E-07			8.88E-07			8.66E-08		
Filistovic-body surface	2.29E-06			2.44E-06			2.38E-07		
Homma (1)	2.3E-07	4.1E-08	4.5E-07	4.5E-07	9.4E-08	7.5E-07	1.7E-06	4.7E-08	4.5E-06
Homma (2)	1.4E-07			1.4E-07			1.5E-08		
Kryshev	9.00E-08	3.00E-08	1.50E-07	1.60E-07	5.00E-08	2.70E-07	1.40E-08	4.00E-09	2.40E-08
Krajewski-man	2.44E-07	8.13E-08	7.32E-07	3.46E-07	1.15E-07	1.04E-06	7.42E-08	2.47E-08	2.23E-07
Krajewski-woman	2.44E-07	8.13E-08	7.32E-07	3.46E-07	1.15E-07	1.04E-06	7.42E-08	2.47E-08	2.23E-07
Krajewski-child (1 yr)	3.08E-07	1.03E-07	9.24E-07	4.37E-07	1.46E-07	1.31E-06	9.38E-08	3.13E-08	2.81E-07
Krajewski-boy (4 yr)				3.87E-07	1.29E-07	1.16E-06			
Krajewski-girl (8 yr)				3.87E-07	1.29E-07	1.16E-06			
Kanyar/Nenyei	4.70E-08	2.10E-08	9.50E-08	1.10E-07	5.00E-08	2.00E-07	3.90E-09	1.60E-09	8.90E-09
Napier (HEDR)	5E-07	2E-07	2E-06	9E-07	3E-07	3E-06	7E-08	2E-08	2E-07

	Eltopia	lower	upper	Pasco	lower	upper	Ringold	lower	upper
Filistovic-thyroid	1.77E-07			1.53E-07					
Filistovic-body surface	4.86E-07			4.19E-07					
Homma (1)	7.0E-07	2.4E-08	1.3E-06	1.2E-07	6.8E-09	2.6E-07	2.5E-06	6.20E-07	4.60E-06
Homma (2)	7.5E-08			1.4E-06			8.6E-07		
Kryshev	1.80E-08	5.00E-09	3.10E-08	1.50E-08	5.00E-09	2.50E-08			
Krajewski-man	6.04E-08	2.01E-08	1.81E-07	9.30E-08	3.10E-08	2.79E-07			
Krajewski-woman	6.04E-08	2.01E-08	1.81E-07	9.30E-08	3.10E-08	2.79E-07			
Krajewski-child (1 yr)	7.63E-08	2.54E-08	2.29E-07	1.18E-07	3.93E-08	3.54E-07			
Kanyar/Nenyei	6.50E-09	3.10E-09	1.20E-08	5.90E-09	2.80E-09	1.10E-08	2.60E-08	1.30E-08	5.00E-08
Napier (HEDR)	3E-07	9E-08	8E-07	7E-07	2E-07	2E-06			

TABLE. III–IX. PREDICTED EXTERNAL DOSES FROM GROUND EXPOSURE, 2–5 SEPTEMBER (mSv)

	Farm A	lower	upper	Farm B	lower	upper
Filistovic-thyroid	9.55E-06			1.32E-05		
Filistovic-body surface	2.54E-05			3.50E-05		
Kryshev	8.00E-06	2.40E-06	1.36E-05	1.40E-05	4.00E-06	2.40E-05
Kanyar/Nenyei	2.50E-06			5.70E-06		

	Mesa	lower	upper	Eltopia	lower	upper
Filistovic-thyroid	3.45E-09			9.89E-07		
Filistovic-body surface	9.16E-09			2.63E-06		
Kryshev	1.00E-06	3.00E-07	1.70E-06	2.00E-06	6.00E-07	3.40E-06
Kanyar/Nenyei	2.10E-07			3.90E-07		

	Pasco	lower	upper	Ringold	lower	upper
Filistovic-thyroid	8.12E-07					
Filistovic-body surface	2.16E-06					
Kryshev	1.00E-06	3.00E-07	1.70E-06			
Kanyar/Nenyei	3.20E-07			1.40E-06		

TABLE. III–X. PREDICTED DOSES FROM GROUND EXPOSURE, 2 SEPTEMBER – 1 OCTOBER (mSv)

	Farm A	lower	upper	Farm B	lower	upper	Mesa	lower	upper
Filistovic-thyroid	2.64E-05			3.59E-05			1.63E-06		
Filistovic-body surface	7.01E-05			9.52E-05			4.32E-06		
Homma (1)	2.6E-05	5.5E-06	4.8E-05	5.5E-05	1.1E-05	1.2E-04	1.5E-04	1.7E-05	4.5E-04
Homma (2)	1.4E-05			1.4E-05			1.6E-06		
Kryshev	2.10E-05	6.00E-06	3.60E-05	3.60E-05	1.10E-05	6.10E-05	3.00E-06	1.00E-06	5.00E-06
Krajewski-man	2.37E-05	7.90E-06	7.11E-05	3.37E-05	1.12E-05	1.01E-04	7.19E-06	2.40E-06	2.16E-05
Krajewski-woman	2.37E-05	7.90E-06	7.11E-05	3.37E-05	1.12E-05	1.01E-04	7.19E-06	2.40E-06	2.16E-05
Krajewski-child (1 yr)	3.19E-05	1.06E-05	9.57E-05	4.54E-05	1.51E-05	1.36E-04	9.68E-06	3.23E-06	2.90E-05
Krajewski-boy (4 yr)				3.70E-05	1.23E-05	1.11E-04			
Krajewski-girl (8 yr)				3.70E-05	1.23E-05	1.11E-04			
Kanyar/Nenyei	8.00E-06			1.80E-05			6.50E-07		
Napier (HEDR)	5E-06	2E-06	2E-05	1E-05	3E-06	3E-05	1E-06	3E-07	3E-06

	Eltopia	lower	upper	Pasco	lower	upper	Ringold	lower	upper
Filistovic-thyroid	4.55E-06			3.91E-06					
Filistovic-body surface	1.21E-05			1.04E-05					
Homma (1)	5.9E-05	1.9E-05	9.3E-05	1.0E-05	3.5E-06	1.6E-05	3.0E-04	6.0E-05	6.4E-04
Homma (2)	7.5E-06			1.4E-04			8.6E-05		
Kryshev	4.00E-06	1.00E-06	7.00E-06	3.00E-06	1.00E-06	5.00E-06			
Krajewski-man	4.48E-06	1.49E-06	1.34E-05	9.05E-06	3.02E-06	2.72E-05			
Krajewski-woman	4.48E-06	1.49E-06	1.34E-05	9.05E-06	3.02E-06	2.72E-05			
Krajewski-child (1 yr)	6.03E-06	2.01E-06	1.81E-05	1.22E-05	4.07E-06	3.66E-05			
Kanyar/Nenyei	1.10E-06			1.00E-06			4.40E-06		
Napier (HEDR)	2E-06	7E-07	6E-06	8E-06	2E-06	2E-05			

TABLE. III–XI. PREDICTED DOSES TO THE THYROID FROM INHALATION (mSv)

	Farm A	lower	upper	Farm B	lower	upper	Mesa	lower	upper
Filistovic	4.25E-03	1.92E-04	1.39E-02	6.03E-03	4.41E-04	2.00E-02	9.64E-04	8.45E-05	2.63E-03
Homma (1)	9.3E-04	1.6E-04	1.8E-03	1.8E-03	3.7E-04	3.0E-03	6.7E-03	1.9E-04	1.8E-02
Homma (2)	5.6E-04			5.6E-04			6.0E-05		
Kryshev	3.80E-04	1.10E-04	6.50E-04	6.40E-04	1.90E-04	1.09E-03	5.50E-05	1.70E-05	9.30E-05
Krajewski-man	1.04E-03	3.46E-04	3.10E-03	1.47E-03	4.90E-04	4.42E-03	3.16E-04	1.05E-04	9.48E-04
Krajewski-woman	9.08E-04	3.02E-04	2.72E-03	1.29E-03	4.30E-04	3.87E-03	2.76E-04	9.20E-05	8.28E-04
Krajewski-child (1 yr)	1.68E-04	5.60E-05	5.04E-04	2.38E-04	7.94E-05	7.14E-04	5.12E-05	1.71E-05	1.54E-04
Krajewski-boy (4 yr)				3.16E-04	5.10E-05	4.59E-04			
Krajewski-girl (8 yr)				1.18E-04	3.93E-05	3.54E-04			
Kanyar/Nenyei (adult)	1.50E-04	6.50E-05	3.20E-04	3.30E-04	1.30E-04	6.50E-04	1.20E-05	4.00E-06	2.50E-05
Napier-4-yr boy				5.40E-03	1.40E-03	2.20E-02			
Napier-8-yr-girl				5.00E-03	1.20E-03	2.00E-02			

	Eltopia	lower	upper	Pasco	lower	upper	Ringold	lower	upper
Filistovic	1.86E-03	1.85E-04	6.99E-03	1.70E-03	6.00E-05	5.68E-03			
Homma (1)	2.8E-03	9.5E-05	5.3E-03	4.9E-04	2.7E-05	1.0E-03	9.7E-03	2.4E-03	1.8E-02
Homma (2)	3.0E-04			5.6E-02			3.4E-03		
Kryshev	7.30E-05	2.20E-05	1.24E-04	5.60E-05	1.70E-05	9.50E-05			
Krajewski-man	2.56E-04	8.54E-05	7.68E-04	3.96E-04	1.32E-04	1.19E-03			
Krajewski-woman	2.24E-04	7.46E-05	6.72E-04	3.46E-04	1.15E-04	1.04E-03			
Krajewski-child (1 yr)	4.16E-05	1.39E-05	1.25E-04	6.42E-05	2.14E-05	1.93E-04			
Kanyar/Nenyei (adult)	2.00E-05	8.00E-06	4.50E-05	1.90E-05	7.00E-06	4.20E-05	8.10E-05	3.60E-05	1.70E-04

TABLE. III–XII. PREDICTED DOSES TO THE THYROID FROM INGESTION FOR REFERENCE INDIVIDUALS (mSv)

	Farm A	lower	upper	Farm B	lower	upper	Mesa	lower	upper
Filistovic-male >20	1.56E-02	2.54E-03	4.46E-02	2.17E-02	2.84E-03	6.61E-02	9.25E-04	1.47E-04	2.67E-03
Filistovic-female >20	1.46E-02	1.88E-03	4.48E-02	1.97E-02	2.80E-03	5.85E-02	8.77E-04	1.11E-04	2.69E-03
Filistovic-male <1	2.65E-02	3.65E-03	7.96E-02	3.54E-02	5.49E-03	1.03E-01	1.47E-03	2.16E-04	4.33E-03
Filistovic-female <1	3.18E-02	3.59E-03	1.01E-01	4.65E-02	5.21E-03	1.47E-01	2.05E-03	2.34E-04	6.48E-03
Homma (1) (adult)	7.2E-03	6.8E-04	2.7E-02	1.6E-02	1.2E-03	5.6E-02	4.2E-02	1.7E-03	1.5E-01
Homma (2) (adult)	5.4E-03			5.4E-03			5.8E-04		
Kryshev-female > 20	1.2E-02	3.0E-03	2.1E-02	2.0E-02	4.0E-03	3.6E-02	1.4E-03	3.0E-04	2.5E-03
Kryshev-child (1 y)	2.6E-02	6.0E-03	4.6E-02	4.5E-02	1.0E-02	8.0E-02	3.0E-03	7.0E-04	5.3E-03
Krajewski-man	1.01E-02	3.37E-03	3.03E-02	1.40E-02	4.67E-03	4.20E-02	2.93E-03	9.77E-04	8.79E-03
Krajewski-woman	8.02E-03	2.67E-03	2.41E-02	1.15E-02	3.83E-03	3.45E-02	2.51E-03	8.37E-04	7.53E-03
Krajewski-child (1 yr)	1.63E-01	5.43E-02	4.89E-01	2.60E-01	8.67E-02	7.80E-01	6.08E-02	2.03E-02	1.82E-01
Kanyar/Nenyei (adult)	1.20E-02			3.30E-02			4.90E-04		

	Eltopia	lower	upper	Pasco	lower	upper	Ringold	lower	upper
Filistovic-male >20	2.64E-03	4.16E-04	7.64E-03	2.23E-03	3.49E-04	6.15E-03			
Filistovic-female >20	2.47E-03	2.46E-04	8.04E-03	2.10E-03	2.97E-04	6.25E-03			
Filistovic-male <1	4.47E-03	6.48E-04	1.32E-02	3.65E-03	5.09E-04	1.09E-02			
Filistovic-female <1	5.37E-03	5.94E-04	1.71E-02	4.79E-03	5.16E-04	1.53E-02			
Homma (1) (adult)	1.7E-02	1.3E-03	6.8E-02	3.0E-03	3.0E-04	1.1E-02	8.2E-02	5.8E-03	3.0E-01
Homma (2) (adult)	2.8E-03			5.4E-02			3.2E-02		
Kryshev-female > 20	2.1E-03	5.0E-04	3.7E-03	2.1E-03	5.0E-04	3.7E-03			
Kryshev-child (1 y)	5.0E-03	1.2E-03	8.8E-03	5.0E-03	1.2E-03	8.8E-03			
Krajewski-man	1.82E-03	6.07E-04	5.46E-03	3.74E-03	1.25E-03	1.12E-02			
Krajewski-woman	1.55E-03	5.17E-04	4.65E-03	3.12E-03	1.04E-03	9.36E-03			
Krajewski-child (1 yr)	3.62E-02	1.21E-02	1.09E-01	7.24E-02	2.41E-02	2.17E-01			
Kanyar/Nenyei (adult)	9.90E-04			1.40E-03			3.50E-03		

TABLE. III–XIII. PREDICTED DOSES TO THE THYROID FROM INGESTION FOR CHILDREN AT FARM B (mSv)

	boy (4 yr)	lower	upper
Filistovic	3.02E-02	6.41E-03	7.93E-02
Kryshev	3.1E-01	7.0E-02	5.5E-01
Krajewski	4.09E-01	1.36E-01	1.23E+00
Napier	4.50E-01	1.10E-01	1.80E+00

	girl (8 yr)	lower	upper
Filistovic	3.37E-02	8.25E-03	8.37E-02
Kryshev	8.0E-02	2.0E-02	1.4E-01
Krajewski	8.27E-02	2.76E-02	2.48E-01
Napier	1.10E-01	2.80E-02	4.40E-01

TABLE. III–XIV. PREDICTED TOTAL DOSES, 2 SEPTEMBER – 1 OCTOBER (mSv)

	Farm A	lower	upper	Farm B	lower	upper	Mesa	lower	upper
Filistovic	1.80E-02			2.63E-02			1.35E-03		
Homma (1)	8.2E-03	1.5E-03	2.8E-02	1.7E-02	3.3E-03	5.7E-02	4.9E-02	2.9E-03	1.7E-01
Homma (2)	6.0E-03			6.0E-03			6.4E-04		
Kryshev	1.74E-02	3.50E-03	3.60E-02	2.97E-02	5.90E-03	6.10E-02	2.10E-03	4.00E-04	4.00E-03
Krajewski-man	1.02E-02			1.41E-02			2.95E-03		
Krajewski-woman	8.09E-03			1.16E-02			2.53E-03		
Krajewski-child (1 yr)	1.63E-01			2.60E-01			6.08E-02		
Krajewski-boy (4 yr)				4.09E-01					
Krajewski-girl (8 yr)				8.29E-02					
Kanyar/Nenyei	1.20E-02			3.30E-02			4.90E-04		
Napier-4-yr boy				4.50E-01	1.10E-01	1.80E+00			
Napier-8-yr-girl				1.20E-01	2.80E-02	4.40E-01			

	Eltopia	lower	upper	Pasco	lower	upper	Ringold	lower	upper
Filistovic	3.23E-03			2.48E-03					
Homma (1)	2.0E-02	1.9E-03	6.9E-02	3.5E-03	6.5E-04	1.2E-02	9.2E-02	1.4E-02	3.0E-01
Homma (2)	3.1E-03			6.0E-02			3.5E-02		
Kryshev	3.10E-03	6.00E-04	6.00E-03	3.10E-03	6.00E-04	6.00E-03			
Krajewski-man	1.84E-03			3.77E-03					
Krajewski-woman	1.57E-03			3.15E-03					
Krajewski-child (1 yr)	3.62E-02			7.24E-02					
Kanyar/Nenyei	9.90E-04			1.40E-03			9.50E-03		

CONTRIBUTORS TO DRAFTING AND REVIEW

Filistovic, V.	Institute of Physics, Lithuania
Homma, T.	Japan Atomic Energy Research Institute, Japan
Kanyár, B.	University of Veszprém, Hungary
Krajewski, P.	Central Laboratory for Radiological Protection, Poland
Kryshev, A.	Institute of Experimental Meteorology, SPA "Typhoon", Russian Federation
Napier, B.	Battelle Pacific Northwest National Laboratories, United States of America
Nedveckaite, T.	Institute of Physics, Lithuania
Nenyei, A.	University of Veszprém, Hungary
Robinson, C.	International Atomic Energy Agency
Sazykina, T.	Institute of Experimental Meteorology, SPA "Typhoon", Russian Federation
Sjöblom, K-L.	International Atomic Energy Agency
Thiessen, K.	SENES Oak Ridge Inc., Center for Risk Analysis, United States of America
Tveten, U.	Institute for Energy Technology (IFE), Norway

Meetings

BIOMASS Theme 2 Planning Meeting, Vienna, Austria: 24–28 June 1996

BIOMASS Dose Reconstruction WG Planning Meeting, Mol, Belgium: 11–13 June 1997

BIOMASS Plenary and Working Group Meetings, Vienna, Austria: 20–24 October 1997

BIOMASS Dose Reconstruction WG Meeting, Veszprém, Hungary: 8–12 June 1998

BIOMASS Research Co-ordination, Plenary and Working Group Meetings, Vienna, Austria: 5–9 October 1998

BIOMASS Dose Reconstruction WG Meeting, Vienna, Austria: 31 May–1 June 1999

BIOMASS Research Co-ordination, Plenary and Working Group Meetings, Vienna, Austria: 4–8 October 1999

BIOMASS Dose Reconstruction WG Meeting, Kjeller, Norway: 25–26 May 2000

BIOMASS Research Co-ordination, Plenary and Working Group Meetings, Vienna, Austria: 6–10 November 2000